ABC Imagem Cardiovascular

Volume 38 | Number 2

April/May/June 2025

Sociedade Brasileira de Cardiologia
ISSN-2675-312X

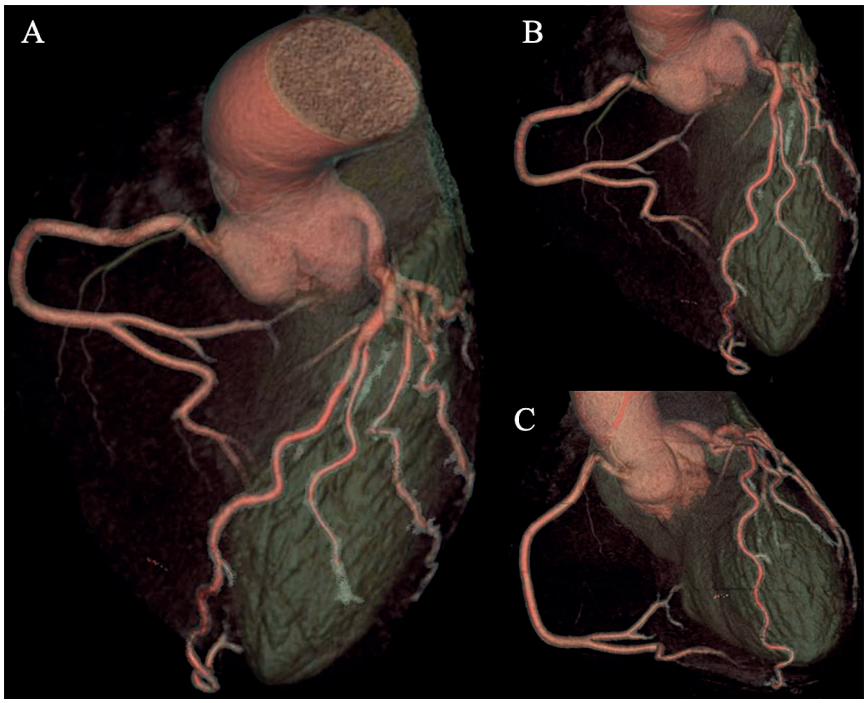

Figure 2 of the article: Coronary Artery Dissection Following Pharmacologic Stress Echocardiography and the Follow-Up of Clinical Management: A Case Report

DIC | SOCIEDADE BRASILEIRA DE CARDIOLOGIA SBC 1943 | ABC Imagem Cardiovascular

Contents

Click on the title to read the article

Case Report

Image

Departament of Cardiovascular Imaging

President
Silvio Henrique Barberato - PR

Vice President of Echocardiography
Daniela do Carmo Rassi Frota - GO

Vice President of Nuclear Cardiology
Cláudio Tinoco Mesquita – RJ

Vice President of Vascular Echography
Salomon Israel do Amaral – RJ

Vice President of Magnetic Resonance Imaging
Isabela Bispo Santos da Silva Costa – SP

Vice President of Computed Tomography
Jorge Andion Torreão – BA

Vice President of Congenital Heart Disease and Pediatric Cardiology
Andressa Mussi Soares – ES

Managing Director
Adenalva Lima de Souza Beck – DF

Financial Director
Gláucia Maria Penha Tavares - SP

Journal Editor
Marcelo Dantas Tavares de Melo – PB

Consulting Board

Members
André Luiz Cerqueira de Almeida - BA
Arnaldo Rabischoffsky - RJ
Carlos Eduardo Rochitte - SP
Marcelo Luiz Campos Vieira - SP
Samira Saady Morhy - SP

Scientific Committee

Coordinator
Daniela do Carmo Rassi Frota - GO

Members
Andressa Mussi Soares - ES
Cláudio Tinoco Mesquita - RJ
Isabela Bispo Santos da Silva Costa - SP
Jorge Andion Torreão - BA
Salomon Israel do Amaral - RJ

Echocardiography Certification Committee

Coordinator
Tatiane Mascarenhas Santiago Emerich - ES
Andrea de Andrade Vilela - SP

Adult Echo Members
Antonio Amador Calvilho JR. - SP
Antonio Tito Paladino Filho - SP
Eliza de Almeida Gripp - RJ
Jaime Paula Pessoa Linhares Filho - CE
João Carlos Moron Saes Braga - SP
Marcio Mendes Pereira - MA
Paulo Henrique Nunes Pereira - PA
Renato de Aguiar Hortegal - SP
Tiago Costa Bignoto - SP
Wanessa Nakamura Guimarães - DF

Congenital Echo Members
Barbara Neiva Tanaka - MA
Daniela Lago Kreuzig - SP
Danielle Lopes Rocha - ES
Halsted Alarcao Gomes Pereira da Silva - SP
Leandro Alves Freire - SP
Marcio Miranda Brito - TO
Maria Elisa Martini Albretch - SP

Seniors
Andrea de Andare Vilela - SP
Glaucia Maria Penha Tavares - SP
José Luiz Barros Pena - MG
Maria Estefania Bosco Otto - DF
Mohamed Hassan Saleh - SP
Solange Bernardes Tatani - SP

Social Media Committee

Coordinator
Alex dos Santos Félix - RJ
Antonio Carlos Leite de Barros Filho - SP

Members
Barbara Athayde Linhares Martins Vrandecic - MG
Cristiane Nunes Martins - MG
José Roberto Matos Souza - SP
Simone Cristina Soares Brandão - PE

Professional Defense and Institutional Relations Committee

Members
Fabio Cañellas Moreira - RS
Jorge Yussef Afiune - DF
Marcelo Haertel Miglioranza - RS
Mohamed Hassan Saleh - SP
Wagner Pires de Oliveira Júnior - DF

Committee of Education and Accreditation

Coordinator
Edgar Bezerra de Lira Filho - SP

Members
Andrea de Andare Vilela - SP
Sandra Nívea dos Reis Saraiva Falcão - CE

Intersociety Committee

Coordinator
Marcelo Luiz Campos Vieira - SP

Members
Ana Cristina de Almeida Camarozano - PR
José Luiz Barros Pena - MG
Marcelo Haertel Miglioranza - RS

DIC Youth Committee

Coordinator
Bruna Morhy Borges Leal Assunção - SP
Márcio Miranda Brito - TO

Adult Echo Members
Carolina da Costa Mendes - SP
Manoela Falsoni - SP
Talita Beithum Ribeiro Mialski - PR
Tauin Raoni Do Couto - PA

CR/MR Members
Maria Júlia Silveira Souto - SP

Vascular Ultrasound Member
Larissa Chaves Nunes de Carvalho - SP

Member Of Congenital Heart Diseases
Isabela de Sousa Lobo Silva - SP

Committee on Echocardiography, Congenital and Pediatric Cardiology

Coordinator
Andressa Mussi Soares - ES

Members
Cláudia Regina Pinheiro de Castro Grau - SP
Laura Mercer Rosa - USA
Márcia Ferreira Alves Barberato - PR

PORTAL DIC

Coordinator
Alex dos Santos Félix - RJ

Administrative Council – Year 2025 (Brazilian Society of Cardiology)

North/Northeast
Nivaldo Menezes Filgueiras Filho (BA) – Vice-President of the Administrative Council of SBC
Sérgio Tavares Montenegro (PE)

East
Denilson Campos de Albuquerque (RJ)
Evandro Tinoco Mesquita (RJ)

State of São Paulo
Ricardo Pavanello (SP)
Miguel Moretti (SP)

Center
Carlos Eduardo de Souza Miranda (MG)
Renault M. Ribeiro Junior (DF)

South
Paulo Ricardo Avancini Caramori (RS) – President of the Administrative Council of SBC
Gerson Luiz Bredt Júnior (PR)

Scientific Committee
Sérgio Tavares Montenegro (PE)
Miguel Moretti (SP)
Angelo de Paola (SP)

National Editorial Board

ABC Imagem Cardiovascular

Volume 38, Nº 2, April/May/June 2025

Indexing: Lilacs (Latin American and Caribbean Health Sciences Literature), Latindex (Regional Cooperative Online Information System for Scholarly Journals from Latin America, the Caribbean, Spain and Portugal) and DOAJ (Directory of Open Access Journals)

Address: Av. Marechal Câmara, 160 - 3º andar - Sala 330
20020-907 • Centro • Rio de Janeiro, RJ • Brazil
Phone.: (21) 3478-2700
E-mail: abcimaging@cardiol.br
https://www.abcimaging.org/

Commercial Department
Phone: (11) 3411-5500
E-mail: comercialsp@cardiol.br

Editorial Production
SBC - Scientific Department

Graphic Design and Diagramming
SBC - Scientific Department

Editorial

Intracardiac Echocardiography: Current Status, Clinical Benefits, and Future Perspectives

Renner Augusto Raposo Pereira,[1,2] *Daniel Moreira Costa Moura*[1,2]

Hospital Nossa Senhora das Neves,[1] *João Pessoa, PB – Brazil*
Hospital Metropolitano DJMP,[2] *Santa Rita, PB – Brazil*

Intracardiac echocardiography (ICE) is an ultrasound imaging technique capable of providing real-time, high-quality visualization of cardiac structures and their adjacent tissues through a catheter with a transducer inserted directly into the heart chambers, typically via transfemoral venous access. By allowing direct and precise visualization of intracardiac anatomy, ICE has been increasingly used to guide structural interventions and catheter ablations for cardiac arrhythmias, as well as to enable immediate detection of intraoperative complications.[1]

Initial clinical investigations began in the 1960s, focusing on the assessment of atrial septal defects. Since then, ICE has evolved significantly.[2] The introduction of the phased-array transducer, the addition of color Doppler functionality, and advancements in manipulation systems have enabled its widespread clinical application. The latest version of phased-array ICE features a position sensor at the catheter tip, allowing real-time integration with three-dimensional electroanatomic mapping systems used in complex ablations. The ability to precisely maneuver the catheter, combined with its versatile positioning, makes ICE a valuable tool for anatomic navigation and real-time monitoring during complex interventions.[3]

Initially, ICE was used to guide the percutaneous closure of atrial septal defects, serving as an alternative to transesophageal echocardiography (TEE), with comparable imaging quality and better tolerability.[1] Currently, ICE is the preferred imaging modality in various electrophysiology procedures, as it eliminates the need for general anesthesia and allows the operator to manage the imaging, optimizing time and resources.[4]

In electrophysiology, ICE has become an essential tool. In atrial fibrillation ablation, ICE safely guides transseptal puncture and provides real-time visualization of the left atrium, pulmonary veins, atrial appendage, and adjacent structures, such as the esophagus and pulmonary arteries, allowing precise delineation of the ablation area and preventing thermal complications. In atrial tachyarrhythmia ablations, such as atypical atrial flutter, ICE helps identify complex anatomical structures and reentry pathways, guiding catheter positioning around scars or critical zones.[5]

In ventricular arrhythmias, ICE has been increasingly used. In the ablation of extrasystoles or tachycardias originating from the right ventricular outflow tract, ICE enables precise anatomical positioning between the outflow tract and adjacent structures. For arrhythmias originating from the left ventricular outflow tract and the left ventricular summit, ICE assists in guiding transseptal or retroaortic approaches, improving procedure efficacy and safety. Its role is even more crucial in coronary cusp arrhythmias, as it provides clear visualization of catheter contact with the cusp, Valsalva sinus, and coronary artery ostium. In cases of arrhythmias originating from the papillary muscles, ICE is particularly valuable, as it allows direct visualization of these mobile structures and continuous catheter contact with the target, which is challenging using electroanatomic mapping alone, enabling more effective procedures. In scar-related ventricular tachycardia, ICE complements electroanatomic mapping by identifying areas of myocardial thinning, aneurysms, and akinetic walls, as well as fibrotic regions associated with the arrhythmogenic substrate, while also monitoring real-time catheter stability during ablation.[6]

Another highlight is the use of ICE in the closure of left atrial appendage. In addition to transseptal puncture, ICE provides visualization of the appendage anatomy, diameter assessment, and guidance for device deployment, while reducing the use of iodinated contrast and fluoroscopy. In many centers, ICE has replaced TEE in this scenario, allowing the procedure to be performed under conscious sedation. This approach is particularly useful when combining atrial fibrillation ablation with LAA closure.[7]

ICE has been gaining ground in interventional cardiology, especially with the development of 3D ICE, serving as a valuable complement and even an alternative to TEE in certain cases. In adults, its application stands out in the percutaneous closure of atrial septal defects and patent foramen ovale, where image quality is superior, and the procedure can be performed under conscious sedation.Initial results are promising for transcatheter mitral valve repair, and more recently, ICE has been studied for percutaneous tricuspid valve procedures and paravalvular leak closure. In transcatheter aortic valve implantation, fluoroscopy remains the standard imaging method, but in more complex cases, 3D ICE can add value and serve as an alternative to TEE.[8]

In percutaneous treatment of congenital heart diseases, ICE has been explored in structural interventions beyond atrial septal defect closure, including ventricular septal defect interventions, patent ductus arteriosus procedures, and pulmonary valve disease treatments. Its use reduces radiation

Keywords

Echocardiography; Cardiac Electrophysiology; Patient Safety

Mailing Address: Renner Augusto Raposo Pereira •
Hospital Nossa Senhora das Neves. R. Etelvina Macedo de Mendonça, 531. Postal code: 58040-530. João Pessoa, PB – Brazil
E-mail: rennerarp@gmail.com

DOI: https://doi.org/10.36660/abcimg.20250031i

exposure and minimizes the need for prolonged general anesthesia, providing significant benefits for pediatric and adult patients with congenital heart disease.[1,9]

ICE is a safe alternative for identifying thrombi in the left atrial appendage, significantly enhancing procedural safety by reducing complications such as cardiac tamponade, thrombosis, and pulmonary vein stenosis.[10] Performing ablations with minimal or even no radiation exposure is now a reality, making it especially relevant for young patients and pregnant women, while also significantly reducing occupational risks for the medical team.[1,10,11]

Additionally, the implementation of ICE in daily practice is feasible after a short learning curve, allowing for rapid adoption without compromising procedure safety or efficacy.[12]

Despite advancements, cost remains a barrier to the widespread dissemination of ICE, primarily due to the high price of disposable catheters. However, considering reduced procedure time, fewer complications, and decreased need for general anesthesia, the total cost of the procedure may be comparable to that of TEE.[1,13]

Emerging technologies, such as real-time three-dimensional ICE, are already being applied and promise to further enhance the precision of interventions.[8] The miniaturization of catheters, improvement in image resolution, and integration with artificial intelligence algorithms for automatic segmentation and structure identification are expected soon.[1,9]

ICE represents one of the major innovations in cardiovascular imaging for contemporary interventional practice. Its growing use is driven by its ability to combine image quality, safety, and efficiency, making it a fundamental tool for high-complexity procedures in electrophysiology and structural cardiology, with a positive impact on procedural safety and efficacy.

References

1. Jingquan Z, Deyong L, Huimin C, Hua F, Xuebin H, Chenyang J, et al. Intracardiac Echocardiography Chinese Expert Consensus. Front Cardiovasc Med. 2022;9:1012731. doi: 10.3389/fcvm.2022.1012731.
2. Kossoff G. Diagnostic Applications of Ultrasound in Cardiology. Australas Radiol. 1966;10(2):101-6. doi: 10.1111/j.1440-1673.1966.tb00774.x.
3. Singh SM, Heist EK, Donaldson DM, Collins RM, Chevalier J, Mela T, et al. Image Integration Using Intracardiac Ultrasound to Guide Catheter Ablation of Atrial Fibrillation. Heart Rhythm. 2008;5(11):1548-55. doi: 10.1016/j.hrthm.2008.08.027.
4. Liu CF. The Evolving Utility Of Intracardiac Echocardiography In Cardiac Procedures. J Atr Fibrillation. 2014;6(6):1055. doi: 10.4022/jafib.1055.
5. Saad EB, Costa IP, Camanho LE. Use of Intracardiac Echocardiography in the Electrophysiology Laboratory. Arq Bras Cardiol. 2011;96(1):e11-7. doi: 10.1590/S0066-782X2011000100019.
6. Asvestas D, Xenos T, Tzeis S. The Contribution of Intracardiac Echocardiography in Catheter Ablation of Ventricular Arrhythmias. Rev Cardiovasc Med. 2022;23(1):25. doi: 10.31083/j.rcm2301025.
7. Beneki E, Dimitriadis K, Theofilis P, Pyrpyris N, Iliakis P, Kalompatsou A, et al. Intracardiac or Transesophageal Echocardiography for Left Atrial Appendage Occlusion: An Updated Systematic Review and Meta-Analysis. Int J Cardiovasc Imaging. 2025;41:489-505. doi: 10.1007/s10554-025-03330-z.
8. Tang GHL, Zaid S, Hahn RT, Aggarwal V, Alkhouli M, Aman E, et al. Structural Heart Imaging Using 3-Dimensional Intracardiac Echocardiography: JACC: Cardiovascular Imaging Position Statement. JACC Cardiovasc Imaging. 2025;18(1):93-115. doi: 10.1016/j.jcmg.2024.05.012.
9. Ghantous E, Aboulhosn JA. The Growing Role of Intracardiac Echo in Congenital Heart Disease Interventions. J Clin Med. 2025;14(7):2414. doi: 10.3390/jcm14072414.
10. Isath A, Padmanabhan D, Haider SW, Siroky G, Perimbeti S, Correa A, et al. Does the Use of Intracardiac Echocardiography during Atrial Fibrillation Catheter Ablation Improve Outcomes and Cost? A Nationwide 14-Year Analysis from 2001 to 2014. J Interv Card Electrophysiol. 2021;61(3):461-8. doi: 10.1007/s10840-020-00844-5.
11. Saad EB, Slater C, Inácio LAO Jr, Santos GVD, Dias LC, Camanho LEM. Catheter Ablation for Treatment of Atrial Fibrillation and Supraventricular Arrhythmias without Fluoroscopy Use: Acute Efficacy and Safety. Arq Bras Cardiol. 2020;114(6):1015-26. doi: 10.36660/abc.20200096.
12. Zei PC, Hunter TD, Gache LM, O'Riordan G, Baykaner T, Brodt CR. Low-Fluoroscopy Atrial Fibrillation Ablation with Contact Force and Ultrasound Technologies: A Learning Curve. Pragmat Obs Res. 2019;10:1-7. doi: 10.2147/POR.S181220.
13. Sant'Anna RT, Lima GG, Saffi MAL, Kruse ML, Leiria TLL. Atrial Fibrillation Ablation: Impact of Intracardiac Echocardiography in Reducing Procedure Time and Hospitalization. Arq Bras Cardiol. 2023;120(5):e20220306. doi: 10.36660/abc.20220306.

Photon-Counting Computed Tomography in Cardiovascular Imaging: Where We Are and What Lies Ahead

Paulo Savoia,[1] *Rodrigo Bello*[1]

University of Iowa Hospitals and Clinics,[1] *Iowa City, Iowa – USA*

Computed Tomography Angiography (CTA) has been an important asset in cardiovascular diagnosis for decades. The continuous improvement of rapid data acquisition with often higher spatial resolution has established the method as indispensable for diagnosing and managing multiple cardiovascular entities such as aneurysms, aortic dissection, and pulmonary embolism.[1,2] The use of CTA in heart and coronary imaging has also gained important territory and relevance.[3,4] Computed Tomography (CT) techniques have been advancing significantly since its introduction in the medical field. Starting with single detectors, then helicoidal scanners, multidetector scanners with high pitch, improvement of reconstruction algorithms, the appearance of dual-energy technology, and lately the ability to acquire images of the whole heart in just one heartbeat with information from the entire cardiac cycle, are incredible milestones. Fractional Flow Reserve CT (FFR-CT) is also a very promising technique.[5] Progression does not come without downsides: ionizing radiation is still concerning, and despite ways to reduce it such as dose modulation, some cardiovascular CTA exams still show relatively high levels of absorbed radiation, especially exams with multiple series, extremely thin slices, and retrospective reconstruction of larger parts of the cardiac cycle. Following this trend of improving image quality with less ionizing radiation as possible, a new complex technique emerged: Photon-counting CT (PCCT).

The main distinction between conventional CT and PCCT is in the detectors of X-rays. The conventional CT detector is based on receiving the X-ray photons that interact with the patient, converting them into light photons (it is an indirect system), and then converting this light into electrical signals that ultimately are going to be converted into digital signals. This system is called an Energy-Integrating Detector (EID). Basically, more light means more X-rays arriving and less interaction / more penetration in the patient's tissues. It is not possible to differentiate exactly how many X-rays are arriving, nor the different energy levels of each X-ray photon. Moreover, the septa between each of the detectors also limit the reception of X-rays.[6,7] On the other hand, PCCT detectors can detect separately each X-ray photon that is arriving and measure the energy of each one of the X-ray photons directly. This is possible because the PCCT detector has a high-voltage crystal layer that relocates electrons for each X-ray photon received, and the number of electrons relocated is proportional to the energy of each X-ray. The relocated electrons generate the electrical pulse that is going to be finally converted into the digital signal. And even smaller energy X-rays can be detected, improving the image contrast-to-noise ratio. It is a direct system, and there is no septa between the detectors. In the end, less X-rays are necessary (therefore less radiation) and it is possible to separate the X-rays according to the energy of each one, leading to applications of tissue recognition (different known energy X-rays are likely to have interacted with different known tissues) functioning as a dual energy CT.[8,9]

As far as this new technology became available, the scientific community was excited about the advances, and interesting publications were released. In mid-2022, Esquivel *et al*.[6] published interesting concepts about PCCT for radiologists: "Key Points Radiologists Should Know", which helped spread the information and knowledge amongst the international Radiology Community. The possibility of improving characterization of small vessels (e.g., distal coronary arteries, peripheral run-off arteries, artery of Adamkiewicz, and small arterial flaps) was highlighted. Still in 2022, Si-Mohamed *et al*.[10] published the first In-Human Results for Coronary CT Angiography with PCCT: despite being a small group of fourteen participants, this prospective study showed significant improvements in overall image quality, diagnostic quality, and diagnostic confidence in PCCT compared to an EID dual-layer CT analyzing multiple variants such as distal coronary lumen, calcification sharpness, stents – classic scenarios of partially limited evaluation with the CT technology available before PCCT.

In 2023, Cademartiri *et al* published a complete paper regarding PCCT cardiac and coronary applications.[11] They revised the PCCT physics, analyzed publications released up to the moment that discussed the matter, and discussed that PCCT allegedly is beneficial in evaluating coronary lumen, coronary stents, prosthetic valves, plaque composition, myocardial tissue imaging, as well as radiation dose reduction, contrast media reduction and improved contrast-to-noise ratio. The reduction in contrast media usage could be around 50%. About the radiation dose reduction, it is calculated between 19-32% according to some authors.[12,13]

Lately, after all these interesting improvements published in small groups of patients and pictorial essays, it is time to finally test the method in wide clinical practice. The theory and cases demonstrated so far are very promising. We have summarized the PCCT key quality improvements in Table 1. The next step is probably to publish data with larger patients' samples, more centers, and mainly, to determine if there are significant changes in patient outcomes. The experience at our Institution, where

Keywords

Computed Tomography Angiography; Cardiovascular Diagnostic Techniques; Cardiology; Radiology

Mailing Address: Paulo Savoia MD PhD •
University of Iowa Hospitals and Clinics. Hawkins Dr., 200. sala 3884 JPP
Postal code: 52242. Iowa City, Iowa – USA
E-mail: paulo-savoia@uiowa.edu

DOI: https://doi.org/10.36660/abcimg.20250035i

Table 1 – PCCT Key Quality Improvements

1. Superior Spatial Resolution Smaller detector elements allow for sharper images with enhanced anatomic detail, benefiting applications like coronary artery visualization, but also lung imaging and inner ear for example.
2. Enhanced Tissue Contrast and Material Differentiation Multi-energy detection enables material decomposition (e.g., calcium, iodine, uric acid), improving lesion characterization and reducing diagnostic ambiguity.
3. Lower Radiation Dose Due to higher detector efficiency and reduced noise, diagnostic-quality images can often be achieved with significantly less radiation exposure.
4. Reduction of Artifacts PCCT minimizes beam hardening and metal artifacts, improving image fidelity in challenging cases such as prosthetic valves, implants and regions near to the bones.
5. Native Spectral Imaging Without Dose Penalty Unlike dual-energy CT, PCCT delivers spectral data in every scan, without requiring specialized protocols or increased dose.

we have the opportunity to work with three PCCT Scanners (one 100% dedicated to research and two for clinical assessment), is also leaning towards this direction, trying to measure differences in dose radiation, contrast media utilization, and significantly changing patient management. We have started using the PCCT scanner at the beginning of 2022. On the other hand, of course there are multiple challenges involved in PCCT worldwide: young clinical experience with the new method, optimization of protocols to extract the maximum possible of the technique (since we have multiple new protocols and Kernels available, with countless reconstruction parameters), robust / updated image viewers to deal with the extremely large number of images one single exam loads (the slice thickness can achieve up to 0.2 mm generating 11,000 images in one single Cardiac CTA) and, of course, the money invested in these novel scans. Figure 1 shows an example of a PCCT heart image acquisition of one of our patients with a prosthetic valve: notice the minimal or almost nonexistent beam hardening or blooming artifacts. Figure 2 shows the left anterior descending coronary artery of another patient scanned in our Institution with PCCT compared with a prior acquisition of the same artery in a multi-detector "conventional" CT.

Finally, we can state that there is no doubt that the new PCCT technology has brought significant advances in image quality, with ultra-high resolution images, an important improvement in the signal-to-noise ratio, and overall reduction in radiation doses, potentially increasing the accuracy of reading physicians and maximizing patient-centered care. PCCT will likely be the future of our CT scanners.

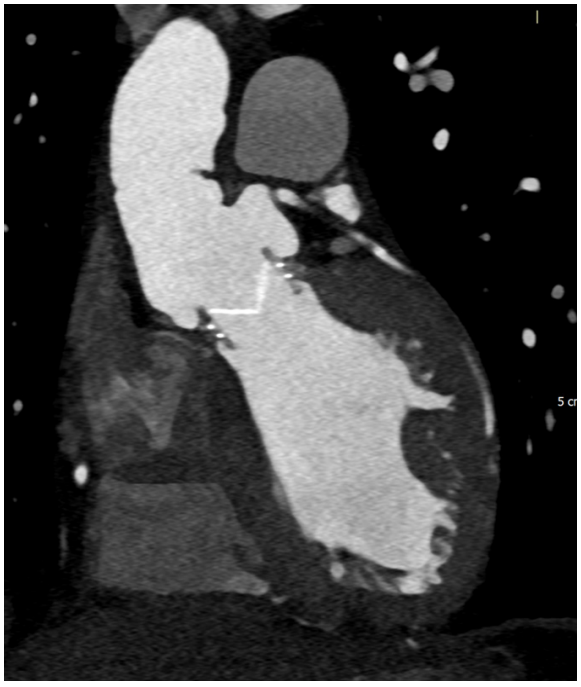

Figure 1 – *PCCT acquisition of one of our patients' heart with a prosthetic valve: notice the minimal or almost nonexistent beam hardening or blooming artifacts.*

Editorial

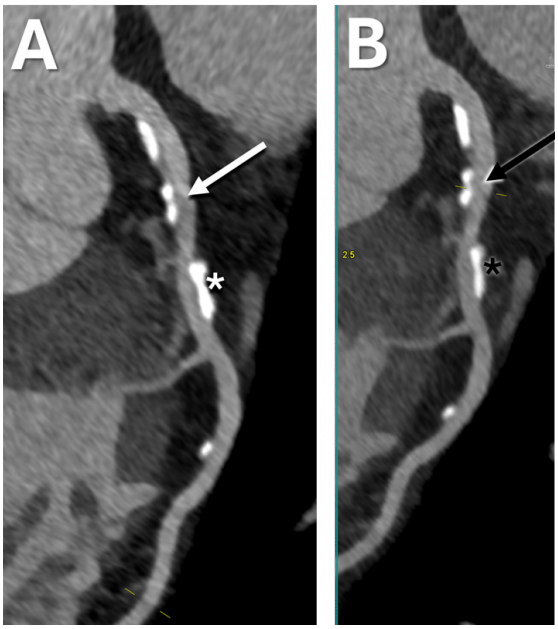

Figure 2 – *Left anterior descending coronary artery of another patient scanned in our Institution with PCCT (Figure 2B) compared to a few months prior acquisition of the same artery in a multi-detector "conventional" dual-source CT (2x192 detector rows) (Figure 2A). The "conventional" acquisition shows more beam hardening artifacts adjacent to a calcified plaque (hypoattenuating area – white arrow) in comparison to the PCCT acquisition- black arrow (Figure 2B). Additionally, there is also less blooming artifact of a calcified plaque in the PCCT acquisition (Figure 2B) – black asterisk - in comparison to the "conventional" acquisition (Figure 2A) – white asterisk. The blooming artifact is a known cause for luminal stenosis overestimation in calcified plaques, and indeed the plaque looks larger in the "conventional" acquisition.*

References

1. Sun Z, Al Moudi M, Cao Y. CT Angiography in the Diagnosis of Cardiovascular Disease: A Transformation in Cardiovascular CT Practice. Quant Imaging Med Surg. 2014;4(5):376-96. doi: 10.3978/j.issn.2223-4292.2014.10.02.
2. Zantonelli G, Cozzi D, Bindi A, Cavigli E, Moroni C, Luvarà S, et al. Acute Pulmonary Embolism: Prognostic Role of Computed Tomography Pulmonary Angiography (CTPA). Tomography. 2022;8(1):529-39. doi: 10.3390/tomography8010042.
3. Sun Z, Choo GH, Ng KH. Coronary CT Angiography: Current Status and Continuing Challenges. Br J Radiol. 2012;85(1013):495-510. doi: 10.1259/bjr/15296170.
4. Cademartiri F, Casolo G, Clemente A, Seitun S, Mantini C, Bossone E, et al. Coronary CT Angiography: A Guide to Examination, Interpretation, and Clinical Indications. Expert Rev Cardiovasc Ther. 2021;19(5):413-25. doi: 10.1080/14779072.2021.1915132.
5. Chen J, Wetzel LH, Pope KL, Meek LJ, Rosamond T, Walker CM. FFRCT: Current Status. AJR Am J Roentgenol. 2021;216(3):640-8. doi: 10.2214/AJR.20.23332.
6. Esquivel A, Ferrero A, Mileto A, Baffour F, Horst K, Rajiah PS, et al. Photon-Counting Detector CT: Key Points Radiologists Should Know. Korean J Radiol. 2022;23(9):854-65. doi: 10.3348/kjr.2022.0377.
7. Remy-Jardin M, Hutt A, Flohr T, Faivre JB, Felloni P, Khung S, et al. Ultra-High-Resolution Photon-Counting CT Imaging of the Chest: A New Era for Morphology and Function. Invest Radiol. 2023;58(7):482-7. doi: 10.1097/RLI.0000000000000968.
8. Willemink MJ, Persson M, Pourmorteza A, Pelc NJ, Fleischmann D. Photon-Counting CT: Technical Principles and Clinical Prospects. Radiology. 2018;289(2):293-312. doi: 10.1148/radiol.2018172656.
9. Sartoretti T, Wildberger JE, Flohr T, Alkadhi H. Photon-Counting Detector CT: Early Clinical Experience Review. Br J Radiol. 2023;96(1147):20220544. doi: 10.1259/bjr.20220544.
10. Si-Mohamed SA, Boccalini S, Lacombe H, Diaw A, Varasteh M, Rodesch PA, et al. Coronary CT Angiography with Photon-Counting CT: First-In-Human Results. Radiology. 2022;303(2):303-13. doi: 10.1148/radiol.211780.
11. Cademartiri F, Meloni A, Pistoia L, Degiorgi G, Clemente A, Gori C, et al. Dual-Source Photon-Counting Computed Tomography-Part I: Clinical Overview of Cardiac CT and Coronary CT Angiography Applications. J Clin Med. 2023;12(11):3627. doi: 10.3390/jcm12113627.
12. Flohr T, Schmidt B, Ulzheimer S, Alkadhi H. Cardiac Imaging with Photon Counting CT. Br J Radiol. 2023;96(1152):20230407. doi: 10.1259/bjr.20230407.
13. Dobrolinska MM, van der Werf NR, van der Bie J, de Groen J, Dijkshoorn M, Booij R, et al. Radiation Dose Optimization for Photon-Counting CT Coronary Artery Calcium Scoring for Different Patient Sizes: A Dynamic Phantom Study. Eur Radiol. 2023;33(7):4668-75. doi: 10.1007/s00330-023-09434-1.

Editorial

Mental Traps That Impact Diagnostic Imaging

Maurício Rodrigues Jordão,[1] *Marcelo Tavares,*[2] *Fábio Fernandes*[3]

Hospital 9 de Julho,[1] *São Paulo, SP – Brazil*
Universidade Federal da Paraíba,[2] *João Pessoa, PB – Brazil*
Universidade de São Paulo, Instituto do Coração,[3] *São Paulo, SP – Brazil*

Daniel Kahneman reinforced and popularized the idea of two distinct modes of thinking.[1] System 1 relies on pattern recognition, detecting simple relationships, correlating stereotypes, and associating ideas in a search for coherence. It is fast, intuitive, automatic, and requires little or no effort or energy. It cannot be turned off and continuously monitors the environment, driven by a survival need rooted in our ancestral past. System 2, on the other hand, demands attention, compares objects based on various attributes, and makes deliberate choices among options. It evaluates scenarios using logical and statistical reasoning. Because it requires attention, its activity is interrupted when that attention is diverted. Therefore, tasks that require effort interfere with one another (for instance, making a turn while driving and performing a complex calculation simultaneously is impossible). However, System 2 is slow, deliberate, effortful, and orderly. The two systems are interconnected: System 1 effortlessly generates impressions and feelings that serve as the main source for the explicit beliefs and deliberate choices made by System 2. In daily life, we often make decisions based on heuristics—mental shortcuts closely linked to System 1—used to save time and energy. While extremely efficient, this faster way of thinking opens the door to cognitive biases, which are systematic tendencies that distort logical reasoning and lead to flawed decisions.

The causes of error in diagnostic medicine can be categorized into two main groups: perceptual errors and interpretive errors. Perceptual errors occur when an abnormality is present on the image but goes undetected. These may be related to image acquisition, post-processing, or equipment quality. Interpretive errors arise when the abnormality is seen but its significance is misunderstood. In such cases, cognitive biases may be involved and are estimated to account for up to 74% of diagnostic errors.[2-4] Approximately 30 types of cognitive biases have been described in literature.[5] In diagnostic imaging, the most relevant include anchoring, confirmation bias, availability bias, attribution bias, framing effect, and satisfaction of search.[2-4,6]

Anchoring refers to the disproportionate influence of initial impressions or salient information — typically presented at the beginning of a case — on subsequent analytical processes. This bias occurs when a clinician remains fixated on an initial hypothesis and fails to adequately incorporate new clinical or imaging data that emerge during the diagnostic investigation. It is a phenomenon linked to the so-called "anchoring effect," in which the first piece of information received tends to exert a significant impact on decision-making. A classic example involves numerical estimation: when a group is asked whether the Golden Gate Bridge is more or less than 2,500 meters long, and then prompted to estimate its actual length, the responses often cluster around the suggested figure — demonstrating anchoring to the initial reference. This bias becomes even more detrimental when combined with confirmation bias. In such cases, the reasoning process begins with a belief or preconceived notion, so that information supporting this initial hypothesis is readily accepted, while contradictory data are more easily dismissed.

Another important bias is availability bias, which refers to the tendency to judge the likelihood of an event based on how easily it comes to mind. The most readily available information is typically the most recent, frequent, or emotionally charged (especially if extreme, vivid, or negative), and therefore tends to be considered first in the diagnostic process. Attribution bias occurs when certain findings are interpreted based on patient characteristics or stereotypes — usually derived from clinical history. Factors such as ethnicity, geographic origin, or age group may influence diagnostic reasoning, as certain genetic or infectious diseases have higher prevalence in specific populations. A common example is the tendency to underestimate the likelihood of atherosclerotic coronary artery disease in young patients presenting with acute coronary syndrome.

One of the main strategies to mitigate the impact of these biases is to analyze imaging studies without clinical context initially, followed by a subsequent review in light of the clinical scenario. This approach is also useful in addressing the so-called "framing effect," in which different diagnostic conclusions may be drawn from the same information depending on how the case is presented. The way the clinician describes the case or formulates the imaging request can influence interpretation — sometimes in suboptimal ways. It is well established that appropriate clinical information tends to enhance diagnostic sensitivity without compromising specificity. However, imaging requests are often incomplete, inadequate, or, in some cases, incorrect.

Satisfaction of search is another cognitive bias frequently encountered in radiologic practice. It refers to the decrease

Keywords

Diagnostic Errors; Heuristics; Healthcare Near Miss; Bias

Mailing Address: Maurício Rodrigues Jordão •
Hospital 9 de Julho. Rua Peixoto Gomide, 545. Postal code: 01409-902. São Paulo, SP – Brazil
E-mail: mrjordao@gmail.com

DOI: https://doi.org/10.36660/abcimg.20250040i

in vigilance or attention to additional abnormalities after the first finding has been identified. Naturally, the likelihood of detecting a second or third abnormality diminishes once an initial anomaly has been recognized.

Several other biases may also be present, all of which have a direct impact on everyday medical practice. When these are understood as cognitive traps, a critical question arises: how can they be avoided? Metacognition[3] — defined as "thinking about one's own thinking" — is a multifaceted process that involves recognizing the limitations of memory, understanding the context and perspectives that influence decision-making, and cultivating self-awareness and critical reflection. These strategies aim to promote conscious questioning of the main sources of cognitive bias. However, evidence regarding their effectiveness in reducing diagnostic errors remains inconclusive.

Although artificial intelligence-based methods[7] hold promise in supporting diagnostic decision-making in imaging, with the potential to mitigate cognitive biases, studies have shown that these systems can internalize certain preexisting biases and introduce new ones inherent to the models themselves, ultimately compromising clinical outcomes.

For the foreseeable future, it will remain the human perspective — grounded in knowledge and experience — that serves as the primary driver of clinical decisions. When this central role is combined with a deeper understanding of our own cognitive processes and a humble acknowledgment that the capacity for error is as intrinsic as the ability to perform with expertise, a new pathway emerges. This path leads to a culture that embraces error recognition, fosters learning from mistakes, and, consequently, enhances strategies for bias mitigation.

References

1. Kahneman D. Rápido e Devagar - Duas Formas de Pensar. Rio de Janeiro: Objetiva; 2011.
2. Itri JN, Patel SH. Heuristics and Cognitive Error in Medical Imaging. AJR Am J Roentgenol. 2018;210(5):1097-105. doi: 10.2214/AJR.17.18907.
3. Busby LP, Courtier JL, Glastonbury CM. Bias in Radiology: The How and Why of Misses and Misinterpretations. Radiographics. 2018;38(1):236-47. doi: 10.1148/rg.2018170107.
4. Waite S, Scott J, Gale B, Fuchs T, Kolla S, Reede D. Interpretive Error in Radiology. AJR Am J Roentgenol. 2017;208(4):739-49. doi: 10.2214/AJR.16.16963.
5. Croskerry P. Cognitive Forcing Strategies in Clinical Decisionmaking. Ann Emerg Med. 2003;41(1):110-20. doi: 10.1067/mem.2003.22.
6. Zhang L, Wen X, Li JW, Jiang X, Yang XF, Li M. Diagnostic Error and Bias in the Department of Radiology: A Pictorial Essay. Insights Imaging. 2023;14(1):163. doi: 10.1186/s13244-023-01521-7.
7. Koçak B, Ponsiglione A, Stanzione A, Bluethgen C, Santinha J, Ugga L, et al. Bias in Artificial Intelligence for Medical Imaging: Fundamentals, Detection, Avoidance, Mitigation, Challenges, Ethics, and Prospects. Diagn Interv Radiol. 2025;31(2):75-88. doi: 10.4274/dir.2024.242854.

New Tools for Optimizing HF Management: The Role of POCUS in the Office

Luiz Claudio Danzmann,[1,2] *Elisa Kalil,*[2] *Soraya Abunader Kalil*[3,4]

Complexo Hospitalar Santa Casa de Porto Alegre,[1] *Porto Alegre, RS – Brazil*
Universidade Luterana do Brasil,[2] *Canoas, RS – Brazil*
Hospital de Clínicas de Porto Alegre,[3] *Porto Alegre, RS – Brazil*
Grupo Hospitalar Conceição,[4] *Porto Alegre, RS – Brazil*

A Reflection on Clinical and Subclinical Circulatory Congestion

The management of heart failure (HF) has improved over the past 20 years, mainly due to advances in diagnostic methods and circulatory decongestion strategies. Several management strategies have demonstrated efficacy in reducing symptoms, lowering rates of HF decompensation events, decreasing mortality indices, and improving surrogate markers of clinical events, such as left ventricular ejection fraction (LVEF).[1] In HF management, the need for detecting and monitoring circulatory congestion is justified by its strong association with neurohormonal activation and systemic inflammation, which contribute to the progressive worsening of HF and, consequently, a higher incidence of clinical events.[2]

But what is the evidence supporting decongestion strategies with diuretics in reducing hard outcomes? In the outpatient setting, the STRONG-HF clinical trial[3] is a good example. Comparing intensive optimization strategy versus usual HF treatment after hospital discharge, the study demonstrated that the group with more frequent visits and more intensive management achieved an absolute risk reduction of 8.1% (15.2% vs. 23.3%, P=0.0021) in the combined outcome of all-cause mortality and/or HF hospitalization within 180 days of follow-up.[3] The statistically significant reduction in clinical signs of congestion, along with a 27% decrease in natriuretic peptide (NP) levels after three months, provided proof of concept for the relationship between decongestion and clinical benefit. This evidence reinforces the need to detect subclinical congestion, especially during the vulnerable phase of HF, which occurs between one and three months after an HF hospitalization, a period in which most potentially preventable events take place.[4]

The State of the Art in Congestion Detection and Monitoring in 2025

The identification of orthopnea, jugular vein distension, and third heart sound offers high specificity for diagnosing congestion, whereas ankle edema and crackling rales demonstrate lower diagnostic accuracy.[5] Among the complementary methods already tested to increase accuracy in detecting fluid overload, serum NP levels and various ultrasound techniques are already recommended by current guidelines and have established applicability in emergency and inpatient settings.[1,6] However, the incorporation of these complementary diagnostic tests in the outpatient setting has been slower in Brazil compared to the rest of the world, especially regarding the point-of-care ultrasound (POCUS) technique.

Is POCUS in the office useful? What is the evidence?

Similar to its proven utility in emergency rooms, the goal of POCUS in the office setting is to identify and monitor pulmonary and systemic venous congestion, with the option to include imaging of cardiac structure and function.[7,8] From a practical standpoint, a quick assessment of the lungs and inferior vena cava – including the identification of vertical echogenic pulmonary lines originating from the pleura (B-lines) with three or more lines in more than one bilateral lung field – the absence of echoes in the pleural space, indicating effusion, and changes in the inferior vena cava diameter (with a diameter greater than 21mm and inspiratory collapse of less than 50%) provides strong diagnostic accuracy for detecting subclinical congestion.[8,9]

The association of imaging with clinical events in outpatients has been extensively investigated. In the outpatient setting, a 2013 study allocated a cohort of 97 outpatients with HF who underwent pulmonary ultrasound (PU) using a 28-lung-field model, echocardiography, and NP measurement. In assessing diagnostic accuracy for HF decompensation, PU outperformed other methods, with a sensitivity of 85% and specificity of 83% for a ≥15 B-lines cutoff, demonstrating its ability to reliably and early detect clinical congestion.[10] In another study, Platz et al.[11] used a more contemporary PU model, recording four bilateral lung fields in a population of 195 HF patients with NYHA functional class II-IV. During outpatient consultation, patients in the third tertile of congestion line distribution (≥3 B-lines) had a fourfold increased risk of the primary outcome (adjusted HR: 4.08, 95% CI: 1.95-8.54; $p < 0.001$) and fewer days alive and out of the hospital (125 days vs. 165 days; adjusted $p < 0.001$).[11] Additionally, in an outpatient setting of HF patients with preserved ejection fraction, in whom clinical congestion signs are often not apparent, POCUS also demonstrated a significant correlation between B-line count and NT-proBNP levels ($p < 0.001$). Notably, among individuals in the upper tertile of B-lines, 76% had no crackles

Keywords

Heart Failure; Ultrasonography; Ambulatory Care

Mailing Address: Luiz Claudio Danzmann •
Complexo Hospitalar Santa Casa de Porto Alegre. Rua Professor Annes Dias, 295. Postal code: 90020-090. Porto Alegre, RS – Brazil
E-mail: luizdanzmann@gmail.com

DOI: https://doi.org/10.36660/abcimg.20250039i

on auscultation, and 50% did not show elevated NT-proBNP levels, highlighting ultrasound's ability to detect subclinical congestion early.[12]

Therefore, the use of POCUS in the office setting is associated with practicality and scientific evidence of better diagnostic and prognostic accuracy compared to standard management, especially when considering the detection of subclinical congestion.

Limitations of POCUS in the office

In PU and inferior vena cava assessment, several limitations must be considered in clinical practice. In pulmonary fibrosis, the usual reverberation pattern is altered due to the destruction of alveolar structures and the formation of consolidation areas and interstitial thickening, which reduces the visualization of A-lines and hinders the proper interpretation of B-lines, potentially leading to false positives for pulmonary congestion. In atelectasis, pulmonary collapse also alters echogenicity, potentially resembling both infectious consolidations and congestion signs, making it difficult to differentiate between infectious and hemodynamic causes. In the case of pulmonary infections, such as pneumonia, the formation of consolidation areas and mixed artifacts distorts the expected ultrasound pattern, masking or mimicking edema conditions. In obese individuals, the increased thickness of the thoracic wall compromises ultrasound beam penetration, reducing image quality and making it difficult to identify A and B lines as well as to accurately assess the inferior vena cava. In these situations, the scarcity of lines may be misinterpreted as clinical improvement, when in reality it is merely a technical limitation. Additionally, the cost of technology in Brazil remains a significant barrier to the widespread adoption of these diagnostic tools in the outpatient setting.[13]

POCUS in the office: seeing fluids at the bedside

POCUS has been called the stethoscope of the 21st century—but is it? The term 'integration' with traditional examination seems more accurate, as imaging offers greater reproducibility, the possibility of storage for evolutionary follow-up, and a growing body of evidence correlating its findings with adverse clinical outcomes. POCUS does not replace the traditional approach but complements it. In 2025, POCUS expands our senses. Beyond touching and listening to the excess of organic fluids at the bedside, we can now see them (Figure 1).

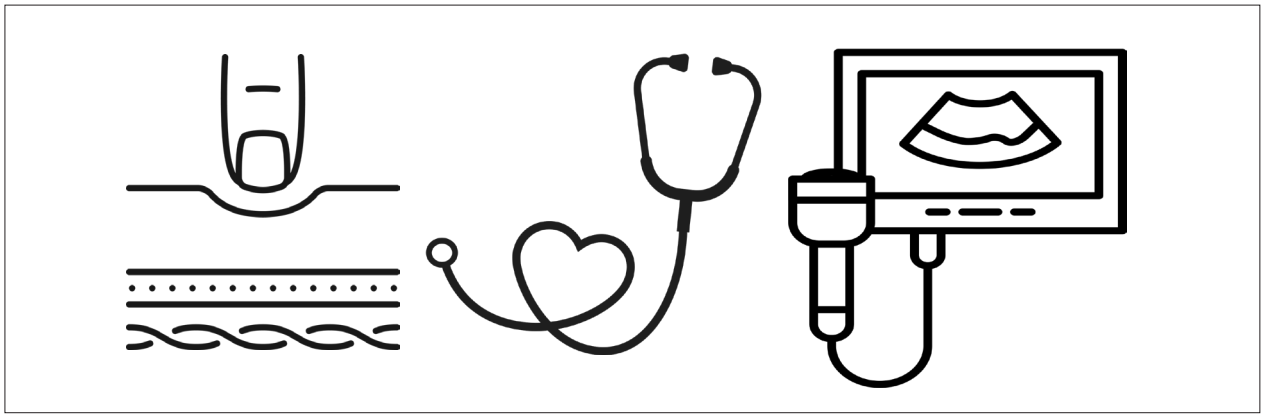

Figure 1 – *Touch, hear and see congestion: POCUS in the office.*

References

1. Marcondes-Braga FG, Moura LAZ, Issa VS, Vieira JL, Rohde LE, Simões MV, et al. Emerging Topics Update of the Brazilian Heart Failure Guideline - 2021. Arq Bras Cardiol. 2021;116(6):1174-212. doi: 10.36660/abc.20210367.
2. Kumric M, Kurir TT, Bozic J, Slujo AB, Glavas D, Miric D, et al. Pathophysiology of Congestion in Heart Failure: A Contemporary Review. Card Fail Rev. 2024;10:e13. doi: 10.15420/cfr.2024.07
3. Mebazaa A, Davison B, Chioncel O, Cohen-Solal A, Diaz R, Filippatos G, et al. Safety, Tolerability and Efficacy of Up-Titration of Guideline-Directed Medical Therapies for Acute Heart Failure (STRONG-HF): A Multinational, Open-Label, Randomised, Trial. Lancet. 2022;400(10367):1938-52. doi: 10.1016/S0140-6736(22)02076-1.
4. Greene SJ, Mentz RJ, Felker GM. Outpatient Worsening Heart Failure as a Target for Therapy: A Review. JAMA Cardiol. 2018;3(3):252-9. doi: 10.1001/jamacardio.2017.5250.
5. Gheorghiade M, Filippatos G, De Luca L, Burnett J. Congestion in Acute Heart Failure Syndromes: An Essential Target of Evaluation and Treatment. Am J Med. 2006;119(12 Suppl 1):S3-S10. doi: 10.1016/j.amjmed.2006.09.011.
6. Danzmann LC. Fluxograma de utilização das ferramentas diagnósticas na insuficiência cardíaca aguda. In: Figueiredo Neto JA, Marcondes-Braga FG, Mesquita ET, Moura LAZ, eds. Insuficiência Cardíaca DEIC-SBC. Barueri: Manole; 2021. p. 459–463.
7. Platz E, Merz AA, Jhund PS, Vazir A, Campbell R, McMurray JJ. Dynamic Changes and Prognostic Value of Pulmonary Congestion by Lung Ultrasound in Acute and Chronic Heart Failure: A Systematic Review. Eur J Heart Fail. 2017;19(9):1154-63. doi: 10.1002/ejhf.839
8. Pellicori P, Shah P, Cuthbert J, Urbinati A, Zhang J, Kallvikbacka-Bennett A, et al. Prevalence, Pattern and Clinical Relevance of Ultrasound Indices of Congestion in Outpatients with Heart Failure. Eur J Heart Fail. 2019;21(7):904-16. doi: 10.1002/ejhf.1383.

9. Kunst L, Danzmann LC, Cuchinski KK, Zimmer JRC. Point-of-Care Ultrasound in Acute Heart Failure: Basic Concepts for Clinical Practice. ABC Heart Fail Cardiomyop. 2023;3(2):e20230073. doi: 10.36660/abchf.20230073

10. Miglioranza MH, Gargani L, Sant'Anna RT, Rover MM, Martins VM, Mantovani A, et al. Lung Ultrasound for the Evaluation of Pulmonary Congestion in Outpatients. JACC Cardiovascular Imaging. 2013;6(11):1141-51. doi: 10.1016/j.jcmg.2013.08.004.

11. Platz E, Jhund PS, Campbell RT, et al. Lung ultrasound in acute and chronic heart failure: systematic review and meta-analysis. JACC Heart Fail. 2016;4(8):659-666.

12. Platz E, McDowell K, Gupta DK, Claggett B, Brennan A, Charles LJ, et al. Pulmonary Congestion on Lung Ultrasound in Ambulatory Patients with Heart Failure with Preserved Ejection Fraction. J Card Fail. 2025:S1071-9164(25)00099-5. doi: 10.1016/j.cardfail.2025.02.013.

13. Muniz RT, Mesquita ET, Souza CV Jr, Martins WA. Pulmonary Ultrasound in Patients with Heart Failure - Systematic Review. Arq Bras Cardiol. 2018;110(6):577-84. doi: 10.5935/abc.20180097.

Do Patients with Homozygosity and Compound Heterozygosity for Variants in the Transthyretin Amyloidosis TTR Gene Have More Severe and Earlier Clinical Conditions?

Tonnison de Oliveira Silva,[1,2] *Samuel Ulisses Chaves Nogueira do Nascimento*[3]
Escola Bahiana de Medicina e Saúde Pública,[1] *Salvador, BA – Brazil*
Cardio Pulmonar Hospital,[2] *Salvador, BA – Brazil*
Universidade Federal da Bahia,[3] *Salvador, BA – Brazil*

The prevalence of homozygotes for the Val142Ile genetic variant in the transthyretin (TTR) gene is extremely low in the general population (0.72%). This prevalence is slightly higher in endomyocardial biopsy studies (6% to 10%) and in cohorts involving reference centers for TTR cardiac amyloidosis (4% to 14%).[1,2]

Homozygotes represent a distinct subpopulation within the spectrum of cardiac amyloidosis, with clinical characteristics that appear to differ substantially from those of heterozygotes. This genetic variation has been associated with an onset of clinical manifestations in younger patients compared with heterozygotes and also with a higher risk of serious cardiovascular events, such as heart failure and ventricular arrhythmias.[3] Besides the earlier onset, observational studies indicate that the disease has a more aggressive phenotypic behavior in homozygous patients, characterized by greater ventricular thickening, worse diastolic function, and a higher load of amyloid fibrils in the heart.[3] Thus, homozygotes usually have a higher risk of developing early and more severe heart failure than heterozygotes.[1-3]

Homozygosity, defined as the inheritance of two identical copies of a mutated allele in the same gene locus, and compound heterozygosity, characterized by the presence of two distinct pathogenic variants in different alleles, are genetic conditions that may exacerbate the severity and anticipate the disease onset due to the absence of a compensatory functional allele.[4] However, incomplete penetrance and variable expressivity significantly modulate the clinical phenotype of this pathology.[4]

Incomplete penetrance means that not all carriers of pathogenic variants in the TTR gene will manifest the disease. Variable expressivity reflects the diversity of clinical manifestations between carriers of the same variant. For instance, Val50Met is associated with early-onset polyneuropathy in endemic regions, such as Portugal and Japan, but may have a predominantly ocular or cardiac phenotype in other regions, such as Sweden.[5] A study of 13 homozygotes for Val142Ile revealed the onset of cardiac symptoms about a decade earlier (63 years) compared with heterozygotes (72 years).[6] However, these findings are not universal. In the Val50Met variant, Swedish homozygotes showed a predominantly ocular phenotype, with no significant difference in age of onset compared with heterozygotes, suggesting that severity depends on the specific variant and genetic background.[5]

Compound heterozygosity also seems to predispose to earlier and more aggressive cases. Cases with combinations, such as Val142Ile/Ile88Leu or Val142Ile/Thr80Ala, showed cardiac symptoms in the fifth or sixth decade of life, significantly earlier than homozygotes or heterozygotes for Val142Ile alone.[6]

Micaglio et al. observed that compound heterozygosity causes important cardiac impairment in patients, similar to that observed in homozygotes, suggesting that the combined effect of the genetic variants exacerbates the deposition of amyloid fibrils and leads to a faster progression of cardiomyopathy.[7] Despite these associations between compound homozygosity/heterozygosity and greater disease severity and precocity, factors, such as gender, geographical location, ancestry, and genetic modifiers, as well as the variable penetrance and expressivity of the TTR gene, influence phenotypic expression and sometimes hinder clinical predictions.

In short, homozygosity and compound heterozygosity are often associated with more severe and earlier conditions, but incomplete penetrance and variable expressivity, interacting with epigenetic factors, limit generalizations. Moreover, the treatment with the best clinical applicability for this group with more complex diseases may be the TTR stabilizers associated with RNA silencers.

Keywords

Amyloidosis; Prealbumin; Homozygote

Correspondência: Tonnison de Oliveira Silva •
Escola Bahiana de Medicina e Saúde Pública. Rua Dom João VI. Postal code: 40285-001. Brotas, Salvador, BA – Brazil
E-mail: tonnisonsilva@hotmail.com

DOI: https://doi.org/10.36660/abcimg.20250027i

References

1. Dungu JN, Papadopoulou SA, Wykes K, Mahmood I, Marshall J, Valencia O, et al. Afro-Caribbean Heart Failure in the United Kingdom: Cause, Outcomes, and ATTR V122I Cardiac Amyloidosis. Circ Heart Fail. 2016;9(9):e003352. doi: 10.1161/CIRCHEARTFAILURE.116.003352.
2. Brown EE, Lee YZJ, Halushka MK, Steenbergen C, Johnson NM, Almansa J, et al. Genetic Testing Improves Identification of Transthyretin Amyloid (ATTR) Subtype in Cardiac Amyloidosis. Amyloid. 2017;24(2):92-5. doi: 10.1080/13506129.2017.1324418.
3. Buxbaum JN, Ruberg FL. Transthyretin V122I (pV142I)* Cardiac Amyloidosis: An Age-Dependent Autosomal Dominant Cardiomyopathy Too Common to be Overlooked as a Cause of Significant Heart Disease in Elderly African Americans. Genet Med. 2017;19(7):733-42. doi: 10.1038/gim.2016.200.
4. Nussbaum RL, McInnes RR, Willard HF. Thompson & Thompson Genetics and Genomics in Medicine. 10th ed. Philadelphia: Elsevier; 2023.
5. Holmgren G, Hellman U, Lundgren HE, Sandgren O, Suhr OB. Impact of Homozygosity for an Amyloidogenic Transthyretin Mutation on Phenotype and Long Term Outcome. J Med Genet. 2005;42(12):953-6. doi: 10.1136/jmg.2005.033720.
6. Reddi HV, Jenkins S, Theis J, Thomas BC, Connors LH, Van Rhee F, et al. Homozygosity for the V122I Mutation in Transthyretin is Associated with Earlier Onset of Cardiac Amyloidosis in the African American Population in the Seventh Decade of Life. J Mol Diagn. 2014;16(1):68-74. doi: 10.1016/j.jmoldx.2013.08.001.
7. Micaglio E, Santangelo G, Moscardelli S, Rusconi D, Musca F, Verde A, et al. Case Report: A Rare Homozygous Patient Affected by TTR Systemic Amyloidosis with a Prominent Heart Involvement. Front Cardiovasc Med. 2023;10:1164916. doi: 10.3389/fcvm.2023.1164916.

Original Article

Classifying the Size of an Atrial Septal Defect According to Echocardiographic Parameters and its Association with the Clinical Presentation in Pediatrics

Lívia de Castro Ribeiro,[1] *Rose Mary Ferreira Lisboa da Silva,*[1] *Henrique de Assis Fonseca Tonelli,*[1] *Adriana Furletti Machado Guimarães,*[1] *Fátima Derlene da Rocha Araújo,*[1] *Zilda Maria Alves Meira,*[1] *Sandra Regina Tolentino Castilho,*[1] *Alan Alvarez Conde,*[1] *Lícia Campos Valadares*[1]

Universidade Federal de Minas Gerais,[1] *Belo Horizonte, MG – Brazil*

Abstract

Background: **Few studies are using linear echocardiographic measurements for classifying the size of Atrial Septal Defect (ASD).**

Objectives: **Investigate the relationship between ASD hemodynamic repercussions and ASD diameter to the mitral annulus diameter (MI/ASD) ratio and ASD diameter to the interatrial septum diameter (ASD/septum) ratio, and describe cutoff points to classify the size of the defect.**

Methods: **An observational, prospective, cross-sectional study, including subjects aged 1 month and 18 years diagnosed with isolated ASD. Hemodynamic repercussion was quantified by clinical evaluation, tricuspid annulus (TA) Z-score, subjective estimation of the enlargement of the right chambers, and the relationship between systemic and pulmonary flows (QP/QS) on echocardiography. Its association with ASD/septum and MI/ASD measurements was also studied. A value of $p < 0.05$ was considered statistically significant.**

Results: **Thirty-five subjects, mean age 6.3 years, 69% female, mean ASD 13.5 mm. There was a correlation between MI/ASD and the clinical classification of ASD (Pearson: -0.61; $p < 0.001$), ASD/septum (Pearson: -0.80; $p < 0.001$), and QP/QS (-0.76; $p < 0.001$). There was a correlation between ASD/septum and the clinical classification of ASD (Pearson: 0.56; $p < 0.001$), QP/QS (0.63; $p = 0.001$), subjective assessment of the right chambers (0.62; $p < 0.001$), and a weak correlation with the TA Z-score (0.35; $p = 0.04$). According to the operating characteristic curve for the stable variable classification of ASD according to the subjective right chamber's size, an area of 0.85 was obtained for ASD/septum ($p = 0.001$). The cutoff point of 0.27 for large ASD showed sensitivity of 85%, specificity of 86.7%, positive predictive value (PPV) of 86%, negative predictive value (NPV) of 85.2%, and positive likelihood ratio of 6.39.**

Conclusions: **ASD/septum was associated with the hemodynamic repercussion of ASD and was useful in detecting large ASD.**

Keywords: **Atrial Heart Septal Defects; Echocardiography; Tricuspid Valve; Atrial Septum.**

Introduction

Atrial Septal Defect (ASD) is a congenital structural alteration of the heart in which blood is mixed between the atria through a defect in the Atrial Septum or adjacent structures. Isolated ASD is the third most common cardiac malformation, corresponding to approximately 15% of all congenital heart diseases.[1] The prevalence of ASD is twice as high among females compared to males.[2] Transthoracic echocardiographic examination is the most widely used method for diagnosing and evaluating ASD in the pediatric population and is sufficient for adequately defining the lesion and its hemodynamic repercussions in most cases. The linear measurement of the defect, the Atrial Septum Size defect ratio (ASD/septum), the repercussion in the right chambers (signs of volumetric overload), and the measurement of the pulmonary flow/systemic flow (QP/QS) ratio are commonly used to assess the defect size. The ASD/septum measurement has been used informally in clinical practice, with no systematization based on studies and without reliable cutoff points for size classification. The measurement of QP/QS during echocardiography has a major limitation, represented by low reproducibility[3] and difficulty performing.[4] The objectives of the study were to investigate, through clinical and echocardiographic assessments, the relationship between ASD hemodynamic repercussion and the measurements of the Mitral Annulus diameter to the ASD diameter (MI/ASD) ratio and the (ASD/septum) ratio, and describe the cutoff points of these

Mailing Address: Livia de Castro Ribeiro •
Hospital das Clínicas da Universidade Federal de Minas Gerais. Rua Alfredo Balena, 110. Postal code: 30130-100. Belo Horizonte, MG – Brazil
E-mail: liviadecastromed85@gmail.com
Manuscript received September 17, 2024; revised January 30, 2025; accepted February 12, 2025
Editor responsible for the review: Karen Saori Shiraishi Sawamura

DOI: https://doi.org/10.36660/abcimg.20240089i

Central Illustration: Classifying the Size of an Atrial Septal Defect According to Echocardiographic Parameters and tts Association with the Clinical Presentation in Pediatrics

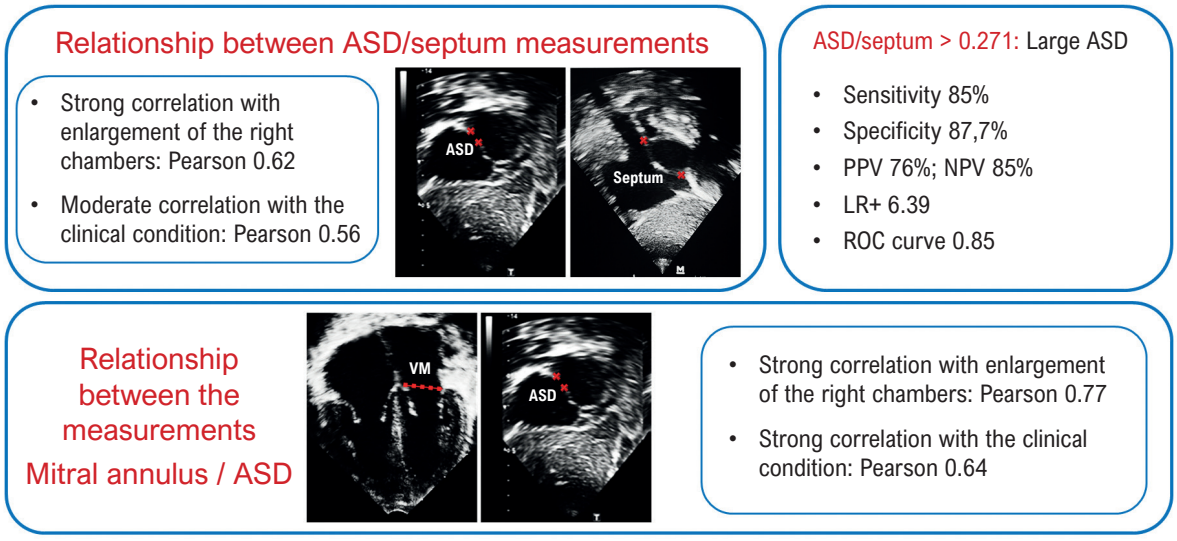

Arq Bras Cardiol: Imagem cardiovasc. 2025;38(2):e20240089

PPV: positive predictive value; ASD: Atrial Septal Defect; NPV: negative predictive value; LR: likelihood ratio; ROC: receiver operating characteristic.

ratios that would allow the defect to be classified based on its size.

Methods

This was an observational, prospective, cross-sectional study. The population consisted of 35 subjects with isolated ASD with a single orifice on echocardiographic examination, of both genders, aged between 1 month and 18 years. The study, the Informed Consent Form (ICF), and the Understanding Form (UF) were approved by the Ethics and Research Committee of the university hospital where the research was carried out. The subjects signed the ICF or UF and then underwent echocardiographic examination and clinical evaluation. Those with significant congenital heart disease (excluding patent foramen ovale, mild mitral, tricuspid, and aortic regurgitation, and bicuspid aortic valve without stenosis), cardiomyopathy (primary or secondary), chronic anemia, and pulmonary hypertension not attributed to the presence of ASD were excluded. The convenience sampling method was used.

The echocardiographic examination was performed with a TOSHIBA device, model APLIO 400, with pediatric and adult transducers with frequencies of 2.5 MHz and 5.0 MHz, respectively, by a pediatric echocardiographer, and the clinical evaluation was performed by a pediatric cardiologist, both members of the team, and blinded to the clinical assessment and vice versa. The clinical assessment was performed on the same day as the echocardiographic evaluation, immediately after it. The degree of repercussion in the right chambers was assessed subjectively, comparing the areas of the Right Atrium (RA) to those of the Left Atrium (LA) and the areas of the Right Ventricle (RV) to those of the Left Ventricle (LV), in a two-dimensional mode, apical four-chamber view,[5] since linear and area measurements of the RA and RV have not been consistently standardized for the pediatric population.[6-8] Comparatively, if the right chambers had a smaller, equal, or larger area than the left chambers, the increase was considered absent or mild, moderate, or significant, respectively. Measurements of the interatrial septum and the ASD diameter were performed in two-dimensional mode, in the subcostal section of the Atrial Septum, with the aid of Color Doppler to identify the edges of the defect.[6] To measure the Atrial Septum, the vertical distance between the end of each vena cava was standardized. The ASD was measured in the region with the greatest distance between the edges throughout the cardiac cycle. The ASD/septum ratio was calculated, and this measurement was compared with the hemodynamic repercussion. The magnitude of the shunt through the ASD was estimated by calculating the systemic flow/pulmonary flow (QP/QS) ratio.[6] The diameters of the Mitral and Tricuspid Annuli were measured in two-dimensional mode, in protodiastole. The parasternal longitudinal long axis view of the LV and RV inflow tract were used to measure the anteroposterior diameters (mitral and tricuspid, respectively) and the apical four-chamber view to measure the laterolateral diameters[7] (Figure 1). The diameters were indexed in the form of a Z-score using the Boston reference.[9-11] The Tricuspid Annulus (TA) Z-score values were also used to classify the degree of ASD repercussion in the right chambers. The

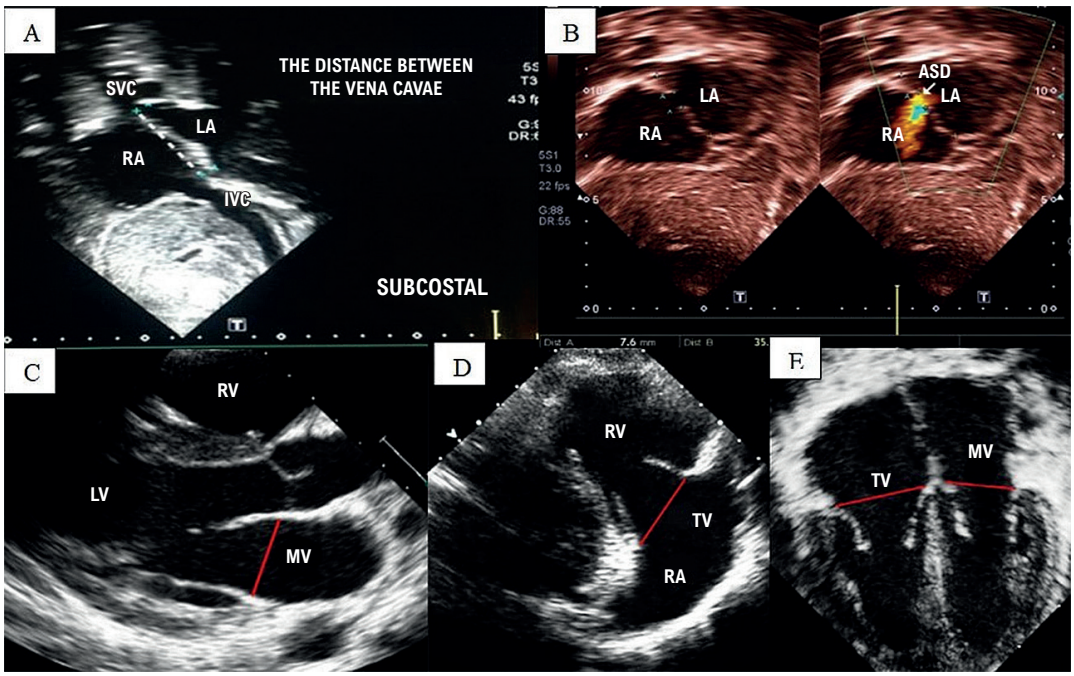

Figure 1 – *Measurement of the interatrial septum, ASD, and mitral and tricuspid annuli on echocardiographic examination. RA: right atrium; LA: left atrium; RV: right ventricle; LV: left ventricle; ASD: Atrial Septal Defect; IVN: inferior vena cava; SVC: superior vena cava; TV: tricuspid valve; MV: mitral valve.*

MI/ASD ratio was calculated, and this measurement was compared with the hemodynamic repercussion. ASD size classification by echocardiographic criteria was performed by subjective analysis and Z-score: Small ASD: the right chamber area is smaller than left chamber area and the TA Z-score ranges from +2 to +2.5; medium ASD: the right chamber area is equal to the left chamber area and the TA Z-score ranges from +2.5 to +3; large ASD: the right chamber area is larger than the left chamber area and the TA Z-score is > +3.

The clinical evaluation consisted of an examination of the cardiovascular system guided by criteria that allowed inferences to be made about the size of the ASD.[12] ASD size classification by clinical evaluation was performed according to Table 1, and the presence of at least three of the four findings for each column was considered.

Statistical analysis: Statistical analysis was performed using Statistical Package for Social Science (SPSS) software version 16.0. The results were expressed as numbers and proportions for categorical variables and as means ± standard deviation for continuous variables. The Shapiro-Wilk test was used to check the normal distribution of variables. Proportions were compared using the Chi-square test or Fisher's exact test when appropriate. For continuous data, the unpaired Student's T-test was used for two variables, or the One-Way ANOVA test was used to compare three or more variables. The Pearson coefficient was used to check the correlation between continuous. The correlation based on the coefficient (positive or inverse) was considered very weak (0.00–0.20), weak (0.21–0.40), moderate (0.41–0.60), strong (0.61–0.80), and very strong (0.81–1.00). The operating characteristic curve was applied to evaluate sensitivity, specificity, Positive Predictive Value (PPV), Negative Predictive Value (NPV), and the positive likelihood ratio of the ASD/septum ratio, considering the size of the septal defect. A P-value of < 0.05 was considered statistically significant.

Results

Among the 35 subjects, 24 (69%) were female. The mean age was 6.3 ± 3.9 years, ranging from 0.4 to 17.2 years. The average weight, height, and body surface area were 21.2 kg, 112 cm, and 0.8 m², respectively. Comorbidities were present in 14% of the subjects (n = 5), including asthma (3), genetic syndrome under investigation (1), and neurological and psychomotor development delay in propaedeutics (1).

Regarding the findings on physical examination, 14 subjects (40%) had fixed splitting of the second heart sound, and 5 (14%) had a diastolic murmur in the tricuspid area. A systolic murmur in the pulmonary area was not detected in six subjects, was grade II in 16 subjects (46%), and grade III ≥ in 13 subjects (37%). RV impulse was not detected in 19 (54%) subjects.

On echocardiographic examination, all subjects had ostium secundum-type ASD. The data collected are summarized in Table 2.

Table 1 – Classification of ASD size according to clinical criteria

Clinical Parameter	Size Classification		
	Small	Medium	Large
Impulse in BEEI and subxiphoid region	Absent	Present	Present
Splitting of the second heart sound	Physiological	Fixed	Fixed
Ejection systolic murmur in the pulmonary area	Absent or grade I/VI	Grade II/VI	Grade > III/VI
Diastolic murmur in the tricuspid area	Absent	Absent	Present

BEEI: lower left sternal border.

Association and correlation between the variables

Table 3 shows the comparisons between clinical signs and echocardiographic measurements. There was no association between gender and any of the variables studied, whether in the clinical or echocardiographic context.

Twelve ASDs were clinically classified as small, 18 as medium, and 5 as large. The correlation between ASD size by clinical classification and echocardiographic findings is summarized in Table 4.

The MI/ASD diameter ratios showed a strong inverse correlation with the ASD/septum measurement. The Pearson coefficient with the anteroposterior and laterolateral measurements was -0.80 ($p < 0.001$). There was also a strong inverse correlation with the QP/QS measurement, with a Pearson coefficient of -0.71 ($p < 0.001$) for the anteroposterior measurement and -0.76 ($p < 0.001$) for the laterolateral measurement.

The ASD/septum diameter ratio showed a strong correlation with the QP/QS ratio with a Pearson coefficient of 0.63 ($p = 0.001$).

Regarding the size of the RV in the subjective assessment, the RV was larger than the LV in 17 subjects, was smaller in 10 subjects, and eight subjects had chambers of equivalent sizes. When assessing the RA, it was larger than the LA in 20 subjects, smaller in eight subjects, and seven subjects had chambers of equivalent sizes. The comparison and correlation between the degree of enlargement of the right chambers and the echocardiographic variables are shown in Tables 5 and 6.

Considering the TA Z-score to classify the size of the ASDs, 25 were small, 5 were medium, and 5 were large. This classification was not associated with the clinical classification of ASD nor with the echocardiographic classification made according to the subjective assessment of the right chambers.

Operating characteristic curve

Applying the operating characteristic curve, considering as the stable variable the classification of the ASD based on the subjective size of the right chambers, an area under the curve of 0.85 was obtained for the ASD/septum ratio. The curve and data with p-value and 95% confidence intervals are shown in Figure 2. The best cutoff point was 0.27, with a sensitivity of 85% and specificity of 86.7% for diagnosing large ASD. The PPV was 76%, and the NPV was 85.2%. The positive likelihood ratio was 6.39.

Regarding the variable classification of ASD according to the subjective size of the right chambers, an area under the curve of 0.14 was obtained for the MI/ASD ratio.

Discussion

The main findings of this study were the strong inverse correlation between the MI/ASD ratio and the clinical classification of the ASD, and the 6.39 probability of diagnosing a large ASD based on an ASD/septum ratio greater than 0.27, according to the subjective size of the right chambers as summarized in the Central Illustration.

The universal form used by cardiologists to classify ASD size is based on several subjective factors in a clinical and echocardiographic context. The presence of symptoms, changes found during the physical examination, and echocardiographic findings are evaluated. Considering there is great variability in body surface area values in the pediatric population, the ASD diameter alone is not an adequate parameter to quantify the size of the lesion. Other parameters are taken into consideration to assess the size of the lesion, such as the QP/QS ratio,[6] the ASD/interatrial septum diameter ratio, and assessment of the degree of enlargement of the right chambers.[4,5]

At the time of the study, there was only one study[13] presenting normal values for linear and area measurements of the RA and RV, as indicated by the echocardiogram measurement guideline[7] for the pediatric population. This study had the limitations of being a single-center study carried out only with a Caucasian population aged 0 to 3 years. Therefore, the study could not be incorporated into clinical practice as it did not cover all pediatric age groups. Since then, two new publications[14,15] of reference values in pediatrics have emerged. Rajagopal *et al.*, described measurements of the area of the RA, but this was a single-center and retrospective study, the results of which have not yet been incorporated into clinical practice.[14] Gokhroo *et al.*, mentioned reference values for measurements, as recommended by the guideline, but the study was limited to the age group of 5 to 15 years.[15] Therefore, the enlargement of the right chambers is estimated subjectively, visually

Table 2 – Measurements and ratio calculation of echocardiographic measurements

Variables	Medium	Minimum	Maximum	Standard deviation
ASD diameter (mm)	13.46	2.70	37.70	8.33
MI/ASD - LL	2.04	0.62	6.30	1.49
MI/ASD - AP	2.00	0.52	6.80	1.48
ASD/septum	0.30	0.06	0.65	0.15
QP/QS	2.56	1.10	4.48	0.99
TA diameter - LL (mm)	23.38	14.40	38.60	5.14
TA Z-score - LL	+1.40	-1.63	+5.28	1.74
TA diameter - AP (mm)	22.48	10.90	37.40	5.77
TA Z-score - AP	+1.11	-2.34	+3.76	1.28
MA diameter - LL (mm)	18.18	11.40	25.80	3.41
MA Z-score - LL	-0.39	-2.34	+2.09	1.15
MA diameter - AP (mm)	17.87	9.80	25.40	3.25
MA Z-score - AP	-0.07	-1.89	+1.93	0.91

ASD: atrial septal defect; mm: millimeters; MI/ASD: mitral annulus diameter/atrial septal defect diameter; LL: laterolateral; AP: anteroposterior; ASD/septum: atrial septal defect diameter/atrial septum diameter; QP/QS: pulmonary flow/systemic flow; TA: tricuspid annulus; AM: mitral annulus.

Table 3 – Comparison between clinical and echocardiographic parameters

Clinical Parameter	P-Value					
	MI/ASD – AP	MI/ASD – LL	ASD/septum	QP/QS	ASD SIZE according to ASCD*	TA Z-score
RV impulses	0.028	0.018	0.15	0.35	0.025	0.56
Splitting of the S2	< 0.001	< 0.001	< 0.001	0.006	< 0.001	0.12
Pulmonary systolic murmur	0.015	0.006	0.022	0.037	0.002	0.41
Tricuspid diastolic murmur	0.055	0.045	0.015	0.016	0.29	0.019

** Fisher's test. Other variables were analyzed using the unpaired Student's t-test. MI/ASD: mitral annulus diameter/atrial septal defect diameter; AP: anteroposterior; LL: laterolateral; ASD/septum: atrial septal defect diameter/atrial septal diameter; QP/QS: pulmonary flow/systemic flow; ASCD: subjective assessment of the right chambers; TA: tricuspid annulus; RV: right ventricle; S2: second heart sound.*

comparing the area of the right chambers with that of the left chambers in the apical four-chamber view in two-dimensional mode. The QP/QS ratio, despite being an objective measure, is very prone to errors and difficult to measure.[16]

Rao *et al.,* presented the method of classifying the size of the residual shunt after ASD percutaneous closure considering the parameters of flow diameter greater than 2 mm and RV measurements with a percentile > 95% but did not propose a classification of the magnitude of the lesion itself.[17]

There are no studies in the literature that evaluate the ASD/septum ratio to classify ASD size. Lin *et al.*, used measurements of the Interatrial Septum and ASD in two-dimensional and color mode with the use of artificial intelligence in a population with an average age of 3 years and demonstrated good accuracy in detecting defects and cases that could be subjected to percutaneous closure of the lesion by measuring the free edges of the septum. However, this study did not evaluate the degree of hemodynamic repercussion, the classification of the lesion size, or the need for treatment.[18] The measurements chosen in this study were the MI/ASD and ASD/septum ratios, as a way of indexing ASD measurement to a cardiac structure, and should be easy to measure. The ASD was measured using the largest linear diameter.

Table 4 – Correlation between ASD size by clinical classification and echocardiographic variables

Echocardiographic variables	Pearson coefficient	P-Value
ASD size: subjective assessment of the right chambers	0.52	0.001
ASD size: TA Z-score assessment	0.26	0.13
TA Z-score - Anteroposterior	0.34	0.045
TA Z-score - Laterolateral	0.34	0.048
ASD/septum	0.56	<0.001
QP/QS	0.62	0.002
MI/ASD - Anteroposterior	-0.58	<0.001
MI/ASD - Laterolateral	-0.61	<0.001

ASD: atrial septal defect; TA: tricuspid annulus; ASD/septum: atrial septal defect diameter/atrial septal diameter; QP/QS: pulmonary flow/systemic flow; MI/ASD: mitral annulus diameter/atrial septal defect diameter.

Considering that lesions may be asymmetrical, the diameter measurements taken may not necessarily reflect the largest diameter of the lesion. The most reliable measurement would be calculating the ASD area, which is done through 3D echocardiography and magnetic resonance imaging, but these exams are not as widely available in clinical practice.[19,20] Thus, to avoid greater bias, diameter measurements were performed with images of good technical quality and using the same subcostal view in all subjects. The subcostal view is very similar to the mid-esophageal bicaval view of the transesophageal echocardiographic examination, which is used to guide percutaneous closure of the ASD with a prosthesis.[6] Boon *et al.*, demonstrated that 2D echocardiographic examination is a reliable method for measuring the diameter of the ASD, especially in cases where the septum is firm, corresponding to 85% of the cases of ostium secundum ASD.[21]

The MI/ASD measurement showed a strong inverse correlation with the clinical classification of ASD and with the classification by subjective assessment of the right chambers. Despite this, it was not possible to define cut-off points for this variable to classify the size of the defect. Although it is intuitive to imagine that the smaller the ratio, the greater the deficit in LV filling and mitral annulus development, it can be speculated that such a relationship is not so linear with the size of the ASD to the point of enabling assertive size calculation.

The ASD/septum measurement showed a moderate correlation with the clinical classification of ASD and a strong correlation with the classification by subjective assessment of the right chambers. It was not possible to define cutoff points for classifying the magnitude of ASD considering its clinical classification. This finding may be explained by the small number of large ASDs classified by the clinical method. A cutoff point of 0.27 was found for the ASD/septum ratio to identify large ASDs compared with the subjective assessment of the size of the right chambers. The same was not possible for medium-sized ASDs, perhaps also due to the small number of subjects with medium ASD according to the classification by subjective assessment of the right chambers.

The QP/QS ratio is one of the parameters found in the guidelines for indicating ASD closure in the adult population.[22] It showed a strong correlation with the MI/ASD and ASD/septum measurements and with the clinical and echocardiographic classification of ASD by a subjective assessment of the right chambers. It may have great

Table 5 – Comparison between the degree of enlargement of the right chambers according to subjective assessment and echocardiographic variables

Variables	Degree of enlargement of the right chambers						p-value (ANOVA)
	Mild	Standard deviation	Moderate	Standard deviation	Major	Standard deviation	
ASD diameter (mm)	5.15	2.27	11.8	6.12	17.37	8.01	0.001
MI/ASD -AP	4.07	1.69	1.78	0.84	1.24	0.48	< 0.001
MI/ASD -LL	4.15	1.58	1.86	0.85	1.25	0.52	< 0.001
ASD/septum	0.13	0.06	0.29	0.14	0.36	0.13	< 0.001
QP/QS	1.19	0.10	2.45	0.93	3.05	0.84	0.007
TA Z-score -AP	-0.17	0.00	+1.00	1.28	+1.66	1.04	0.001
TA Z-score - LL	-0.04	1.30	+1.17	0.75	+2.06	1.81	0.01

ASD: atrial septal defect; mm: millimeters; RA: right atrium; RV: right ventricle; MI/ASD: mitral annulus diameter/atrial septal defect diameter; AP: anteroposterior; LL: laterolateral; ASD/septum: atrial septal defect diameter/atrium septal diameter; QP/QS: pulmonary flow/systemic flow; TA: tricuspid annulus.

Table 6 – Correlation between the degree of enlargement of the right chambers according to subjective assessment and echocardiographic variables

Variables	Pearson coefficient	P-Value
ASD diameter (mm)	0.61/0.66 RA/RV	< 0.001 RA/RV
MI/ASD -AP	-0.75	<0.001
MI/ASD -LL	-0.77	<0.001
ASD/septum	0.62	<0.001
QP/QS	0.61	0.002
TA Z-score -AP	0.58	<0.001
TA Z-score - LL	0.50	0.002

ASD: atrial septal defect; mm: millimeters; RA: right atrium; RV: right ventricle; MI/ASD: mitral annulus diameter/atrial septal defect diameter; AP: anteroposterior; LL: laterolateral; ASD/septum: atrial septal defect diameter/atrium septal diameter; QP/QS: pulmonary flow/systemic flow; TA: tricuspid annulus.

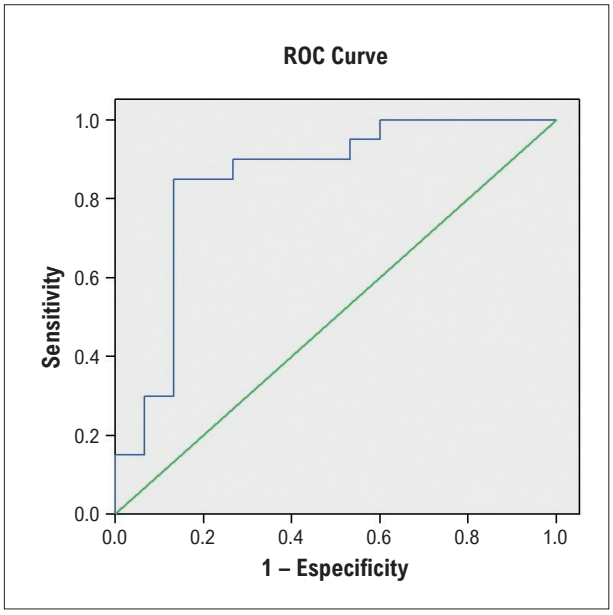

Figure 2 – *Operating characteristic curve for the ASD/septum ratio, considering as the stable variable the classification of the ASD based on the subjective size of the right chambers. ROC: receiver operating characteristic.*

variability[3,4] because of how the relationship is calculated, with four measurements being required: the radius and the velocity-time integral of the RV and LV outflow tract. An error in any of the four measurements can alter the final value of the relationship. Furthermore, the radius measurement is squared, which causes a radius measurement error to also be squared in the calculation.[16] Faherty *et al.*, correlated the QP/QS calculation values on echocardiography with those obtained by oximetry on catheterization in patients with hemodynamically significant ostium secundum ASD and found a weak correlation between the methods, with the echocardiographic method tending to overestimate the values obtained by oximetry.[23]

In clinical practice, it is common to repeat the measurement when the echocardiographer finds a value considered to be incompatible with the other findings. Therefore, the measurement is influenced by a subjective bias. In the study data collection protocol, the number of measurement repetitions for calculating the QP/QS ratio was not limited. Consequently, echocardiographers were free to choose the calculation value they considered to be the most reliable. This subjectivity bias may have contributed to the finding of a strong correlation between this measurement and the other variables studied.

The TA Z-score measurement showed a weak correlation with the clinical classification of ASD and a moderate correlation with the classification based on a subjective assessment of the right chambers. One explanation for such findings may be the lack of normalization of Z-score reference values for TA measurements in the literature. Despite the standardization of the measurement method of the most recent studies and their larger sample size compared to older studies,[24-26] there are still differences between the nomograms, which result in Z-scores that are very discordant with each other. The studies show differences between them, such as the body surface formula used, gender differentiation or lack of it, age range used, and intra-observer and interobserver variability.[27] Snyder *et al.*, demonstrated that there was no strong linear relationship between RV volume on cardiac magnetic resonance imaging and tricuspid valve Z-score on echocardiography in patients in the late postoperative period of Tetralogy of Fallot. Among patients with RV enlargement on MRI, the TA Z-score measurement on echocardiography showed a sensitivity of 45% to identify enlargement, with a Z-score $> +2$.[28] In the present study, the tricuspid valve diameter Z-score was observed within the normal range despite enlarged RV on a two-dimensional assessment compared to the LV in some subjects.

The classification of the magnitude of ASD by the TA Z-score value as described in the methodology was not associated with any of the parameters investigated in the physical examination and, consequently, with the clinical classification of ASD, nor it was associated with the classification of ASD according to a subjective assessment of the right chambers. In addition to the already-mentioned variability of Z-score normality values in the pediatric population, the choice of the Z-score range used for classification must be considered. In the study, different Z-score ranges were not compared, and the association of each of them with other methods of classifying ASD size was not evaluated.

Many of the results found in the study are in agreement with the literature data. Among them, the frequency of findings on physical examination and the proportion between genders.

The frequency was higher in females, in a proportion of 2.2:1, very close to that described in the literature of 2:1.[2] The percentages found of wide and fixed splitting of the second heart sound (S2), systolic murmur in the pulmonary

area, and diastolic murmur in the tricuspid area were 66%, 83%, and 15%, respectively, similar to the values of 66%, 90%, and 12% described in the literature, respectively.[29] Regarding RV impulses, the presence and intensity of such a finding depend greatly on the patient's biotype.

The ASD type most frequently found is ostium secundum, responsible for approximately 85% of the cases.[30] In the study, it was the only type found, a finding that can be explained by the small sample size.

Among the parameters investigated by physical examination, all were associated with the subjective classification of the right chambers, except for the diastolic murmur in the tricuspid area. This fact can be explained by the low sensitivity of this parameter for the diagnosis of ASD.[29]

Limitations

This study has some limitations because it is a single-center, cross-sectional study with a small sample size and a large age standard deviation. Furthermore, it was not possible to assess the intra-observer and interobserver variability regarding the clinical method and the echocardiographic examination, but the team was previously trained on the measurement protocol. No post hoc test was used to verify significant differences between the echocardiographic parameter measurements and the subjective assessment of the enlargement of the right chambers.

Conclusions

The MI/ASD and ASD/septum measurements were associated with ASD size classification concerning the clinical parameters and subjective assessment of the size of the right chambers during an echocardiogram. The measurement of the ASD/septum ratio above 0.27 proved to be useful in identifying large ASDs based on the subjective enlargement of the right chambers, which was not found in small and medium-sized ASDs. It was not possible to define cut-off points for the MI/ASD measurement to classify ASD size. The TA Z-score measurement was not a good parameter for classifying ASD size.

Author Contributions

Conception and design of the research: Tonelli HAF; acquisition of data: Ribeiro LC, Tonelli HAF, Araújo FDR, Furletti A, Meira ZMA, Castilho SRT, Valadares LC, Conde AA; analysis and interpretation of the data and writing of the manuscript: Ribeiro LC; statistical analysis: Silva RMFL; critical revision of the manuscript for intellectual content: Silva RMFL, Tonelli HAF.

Potential Conflict of Interest

No potential conflict of interest relevant to this article was reported.

Sources of Funding

There were no external funding sources for this study.

Study Association

This article is part of the thesis of master submitted by Lívia de Castro Ribeiro, from Universidade Federal de Minas Gerais.

Ethics Approval and Consent to Participate

This study was approved by the Ethics Committee of the UFMG under the protocol number 53353116.3.0000.5149. All the procedures in this study were in accordance with the 1975 Helsinki Declaration, updated in 2013. Informed consent was obtained from all participants included in the study.

References

1. Liu Y, Chen S, Zühlke L, Black GC, Choy MK, Li N, et al. Global Birth Prevalence of Congenital Heart Defects 1970-2017: Updated Systematic Review and Meta-Analysis of 260 Studies. Int J Epidemiol. 2019;48(2):455-63. doi: 10.1093/ije/dyz009.
2. Engelfriet P, Mulder BJ. Gender Differences in Adult Congenital Heart Disease. Neth Heart J. 2009;17(11):414-7. doi: 10.1007/BF03086294.
3. Quiñones MA, Otto CM, Stoddard M, Waggoner A, Zoghbi WA; Doppler Quantification Task Force of the Nomenclature and Standards Committee of the American Society of Echocardiography. Recommendations for Quantification of Doppler Echocardiography: A Report from the Doppler Quantification Task Force of the Nomenclature and Standards Committee of the American Society of Echocardiography. J Am Soc Echocardiogr. 2002;15(2):167-84. doi: 10.1067/mje.2002.120202.
4. Lai WW, Mertens LL, Cohen MS, Geva T, editors. Anomalies of the Atrium Septum. Echocardiography In Pediatric And Congenital Heart Disease: From Fetus to Adults. Hoboken: Wiley-Blackwell; 2009.
5. Anderson RH, Baker EI, Penny D, Redington AN, Rigby ML, Wernovsky G. Interatrial Communications. Paediatric Cardiology. Philadelphia: Churchill Livingstone; 2010. p. 523-46.
6. Silvestry FE, Cohen MS, Armsby LB, Burkule NJ, Fleishman CE, Hijazi ZM, et al. Guidelines for the Echocardiographic Assessment of Atrial Septal Defect and Patent Foramen Ovale: From the American Society of Echocardiography and Society for Cardiac Angiography and Interventions. J Am Soc Echocardiogr. 2015;28(8):910-58. doi: 10.1016/j.echo.2015.05.015.
7. Lopez L, Colan SD, Frommelt PC, Ensing GJ, Kendall K, Younoszai AK, et al. Recommendations for Quantification Methods During the Performance of a Pediatric Echocardiogram: A Report from the Pediatric Measurements Writing Group of the American Society of Echocardiography Pediatric and Congenital Heart Disease Council. J Am Soc Echocardiogr. 2010;23(5):465-95. doi: 10.1016/j.echo.2010.03.019.
8. Lang RM, Badano LP, Mor-Avi V, Afilalo J, Armstrong A, Ernande L, et al. Recommendations for Cardiac Chamber Quantification by Echocardiography in Adults: An Update from the American Society of Echocardiography and the European Association of Cardiovascular Imaging. J Am Soc Echocardiogr. 2015;28(1):1-39.e14. doi: 10.1016/j.echo.2014.10.003.
9. zscore.chboston.org [Internet]. Boston: Boston Children's Hospital; 2023 [cited 2025 Mar 7]. Available from:: hhttps://zscore.chboston.org/.

10. Sluysmans T, Colan SD. Structural Measurements and Adjustments for Growth. In: Lai WW, Mertens LL, Cohen MS, Geva T, editors. Anomalies of the Atrium Septum. Echocardiography In Pediatric And Congenital Heart Disease: From Fetus to Adults. Hoboken: Wiley-Blackwell; 2009. p.158-74.

11. Colan SD. Normal Echocardiographic Values for Cardiovascular Structures. In: Lai WW, Mertens LL, Cohen MS, Geva T, editors. Anomalies of the Atrium Septum. Echocardiography In Pediatric And Congenital Heart Disease: From Fetus to Adults. Hoboken: Wiley-Blackwell; 2009. p. 765-85.

12. Sachdeva, R. Atrial septal defect. In: Allen HD, Driscoll DJ, Shaddy RE, Feltes TF, editors. Moss and Adams' Heart Disease in Infants, Children, and Adolescents: Including the Fetus and Young Adult. Philadelphia: Lippincott Williams & Wilkins; 2016. p. 739-56.

13. Cantinotti M, Scalese M, Murzi B, Assanta N, Spadoni I, De Lucia V, et al. Echocardiographic Nomograms for Chamber Diameters and Areas in Caucasian Children. J Am Soc Echocardiogr. 2014;27(12):1279-92.e2. doi: 10.1016/j.echo.2014.08.005.

14. Rajagopal H, Uppu SC, Weigand J, Lee S, Karnik R, Ko H, et al. Validation of Right Atrial Area as a Measure of Right Atrial Size and Normal Values of in Healthy Pediatric Population by Two-Dimensional Echocardiography. Pediatr Cardiol. 2018;39(5):892-901. doi: 10.1007/s00246-018-1838-3.

15. Gokhroo RK, Anantharaj A, Bisht D, Kishor K, Plakkal N, Aghoram R, et al. A Pediatric Echocardiographic Z-Score Nomogram for a Developing Country: Indian Pediatric Echocardiography Study - The Z-score. Ann Pediatr Cardiol. 2017;10(1):31-8. doi: 10.4103/0974-2069.197053.

16. Otto CM. Cardiopatias Congênitas em Adultos: Fundamentos de Ecocardiografia Clínica. Rio de Janeiro: Elsevier; 2010.

17. Rao PS. Role of Echocardiography in the Diagnosis and Interventional Management of Atrial Septal Defects. Diagnostics. 2022;12(6):1494. doi: 10.3390/diagnostics12061494.

18. Lin X, Yang F, Chen Y, Chen X, Wang W, Li W, et al. Echocardiography-Based AI for Detection and Quantification of Atrial Septal Defect. Front Cardiovasc Med. 2023;10:985657. doi: 10.3389/fcvm.2023.985657.

19. Mweri ST, Deng Y, Cheng P, Lin H, Wang H, Mkangara OB, et al. Evaluation of Atrial Septal Defect Using Real-Time Three-Dimensional Echocardiography: Comparison with Surgical Findings. J Huazhong Univ Sci Technolog Med Sci. 2009;29(2):257-9. doi: 10.1007/s11596-009-0225-y.

20. Beerbaum P, Körperich H, Esdorn H, Blanz U, Barth P, Hartmann J, et al. Atrial Septal Defects in Pediatric Patients: Noninvasive Sizing with Cardiovascular MR Imaging. Radiology. 2003;228(2):361-9. doi: 10.1148/radiol.2282020798.

21. Boon I, Vertongen K, Paelinck BP, Demulier L, van Berendoncks A, Maeyer C, et al. How to Size ASDs for Percutaneous Closure. Pediatr Cardiol. 2018;39(1):168-75. doi: 10.1007/s00246-017-1743-1.

22. Stout KK, Daniels CJ, Aboulhosn JA, Bozkurt B, Broberg CS, Colman JM, et al. 2018 AHA/ACC Guideline for the Management of Adults with Congenital Heart Disease: A Report of the American College of Cardiology/American Heart Association Task Force on Clinical Practice Guidelines. Circulation. 2019;139(14):e698-e800. doi: 10.1161/CIR.0000000000000603.

23. Faherty E, Rajagopal H, Lee S, Love B, Srivastava S, Parness IA, et al. Correlation of Transthoracic Echocardiography-Derived Pulmonary to Systemic Flow Ratio with Hemodynamically Estimated Left to Right Shunt in Atrial Septal Defects. Ann Pediatr Cardiol. 2022;15(1):20-6. doi: 10.4103/apc.apc_139_21.

24. Sluysmans T, Colan SD. Theoretical and Empirical Derivation of Cardiovascular Allometric Relationships in Children. J Appl Physiol. 2005;99(2):445-57. doi: 10.1152/japplphysiol.01144.2004.

25. Zilberman MV, Khoury PR, Kimball RT. Two-Dimensional Echocardiographic Valve Measurements in Healthy Children: Gender-Specific Differences. Pediatr Cardiol. 2005;26(4):356-60. doi: 10.1007/s00246-004-0736-z.

26. Pettersen MD, Du W, Skeens ME, Humes RA. Regression Equations for Calculation of z Scores of Cardiac Structures in a Large Cohort of Healthy Infants, Children, and Adolescents: An Echocardiographic Study. J Am Soc Echocardiogr. 2008;21(8):922-34. doi: 10.1016/j.echo.2008.02.006.

27. Cantinotti M, Scalese M, Molinaro S, Murzi B, Passino C. Limitations of Current Echocardiographic Nomograms for Left Ventricular, Valvular, and Arterial Dimensions in Children: A Critical Review. J Am Soc Echocardiogr. 2012;25(2):142-52. doi: 10.1016/j.echo.2011.10.016.

28. Snyder K, Drant S, Carris E, Christopher A, Allada V. Tricuspid Valve Size Relationship to Right Ventricular Volume in Post-Operative Tetralogy of Fallot Patients. Pediatr Cardiol. 2022;43(4):887-93. doi: 10.1007/s00246-021-02800-0.

29. Geggel RL. Clinical Detection of Hemodynamically Significant Isolated Secundum Atrial Septal Defect. J Pediatr. 2017;190:261-4.e1. doi: 10.1016/j.jpeds.2017.07.037.

30. Naqvi N, McCarthy KP, Ho SY. Anatomy of the Atrial Septum and Interatrial Communications. J Thorac Dis. 2018;10(Suppl 24):2837-47. doi: 10.21037/jtd.2018.02.18.

Original Article

The Impact of Anxiety on Patients Referred for Transesophageal Echocardiography

João Afonso Astolfi Martins,[1] Amanda de Vasconcelos Eng,[1] Edgar Lira Filho,[1] Claudio Henrique Fischer,[1] Claudia Gianini Monaco,[1] Alessandra Joslin Oliveira,[1] Fernando Rodrigues da Camara Oliveira,[1] Marcelo Luiz Campos Vieira,[1] Samira Saady Morhy,[1] Ana Clara Tude Rodrigues[1]

Hospital Israelita Albert Einstein,[1] São Paulo, SP – Brazil

Abstract

Background: Anxiety is an important factor that influences patient experience during medical procedures. Transesophageal echocardiography (TEE) is an exam that requires sedation, which can exacerbate anxiety and affect its practice.

Objective: To assess variables that influence the degree of anxiety experienced by patients undergoing TEE and its correlation with sedation.

Methods: We assessed patients of both sexes, age >18 years, referred for TEE. We applied an anxiety questionnaire (none, mild, moderate, and high) and collected demographic, clinical, and physiological data. For comparison purposes, patients were divided into the following 2 groups: no/mild anxiety and moderate/severe anxiety.

Results: We studied 63 patients, 41 (66%) of whom were male. The majority were White (87.3%), and the mean age was 52.5 ± 14.7 years. Only 35% of patients had comorbidities, the most frequent being hypertension (63.6%), and 70% patients were undergoing TEE for the first time. The main indication for TEE was valvular disease (30%). The majority of patients (62%) reported some degree of anxiety, as follows: 25 (40%) mild, 10 (16%) moderate, and 4 (6%) severe. Patients with moderate/severe anxiety (p = 0.03) and younger patients (p = 0.001) required higher doses of midazolam for sedation.

Conclusion: Anxiety was common in patients referred for TEE, and it appeared to be less influenced by clinical variables. However, we concluded that more anxious and younger patients required higher doses of sedation.

Keywords: Echocardiography; Anxiety; Conscious Sedation.

Introduction

Transesophageal echocardiography (TEE) is a widely used tool in cardiology; due to the anatomical proximity between the heart and the esophagus, it allows the assessment of functional and/or structural cardiac alterations with high accuracy,[1] for example, valvular heart disease, thrombi and masses, aortopathies, among other diseases.[2] It is considered a semi-invasive examination, as it requires the introduction of an esophageal probe; in order to provide comfort to patients, light or moderate sedation is performed,[3] generally using benzodiazepines (midazolam) in combination with an opioid (fentanyl). It is important to emphasize that the examination is not without risks, which are often associated with sedation itself. The most common complications include hypoventilation, hypoxemia,[4] and hypotension.[5] Furthermore, some factors associated with the patient or the examination may contribute to an increased level of anxiety related to medical procedures; non-White ethnicities,[6] female sex,[7] and history of chronic diseases[7] have been related to the development of anxiety in the general population. Higher anxiety levels have also been related to prolonged duration of medical procedures and eventual use of higher sedative doses.[8] Therefore, it is important to define factors that could influence the level of anxiety related to TEE and its impact on sedation, in order to optimize patient management during examination.

Objectives

The objectives of this study were to determine the prevalence of anxiety related to TEE, to assess factors related to the examination and/or patients that could influence the degree of anxiety experienced by patients, and to verify whether the amount of anesthetic administered during the procedure could correlate with the degree of anxiety and/or other clinical variables.

Mailing Address: João Afonso Astolfi Martins •
Hospital Israelita Albert Einstein. Avenida Albert Einstein, 627. Postal code: 05652-900. São Paulo, SP – Brazil
E-mail: astolfimartins@gmail.com
Manuscript received February 4, 2025; revised February 18, 2025; accepted March 10, 2025
Editor responsible for the review: Maria Otto

DOI: https://doi.org/10.36660/abcimg.20250005i

Central Illustration: The Impact of Anxiety on Patients Referred for Transesophageal Echocardiography

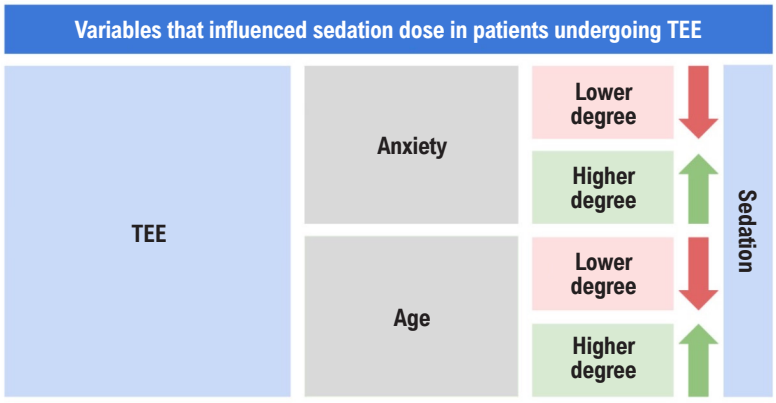

Arq Bras Cardiol: Imagem cardiovasc. 2025;38(2):e20250005

TEE: transesophageal echocardiography.

Methods

Patients

This study prospectively assessed patients aged 18 years or older of both sexes who were referred for TEE, as outpatients or inpatients at a tertiary hospital located in the South Zone of the city of São Paulo, Brazil. We only included patients who provided written informed consent via a free and informed consent form.

Regarding the exclusion criteria, this study excluded patients with contraindications to TEE, patients with impaired cognition, and patients who required sedation under anesthesiologist supervision.

TEE and sedation

After the routine transthoracic examination, TEE was performed in the routine manner, with the prescribed sedation and under the guidance of the cardiologist and echocardiographer responsible for performing the examination. Following oropharyngeal anesthesia with lidocaine spray, with patients in the left lateral decubitus position, sedation with intravenous fentanyl (50 or 100 mcg) was performed, followed by intravenous midazolam in an initial dose of 1 to 2 mg, with additional doses of 1 mg administered for conscious sedation. If necessary, additional doses of midazolam could be administered to continue the examination.[9]

Anxiety questionnaire

To assess the level of anxiety, we used a mini-questionnaire adapted from Cao,[10] consisting of a simple visual self-assessment scale, to analyze each study participant's anxiety level. Patients were asked to choose among facial drawings showing different levels of anxiety, marking the one that described their state of anxiety at that time (Figure 1). For comparative purposes, the patients were divided into 2 groups, one including patients with no/mild anxiety and the other with moderate/high levels of anxiety.

Clinical variables

We recorded data such as blood pressure, heart rate, respiratory rate, and oximetry. The presence of comorbidities (diabetes, hypertension, cardiovascular diseases, and others), routine use of anxiolytics, and the indication for the examination were also recorded.

Statistical analysis

The variables were described based on absolute and relative frequencies, means and standard deviations, or medians and quartiles. Comparisons of patient characteristics with anxiety levels were performed using Student's t test or Mann-Whitney test for quantitative variables, according to their distribution, and chi-square or Fisher's exact test were used for qualitative variables. Data normality was assessed using the Shapiro-Wilk test. To correlate variables with sedative dose, we used Pearson or Spearman correlation, as appropriate. Analyses were performed using SPSS statistical software, version 26.0. Study data were entered into a data storage platform dedicated to REDCap research for later analysis.[11] This study is part of a research project aimed at evaluating music therapy as an adjunct measure to sedation in patients referred to TEE. The study received approval from the institutional research ethics committee.

Results

We assessed 65 patients, 2 of whom were excluded (1 due to refusal to participate and 1 due to contraindication to TEE), leaving 63 patients who fulfilled the inclusion criteria and

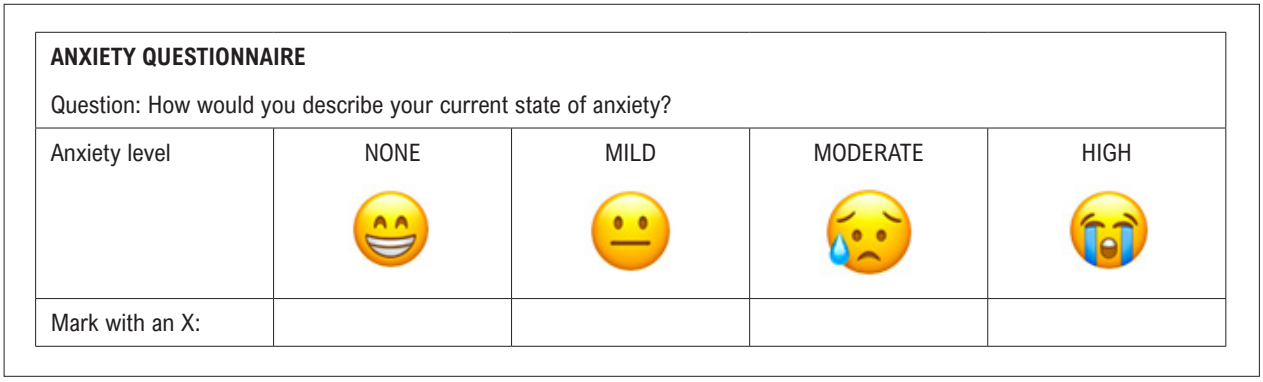

Figure 1 – *Anxiety questionnaire*

signed the free and informed consent form. Most patients were male (65%). The mean age was 52 ± 14 years, and the majority were White (87%). The majority of patients had completed secondary education (95%). Regarding origin of patients, only 11 were hospitalized at the time of the examination, while the remainder underwent the examination on an outpatient basis. Comorbidities were infrequent (35% of patients), the most frequent being systemic arterial hypertension. For 66% of patients, the examination was being performed for the first time. For 24%, it was the second time, and only 10% had undergone more than 2 examinations. Regarding indications, valvular heart disease was the most frequent (30%), followed by stroke (20%), arrhythmias (13%), and suspected endocarditis (9.5%). Other less frequent indications included investigation of patent foramen ovale, cardiac masses, and evaluation of the aorta. When asked, almost all patients (95%) confirmed that they had received detailed instructions about the examination, including about complications. None of the patients who had previously undergone the examination reported a negative previous experience with TEE, and only 11% used routine anxiolytics. Table 1 displays the patients' characteristics.

Table 1 – Characteristics of patients referred for TEE (n = 63)

Characteristic	Mean ± standard deviation or n (%)
Age (years)	52.5 ± 14.8
Weight (kg)	77.8 ± 15.3
Height (cm)	172.2 ± 8.9
BMI (kg/m^2)	26.1 ± 3.9
Male sex	41 (65)
White ethnicity	55 (87.3)
Multiracial (*Pardo*) ethnicity	8 (12.7)
Complete secondary education	58 (92)
Inpatients	11 (17.5)
Outpatients	52 (82.5)
No comorbidities	41 (65)
Systemic arterial hypertension	14 (22.2)
Obesity	6 (9.5)
Diabetes mellitus	1 (1.5)

BMI: body mass index.

Anxiety level and influence of patient-related variables

Regarding anxiety level, the majority of patients (62%) were anxious before the procedure, with mild anxiety in 40%, moderate anxiety in 16%, and high anxiety in 6% (Figure 2). We did not observe any correlation between demographic variables (sex, age, and ethnicity), education level, indication for the examination, routine use of anxiolytics, or patient origin with the presence of anxiety before TEE.

Comparison between sedative dose used, anxiety level, and variables related to the examination

The mean fentanyl dose was 55.5 ± 17.6 mcg. The mean initial dose of midazolam was 4.8 ± 2.2 mg, and the mean additional midazolam dose was 1.32 ± 1.6 mg. The midazolam doses required for sedation were similar for men and women. No difference was observed between the midazolam dose and education level or ethnicity. On the other hand, patients with comorbidities required lower midazolam doses for sedation ($p = 0.04$), whereas outpatients required higher sedative doses when compared to inpatients ($p = 0.01$). These findings are displayed in Figure 3.

Regarding the sedative dose used, when comparing the subgroups of patients with no anxiety/mild anxiety and patients with moderate/high anxiety, a significant difference was observed only for the additional dose of midazolam required for sedation ($p = 0.03$). Patients with moderate/high anxiety levels used a larger additional amount of midazolam (2 mg [2 to 3 mg]) compared to those with mild/no anxiety (1.5 mg [1 to 2 mg]), as shown in Figure 4. There was no difference between anxiety levels and variables such as instructions received, indication for the examination, routine use of anxiolytics, or the number of transesophageal examinations previously undergone. Only 2 patients required anesthesia to complete the procedure; therefore, there was no difference between groups for this variable.

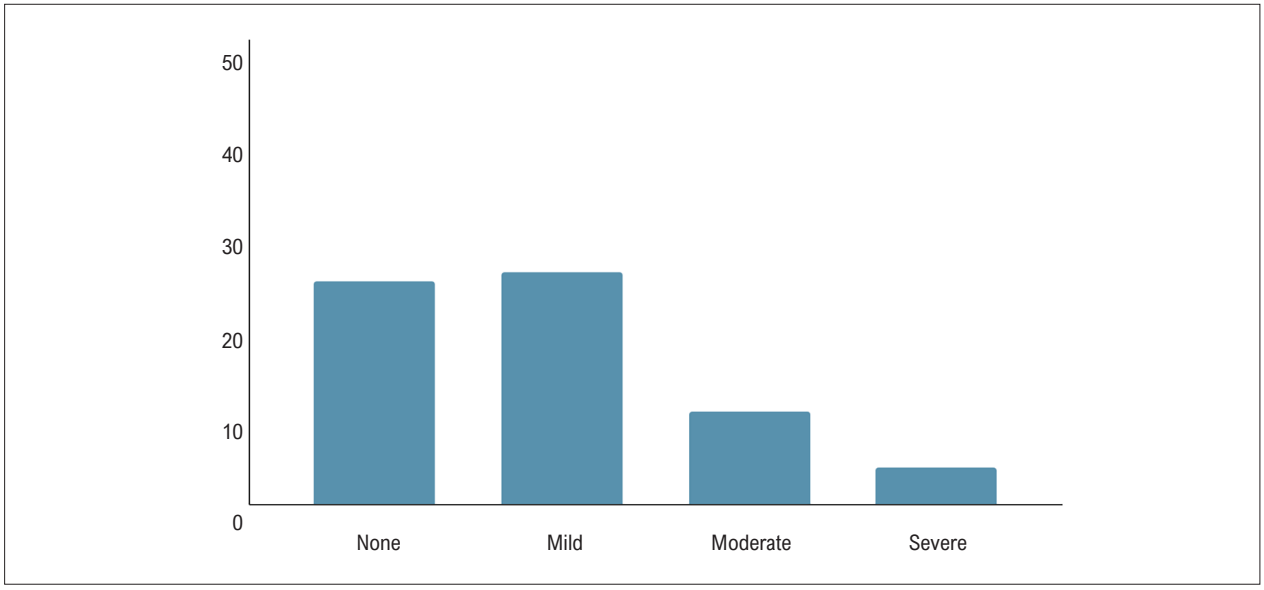

Figure 2 – *Anxiety level in patients referred for TEE (n = 63)*

Table 2 – Correlation between patient characteristics and total midazolam dose (n = 63)

Variable	r	p
Age (years)	–0.41	0.001
Weight (kg)	–0.009	0.942
Height (cm)	–0.20	0.114
BMI (kg/m2)	–0.15	0.223
Systolic blood pressure (mmHg)	–0.07	0.574
Diastolic blood pressure (mmHg)	0.11	0.356
Heart rate (bpm)	0.06	0.592
Respiratory rate (breaths per minute)	–0.28	0.026
Oximetry (%)	0.39	0.001

BMI: body mass index.

Correlation between sociodemographic variables and anesthetic dose administered

The variables that showed a significant correlation with the total dose of midazolam were age, with a moderate negative correlation ($r = -0.41$, $p = 0.001$); oximetry, with a moderate positive correlation ($r = 0.39$); and respiratory rate, with a slight negative correlation ($r = -0.28$). Table 2 displays these data.

Discussion

TEE is a widely used tool in cardiology; it is a semi-invasive technique, as it requires the introduction of an esophageal probe. In order to provide comfort to patients, it is often accompanied by mild or moderate sedation, generally using benzodiazepines (midazolam) in combination with an opioid (fentanyl). TEE is not without risks, which are often associated with sedation itself. The most common complications are hypoventilation, hypoxemia, and hypotension. It is known that the anxiety experienced by patients is a determining factor for additional difficulties in performing procedures, requiring greater management skills and more time from the team to perform the procedure.[12] Furthermore, in addition to the resulting technical difficulties, anxiety could contribute to negative patient experience during the procedure. The quality of the examination is also directly related to the quality of the sedation performed. In this sense, when we evaluated the relationship between factors related to the exam/patient and the level of anxiety reported, we observed that the dose required for sedation was higher for outpatients when compared to inpatients. One possible explanation might be exposure to the hospital environment, which is unfamiliar to the patient, causing greater anxiety, whereas inpatients, in addition to being previously exposed to the environment, are often using sedative medications. We also noted that patients with comorbidities required lower sedation doses when compared to patients without comorbidities. In patients referred for endoscopic procedures, it was observed that those with higher American Society of Anesthesiologists (ASA) classification for pre-anesthesia surgical risk require less sedation. Since the ASA class increases according to the number of comorbidities presented, this could explain the correlation with comorbidities found in our study.[12]

It is known that non-White ethnicities,[6] female sex, and history of chronic diseases[7] are risk factors for the development of anxiety. However, in this study, we did not observe a correlation between anxiety and these variables. One possible explanation for the lack of correlation is that anxiety in a social context presents different risk factors compared to anxiety related to a medical examination, as in the case of TEE. Moreover, other authors, when studying

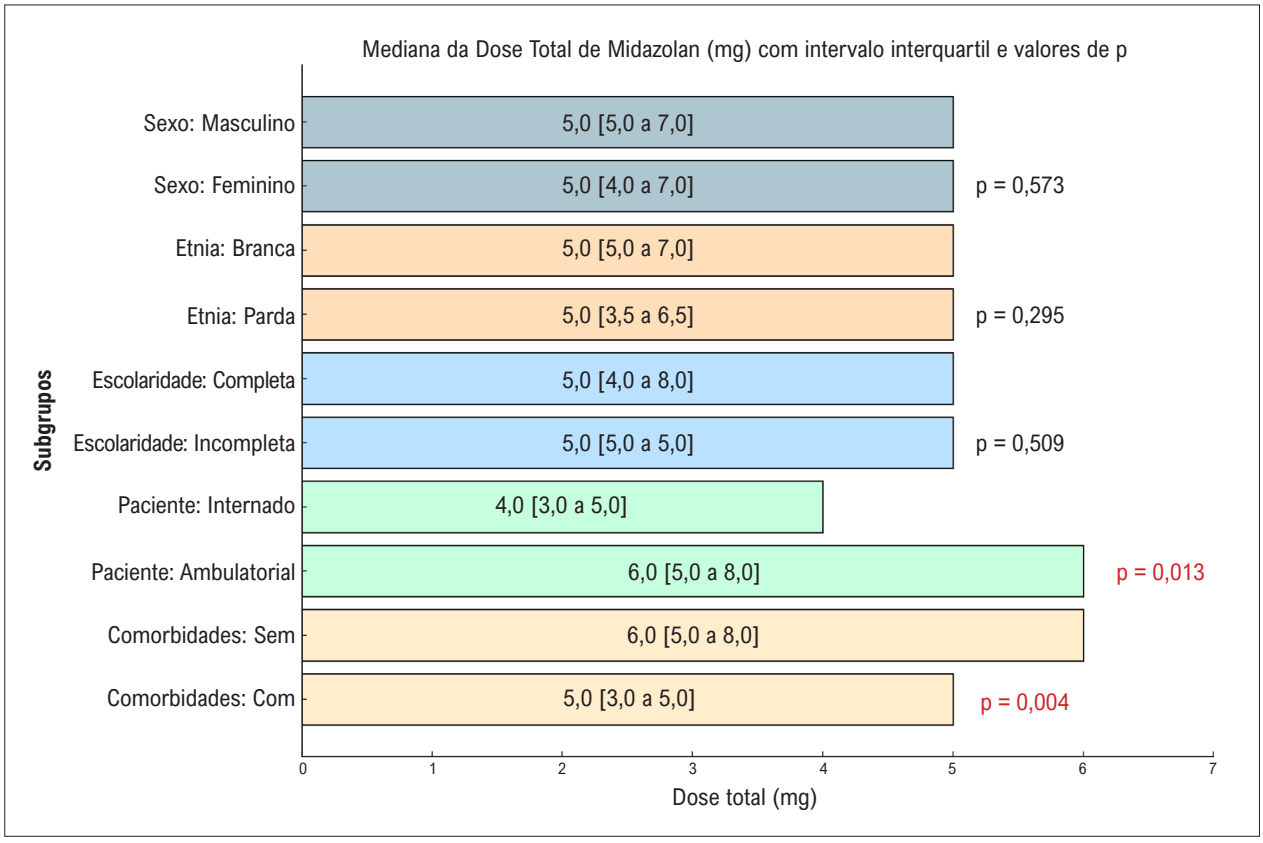

Figure 3 – *Comparison of patient characteristics with midazolam dose*

patients undergoing endoscopic procedures (similar to TEE), also did not find a correlation between sex and anxiety.[8]

Regarding the correlation between the variables and sedative doses, we observed that age presented a negative correlation coefficient; in other words, the younger the patient, the higher the dose of midazolam required for sedation, a finding already reported in the literature.[8] Furthermore, it is known that elderly patients are more sensitive to the use of medications due to pharmacokinetic and pharmacodynamic changes resulting from age;[13] consequently, they have greater adverse effects with the use of sedation. Accordingly, given that elderly patients are more sensitive, the physician responsible for sedation would be expected to be more cautious, administering a lower dose of sedative.

Finally, in relation to anxiety and the dose of anesthetic administered, we observed that the additional midazolam dose was higher in patients with moderate/high anxiety level ($p = 0.033$). Although some authors have reported no correlation between the level of pre-procedure anxiety and the sedative dose used,[14] similar to our findings, other studies have shown that the anesthetic dose required to perform the procedure may increase according to the anxiety level.[15] A possible explanation would be greater activation of the neuroaxis due to the increased release of adrenocorticotropic hormone and corticosteroids in anxious patients,[16] thus requiring greater anesthetic doses to achieve the same level of sedation as non-anxious patients for the same procedure.[14]

Limitations

It is worth noting the main limitation inherent to this study. The study sample was small, restricting the possible influence of other factors, such as sex or ethnicity, on the level of anxiety presented. However, we were able to identify other factors that were significantly related to anxiety level, even with the sample studied.

Conclusion

Anxiety is a common symptom in patients referred for TEE. As a result of this study, we have understood that more anxious and younger patients required higher doses of sedation to perform the procedure (Central Figure).

Author Contributions

Conception and design of the research and analysis and interpretation of the data: Martins JAA, Eng AV, Lira Filho E, Morhy SS, Rodrigues ACT; acquisition of data and critical revision of the manuscript for intellectual content: Martins JAA, Eng AV, Lira Filho E, Fischer CH, Monaco CG, Oliveira AJ, Oliveira FRC, Vieira MLC, Morhy SS, Rodrigues ACT; statistical analysis: Martins JAA, Eng AV, Morhy SS, Rodrigues ACT; writing of the manuscript: Martins JAA, Lira Filho E, Morhy SS, Rodrigues ACT; performance of transesophageal echocardiography: Lira

Filho E, Fischer CH, Monaco CG, Oliveira AJ, Oliveira FRC, Vieira MLC, Morhy SS, Rodrigues ACT.

Potential Conflict of Interest

No potential conflict of interest relevant to this article was reported.

Sources of Funding

There were no external funding sources for this study.

Study Association

This article is part of the undergraduate thesis submitted by João Afonso Astolfi Martins, from Faculdade Israelita de Ciências da Saúde Albert Einstein.

Ethics Approval and Consent to Participate

This study was approved by the Ethics Committee of the Hospital Israelita Albert Einstein under the protocol number 64738222.7.0000.0071. All the procedures in this study were in accordance with the 1975 Helsinki Declaration, updated in 2013. Informed consent was obtained from all participants included in the study.

Use of Artificial Intelligence

The authors did not use any artificial intelligence tools in the development of this work.

Availability of Research Data and Other Materials

The underlying content of the research text is contained within the manuscript.

References

1. Bruijn SF, Agema WR, Lammers GJ, van der Wall EE, Wolterbeek R, Holman ER, et al. Transesophageal Echocardiography is Superior to Transthoracic Echocardiography in Management of Patients of Any Age with Transient Ischemic Attack or Stroke. Stroke. 2006;37(10):2531-4. doi: 10.1161/01.STR.0000241064.46659.69.
2. Mansour IN, Lang RM, Furlong KT, Ryan A, Ward RP. Evaluation of the Application of the ACCF/ASE Appropriateness Criteria for Transesophageal Echocardiography in an Academic Medical Center. J Am Soc Echocardiogr. 2009;22(5):517-22. doi: 10.1016/j.echo.2009.02.009.
3. Aeschbacher BC, Portner M, Fluri M, Meier B, Lüscher TF. Midazolam Premedication Improves Tolerance of Transesophageal Echocardiography. Am J Cardiol. 1998;81(8):1022-6. doi: 10.1016/s0002-9149(98)00083-6.
4. Bailey PL, Pace NL, Ashburn MA, Moll JW, East KA, Stanley TH. Frequent Hypoxemia and Apnea after Sedation with Midazolam and Fentanyl. Anesthesiology. 1990;73(5):826-30. doi: 10.1097/00000542-199011000-00005.
5. Stoddard MF, Longaker RA. The Safety of Transesophageal Echocardiography in the Elderly. Am Heart J. 1993;125(5 Pt 1):1358-62. doi: 10.1016/0002-8703(93)91007-2.
6. Smolen JR, Araújo EM. Race/Skin Color and Mental Health Disorders in Brazil: A Systematic Review of the Literature. Cien Saude Colet. 2017;22(12):4021-30. doi: 10.1590/1413-812320172212.19782016.
7. Costa CO, Branco JC, Vieira IS, Souza LDM, Silva RA. Prevalence of Anxiety and Associated Factors in Adults. J Bras Psiquiatr. 2019;68(2):92-100. doi: 10.1590/0047-2085000000232.
8. Gürbulak B, Üçüncü MZ, Yardımcı E, Kırlı E, Tüzüner F. Impact of Anxiety on Sedative Medication Dosage in Patients Undergoing Esophagogastroduodenoscopy. Wideochir Inne Tech Maloinwazyjne. 2018;13(2):192-8. doi: 10.5114/wiitm.2018.73594.
9. Silva CE, Tasca R, Weitzel LH, Moisés VA, Ferreira LD, Tavares GM, et al Standardization of Equipment and Techniques for Conducting Echocardiographic Examinations. Arq Bras Cardiol. 2004;82(Suppl 2):1-10. doi: 10.1590/S0066-782X2004000800001.
10. Cao X, Yumul R, Lazo OLE, Friedman J, Durra O, Zhang X, et al. A Novel Visual Facial Anxiety Scale for Assessing Preoperative Anxiety. PLoS One. 2017;12(2):e0171233. doi: 10.1371/journal.pone.0171233.
11. Harris PA, Taylor R, Minor BL, Elliott V, Fernandez M, O'Neal L, et al. The REDCap Consortium: Building an International Community of Software Platform Partners. J Biomed Inform. 2019;95:103208. doi: 10.1016/j.jbi.2019.103208.
12. Silva MRA, Espírito Santo ACG. Intervenção Dialógica e Atenuação da Ansiedade no Exame de Endoscopia Digestiva Alta [cited 2025 Mar 29]. Available from:. https://www.ufpe.br/documents/1192056/0/Interven%C3%A7%C3%A3o+dial%C3%B3gica+e+a+atenua%C3%A7%C3%A3o+da+ansiedade+no+exame+de+endoscopia+digestiva+alta.pdf/e51da22f-6b09-4d03-8d7f-9a02aa519a80.
13. Luca E, Schipa C, Cambise C, Sollazzi L, Aceto P. Implication of Age-Related Changes on Anesthesia Management. Saudi J Anaesth. 2023;17(4):474-81. doi: 10.4103/sja.sja_579_23.
14. Chung KC, Juang SE, Lee KC, Hu WH, Lu CC, Lu HF, et al. The Effect of Pre-Procedure Anxiety on Sedative Requirements for Sedation During Colonoscopy. Anaesthesia. 2013;68(3):253-9. doi: 10.1111/anae.12087.
15. Kil HK, Kim WO, Chung WY, Kim GH, Seo H, Hong JY. Preoperative Anxiety and Pain Sensitivity are Independent Predictors of Propofol and Sevoflurane Requirements in General Anaesthesia. Br J Anaesth. 2012;108(1):119-25. doi: 10.1093/bja/aer305.
16. Graeff FG. Anxiety, Panic and the Hypothalamic-Pituitary-Adrenal Axis. Braz J Psychiatry. 2007;29(Suppl 1):S3-6. doi: 10.1590/s1516-44462007000500002.

Impact of Anxiety on Patients Referred for Transesophageal Echocardiography

Augusto Alberto da Costa Jr.[1]
Escola Paulista de Medicina,[1] *São Paulo, SP – Brazil*

Short Editorial related to the article: The Impact of Anxiety on Patients Referred for Transesophageal Echocardiography

In this issue of ABC Cardiovascular Imaging, anxiety is highlighted not only as a factor in the subjective assessment of patients' experiences during invasive medical procedures (transesophageal echocardiography, TEE) but also for its influence on the amount of sedative drugs administered during the procedure.

The study *The Impact of Anxiety on Patients Referred for Transesophageal Echocardiography,* conducted at a tertiary institution, provides a detailed analysis of multiple characteristics of patients undergoing the exam, its influence on sedation, and revisits important aspects of good medical practice. The study results indicate that anxiety, assessed using easily implemented indicators,[1] was present in 62% of patients. Self-assessment tables show mild anxiety in 40%, moderate anxiety in 16%, and severe anxiety in 6%. It is part of the experience of echocardiographers performing transesophageal exams to deal with patient anxiety, especially among younger individuals.[2,3]

Multiple variables are influential; after a satisfactory consultation time and an excellent doctor-patient relationship, the absence of "questions or need for additional clarifications" from patients may be related to their embarrassment in ignoring details they assumed to be general knowledge in the current "Google era".[4] The previous unrestricted functionality of young individuals contributes to insecurity and anxiety regarding hospital admission. In addition, the array of medical equipment and the fear of a new reality –the possibility of confirming a medical condition with serious consequences – contribute to patient anxiety.

An interesting aspect of this study is that it was conducted in patients with a high sociocultural level, with 92% having completed university education, which is uncommon in our setting. Broad access to information and a higher cultural level did not help reduce pre-procedure anxiety in unfamiliar situations (66% of the studied patients were undergoing TEE for the first time). The excess of available information may play a role in increasing pre-procedure anxiety.[5]

The results obtained confirmed expectations: younger patients and those with a higher self-assessed level of anxiety required higher doses of medication to achieve adequate sedation during the procedure. These findings are consistent with existing literature, both for invasive diagnostic procedures (TEE, colonoscopy)[6] and for achieving appropriate levels of anesthesia during surgical procedures.[7] Also, they were shown to be related to increased activation of the neuroendocrine axis.[8] Among patients whose indication for the test was made after hospitalization, older individuals, with comorbidities that had required previous hospital procedures or admissions, showed lower levels of self-assessed anxiety.[9] In these patients, clinical deterioration requiring intensive treatment may trigger awareness of the possibility of the end of life.[10] This increase in anxiety levels can be further exacerbated by the effects of medications used in critically ill patients (vasopressors, corticosteroids), as well as the need for respiratory support and invasive procedures, including TEE.[10]

The main risks of the procedure analyzed by the authors — an increase in vagal autonomic tone, hypotension, and respiratory depression with hypoxia — may be exacerbated by the need for higher doses of opioids/benzodiazepines.[11]

Identifying contributing factors and understanding and implementing measures to mitigate or control anxiety can help multidisciplinary teams achieve effective management in the perioprocedural period, improving patient experience. There are advantageous benefits, such as better quality of image acquisition, and lower risk of sedation complications in young patients, in individuals with a low body mass index,[6] and in anxious elderly patients with comorbidities who have lower tolerance to additional complications.

Complex procedures, such as endovascular aortic prosthesis implantation, even after significant functional improvement, can still be associated with anxiety symptoms for up to six weeks post-intervention.[12,13] A reasonable rationale would be to seek faster relief through more intensive psychological preparation. Low-cost measures that have shown effectiveness include music therapy and aromatherapy,[14,15] which are already used in percutaneous interventions guided by computed tomography (tumor biopsies, abscess drainage, tumor ablation).

The analysis made by Munn et al. is highly relevant regarding the repercussions of anxiety and the opportunity to reflect on different resources and approaches[15-17] to alleviate patient distress before, during, and after invasive procedures. These procedures have become increasingly frequent, integrated into the routine of various institutions. Sometimes, for this reason, we adopt "conscious sedation" when continuous awareness should be maintained. Invasive procedures often cause concern, anxiety, and distress in patients; this publication invites us to remain alert and vigilant to these possibilities.

Keywords

Anxiety; Patients; Transesophageal Echocardiography

Mailing Address: Augusto Alberto da Costa Jr. •
Escola Paulista de Medicina. Rua Napoleão de Barros, 715. Postal code: 04024-002. Vila Clementino, SP – Brazil
E-mail: augustoacostajr@gmail.com

DOI: https://doi.org/10.36660/abcimg.20250036i

References

1. Cao X, Yumul R, Lazo OLE, Friedman J, Durra O, Zhang X, et al. A Novel Visual Facial Anxiety Scale for Assessing Preoperative Anxiety. PLoS One. 2017;12(2):e0171233. doi: 10.1371/journal.pone.0171233.
2. José GM, Silva CE, Ferreira LD, Novaes YP, Monaco CG, Gil MA, et al. Effective Dose of Sedation in Transesophageal Echocardiography: Relation to Age, Body Surface Area and Left Ventricle Function. Arq Bras Cardiol. 2009;93(6):576-81. doi: 10.1590/s0066-782x2009001200011.
3. Lira-Filho EB, Arruda ALM, Furtado MS, Kowatsch I, Carvalho FP, Felinto CE, et al. Impact of Fentanyl Associated with Midazolam in Sedation for Transesophageal Echocardiography. Arq Bras Cardiol: Imagem Cardiovasc. 2014;27(2):83-6. doi: 10.5935/2318-8219.20140014.
4. Jaeb MA, Pecanac KE. Shame in Patient-Health Professional Encounters: A Scoping Review. Int J Ment Health Nurs. 2024;33(5):1158-69. doi: 10.1111/inm.13323.
5. Meira M, Bitencourt AGV, Travesso DJ, Chojniak R, Barbosa PNVP. Relationship between Anxiety and Internet Searches Before Percutaneous Ultrasound-Guided Diagnostic Procedures: A Prospective Cohort Study. PLoS One. 2022;17(10):e0275200. doi: 10.1371/journal.pone.0275200.
6. Gürbulak B, Üçüncü MZ, Yardımcı E, Kırlı E, Tüzüner F. Impact of Anxiety on Sedative Medication Dosage in Patients Undergoing Esophagogastroduodenoscopy. Wideochir Inne Tech Maloinwazyjne. 2018;13(2):192-8. doi: 10.5114/wiitm.2018.73594.
7. Baagil H, Baagil H, Gerbershagen MU. Preoperative Anxiety Impact on Anesthetic and Analgesic Use. Medicina. 2023;59(12):2069. doi: 10.3390/medicina59122069.
8. Graeff FG. Anxiety, Panic and the Hypothalamic-Pituitary-Adrenal Axis. Braz J Psychiatry. 2007;29(Suppl 1):3-6. doi: 10.1590/s1516-44462007000500002.
9. Patanwala AE, Christich AC, Jasiak KD, Edwards CJ, Phan H, Snyder EM. Age-Related Differences in Propofol Dosing for Procedural Sedation in the Emergency Department. J Emerg Med. 2013;44(4):823-8. doi: 10.1016/j.jemermed.2012.07.090.
10. Boehm LM, Bird CM, Warren AM, Danesh V, Hosey MM, McPeake J, et al. Understanding and Managing Anxiety Sensitivity during Critical Illness and Long-Term Recovery. Am J Crit Care. 2023;32(6):449-57. doi: 10.4037/ajcc2023975.
11. Johnson S. Sedation and Analgesia in the Performance of Interventional Procedures. Semin Intervent Radiol. 2010;27(4):368-73. doi: 10.1055/s-0030-1267851.
12. Bäz L, Wiesel M, Möbius-Winkler S, Westphal JG, Schulze PC, Franz M, et al. Depression and Anxiety in Elderly Patients with Severe Symptomatic Aortic Stenosis Persistently Improves after Transcatheter Aortic Valve Replacement (TAVR). Int J Cardiol. 2020;309:48-54. doi: 10.1016/j.ijcard.2020.03.021.
13. Eide LSP, Fridlund B, Hufthammer KO, Haaverstad R, Packer EJS, Ranhoff AH, et al. Anxiety and Depression in Patients Aged 80 Years and Older Following Aortic Valve Therapy. A Six-Month Follow-Up Study. Aging Clin Exp Res. 2023;35(11):2463-70. doi: 10.1007/s40520-023-02541-5.
14. Fleckenstein FN, Hecker KA, Schusta F, Pöhlmann A, Auer TA, Gebauer B, et al. Prospective Randomized Study on the Effect of Music on Anxiety and Pain Related to CT-Guided Percutaneous Interventions. Eur Radiol. 2025. doi: 10.1007/s00330-025-11441-3.
15. Munn Z, Jordan Z. Interventions to Reduce Anxiety, Distress and the Need for Sedation in Adult Patients Undergoing Magnetic Resonance Imaging: A Systematic Review. Int J Evid Based Healthc. 2013;11(4):265-74. doi: 10.1111/1744-1609.12045.
16. Faymonville EM, Mambourg HP, Joris J, Vrijens B, Fissette J, Albert A, et al. Psychological Approaches during Conscious Sedation. Hypnosis versus Stress Reducing Strategies: A Prospective Randomized Study. Pain. 1997;73(3):361-7. doi: 10.1016/S0304-3959(97)00122-X.
17. Makary MS, Silva A, Kingsbury J, Bozer J, Dowell JD, Nguyen XV. Noninvasive Approaches for Anxiety Reduction during Interventional Radiology Procedures. Top Magn Reson Imaging. 2020;29(4):197-201. doi: 10.1097/RMR.0000000000000238.

Original Article

Assessment of Interrater Reliability in Point-of-Care Ultrasound for Assessing Congestion in Cardiovascular Intensive Care

Marina Petersen Saadi,[1,2] Guilherme Pinheiro Machado,[1] Gustavo Paes Silvano,[1,2] João Pedro da Rosa Barbato,[2] Renato Ferraz Almeida,[2] Fernando Luis Scolari,[1] Guilherme Heiden Telo,[1] Anderson Donelli da Silveira[1,2]

Hospital de Clinicas de Porto Alegre,[1] Porto Alegre, RS – Brazil

Universidade Federal do Rio Grande do Sul,[2] Porto Alegre, RS – Brazil

Abstract

Background: The assessment of congestion is critical for managing patients with cardiovascular conditions, including heart failure (HF). Traditional methods often lack sensitivity, whereas point-of-care ultrasound (POCUS) provides an objective bedside alternative.

Objective: To evaluate the interrater reliability (IRR) of key POCUS variables used to assess hemodynamic, pulmonary, and venous congestion.

Methods: This single-center, prospective study was conducted from January to June 2023 in a cardiovascular intensive care unit (CICU) in Brazil. Adult patients underwent standardized POCUS examinations. Three trained investigators independently assessed lung ultrasound (LUS) (B-lines), left ventricular filling pressures (LVFP) (E/A and E/e′ ratios), inferior vena cava (IVC) measurements, hepatic and portal vein Doppler flow, and modified Venous Excess Ultrasound (mVExUS) Score. IRR was analyzed using intraclass correlation coefficient (ICC).

Results: A total of 23 patients were included, with a median age of 65 years, each undergoing three independent POCUS examinations (69 total assessments). LUS and IVC measurements showed excellent IRR (ICC 0.903). Hepatic and portal vein flows demonstrated good IRR (ICCs 0.808 and 0.796, respectively). mVExUS grading achieved the highest IRR (ICC 0.957). The E wave showed excellent IRR (ICC 0.934), while the A wave and e′ velocity had lower IRRs (0.512 and 0.399, respectively). E/e′ and E/A ratios demonstrated moderate-to-good IRR (ICCs 0.662 and 0.852, respectively). The median exam duration was 10 minutes.

Conclusion: POCUS variables demonstrated high reproducibility, particularly for LUS and mVExUS. The reproducibility of LUS and mVExUS was higher than that of LVFP parameters, suggesting they may be more reliable than traditional measures such as E/e′. These findings support the use of POCUS for standardized assessment of congestion. Further studies are needed to validate its prognostic value.

Keywords: Ultrasonics; Intensive Care Units; Heart Failure; VExUs, modified VExUS.

Introduction

Accurate assessment of hemodynamic and fluid status is critical in critically ill patients, particularly those with cardiovascular diseases such as heart failure (HF).[1] Traditional approaches, including clinical examination and radiological imaging, often fail to provide precise information due to their subjective nature and limited sensitivity,[2] highlighting the need for more objective bedside tools. Lung ultrasound (LUS), echocardiography (TTE), and derived parameters have been developed to enhance the evaluation of these patients.[3]

Mailing Address: Marina Petersen Saadi •
Hospital de Clinicas de Porto Alegre. Rua Ramiro Barcelos, 2350. Postal code: 90410-000. Porto Alegre, RS – Brazil
E-mail: marinapsaadi@gmail.com
Manuscript received April 17, 2025; revised April 17, 2025; accepted April 18, 2025
Editor responsible for the review: Marcelo Tavares

DOI: https://doi.org/10.36660/abcimg.20250022i

LUS has been widely used for over a decade and has demonstrated utility in detecting pulmonary congestion, particularly in HF.[4-6] However, the appearance of B-lines is not exclusive to pulmonary edema and can sometimes be misleading. Therefore, combining LUS findings with other congestion parameters is recommended.[7,8] TTE enables the assessment of hemodynamic congestion through parameters such as the transmitral flow (E/A ratio) and the E/e′ ratio. These relatively simple TTE measures are easy to learn and can be applied at the bedside.[8,9] Venous Excess Ultrasound (VExUS) Score is used to assess systemic venous congestion by evaluating the size and flow patterns of the inferior vena cava (IVC), hepatic vein, and renal vein. Evaluation of systemic congestion through VExUS has also proven useful in predicting cardiorenal syndrome (CRS).[10,11] Integrating pulmonary and hemodynamic congestion parameters, particularly the E/e′ ratio, has been shown to be more accurate than LUS alone for diagnosing HF in emergency settings.[12] Adding systemic congestion parameters would likely further enhance diagnostic accuracy.

Central Illustration: Assessment of Interrater Reliability in Point-of-Care Ultrasound for Assessing Congestion in Cardiovascular Intensive Care

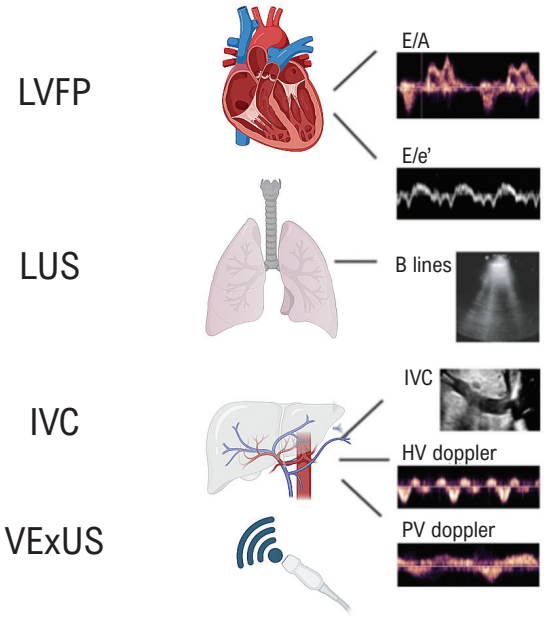

Arq Bras Cardiol: Imagem cardiovasc. 2025;38(2):e20250022

Key POCUS parameters assessed in this study included LVFP, LUS, IVC measurements, and venous congestion evaluation using the mVExUS Score. The variables analyzed were E/A and E/e' ratios for LVFP, B-lines for LUS, IVC diameter and collapsibility, and hepatic vein (HV) and portal vein (PV) Doppler assessments for mVExUS. Created with BioRender.com.

Despite its growing use, the reproducibility of individual point-of-care ultrasound (POCUS) components remains a concern. Interrater reliability (IRR) is essential to ensure consistency across different operators and clinical settings. Most previous studies have evaluated pulmonary, hemodynamic, and systemic congestion parameters individually, aiming to correlate them with congestion severity or clinical outcomes. However, it is important to determine whether the POCUS variables commonly used for congestion assessment demonstrate good IRR and whether the combined evaluation of these selected parameters is feasible in clinical practice.

This study aims to evaluate the IRR of key POCUS variables — specifically LUS, left ventricular filling pressure (LVFP) parameters (E/A and E/e' ratios), IVC measurements, hepatic and portal venous Doppler assessments, and modified VExUS grading (mVExUS) — in patients admitted to a cardiovascular intensive care unit (CICU), assessing their potential for standardized bedside application (Central Illustration).

Methods

Study design

This was a single-center, prospective study conducted in the CICU at a tertiary hospital in Brazil. The study period spanned from January to June 2023 and included adult patients (≥18 years) admitted with various cardiovascular conditions, including HF, acute coronary syndromes, and arrhythmias. The only exclusion criterion was lack of consent to participate.

The study protocol was approved by the Research Ethics Committee of Hospital de Clínicas de Porto Alegre (HCPA) under approval no. 6.468.353 and conducted in accordance with the Brazilian National Health Council Resolution no. 466/12.

Ultrasound assessment

US examinations were performed using a portable US machine (Mindray ME Series; Shenzhen, China) equipped with a 2.5-MHz phased-array sector transducer. Patients were positioned supine with a 30-degree head elevation to standardize imaging conditions. Vital signs were recorded immediately before each evaluation to ensure consistency in hemodynamic status during the examinations. All assessments were conducted with concurrent ECG monitoring. Investigators were blinded to each other's results to minimize bias.

Ultrasound parameters

The following key parameters commonly used to assess pulmonary, hemodynamic, and systemic venous congestion were assessed:

- LUS: assessment of B-lines in eight lung zones.
- LVFP: measurement of E/A and E/e' ratios from the apical four-chamber view.
- IVC: measurement of diameter and collapsibility index.
- Venous Doppler: assessment of hepatic and portal venous flow patterns using pulsed-wave Doppler (PWD).
- mVExUS: grading modified VExUS score based on findings from hepatic and portal venous Doppler flow.

Assessment of hemodynamic congestion

The objective of the hemodynamic evaluation was to detect an increased LVFP. From the apical four-chamber view, the mitral inflow pattern was assessed using PWD at the tips of the mitral valve leaflets. The E/A ratio was categorized into three grades: grade 1 (E/A ≤0.8 and E velocity ≤50 cm/s), considered normal; grade 3 (E/A ≥2), indicating elevated LVFP; and grade 2 (E/A ≤0.8 with E velocity >50 cm/s, or E/A between 0.8 and 2), classified as indeterminate. In cases with a grade 2 E/A ratio, the septal E/e' ratio was used to further differentiate between normal and elevated LVFP.[13]

In the same apical four-chamber view, with angulation to align with the interventricular septum, the medial e' velocity was measured at the mitral annulus using PWD after tissue Doppler imaging (TDI).[14] Medial e' was selected for its feasibility and because most published data on the E/e' ratio are based on this measurement. It is considered the most reliable parameter for estimating LVFP.[15] Increased LVFP was defined as medial E/e' >15 in sinus rhythm or >11 in atrial fibrillation (Figure 1).[16]

Assessment of lung congestion

The chest wall was divided into eight zones, with one scan obtained for each zone. The cardiac transducer was positioned perpendicularly to the ribs along the intercostal spaces, at a depth of approximately 12-18 cm depending on body habitus.[17] Each zone (two anterior and two lateral per hemithorax) was evaluated independently. A zone was considered positive if three or more B-lines were present, and pulmonary congestion was assumed when two or more zones were positive (Figure 2).[6]

Assessment of peripheral venous congestion

The final step included the evaluation of IVC for diameter and collapsibility, along with hepatic and portal venous flows assessed using PWD.

The IVC was evaluated through the subcostal window, approximately 1 cm caudal to its junction with the hepatic vein, to estimate central venous pressure (CVP). CVP was inferred based on IVC diameter and inspiratory variability: a normal CVP of approximately 3 mmHg was suggested when both an IVC diameter ≤2.1 cm and collapsibility ≥50% were present; conversely, an IVC diameter >2.1 cm with <50% collapsibility corresponded to a CVP of approximately 15 mmHg. An intermediate CVP of around 8 mmHg was assigned when only one of these two criteria was met.[18]

If the IVC diameter was ≥2 cm, a modified VExUS assessment was performed using hepatic and portal vein Doppler evaluations. PWD was used in the hepatic vein to assess flow patterns, graded as follows: grade 1 (normal) when the systolic (S) wave was higher than the diastolic (D) wave; grade 2 (mild congestion) when the S wave was lower than the D wave; and grade 3 (severe congestion) when S-wave reversal was present. Portal vein flow was also assessed with PWD and classified into three grades: grade 1 (normal) if nonpulsatile with a maximum-minimum velocity variability <30%; grade 2 (mild congestion) if the pulsatility index was between 30-50%; and grade 3 (severe congestion) if the pulsatility index was ≥50%.[11]

Venous congestion severity by mVExUS was classified into four grades based on IVC diameter and PWD findings. A non-dilated IVC (<2 cm) indicated no significant venous congestion (grade 0). An IVC diameter ≥2 cm with normal or mildly abnormal hepatic or portal vein flow corresponded to mild congestion (grade 1). A plethoric IVC associated with one severely abnormal venous flow pattern (either S-wave reversal in the hepatic vein or ≥50% pulsatility index in the portal vein) defined moderate congestion (grade 2). Severe congestion (grade 3) was diagnosed when severely abnormal flow patterns were present in both the hepatic and portal veins (Figure 3).[19]

Assessment of IRR

Three trained investigators, blinded to each other's evaluations, independently performed real-time POCUS assessments to evaluate IRR. All investigators had received standardized training, consisting of a 4-hour theoretical-practical session followed by a one-month supervised period in the CICU. During this time, each cardiology resident completed at least 50 ultrasound examinations. Exams were not recorded, thereby eliminating retrospective bias and ensuring that IRR reflected real-world clinical practice.

Difficulty scoring

To further characterize the practical applicability of the US protocol, each investigator rated the difficulty of each patient's assessment as easy, average, or hard. An "easy" assessment was defined by clear imaging and straightforward interpretation; an "average" assessment required moderate effort and interpretation; and a "hard" assessment involved significant challenges related to imaging acquisition or interpretation. This subjective evaluation provided additional insight into the feasibility of protocol implementation across varying patient anatomies and clinical conditions.

Statistical analysis

Sample size was calculated assuming a minimum acceptable intraclass correlation coefficient (ICC) of 0.65 and an expected ICC of 0.90. With three raters per subject, a sample of 23 patients provided 90% power at a 0.01 significance level. Continuous variables were reported as mean (standard deviation [SD]) or median (interquartile range [IQR]), according to distribution symmetry assessed by the Shapiro-Wilk test. Categorical variables were presented as

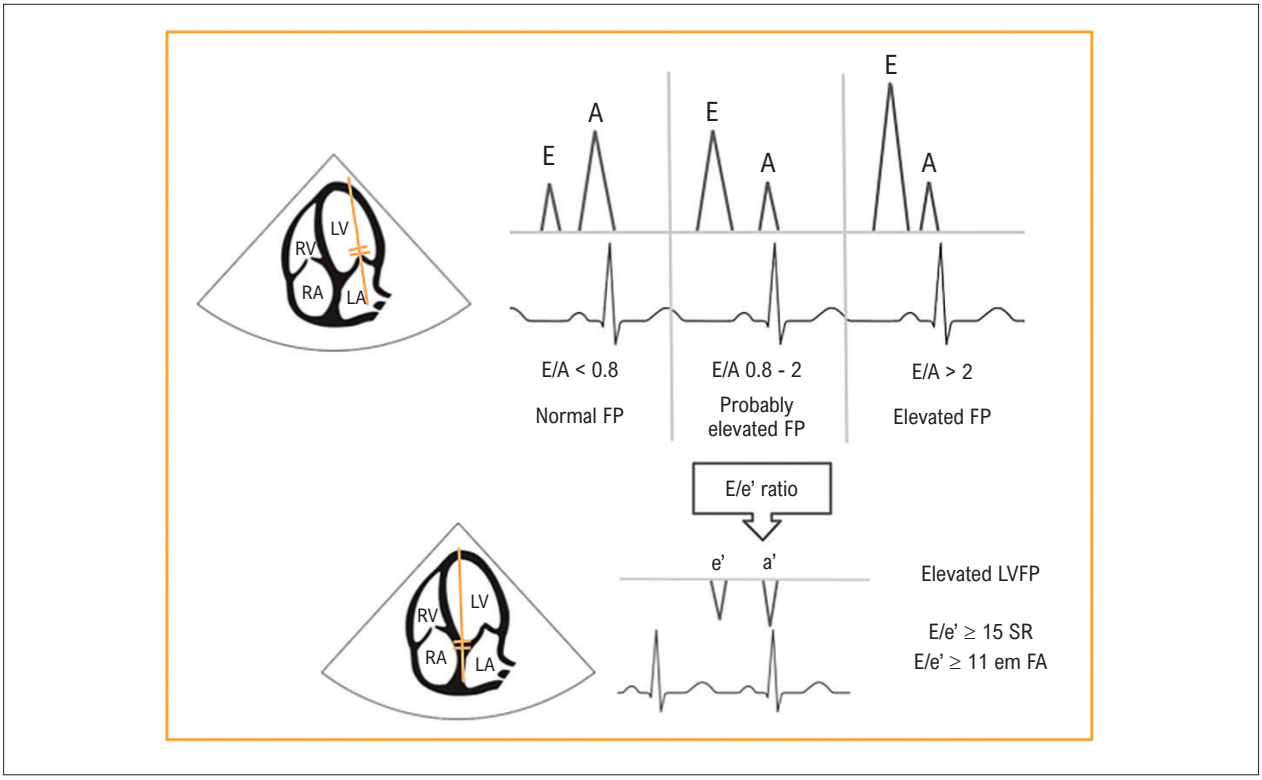

Figure 1 – *The aim of the hemodynamic evaluation is to identify elevated LVFP. The E/A ratio is categorized into three grades, reflecting different levels of LVFP. Patients with a grade 1 E/A ratio are assumed to have normal LVFP, while those with a grade 3 E/A ratio (restrictive pattern) are associated with elevated LVFP. For patients with a grade 2 E/A ratio, the septal E/e' ratio is used to differentiate between normal and elevated LVFP. RV: right ventricle; RA: right atrium; LV: left ventricle; LA: left atrium; FP: LVFP: left ventricular filling pressures; SR: sinus rhythm; AF:atrial fibrillation.*

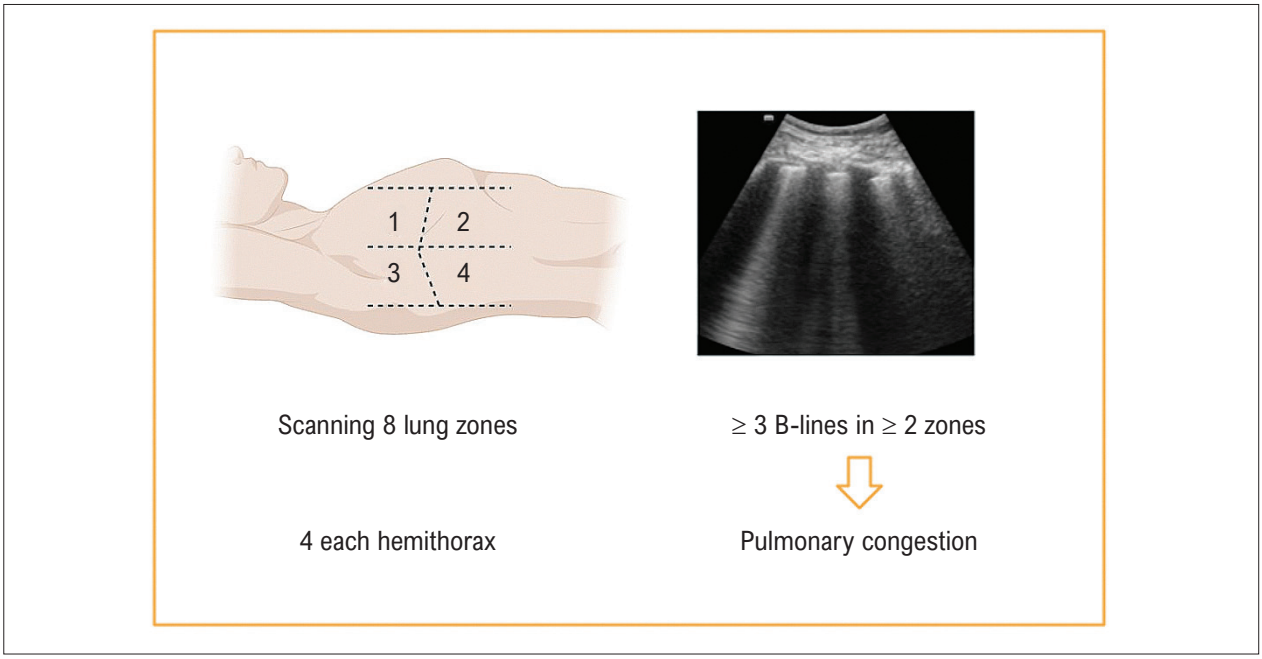

Figure 2 – *For assessing lung congestion, the chest wall is divided into eight zones, with one scan obtained for each zone. Each zone (two anterior and two lateral per hemithorax) is evaluated independently. A zone is considered positive if three or more B-lines are present, and pulmonary congestion is assumed when two or more zones are positive.*

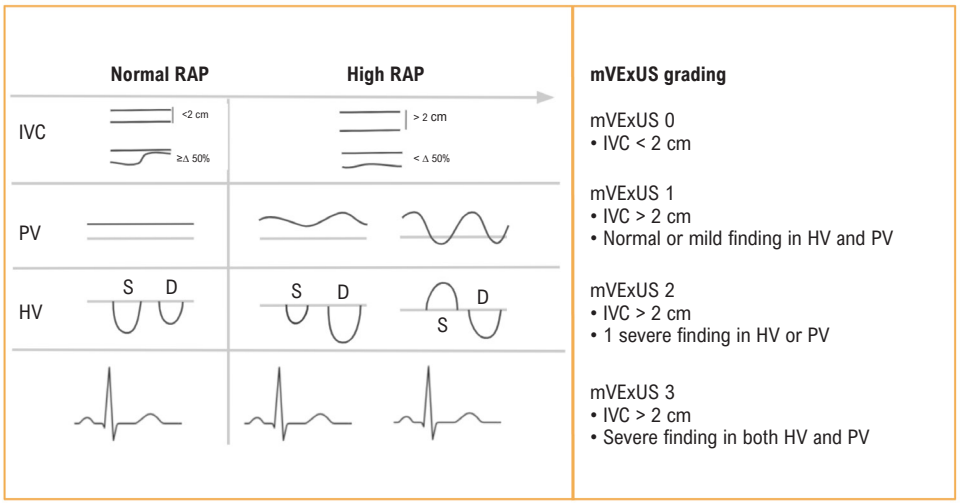

Figure 3 – *Venous congestion by mVExUS is classified into four grades based on IVC assessment and PWD findings. A nondilated IVC (<2 cm) indicates no significant venous congestion (grade 0). When the IVC is ≥2 cm with normal or mildly abnormal findings on hepatic or portal vein Doppler, congestion is considered mild (grade 1). A plethoric IVC associated with one severely abnormal pattern (S-wave reversal in the hepatic vein or ≥50% pulsatility index in the portal vein) defines moderate congestion (grade 2). Severe congestion (grade 3) is indicated by severely abnormal flow patterns in both hepatic and portal veins.*
IVC: inferior vena cava; RAP: mVExUS: modified Venous Excess Ultrasound; HV: hepatic vein; PV: portal vein.

absolute and relative frequencies. ICCs were calculated using a two-way mixed-effects model to assess agreement among the three raters for both continuous and ordinal variables. IRR was classified as poor (<0.50), moderate (0.50-0.75), good (0.75-0.90), or excellent (>0.90). Statistical analyses were performed using SPSS Statistics for macOS, version 29.0 (IBM Corp., Armonk, NY, USA), with significance set at 0.05 (two-tailed).

Results

Between January and June 2023, 23 patients were enrolled in the study. Each patient underwent three independent POCUS assessments, resulting in a total of 69 ultrasound examinations evaluated for IRR. The median age was 65 years (IQR, 53-70), and 60.9% were male. Most admissions to the CICU were due to decompensated HF (65%), followed by ST-elevation myocardial infarction (STEMI) (17%). Parenteral vasodilators were used in 43.5% of patients, inotropes in 21.7%, and vasopressors in 13%.

Regarding cardiac function, 17.4% of patients had preserved left ventricular ejection fraction (LVEF), while 82.6% exhibited reduced LVEF (≤50%). HF etiology was classified as ischemic in 39.1%, nonischemic in 30.4%, and valvular due to severe aortic stenosis in 8.7%. The median LVEF was 33.5% (IQR, 21.7-46.2). During the ultrasound examinations, atrial fibrillation was present in 9% of patients, left bundle branch block in 13%, and 17.4% had an implantable cardioverter-defibrillator. Severe or moderate mitral regurgitation was observed in 43.5% of patients, and severe or moderate tricuspid regurgitation in 39.1%.

A detailed description of the demographic and clinical characteristics of the study population is provided in Table 1, while Appendix Table 1 and Appendix Table 2 summarize POCUS measurements.

IRR

Regarding the IRR of US measurements, excellent agreement was observed for lung positive zone assessments (ICC, 0.903; 95% CI, 0.818-0.954; p<0.001) and IVC measurements (ICC, 0.903; 95% CI, 0.820-0.954; p<0.001), indicating consistent evaluations for pulmonary congestion assessment and CVP estimation.

Subsequent analyses of venous congestion components, including hepatic vein flow, portal vein flow, and mVExUS grading, also demonstrated substantial IRR. Hepatic vein assessment yielded an ICC of 0.808 (95% CI, 0.662-0.906; p<0.001), while portal vein assessment showed an ICC of 0.796 (95% CI, 0.641-0.899; p<0.001). mVExUS grading, reflecting an integrated evaluation of venous congestion, exhibited the highest IRR with an ICC of 0.957 (95% CI, 0.914-0.981; p<0.001) (Table 2).

Further assessments of hemodynamic congestion parameters revealed varying levels of IRR. The E wave demonstrated excellent consistency, with an ICC of 0.934 (95% CI, 0.873-0.969; p<0.001). In contrast, the A wave and septal e′ velocity showed lower IRR, with ICCs of 0.512 (95% CI, 0.176-0.799; p<0.001) and 0.399 (95% CI, 0.146-0.650; p<0.001), respectively. Despite the lower IRR of isolated e′ measurements, the E/e′ ratio demonstrated moderate IRR (ICC, 0.662; 95% CI, 0.449-0.824; p<0.001). The overall classification

of the E/A ratio demonstrated good IRR, with an ICC of 0.852 (95% CI, 0.731-0.928; p<0.001) (Table 2). We additionally evaluated the interobserver agreement for the velocity-time integral (VTI) of the left ventricular outflow tract (LVOT), which, although not part of the standard congestion assessment, has been widely used in ICU settings as a surrogate for cardiac output. Its reproducibility was considered good, with an ICC of 0.820 (95% CI: 0.680–0.912; p<0.001).

The overall examination duration was 10.0 minutes (IQR, 8.0-12.0), reflecting the protocol's efficiency and highlighting its practicality for clinical settings where timely assessments are critical. The concise duration supports the feasibility of integrating the protocol into routine clinical workflows without significant disruption.

Overall, the ICC values for most parameters indicated good to excellent reproducibility among investigators, confirming the protocol's IRR for clinical application. A comprehensive summary of the ICC values for all assessed parameters is provided in Appendix Table 2.

Assessment difficulty

The difficulty ratings assigned by investigators varied, with most assessments classified as easy (50.7%), indicating that the protocol is generally manageable. An additional 36.2% of assessments were rated as average, suggesting the protocol is straightforward in many cases. Only 10.1% were rated as hard, indicating that the protocol remains a reliable tool even under suboptimal imaging conditions. These findings support its practical applicability and suggest it can be effectively implemented across diverse clinical settings, even when ideal acoustic windows are not available.

Discussion

The results of this study underscore the high IRR of the proposed US protocol across its various components, with most ICC values ranging from good to excellent. Furthermore, the findings confirm the feasibility of implementing a novel protocol for hemodynamic assessment at the bedside within a CICU. The high ICC values for lung positive zone assessments indicate excellent IRR in evaluating pulmonary congestion, consistent with previous studies that have demonstrated substantial agreement among observers following short-term training.[20-22]

The IVC diameter and collapsibility also demonstrated excellent IRR, reflecting consistent agreement in estimating CVP as low, normal, or high. However, it is well known that the accuracy of IVC measurements for CVP estimation is greater at the extremes of volume status and less reliable at intermediate values. Additionally, accuracy can be compromised in patients with comorbid conditions such as pulmonary or hepatic disease, obesity, or in those receiving positive pressure ventilation, leading to reduced clinical utility in these scenarios.[23,24]

Evaluating peripheral venous congestion using VExUS is valuable because, in addition to identifying systemic

Table 1 – Clinical characteristics of the sample

Variable	Total (n = 23)
Age, years	65 (53-70)
Male sex (n, %)	14 (60.9%)
Smoking status	
Active smoker (n, %)	2 (8.7%)
Former smoker (n, %)	7 (30.4%)
HF etiology	
Preserved ejection fraction (n, %)	4 (17.4%)
Ischemic (n, %)	9 (39.1%)
Nonischemic (n, %)	7 (30.4%)
Aortic stenosis (n, %)	2 (8.7%)
Previous myocardial infarction (n, %)	13 (56.5%)
Implantable cardioverter-defibrillator (n, %)	4 (17.4%)
Atrial fibrillation (n, %)	2 (8.7%)
Left bundle branch block (n, %)	3 (13%)
LVEF, %	33.5 (21.7-46.2)
Severe or moderate mitral regurgitation (n, %)	10 (43.5%)
Severe or moderate tricuspid regurgitation (n, %)	9 (39.1%)
Diagnosis at admission	
Decompensated HF (n, %)	15 (65.3%)
Acute STEMI (n, %)	4 (17.4%)
Unstable angina (n, %)	1 (4.3%)
Cardiogenic shock (n, %)	1 (4.3%)
Complete atrioventricular block (n, %)	1 (4.3%)
Post-percutaneous coronary intervention (n, %)	1 (4.3%)
Parenteral drugs	
Vasopressor (n, %)	3 (13%)
Venodilator (n, %)	10 (43.5%)
Inotropic (n, %)	5 (21.7%)
Creatinine, mg/dL	2 (1.2-2.6%)
Brain natriuretic peptide, pg/mL	1375 (218.5-2668.5)

Results are expressed as n (%) or median (interquartile range). HF: heart failure; STEMI: ST-elevation myocardial infarction; LVEF: left ventricular ejection fraction.

congestion and predicting CRS, it appears to correlate well with CVP.[24] While the isolated assessment of hepatic and portal vein flows showed good IRR, mVExUS grading demonstrated even better agreement. Our results indicate that although observers did not always agree on the classification of specific hepatic or portal flow patterns, the mVExUS grading still exhibited excellent IRR. This suggests that, for mVExUS grading, the most critical factor is the identification of severely abnormal patterns that shift the congestion category.

Comparing our findings with those from previous studies evaluating IRR in VExUS, it is evident that available data are relatively scarce. One study reported an ICC of 0.83 ($p<0.001$) for the overall VExUS grade, indicating substantial agreement among interpreters. For individual VExUS components, ICCs were 0.71 ($p<0.001$) for the hepatic vein, 0.74 ($p<0.001$) for the portal vein, and 0.48 ($p<0.001$) for the renal vein, reflecting a range from poor to moderate IRR.[25] Additionally, another study reported good IRR for portal pulsatility fraction assessment by transthoracic ECG, with a mean difference of 5.6% between repeated measurements and an ICC of 0.824 ($p<0.001$).[26] This finding aligns with our results and highlights the robustness of portal vein assessments. In our study, similar patterns were observed, with even higher IRR for the hepatic and portal veins. This improvement may be attributed to the consistent use of ECG tracing during all examinations, a practice previously associated with increased concordance.[25] Due to the previously reported poor concordance and time-consuming nature of renal vein assessment,[25] it was excluded from our protocol to streamline the process and improve IRR. This decision is further supported by evidence that a mVExUS score excluding renal venous Doppler has already been validated in patients with CRS admitted to the intensive care unit in a single-center prospective study.[27]

In the evaluation of hemodynamic congestion, the lower ICC values for the A wave and e′ measurements may be attributed to challenges such as patient tachycardia and the prevalence of arrhythmias during the study, both of which can affect the consistency of measurements related to atrial contraction and early diastolic velocities at the septal mitral annulus. Although TDI e′ velocity is generally more robust than transmitral flow assessment, it still presents challenges, particularly in patients with regional myocardial dysfunction.[13,28] Measurement inconsistencies could also result from the US probe not being perfectly aligned parallel to the interventricular septum in the supine position. Including only patients with HF and reduced LVEF could potentially improve the performance and reproducibility of e′ measurements.[29]

The overall classification of the E/A ratio demonstrated good IRR, with an ICC of 0.852 (95% CI, 0.731-0.928; $p<0.001$), while the evaluation of the E/e′ ratio showed moderate IRR (ICC, 0.662; 95% CI, 0.449-0.824; $p<0.001$). Although the E/A and E/e′ ratios are widely used for the assessment of diastolic function in ECG and have been proposed for bedside application, their use by non-echocardiographers in clinical practice has not been extensively studied.[15,30,14]

Table 2 – IRR for each POCUS parameter

Variable	ICC	95% CI	p-value
Lung positive zones	0.903	0.818-0.954	<0.001
IVC	0.903	0.820-0.954	<0.001
CVP estimation	0.955	0.817-0.954	<0.001
E wave	0.934	0.873-0.969	<0.001
A wave	0.512	0.176-0.799	<0.001
Septal e' wave	0.399	0.146-0.650	<0.001
E/A ratio	0.852	0.731-0.928	<0.001
E/e' ratio	0.662	0.449-0.824	<0.001
Hepatic vein Doppler	0.808	0.662-0.906	<0.001
Portal vein Doppler	0.796	0.641-0.899	<0.001
mVExUS grading	0.957	0.914-0.981	<0.001
LVOT-VTI	0.820	0.680- 0.912	<0.001
Difficulty rating	0.298	0.030-0.584	0.014

CI: confidence interval; CVP: central venous pressure; ICC: intraclass correlation coefficient; mVExUS: modified Venous Excess Ultrasound Score ; LVOT-VTI : left ventricular outflow tract velocity-time integral; IVC: inferior vena cava.

Strengths and limitations

This single-center study with a relatively small sample size may limit generalizability and sensitivity to detect subtle variations. Operator dependence could affect reproducibility in less experienced settings; however, the high ICCs observed suggest that adequate training mitigates this concern. Methodological rigor was maintained through real-time, blinded assessments performed by trained investigators, with ECG integration, minimizing biases typically associated with retrospective or video-based analyses. These strengths reinforce the robustness and clinical applicability of the evaluated POCUS variables.

Conclusion

This study demonstrates POCUS variables used to assess hemodynamic, pulmonary, and peripheral venous congestion exhibit high IRR across their components. High reproducibility was observed for lung positive zones, LVFP parameters, IVC measurements, and mVExUS grading. The reproducibility of LUS and mVExUS was higher than that of LVFP assessment, suggesting these parameters may offer greater consistency than traditional measures such as the E/e′ ratio.

Acknowledgements

We would like to thank the staff of the CICU at HCPA for their valuable support in facilitating this study. We also acknowledge the logistical and administrative support

provided by the graduate coordination team at the Universidade Federal do Rio Grande do Sul. Finally, we thank all patients and their families who consented to participate and made this study possible.

Author Contributions

Conception and design of the research: Saadi MP, Machado GP, Silvano GP, Telo G, Silveira AD; acquisition of data: Saadi MP, Silvano GP, Barbato JPR, Almeida RF; analysis and interpretation of the data: Saadi MP, Machado GP, Silvano GP, Telo G; statistical analysis: Saadi MP, Machado GP, Silvano GP; writing of the manuscript: Saadi MP, Silvano GP; critical revision of the manuscript for intellectual content: Saadi MP, Scolari FL, Telo G, Silveira AD.

Potential Conflict of Interest

No potential conflict of interest relevant to this article was reported.

Sources of Funding

There were no external funding sources for this study.

Study Association

This article is part of the thesis of Doctoral submitted by Marina Petersen Saadi, from Universidade Federal do Rio Grande do Sul.

Ethics Approval and Consent to Participate

This study was approved by the Ethics Committee of the Hospital de Clínicas de Porto Alegre under the protocol number 6.468.353. All the procedures in this study were in accordance with the 1975 Helsinki Declaration, updated in 2013. Informed consent was obtained from all participants included in the study.

Use of Artificial Intelligence

The authors did not use any artificial intelligence tools in the development of this work.

Research Data

All datasets supporting the results of this study are available upon request from the corresponding author.

References

1. McDonagh TA, Metra M, Adamo M, Gardner RS, Baumbach A, Böhm M, et al. 2021 ESC Guidelines for the Diagnosis and Treatment of Acute and Chronic Heart Failure. Eur Heart J. 2021;42(36):3599-726. doi: 10.1093/eurheartj/ehab368.
2. Koratala A, Ronco C, Kazory A. Diagnosis of Fluid Overload: From Conventional to Contemporary Concepts. Cardiorenal Med. 2022;12(4):141-54. doi: 10.1159/000526902.
3. Price S, Platz E, Cullen L, Tavazzi G, Christ M, Cowie MR, et al. Expert Consensus Document: Echocardiography and Lung Ultrasonography for the Assessment and Management of Acute Heart Failure. Nat Rev Cardiol. 2017;14(7):427-40. doi: 10.1038/nrcardio.2017.56.
4. Platz E, Jhund PS, Girerd N, Pivetta E, McMurray JJV, Peacock WF, et al. Expert Consensus Document: Reporting Checklist for Quantification of Pulmonary Congestion by Lung Ultrasound in Heart Failure. Eur J Heart Fail. 2019;21(7):844-51. doi: 10.1002/ejhf.1499.
5. Pivetta E, Goffi A, Nazerian P, Castagno D, Tozzetti C, Tizzani P, et al. Lung Ultrasound Integrated with Clinical Assessment for the Diagnosis of Acute Decompensated Heart Failure in the Emergency Department: A Randomized Controlled Trial. Eur J Heart Fail. 2019;21(6):754-66. doi: 10.1002/ejhf.1379.
6. Gargani L, Girerd N, Platz E, Pellicori P, Stankovic I, Palazzuoli A, et al. Lung Ultrasound in Acute and Chronic Heart Failure: A Clinical Consensus Statement of the European Association of Cardiovascular Imaging (EACVI). Eur Heart J Cardiovasc Imaging. 2023;24(12):1569-82. doi: 10.1093/ehjci/jead169.
7. Öhman J, Harjola VP, Karjalainen P, Lassus J. Assessment of Early Treatment Response by Rapid Cardiothoracic Ultrasound in Acute Heart Failure: Cardiac Filling Pressures, Pulmonary Congestion and Mortality. Eur Heart J Acute Cardiovasc Care. 2018;7(4):311-20. doi: 10.1177/2048872617708974.
8. Öhman J, Harjola VP, Karjalainen P, Lassus J. Focused Echocardiography and Lung Ultrasound Protocol for Guiding Treatment in Acute Heart Failure. ESC Heart Fail. 2018;5(1):120-8. doi: 10.1002/ehf2.12208.
9. Nagueh SF. Non-Invasive Assessment of Left Ventricular Filling Pressure. Eur J Heart Fail. 2018;20(1):38-48. doi: 10.1002/ejhf.971.
10. Beaubien-Souligny W, Benkreira A, Robillard P, Bouabdallaoui N, Chassé M, Desjardins G, et al. Alterations in Portal Vein Flow and Intrarenal Venous Flow are Associated with Acute Kidney Injury after Cardiac Surgery: A Prospective Observational Cohort Study. J Am Heart Assoc. 2018;7(19):e009961. doi: 10.1161/JAHA.118.009961.
11. Beaubien-Souligny W, Rola P, Haycock K, Bouchard J, Lamarche Y, Spiegel R, et al. Quantifying Systemic Congestion with Point-Of-Care Ultrasound: Development of the Venous Excess Ultrasound Grading System. Ultrasound J. 2020;12(1):16. doi: 10.1186/s13089-020-00163-w.
12. Öhman J, Harjola VP, Karjalainen P, Lassus J. Rapid Cardiothoracic Ultrasound Protocol for Diagnosis of Acute Heart Failure in the Emergency Department. Eur J Emerg Med. 2019;26(2):112-7. doi: 10.1097/MEJ.0000000000000499.
13. Nagueh SF, Smiseth OA, Appleton CP, Byrd BF 3rd, Dokainish H, Edvardsen T, et al. Recommendations for the Evaluation of Left Ventricular Diastolic Function by Echocardiography: An Update from the American Society of Echocardiography and the European Association of Cardiovascular Imaging. J Am Soc Echocardiogr. 2016;29(4):277-314. doi: 10.1016/j.echo.2016.01.011.
14. Popescu BA, Beladan CC, Nagueh SF, Smiseth OA. How to Assess Left Ventricular Filling Pressures by Echocardiography in Clinical Practice. Eur Heart J Cardiovasc Imaging. 2022;23(9):1127-9. doi: 10.1093/ehjci/jeac123.
15. Ommen SR, Nishimura RA, Appleton CP, Miller FA, Oh JK, Redfield MM, et al. Clinical Utility of Doppler Echocardiography and Tissue Doppler Imaging in the Estimation of Left Ventricular Filling Pressures: A Comparative Simultaneous Doppler-Catheterization Study. Circulation. 2000;102(15):1788-94. doi: 10.1161/01.cir.102.15.1788.
16. Sohn DW, Song JM, Zo JH, Chai IH, Kim HS, Chun HG, et al. Mitral Annulus Velocity in the Evaluation of Left Ventricular Diastolic Function in Atrial Fibrillation. J Am Soc Echocardiogr. 1999;12(11):927-31. doi: 10.1016/s0894-7317(99)70145-8.

17. Duggan NM, Goldsmith AJ, Saud AAA, Ma IWY, Shokoohi H, Liteplo AS. Optimizing Lung Ultrasound: The Effect of Depth, Gain and Focal Position on Sonographic B-Lines. Ultrasound Med Biol. 2022;48(8):1509-17. doi: 10.1016/j.ultrasmedbio.2022.03.015.

18. Rudski LG, Lai WW, Afilalo J, Hua L, Handschumacher MD, Chandrasekaran K, et al. Guidelines for the Echocardiographic Assessment of the Right Heart in Adults: A Report from the American Society of Echocardiography Endorsed by the European Association of Echocardiography, a Registered Branch of the European Society of Cardiology, and the Canadian Society of Echocardiography. J Am Soc Echocardiogr. 2010;23(7):685-713. doi: 10.1016/j.echo.2010.05.010.

19. Koratala A, Reisinger N. Venous Excess Doppler Ultrasound for the Nephrologist: Pearls and Pitfalls. Kidney Med. 2022;4(7):100482. doi: 10.1016/j.xkme.2022.100482.

20. Koo TK, Li MY. A Guideline of Selecting and Reporting Intraclass Correlation Coefficients for Reliability Research. J Chiropr Med. 2016;15(2):155-63. doi: 10.1016/j.jcm.2016.02.012.

21. Gullett J, Donnelly JP, Sinert R, Hosek B, Fuller D, Hill H, et al. Interobserver Agreement in the Evaluation of B-Lines Using Bedside Ultrasound. J Crit Care. 2015;30(6):1395-9. doi: 10.1016/j.jcrc.2015.08.021.

22. Imanishi J, Iwasaki M, Ujiro S, Nakano T, Yamashita T, Eto H, et al. Accuracy of Lung Ultrasound Examinations of Residual Congestion Performed by Novice Residents in Patients with Acute Heart Failure. Int J Cardiol. 2024;395:131446. doi: 10.1016/j.ijcard.2023.131446.

23. Stassen J, Falter M, Herbots L, Timmermans P, Dendale P, Verwerft J. Assessment of Venous Congestion Using Vascular Ultrasound. JACC Cardiovasc Imaging. 2023;16(3):426-31. doi: 10.1016/j.jcmg.2022.12.028.

24. Longino A, Martin K, Leyba K, Siegel G, Gill E, Douglas IS, et al. Correlation between the VExUS Score and Right Atrial Pressure: A Pilot Prospective Observational Study. Crit Care. 2023;27(1):205. doi: 10.1186/s13054-023-04471-0.

25. Longino AA, Martin KC, Leyba KR, Siegel G, Sharma VM, Riscinti M, et al. Reliability and Reproducibility of the Venous Excess Ultrasound (VExUS) Score, a Multi-Site Prospective Study Validating a Novel Ultrasound Technique for Comprehensive Assessment of Volume Status. Research Square. 2024. doi: 10.21203/rs.3.rs-3993434/v1.

26. Eljaiek R, Cavayas YA, Rodrigue E, Desjardins G, Lamarche Y, Toupin F, et al. High Postoperative Portal Venous Flow Pulsatility Indicates Right Ventricular Dysfunction and Predicts Complications in Cardiac Surgery Patients. Br J Anaesth. 2019;122(2):206-14. doi: 10.1016/j.bja.2018.09.028.

27. Bhardwaj V, Vikneswaran G, Rola P, Raju S, Bhat RS, Jayakumar A, et al. Combination of Inferior Vena Cava Diameter, Hepatic Venous Flow, and Portal Vein Pulsatility Index: Venous Excess Ultrasound Score (VEXUS Score) in Predicting Acute Kidney Injury in Patients with Cardiorenal Syndrome: A Prospective Cohort Study. Indian J Crit Care Med. 2020;24(9):783-9. doi: 10.5005/jp-journals-10071-23570.

28. Sunderji I, Singh V, Fraser AG. When does the E/e' Index Not Work? The Pitfalls of Oversimplifying Diastolic Function. Echocardiography. 2020;37(11):1897-907. doi: 10.1111/echo.14697.

29. Robinson S, Ring L, Oxborough D, Harkness A, Bennett S, Rana B, et al. The Assessment of Left Ventricular Diastolic Function: Guidance and Recommendations from the British Society of Echocardiography. Echo Res Pract. 2024;11(1):16. doi: 10.1186/s44156-024-00051-2.

30. Koratala A, Kazory A. Point of Care Ultrasonography for Objective Assessment of Heart Failure: Integration of Cardiac, Vascular, and Extravascular Determinants of Volume Status. Cardiorenal Med. 2021;11(1):5-17. doi: 10.1159/000510732.

***Supplemental Materials**

For additional information, please click here.

The Use of POCUS in Daily Practice: Are We Really Ready to Use it Efficiently?

Angelo Antunes Salgado,[1,2] *Marcos Paulo Lacerda Bernardo*[1]

Universidade do Estado do Rio de Janeiro,[1] *Rio de Janeiro, RJ – Brazil*

Instituto Nacional de Cardiologia,[2] *Rio de Janeiro, RJ – Brazil*

Short Editorial related to the article: Assessment of Interrater Reliability in Point-of-Care Ultrasound for Assessing Congestion in Cardiovascular Intensive Care

Research on congestion in patients with heart failure (HF) is crucial for clinical management and prognosis of the disease. Congestion (i.e., the accumulation of fluids in the body) is the main cause of hospital admission and readmission of patients with HF, and it is associated with increased mortality. Early detection and identification of the extent of congestion are essential for choosing the most appropriate therapy, preventing complications, and improving prognosis.[1] Clinical signs of congestion may be insufficiently sensitive and specific for the diagnosis and management of patients with HF.[2]

The point-of-care ultrasound (POCUS) is a diagnostic tool that allows immediate and dynamic visualization of ultrasound images. This tool can be used at the bedside to obtain additional clinical information for the physical examination of a specific disease or procedure. The practicality and speed with which images are obtained result in their high use at hospitals for critically ill patients. POCUS has been used in various medical specialties, especially in pulmonary and cardiac ultrasound.[3]

The POCUS exam at the bedside of critically ill patients in the intensive care unit or even at the outpatient clinic is becoming increasingly common in medical practice, along with physical examination and other complementary tests. As demonstrated by its excellent sensitivity and specificity, performing the POCUS with a focus on specific clinical questions allows for accurate and rapid diagnosis of the hemodynamics of the patient, as well as systemic volume status and degree of pulmonary congestion, and does not add too much time to its performance.

The steps for performing a complete hemodynamic POCUS are based on assessing the degree of cardiac function impairment (cardiac POCUS), assessing pulmonary congestion (pulmonary US), and assessing systemic congestion (VExUS). The POCUS may be crucial in patients with shock of undetermined cause, cardiac arrest, and sudden dyspnea, but it is increasingly used to optimize therapy in non-critical patients.

Keywords:

Ultrasonography; Heart Failure; Clinical Diagnosis

Mailing Address: Angelo Antunes Salgado •
Universidade do Estado do Rio de Janeiro. Avenida 28 de Setembro, 77.
Postal code: 20550-900. Rio de Janeiro, RJ – Brazil
E-mail: angeloasalgado@gmail.com

DOI: https://doi.org/10.36660/abcimg.20250026i

Cardiac POCUS evaluates the function of the left and right ventricles, the presence of pericardial effusion, and the characteristics of the inferior vena cava. These parameters enable the identification of causes of hypotension, such as hypovolemia, ventricular dysfunction (cardiogenic shock), or obstructive processes (PTE or hemodynamically significant pericardial effusion).

In the cardiovascular field, pulmonary ultrasound plays an important role in the search for B-lines (known as "comet tails"), which commonly occur in patients with decompensated left ventricular function, either due to contractility failure or increased left ventricle diastolic pressure in hypertensive crises or volume overload, causing pulmonary congestion. The presence of B-lines precedes the auscultation of pulmonary crackles on physical examination, making it important for early diagnosis and treatment.

The VExUS protocol is based on the evaluation of the inferior vena cava, suprahepatic vein flow, portal vein flow, and renal interlobar veins.[4] The analysis of the inferior vena cava serves as a guideline for the VExUS protocol; if its diameter is less than 2.0 cm, the protocol is interrupted, indicating that the patient has no signs of systemic overload (VExUS Score grade 0). However, an inferior vena cava diameter greater than or equal to 2.0 cm is indicative of systemic volume overload, and the protocol is continued by analyzing the flow of the suprahepatic vein, portal vein, and renal interlobar vein. According to the characteristics of the flow, systemic overload is classified as VExUS grade 1 (mild overload), grade 2 (moderate overload), or grade 3 (severe overload).

Saadi et al.[5] found a low inter-examiner variability in performing the POCUS in real-world patients among the three examiners trained for this purpose, with an inter-examiner correlation of 0.9 for pulmonary assessment and 0.9 for estimating the diameter of the inferior vena cava. For the assessment of visceral vessels, the correlation of hepatic vein flow was 0.8, and portal vein flow was 0.79, with the correlation with the VExUS score showing the highest correlation in the study (0.95). The evaluation of left ventricle diastolic pressure parameters showed the lowest values (E/e' correlation: 0.66; A wave: 0.51; septal e' wave: 0.39), despite the good E/A correlation (0.85).

Saadi demonstrated that the POCUS exam is feasible for professionals who are not experts in the method and that after a standardized training period of four hours (theoretical-practical sessions) and one month of training, performing at least 50 supervised exams, they become able to perform the exam, adding diagnostic and management power to the patients examined. POCUS is not a substitute for a full

specialist assessment; thus, proper training is essential to ensure accurate diagnoses.

The performance of these exams by a fourth examiner, fully trained in the method, could serve as a gold standard, allowing not only the degree of agreement between trained professionals to be assessed but also diagnostic accuracy.

Doppler ultrasound of the renal interlobar vessels, an important part of the VExUS assessment, is a challenge for professionals with little knowledge of the method and even for qualified professionals. The dorsal decubitus position of the patient, obesity, inability to mobilize, and the lack of cooperation of the patient in apnea may hinder the evaluation of the intrarenal flow. In the original study by Beaubien et al.[6] the degree of renal congestion was more closely related to the development of renal failure than any other parameter; thus, this degree is important in determining the VExUS score. Removing this parameter from the analysis could distort the VExUS score, reducing the sensitivity and specificity of the severity of systemic congestion. However, in situations in which it is difficult to obtain intrarenal flow, the simplified VExUS protocol can be used using only the suprahepatic veins and portal vein, as it will give us a better idea of the volemia of the patient than with information from the inferior vena cava alone.

POCUS is a tool that is here to stay in clinical practice. Greater sensitivity and specificity in detecting hemodynamically relevant conditions not only improves diagnosis but also guides more precise therapeutic interventions, even in outpatients. Therefore, POCUS become an indispensable resource in contemporary medical practice.

References

1. Moreira FL, Silva GW. Não Tratamos a Congestão Pulmonar e Sistêmica na Insuficiência Cardíaca Aguda Adequadamente. LAJEC. 2022;1(3):e21020. doi: 10.54143/jbmede.v1i3.51.
2. Rohde LEP, Montera MW, Bocchi EA, Clausell NO, Albuquerque DC, Rassi S, et al. Diretriz Brasileira de Insuficiência Cardíaca Crônica e Aguda. Arq Bras Cardiol. 2018;111(3):436-539. doi: 10.5935/abc.20180190.
3. Knust L, Danzmann LC, Cuchinski KK, Zimmer JRC. POCUS na Insuficiência Cardíaca Aguda: Conceitos Básicos para a Prática Clínica. ABC Heart Fail Cardiomyop. 2023;3(2):20230073. doi: 10.36660/abcimg.20240026.
4. Salgado AA, Bernardo MPL, Melo F Netto. Como Faço Avaliação da Congestão Venosa Sistêmica: Protocolo VExUS. Arq Bras Cardiol: Imagem Cardiovasc. 2024;37(2):e20240026. doi: 10.36660/abcimg.20240026.
5. Saadi MP, Machado GP, Silvano GP, Barbato JPR, Almeida RF, Scolari FL et al. Avaliação da Concordância Interobservadores do Ultrassom à Beira do Leito na Análise da Congestão em Unidade de Terapia Intensiva Cardiovascular. Arq Bras Cardiol: Imagem cardiovasc. 2025;38(2):e20250022. DOI: https://doi.org/10.36660/abcimg.20250022
6. Beaubien-Souligny W, Rola P, Haycock K, Bouchard J, Lamarche Y, Spiegel R, et al. Quantifying Systemic Congestion with Point-Of-Care Ultrasound: Development of the Venous Excess Ultrasound Grading System. Ultrasound J. 2020;12(1):16. doi: 10.1186/s13089-020-00163-w.

Original Article

Hypertrophic Cardiomyopathy: Analysis of Septal Thickness with Gradient Reduction in Patients Undergoing Radiofrequency Septal Ablation

Andrea de Andrade Vilela,[1,2] Mariane Higa Shinzato,[1] Bruno Pereira Valdigem,[1] Antonio Tito Paladino,[1,3] Edileide de Barros Correia,[1] Jorge Eduardo Assef[1]

Instituto Dante Pazzanese de Cardiologia,[1] São Paulo, SP – Brazil
Hospital Israelita Albert Einstein,[2] São Paulo, SP – Brazil
Hospital Vila Nova Star,[3] São Paulo, SP – Brazil

Abstract

Background: **Hypertrophic obstructive cardiomyopathy (HOCM) is an autosomal dominant genetic disorder. Invasive treatment for intraventricular gradient reduction is indicated in patients (p) who are refractory to clinical treatment with gradient ≥ 50 mmHg. Radiofrequency ablation (RFA) is one of the current options for invasive management.**

Objectives: **To evaluate the correlation between interventricular septal diameter and procedural success, defined as immediate post-procedural gradient reduction, improvement in functional class (FC), and sustained gradient reduction at 6-month follow-up.**

Methods: **Twenty-two patients with HOCM were included. Transthoracic echocardiography was performed before and six months after RFA, while transesophageal echocardiography (TEE) was carried out intraprocedure.**

Results: **The mean age was 56.64 years (± 12.23), with 68.18% of patients being female and 73% hypertensive. An immediate gradient reduction greater than 50% was observed in 72.7% of patients. At the 6-month follow-up, 60% of patients showed a ≥ 50% gradient reduction along with an improvement in FC. A median septal thickness of 18 mm was associated with greater procedural success compared to a median of 15 mm, and no significant change in septal thickness was observed over the 6-month follow-up period.**

Conclusion: **Radiofrequency septal ablation (RFSA) is an effective and safe technique for the invasive management of HOCM. The procedure enables a significant reduction in the intraventricular gradient, accompanied by improved FC and sustained short-term results. Thicker septal were associated with greater intraprocedural gradient reductions; however, there was no reduction in thickness during the 6-month follow-up.**

Keywords: **Hypertrophic Cardiomyopathy; Radiofrequency Ablation.**

Introduction

Hypertrophic cardiomyopathy (HCM) is an autosomal dominant genetic disorder that affects one in 500 individuals[1] and is considered the most common isolated form of hereditary heart disease.[2] In addition to its genetic basis, the disease's pathophysiology involves a combination of diastolic dysfunction, left ventricular outflow tract (LVOT) obstruction, mitral regurgitation, and myocardial ischemia.[3]

This pathophysiological mechanism explains the development of clinical manifestations, which not only present with a highly heterogeneous clinical picture, but can begin at any stage of life.[4-7] This diversity in clinical presentations is largely due to genetic heterogeneity itself, with progression ranging from asymptomatic cases to sudden death as the initial diagnosis.[8]

In the presence of symptoms, treatment for HCM is indicated.[8] Pharmacological therapy is the first-line treatment used to relieve heart failure symptoms. However, in cases of significant obstruction and severe symptoms refractory to drug treatment, more invasive measures may be necessary to improve symptoms and reduce the intraventricular gradient.[9]

Two invasive methods, surgical myectomy and alcohol septal ablation, are used to relieve LVOT obstruction in patients refractory to clinical treatment. Recent studies have reported favorable results of a new interventional procedure, radiofrequency septal ablation (RFSA).

There are few studies in the literature correlating myocardial thickness diameters with the success of this procedure. Therefore, our objective was to assess whether the degree of myocardial wall thickening prior to the

Mailing Address: Andrea de Andrade Vilela •
Instituto Dante Pazzanese de Cardiologia. Av. Dante Pazzanese, 500. Postal Code: 04012-909. São Paulo, SP – Brazil
E-mail: andreadeandradevilela@gmail.com
Manuscript received April 3, 2025; revised April 7, 2025; accepted April 7, 2025
Editor responsible for the review: Marcelo Tavares

DOI: https://doi.org/10.36660/abcimg.20240097i

Central Illustration: Hypertrophic Cardiomyopathy: Analysis of Septal Thickness with Gradient Reduction in Patients Undergoing Radiofrequency Septal Ablation

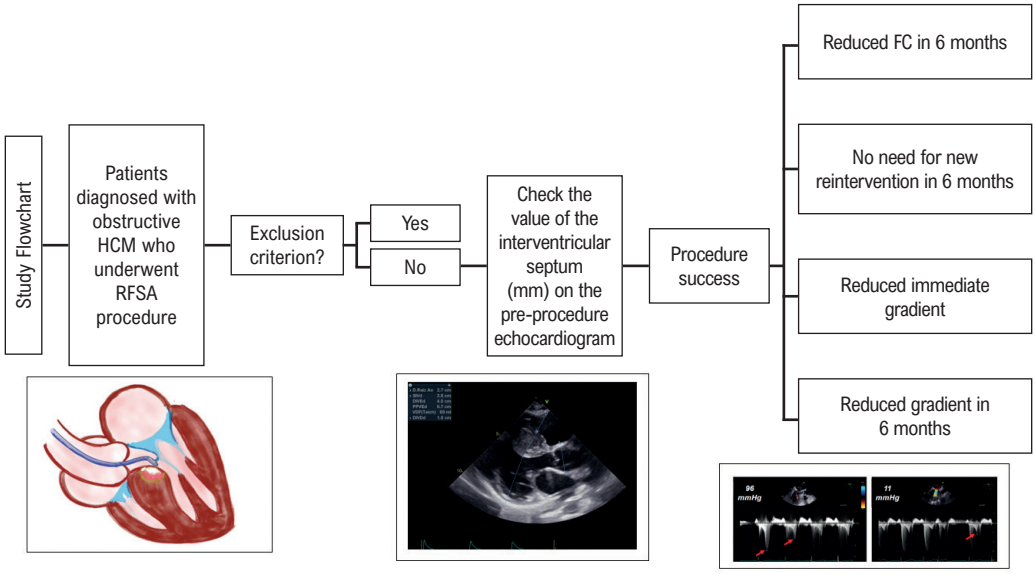

Arq Bras Cardiol: Imagem cardiovasc. 2025;38(2):e20240097

HCM: Hypertrophic cardiomyopathy; RFSA: Radiofrequency septal ablation; FC: functional class.

intervention was associated with greater success in RFSA in patients with hypertrophic obstructive cardiomyopathy (HOCM).

Methods

Study Sample

This is a retrospective observational study based on a review of medical records, approved by our institutional research ethics committee under protocol No. 5133. Patients of both sexes, aged 18 years or older, diagnosed with HOCM, and who underwent RFSA treatment were included. The procedure was performed between May 2017 and October 2019.

Invasive therapy was indicated for patients with HOCM with a maximum gradient at rest or after provocative maneuver ≥ 50 mmHg, were symptomatic, and refractory to clinical treatment. Patients who underwent another concomitant invasive procedure or declined participation were excluded from the study.

RFSA Protocol

The procedure protocol was described by Valdigem et al.[10] RFSAs were performed in an electrophysiology room, with the patient under general anesthesia and mechanical ventilation. The right femoral artery was accessed using an 8F introducer for retroaortic access to the left ventricular septal region. Two additional punctures were made in the right femoral vein (6F introducer) to place one quadripolar catheter in the right septum (to identify the His bundle electrocardiographically) and another in the right ventricular apex.

With the aid of transesophageal echocardiography (TEE), the ventricle-aortic gradient was measured, and the area of greatest flow acceleration—corresponding to the point of greatest obstruction — was identified.

Thus, using TEE morphofunctional analysis and electroanatomical mapping, the therapeutic catheter was positioned at the site of greatest septal obstruction, and radiofrequency energy was applied for 120 seconds (80W, 60 °C). After each application, the gradient was measured by means of TEE. Immediately after the procedure, TEE was used to measure the maximum gradient in the LVOT and to rule out complications such as pericardial effusion, mitral valve injury, or significant mitral regurgitation.

After the sheaths were removed, patients remained in the intensive care unit (ICU) for 24 hours and were then transferred to the inpatient ward for 3 to 5 days.

Research Design Flowchart

Medical records of eligible patients were reviewed according to the established inclusion and exclusion criteria. Clinical data and interventricular septal diameters (measured by pre-procedure transthoracic echocardiography) were analyzed. Procedural success was defined as immediate gradient reduction, absence of reintervention within six months, improvement in NYHA functional class (FC), and gradient reduction at 6-month follow-up (Central Illustration).

Statistical Analysis

Frequency distribution was used to describe categorical variables. Central trend measures (mean and median) and variability (minimum, maximum, and standard deviation) were used to describe numerical variables.

Given the variability in hemodynamic conditions, two assessment settings were defined: intraprocedure and outpatient. Intraprocedure: considering the gradients immediately before ablation and immediately after ablation, with the patient intubated under the effect of positive pressure. Outpatient: considering the gradients estimated by the echocardiogram before the procedure and six months after the procedure.

The nonparametric Mann-Whitney U test was used to verify the association between the septal measurement numerical variable and procedural success. This test was chosen because the normal distribution of the septal measurements was not observed.

A graph was constructed for the evolution of the septal thickness at the time points before the procedure, three months, and six months after the ablation. A mixed linear regression model was used to assess changes in septal thickness over time, treating repeated patient measurements as a random effect.

The paired Student's *t*-test was applied to compare the numerical variable gradient before the procedure and at 6 months, where the normal distribution of the data was identified.

The nonparametric Wilcoxon paired test was applied to compare the numerical variable immediate gradient before the procedure and immediately after, and no normality was observed in the variables data.

The Shapiro-Wilk test was conducted to verify data normality (normal distribution) for each numerical variable.

Box-Plot graphs were used to represent the distribution of the pre and post-immediate gradient at timepoint zero and six months later.

A significance level of 5% was adopted for all statistical tests. The statistical software STATA version 16.0 was used to perform the statistical analyses (ref: StataCorp. 2019. Stata Statistical Software: Release 16.0. College Station, Texas: Stata Corporation).

Results

The study included 22 patients with HOCM who underwent RFSA treatment at a tertiary cardiology hospital between May 2017 and October 2019.

Table 1 shows the clinical characteristics observed before the procedure. Regarding gender, the sample was predominantly female, with seven men (32%) and 15 women (68%). Patient age ranged from 23 to 79 years, with a mean of 56.73 ± 12.20 years. The mean body mass index (BMI) was 29.69 ± 5.46 kg/m².

Regarding medical history, 16 patients (73%) were hypertensive, 11 (50%) had dyslipidemia, six (27%) were diabetic, and three (14%) had a diagnosis of hypothyroidism. Three patients (14%) had associated coronary artery disease.

Table 1 – Clinical profile of patients before RFSA

Clinical Characteristics	Total patients (n = 22)
Age (years) – mean (SD)	56.73 ± 12.20
Female – n (%)	15 (68%)
Male – n (%)	7 (32%)
BMI (kg/m²) – mean (SD)	29.69 ± 5.46
Body surface area (m²) – mean (SD)	1.84 ± 0.23
Smoking - n (%)	2 (9%)
Former smoker – n (%)	2 (9%)
Systemic arterial hypertension	16 (73%)
Dyslipidemia	11 (50%)
Coronary artery disease	3 (14%)
Hypothyroidism	3 (14%)
Diabetes mellitus	6 (27%)
Familial HCM	5 (23%)

N: number of patients; SD: standard deviation; BMI: body mass index; HCM: hypertrophic cardiomyopathy; SD: Standard Deviation.

A known family history of HCM was documented in approximately 23% of the cases.

Among the patients with previous coronary artery disease, only one had undergone prior myocardial revascularization.

Regarding symptoms (Table 2), all 22 patients (100%) had dyspnea, 12 (55%) had angina, six (27%) experienced palpitation, seven (32%) had syncope, and five (23%) reported fainting. Nearly all patients (91%) were in FC III-IV despite clinical treatment. All 22 patients (100%) used beta-blockers, seven (32%) were on calcium channel blockers and two (9%) were using antiarrhythmics (Table 3).

Mean heart rate was 62.45 bpm ± 6.99. The electrocardiogram performed before the procedure showed left ventricular overload in 100% of patients, and eight of them (36.4%) had left bundle branch block.

The mean septal thickness before the procedure was 18.59 mm (± 4.63), ranging from 13 mm to 32 mm (Table 4). Diastolic dysfunction (grades I to III) and mitral insufficiency due to systolic anterior motion of the mitral valve were notable findings. All patients had preserved systolic function, with a mean ejection fraction estimated by Simpson of 68% ± 4.3. As expected, ventricular mass was increased, with a mean value of 341.86 g (± 113.85). The mean, median, and standard deviation values of the echocardiographic parameters are shown in Table 5.

The mean initial maximum gradient estimated during the procedure was 78.18 mmHg (± 33.05). At the end

Table 2 – Symptoms reported by patients before RFSA

Symptoms	Total patients (n = 22)
Dyspnea	22 (100%)
FC I	0
FC II	2 (9%)
FC III	15 (68%)
FC IV	5 (23%)
Angina	12 (55%)
Palpitation	6 (27%)
Syncope	7 (32%)
Fainting	5 (23%)

FC: Function class.

Table 3 – Medications regularly used prior to the RFSA procedure

Medication	Total patients (n = 22)
Beta blocker	22 (100%)
Propranolol	6 (27.3%)
Atenolol	11 (50%)
Metoprolol	5 (22.7%)
Amiodarone	1 (4.6%)
Disopyramide	1 (4.6%)
Calcium channel blocker	7 (31.8%)
Amlodipine	1 (4.6%)
Verapamil	3 (13.6%)
Diltiazem	3 (13.6%)
ARB	4 (19.2%)
Losartan	4 (19.2%)
Diuretics	15 (68.2%)
Furosemide	2 (9.1%)
Hydrochlorothiazide	4 (18.2%)
Chlorthalidone	8 (36.4%)
Spironolactone	13 (59.1%)

ARB: angiotensin receptor blocker.

of the procedure, the mean decreased to 34.09 mmHg (± 28.48).

Two patients developed complications at the puncture site, one pseudoaneurysm and two hematomas, which were resolved conservatively. Seven patients developed left bundle branch block immediately after the procedure and, and two patients had hypotension. There were no deaths or complications requiring surgical intervention during hospitalization. No cases of pericardial effusion or clinical cerebral embolic events were observed.

The mean length of hospital stay was 4.14 days, ranging from two to 10 days.

Before the radioablation procedure, 68% of the patients were in NYHA FC III, and 23% reported FC IV. At the end of one year after the procedure, 77% were in FC I, and 9% were in FC II (Figure 1).

LVOT gradient measurements were performed immediately before and after radioablation, considering the same hemodynamic status (patient sedated, on mechanical ventilation with PEEP of 5, with the same pressure level and inferior vena cava diameter) for accurate analysis of gradient variation related to the procedure (Figure 2). A statistically significant reduction in the LVOT gradient was observed, with the median pre-procedure value at 68 mmHg and the median immediate post-procedure value at 27 mmHg ($p < 0.001$). Obstructive gradients recorded in the outpatient setting prior to the procedure (mean = 110.5 mmHg) were higher than those recorded in the procedure room, as shown in Figure 3, and higher than those measured in the outpatient setting six months post-procedure (45.7 mmHg) compared to the immediate post-procedure values. This difference is likely due to the hemodynamic response under sedation during the radioablation procedure. In both assessments, a significant reduction in the gradient was observed: a mean relative reduction of 58.9% immediately after the procedure and 52% at the 6-month follow-up (Table 6).

There is no established definition of successful outcomes for RFSA in the literature. Ifor this study, success was defined as an immediate gradient reduction of ≥ 50%, with this reduction maintained six months after the procedure. Gradients lower than 50 mmHg and lower than 30 mmHg immediately after the procedure were also considered parameters of procedural success. Table 7 shows the proportion of patients who presented a reduced gradient (immediately after RFSA and at six months) according to success-defining parameters. The nonparametric Mann-Whitney U test was used to verify the association between ventricular septum diameter and RFSA success. Table 8 shows the distribution of septal measurements based on procedural outcomes. When defining success as a gradient reduction of ≥ 50%, septa with a median thickness of 18 mm were associated with better outcomes compared to those with 15 mm ($p < 0.05$). When success was defined as a gradient reduction of ≥ 50% and an absolute gradient below 50 mmHg, septa with a median thickness of 18 mm again showed better outcomes than those with 15 mm ($p < 0.05$). No significant associations were found in the other success categories ($p > 0.05$).

Table 4 – Individual echocardiographic characteristics prior to the RFSA procedure

Patient	Sex	Age	Aortic Root (mm)	LA (mm)	iLA (mm/m²)	LVDD (mm)	Pre-Ablation Septal Thickness (mm)	Posterior Wall (mm)	Septum/ PW Ratio	LV mass (g)	Indexed LV mass (g/m²)	EF (%)
1	M	55	33	50	60.00	44	23	11	2.09	408	178.3	69
2	F	50	32	57	81.00	47	24	12	2.00	345	156	78
3	F	51	32	40	73.00	36	15	11	1.36	201	99	74
4	F	64	29	41	37.00	41	15	10	1.50	229	165	68
5	F	71	32	47	43.00	43	18	13	1.38	341	165	70
6	F	62	30	33	46.00	42	27	19	1.42	427	207	74
7	F	58	29	52	108.00	36	18	14	1.29	214	143	70
8	M	51	36	43	36.00	44	18	12	1.50	335	163	66
9	F	23	29	39	50.00	36	17	8	2.13	189	114	67
10	F	73	34	42	49.00	48	16	13	1.23	362	189	62
11	F	64	29	46	52.00	42	15	11	1.36	252	155	65
12	M	55	35	41	37.00	51	20	11	1.82	438	223	69
13	F	79	34	56	64.00	38	21	18	1.17	367	209	69
14	F	50	36	33	40.00	40	16	14	1.14	292	200	68
15	F	54	31	38	53.00	42	15	10	1.5	237	145	66
16	M	38	33	58	43.00	49	22	13	1.69	497	225	61
17	M	51	36	46	46.00	51	17	12	1.42	397	193	67
18	M	62	37	43	43.00	48	17	13	1.31	381	214	62
19	M	55	34	50	80.00	42	32	16	2.00	686	394	76
20	F	71	32	49	82.00	45	15	15	1.00	346	215	68
21	F	64	37	45	55.00	52	13	12	1.08	331	186	67
22	F	48	31	32	40.00	43	15	10	1.50	246	129	67

LA: left atrium; iLA: indexed left atrium; LVDD: left ventricular end-diastolic diameter; PW: posterior wall; LV: left ventricle; EF: ejection fraction.

The measurement of septal thickness at the pre-procedure, three-months and six-months' time points is shown in Figure 4. The red line represents the mean values. A mixed linear model was used to evaluate the effect of time on septal thickness, considering the dependence between participants. No evidence was found to suggest that the measurements changed over time.

Discussion

To date, this study has shown that RFSA presents favorable results in reducing the ventricular gradient, without fatal complications.

To minimize hemodynamic variability, we compared gradients measured immediately before and after the procedure while the patient was sedated and on mechanical ventilation in the catheterization lab. Similarly, we compared outpatient gradients measured before the procedure with those measured six months post-procedure.

The procedure was largely successful, whether defined as a gradient reduction of more than 50%, an absolute gradient below 50 mmHg or 30 mmHg, or a combination of these criteria. Immediate gradient reduction above 50% occurred in 72.7% of patients.

The result at 6 months also demonstrated a gradient reduction ≥ 50% in 60% of the patients. At six months, the patients benefited

Table 5 – Echocardiographic parameters prior to the RFSA

Parameter	Mean	Median	Standard deviation	Minimum	Maximum
AO (mm)	32.77	32.50	2.67	29	37
LA (mm)	44.59	44.00	7.46	32	58
iLA (mm/m²)	56.36	49.50	18.76	36	108
LVDD (mm)	43.64	43.00	4.87	36	52
IS (mm)	18.59	17.00	4.63	13	32
PW (mm)	12.64	12.00	2.63	8	19
IS/PW	1.50	1.42	0.33	1.00	2.12
LV mass (g)	341.86	343.00	113.85	189	686
Indexed LV mass (g/m²)	184.88	182.15	58.49	99	394
LVEDV (ml)	88.7	85.5	23.10	54	130
EF (%)	68.32	68.00	4.29	61	78

AO: aortic root; LA: left atrium; iLA: indexed left atrial volume; LVDD: left ventricular end-diastolic diameter; IS: interventricular septum; PW: posterior wall; IS/PW: interventricular septum/posterior wall ratio; LV: left ventricle; EDV: end-diastolic volume; EF: ejection fraction; LVEDV: Left Ventricular End Diastolic Volume.

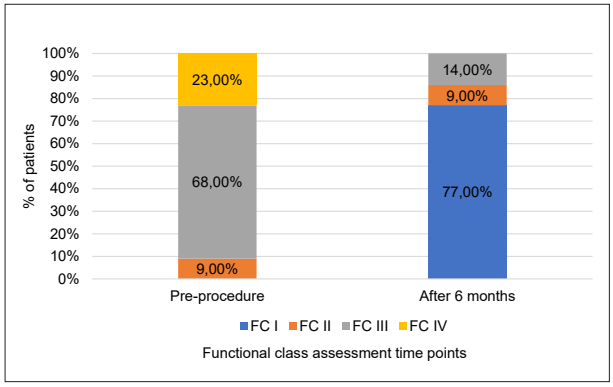

Figure 1 – *Percentage distribution of patients with FC I, II, III and IV before and after 6 months of the RFSA procedure. FC: functional class.*

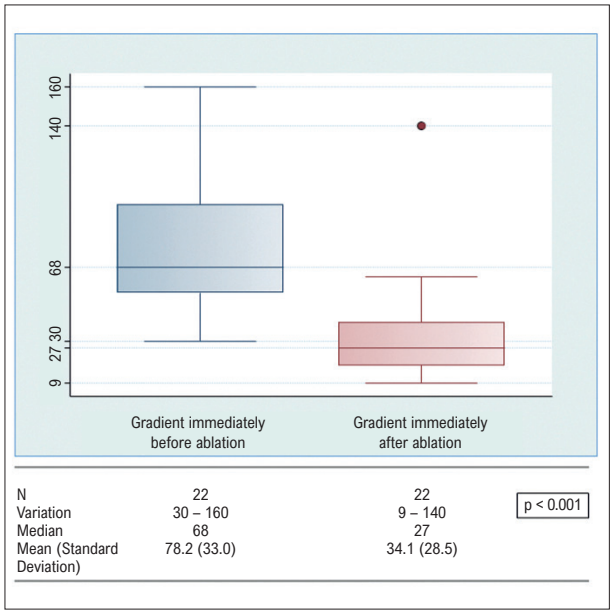

Figure 2 – *Gradients assesment immediately before and after RFSA.*

from the procedure, as demonstrated by improved FC in 100% of the patients, without the need for reintervention.

The results analysis showed that septa with a median of 18 mm tended to have greater success than those with a median of 15 mm. This can be explained by the fact that greater septal thicknesses are related to higher gradients, and the reduction becomes more noticeable in patients who already have greater gradients.

Over the course of six months, the analysis of the septal diameter evolution was influenced by the loss of data, but there was no significant change during this period. These findings suggest that the gradient reduction probably occurs due to the lower motility of the septal segment treated by radioablation, rather than a reduction in its thickness.

Study Limitations

This was a retrospective study with a short follow-up period. As a retrospective study, we acknowledge that including a validated quality of life questionnaire pre- and post-procedure (six months) would have provided additional insight beyond NYHA FC. Likewise, the six-minute walk test and cardiopulmonary test would have offered quantitative parameters, which would certainly contribute more valuable data.

The sample size was small, which limits statistical correlation. The small sample size and retrospective design restricted our ability to perform comparative analyses with other established methods, such as alcohol septal ablation or surgical myectomy.

Since data were obtained from medical records, some cases were excluded due to incomplete information.

Conclusion

RFSA is an effective and safe technique in the invasive management of HOCM. The procedure allows for a significant reduction in intraventricular gradient, improvement in FC, and maintenance of results in short-term follow-up.

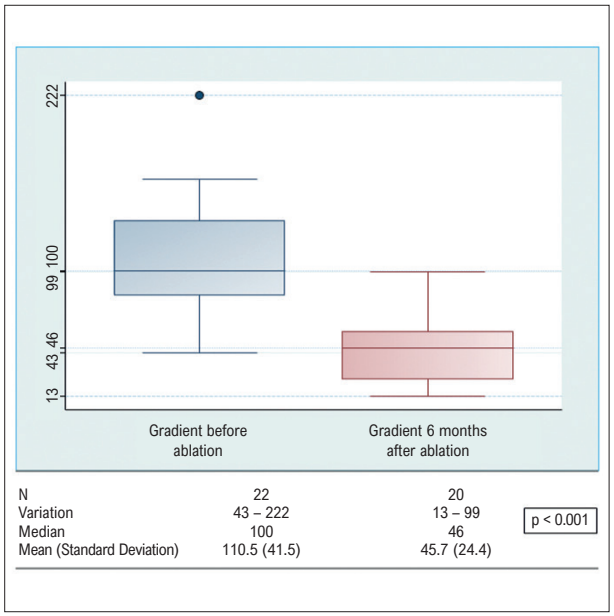

Figure 3 – *Gradients assesment before and after 6 months of the RFSA procedure.*

Multicenter studies comparing RFSA to traditional invasive techniques, with long-term follow-up, are required for this new modality to be considered an alternative for invasive management in HOCM, as outlined in the guidelines.

Author Contributions

Conception and design of the research: Vilela AA, Valdigem BP, Correia EB; acquisition of data: Vilela AA, Shinzato MH, Valdigem BP, Paladino AT, Correia EB; analysis and interpretation of the data, statistical analysis and writing of the manuscript: Vilela AA, Shinzato MH, Valdigem BP; critical revision of the manuscript for intellectual content: Vilela AA, Shinzato MH, Valdigem BP, Paladino AT, Correia EB, Assef JE.

Potential Conflict of Interest

No potential conflict of interest relevant to this article was reported.

Sources of Funding

There were no external funding sources for this study.

Table 6 – Gradient in the pre- and post-intraprocedural time points and at 6 months

Time points	Pre	Post	Absolute Dif. [95% CI]	Relative Reduction % [95% CI]	p-value
Intraprocedural	78.2 ± 33.1	34.1 ± 28.5	-44.1 [-53.3; -34.9]	58.9 [51.1; 66.7]	<0.001
Outpatient	110.5 ± 41.5	45.7 ± 24.4	-60.9 [-80.7; -41.1]	52.0 [38.2; 65.8]	<0.001

CI: Confident interval.

Table 7 – Proportion of patients who reduced gradients comparing pre and immediate post, and comparing pre-outpatient and 6-months post-outpatient

Endpoints	Total
Pre- and Post-Immediate Intraoperative	
Immediate gradient reduction ≥ 50%	16/22 (72.7%)
Post-immediate gradient ≤ 50 mmHg	19/22 (86.4%)
Post-immediate gradient ≤ 30 mmHg	12/22 (54.5%)
Gradient reduction ≥ 50% and Post-immediate gradient ≤ 50 mmHg	16/22 (72.7%)
Gradient reduction ≥ 50% of Post-immediate gradient ≤ 30 mmHg	12/22 (54.5%)
Pre-Outpatient and 6-Months Post-Outpatient	
Gradient reduction in 6 months ≥ 50%	12/20 (60.0%)
Gradient after 6 months ≤ 50 mmHg	12/20 (60.0%)
Gradient after 5 months ≤ 30 mmHg	7/20 (35.0%)
Gradient reduction in 6 months ≥ 50% and after 6 months gradient ≤ 50 mmHg	9/20 (45.0%)
Gradient reduction in 6 months ≥ 50% and after 6 months gradient ≤ 30 mmHg	6/20 (30.0%)

Table 8 – Distribution of septum measurements according to success group

SUCCESS	SEPTUM						
	Category	N	Variation	Median	Mean (SD)		p-value
Immediate gradient dropped MORE than 50%	No	6	15 – 18	15	15.8	(1.3)	0.050
	Yes	16	13 – 32	18	19.6	(5.0)	
Immediate gradient dropped BELOW 50%	No	3	15 – 18	15	16.0	(1.7)	0.300
	Yes	19	13 – 32	17	19.0	(4.8)	
Immediate gradient dropped BELOW 30%	No	10	15 – 27	16	17.9	(4.2)	0.421
	Yes	12	13 – 32	17.5	19.2	(5.0)	
Immediate gradient dropped more than 50% and BELOW 50 mmHg	No	6	15 – 18	15	15.8	(1.3)	0.050
	Yes	16	13 – 32	18	9.6	(5.0)	
Immediate gradient dropped more than 50% and BELOW 30 mmHg	No	10	15 – 27	16	17.9	(4.2)	0.421
	Yes	12	13 – 32	17.5	19.2	(5.0)	
Success 6 months gradient DROPPED more than 50%	No	8	16 – 32	19	20.6	(5.2)	0.137
	Yes	12	13 – 27	16.5	17.8	(4.2)	
Success Gradient 6 months BELOW 50%	No	8	13 – 23	17.5	17.5	(3.1)	0.506
	Yes	12	15 - 32	17.5	19.9	(5.4)	
Success Gradient 6 months DROPPED Below 30 mmHg	No	13	13 – 32	18	19.1	(5.1)	0.984
	Yes	7	15 – 27	17	18.7	(4.1)	
Success gradient 6 months dropped > 50% and below 50 mmHg	No	11	13 – 32	18	19.2	(5.1)	0.751
	Yes	9	15 – 27	17	18.7	(4.4)	
Success gradient 6 months dropped > 50% and below 30 mmHg	No	14	13 – 32	17.5	18.9	(5.0)	0.889
	Yes	6	15 – 27	17.5	19.0	(4.4)	

SD: Standard Deviation. P-value obtained by the Mann-Whitney U test.

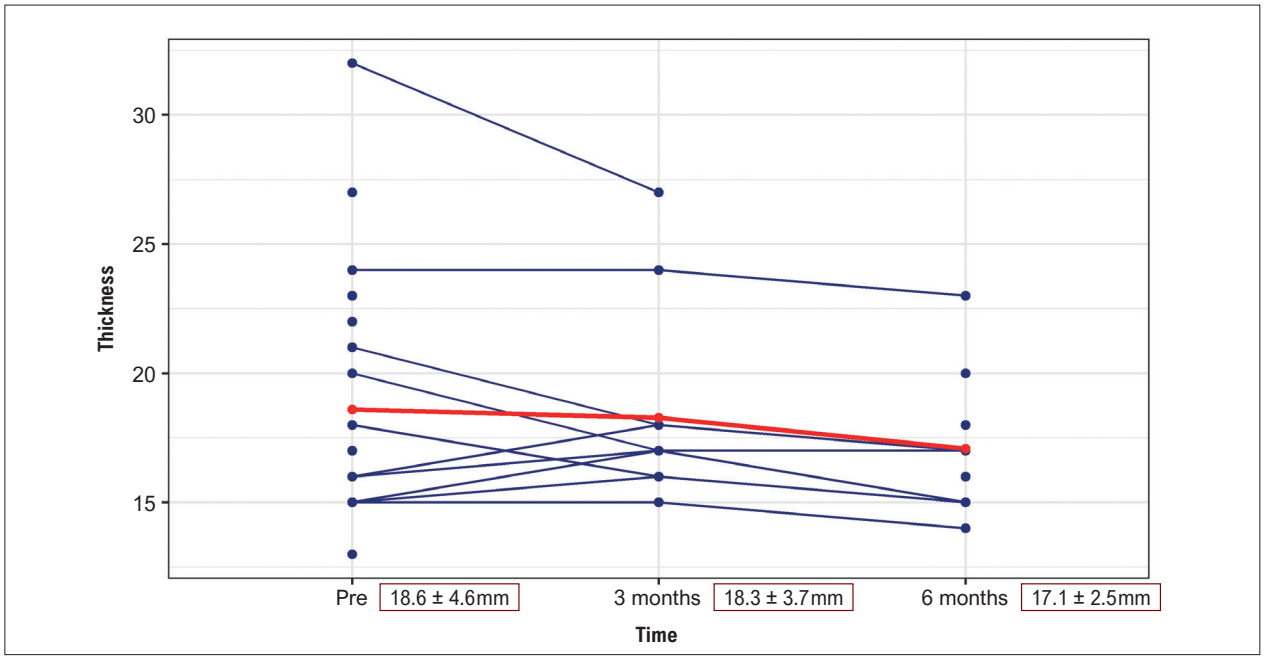

Figure 4 – *Profile graph of the septal thickness evolution (mean and standard deviation) over time.*

Study Association

This article is part of the thesis of Doctoral submitted by Mariane Higa Shinzato, from Dante Pazzanese Institute/São Paulo University.

Ethics Approval and Consent to Participate

This study was approved by the Ethics Committee of the Dante Pazzanese Heart Institute under the protocol number 5133. All the procedures in this study were in accordance with the 1975 Helsinki Declaration, updated in 2013. Informed consent was obtained from all participants included in the study.

Use of Artificial Intelligence

The authors did not use any artificial intelligence tools in the development of this work.

Availability of Research

The underlying content of the research text is contained within the manuscript.

References

1. Maron BJ. Hypertrophic Cardiomyopathy. Lancet. 1997;350(9071):127-33. doi: 10.1016/S0140-6736(97)01282-8.
2. Howell N, Bradlow W. Surgical Management of Left Ventricular Outflow Obstruction in Hypertrophic Cardiomyopathy. Echo Res Pract. 2015;2(1):37-44. doi: 10.1530/ERP-15-0005.
3. Bazan SGZ, Oliveira GO, Silveira CFSMP, Reis FM, Malagutte KNDS, Tinasi LSN, et al. Hypertrophic Cardiomyopathy: A Review. Arq Bras Cardiol. 2020;115(5):927-35. doi: 10.36660/abc.20190802.
4. Elliott PM, Anastasakis A, Borger MA, Borggrefe M, Cecchi F, Charron P, et al. 2014 ESC Guidelines on Diagnosis and Management of Hypertrophic Cardiomyopathy: The Task Force for the Diagnosis and Management of Hypertrophic Cardiomyopathy of the European Society of Cardiology (ESC). Eur Heart J. 2014;35(39):2733-79. doi: 10.1093/eurheartj/ehu284.
5. Maron BJ, Ommen SR, Semsarian C, Spirito P, Olivotto I, Maron MS. Hypertrophic Cardiomyopathy: Present and Future, with Translation Into Contemporary Cardiovascular Medicine. J Am Coll Cardiol. 2014;64(1):83-99. doi: 10.1016/j.jacc.2014.05.003.
6. Maron MS, Maron BJ. Hypertrophic Cardiomyopathy - Authors' Reply. Lancet. 2013;381(9876):1457-8. doi: 10.1016/S0140-6736(13)60922-8.
7. Maron BJ. Hypertrophic Cardiomyopathy: A Systematic Review. JAMA. 2002;287(10):1308-20. doi: 10.1001/jama.287.10.1308.
8. Bittencourt MI, Rocha RM, Albanesi FM Filho. Hypertrophic Cardiomyopathy. Rev Bras Cardiol. 2010;23(1):17-24.
9. Cooper RM, Shahzad A, Hasleton J, Digiovanni J, Hall MC, Todd DM, et al. Radiofrequency Ablation of the Interventricular Septum to Treat Outflow Tract Gradients in Hypertrophic Obstructive Cardiomyopathy: A Novel Use of CARTOSound® Technology to Guide Ablation. Europace. 2016;18(1):113-20. doi: 10.1093/europace/euv302.
10. Valdigem BP, Correia EB, Moreira DAR, Bihan DL, Pinto IMF, Abizaid AAC, et al. Septal Ablation with Radiofrequency Catheters Guided by Echocardiography for Treatment of Patients with Obstructive Hypertrophic Cardiomyopathy: Initial Experience. Arq Bras Cardiol. 2022;118(5):861-72. doi: 10.36660/abc.20200732.

Radiofrequency in Obstructive Hypertrophic Cardiomyopathy: The Role of Imaging in the Assessment of Septal Thickness and Gradient Reduction

Alexandre Costa Souza,[1,2] *Marcus Vinicius Silva Freire de Carvalho*[1,2]

Hospital São Rafael/ Rede D'Or,[1] *Salvador, BA – Brazil*

Instituto D'Or de ensino e pesquisa,[2] *Idor, Salvador, BA – Brazil*

Short editorial referring to the article: Hypertrophic Cardiomyopathy: Analysis Of Septal Thickness With Gradient Reduction In Patients Undergoing Radiofrequency Septal Ablation

Obstructive hypertrophic cardiomyopathy (HCM) is a genetic disorder characterized by pronounced myocardial hypertrophy and varying degrees of fibrosis. The obstruction of the left ventricular outflow tract (LVOT) is an anatomical condition with dynamic behavior that can lead to symptoms such as exercise intolerance and reduced functional class, and is also associated with cases of sudden cardiac death.[1]

The indication for invasive treatment aimed at reducing the intraventricular gradient is reserved for symptomatic patients — those who are refractory to medical therapy — with a gradient ≥ 50 mmHg. Common interventional therapies for this condition include surgical myectomy or, in a less invasive approach, alcohol septal ablation of coronary septal branches. However, these interventions have shown highly variable outcomes in the literature and remain infrequently used in clinical practice.[2,3]

In view of this scenario, catheter-based radiofrequency septal ablation (RFSA), using electroanatomical mapping for improved characterization of the interventricular septum, has been increasingly investigated as a less invasive therapeutic alternative with greater potential for lesion extent control.[4]

In this context, detailed echocardiographic evaluation is essential for procedural selection and follow-up, assessing morphological aspects (distribution of hypertrophy and degree of septal thickening) and functional/hemodynamic aspects (LVOT obstruction, systolic anterior motion of the mitral valve, and consequent mitral regurgitation).[5] Moreover, it enables the diagnosis of potential complications and aids in monitoring the clinical course of patients undergoing interventional therapies, including RFSA.[2,4]

The study by Vilela et al.,[6] published in this issue of *ABC Imagem Cardiovascular*, evaluated 22 patients diagnosed with obstructive HCM who underwent RFSA, aiming to correlate septal thickness with the hemodynamic response achieved through the procedure. To this end, the authors used transthoracic echocardiography for pre-procedural assessments and six-month follow-up, as well as transesophageal echocardiography for intra-procedural measurements.

The primary endpoint was the reduction of the maximal intraventricular gradient, as measured by continuous-wave Doppler at the LVOT. Procedural success was defined by composite criteria: an immediate gradient reduction of ≥ 50%, maintenance of the reduced gradient at six months, and improvement in functional class according to the NYHA classification. In the immediate post-procedural period, 72.7% of patients achieved the proposed gradient reduction, and 60% maintained this result during outpatient follow-up. A significant improvement in functional class was also observed throughout the follow-up period.

The authors found that patients with septal thickness ≥ 18 mm had significantly higher immediate success rates ($p = 0.050$) compared to those with an average thickness of 15 mm. However, no significant reduction in septal thickness was observed over time, suggesting that the gradient reduction was more likely related to functional modification of the treated segment rather than anatomical remodeling. Nonetheless, these findings should be interpreted with caution, given the small sample size ($n = 22$), which limits the generalization of results and restricts subgroup analysis of specific clinical or anatomical profiles.

The results of this study highlight the crucial contribution of cardiovascular imaging, particularly echocardiography, in supporting invasive decision-making in patients with HCM. Septal thickness measurement, accurate documentation of the intraventricular gradient, and functional assessment over time together provide a robust set of data, strengthening the clinical application of RFSA as an emerging therapeutic strategy. Although limited by sample size, the findings reinforce the technical feasibility of the method and its association with favorable clinical outcomes. In a context of ongoing advances in structural therapies, the integration of clinical reasoning with imaging modalities remains central to individualized case selection and management.

Despite the positive findings, the small sample size and retrospective design limit the generalizability of the results. The lack of direct comparison with traditional invasive techniques, such as surgical myectomy or alcohol septal ablation, also prevents definitive conclusions regarding the superiority or equivalence of the method. Prospective, randomized studies with long-term follow-up and objective criteria for clinical and functional success are essential to firmly establish RFSA within the therapeutic algorithm for HCM. The evolution of imaging techniques and their integration with electrophysiology represent a promising pathway toward the individualization of invasive approaches.

Keywords

Radiofrequency Ablation;Cardiomyopathies; Left Ventricular Outflow Obstruction

Mailing Address: Marcus Vinicius Silva Freire de Carvalho •
Hospital São Rafael. Avenida São Rafael, 2152. Postal code: 41253-190. São Marcos, Salvador, BA – Brazil
E-mail: marcusviniciusfrc@hotmail.com

DOI: https://doi.org/10.36660/abcimg.20250024i

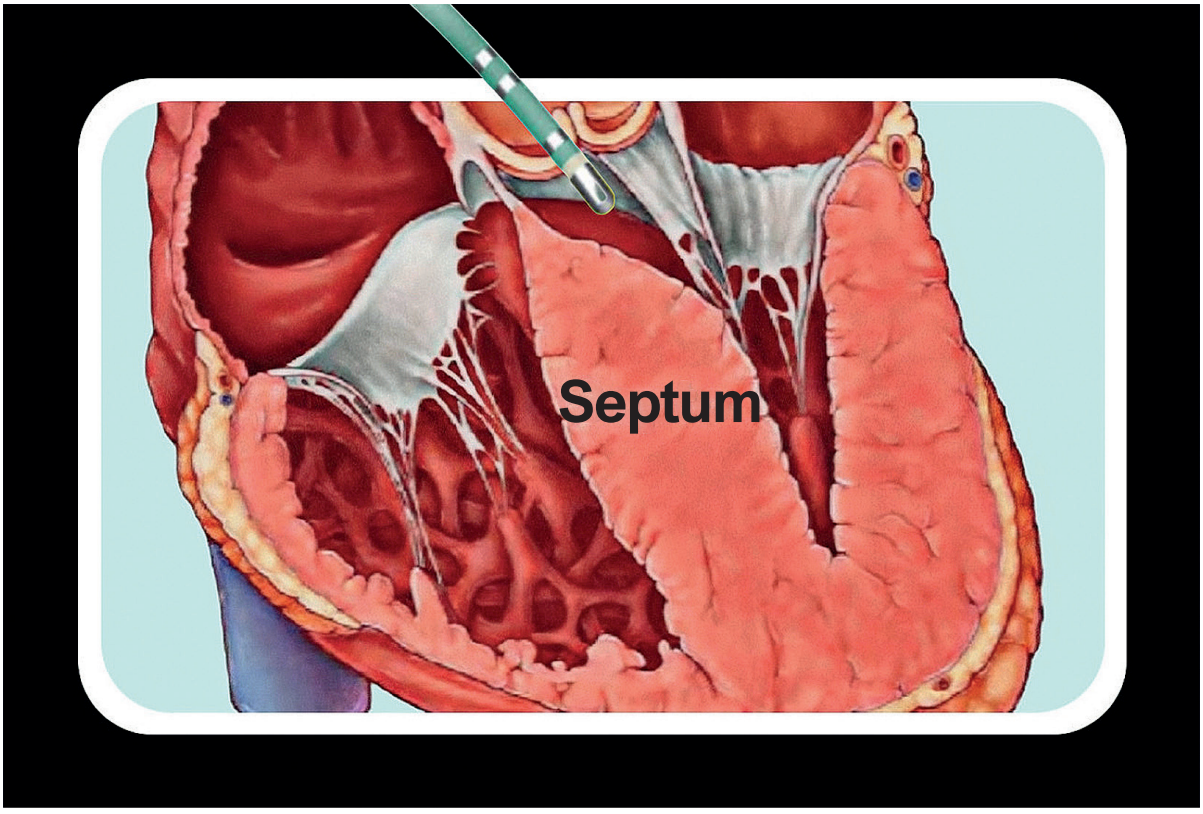

Figure 1 – *Schematic illustration of the catheter-based approach for RFSA, highlighting the thickened interventricular septum frequently involved in LVOT obstruction in obstructive HCM. The image shows the position of the ablation catheter relative to the mitral valve apparatus and the LV outflow tract, the target region for RFSA therapy.*

References

1. Maron BJ, Ommen SR, Semsarian C, Spirito P, Olivotto I, Maron MS. Hypertrophic Cardiomyopathy: Present and Future, with Translation Into Contemporary Cardiovascular Medicine. J Am Coll Cardiol. 2014;64(1):83-99. doi: 10.1016/j.jacc.2014.05.003.
2. Ommen SR, Mital S, Burke MA, Day SM, Deswal A, Elliott P, et al. 2020 AHA/ACC Guideline for the Diagnosis and Treatment of Patients with Hypertrophic Cardiomyopathy: A Report of the American College of Cardiology/American Heart Association Joint Committee on Clinical Practice Guidelines. J Am Coll Cardiol. 2020;76(25):159-240. doi: 10.1016/j.jacc.2020.08.045.
3. Elliott PM, Anastasakis A, Borger MA, Borggrefe M, Cecchi F, Charron P, et al. 2014 ESC Guidelines on Diagnosis and Management of Hypertrophic Cardiomyopathy: the Task Force for the Diagnosis and Management of Hypertrophic Cardiomyopathy of the European Society of Cardiology (ESC). Eur Heart J. 2014;35(39):2733-79. doi: 10.1093/eurheartj/ehu284.
4. Valdigem BP, Correia EB, Moreira DAR, Bihan DL, Pinto IMF, Abizaid AAC, et al. Septal Ablation with Radiofrequency Catheters Guided by Echocardiography for Treatment of Patients with Obstructive Hypertrophic Cardiomyopathy: Initial Experience. Arq Bras Cardiol. 2022;118(5):861-72. doi: 10.36660/abc.20200732.
5. Gersh BJ, Maron BJ, Bonow RO, Dearani JA, Fifer MA, Link MS, et al. 2011 ACCF/AHA Guideline for the Diagnosis and Treatment of Hypertrophic Cardiomyopathy: A Report of the American College of Cardiology Foundation/American Heart Association Task Force on Practice Guidelines. Developed in Collaboration with the American Association for Thoracic Surgery, American Society of Echocardiography, American Society of Nuclear Cardiology, Heart Failure Society of America, Heart Rhythm Society, Society for Cardiovascular Angiography and Interventions, and Society of Thoracic Surgeons. J Am Coll Cardiol. 2011;58(25):212-60. doi: 10.1016/j.jacc.2011.06.011.
6. Vilela AA, Shinzato MH, Valdigem B, Paladino Filho AT, Correia EB, Assef JE. Cardiomiopatia Hipertrófica: Análise da Espessura Septal com a Redução do Gradiente em Pacientes Submetidos à Ablação Septal por Radiofrequência. Arq Bras Cardiol: Imagem cardiovasc. 2025;38(2):e20240097. doi: 10.36660/abcimg.20240097.

Original Article

Conventional and Partially ECG-Gated Triple Rule-Out Computed Tomography Angiography with Extension to Abdominal Aorta: Comparative Radiation Dose and Imaging Quality

Pamela Bertolazzi,[1] Carla Franco Greco Silva,[1] Leonardo Iunes,[1] Fernando Freitas de Oliveira,[1] Fabio Payão Pereira,[1] Publio Cesar Cavalcanti Viana,[1] Isac Castro,[1] Natally Horvat,[2] José Arimateia Batista Araújo-Filho[1]

Hospital Sírio-Libanês,[1] São Paulo, SP – Brazil

Mayo Clinic,[2] Rochester – USA

Abstract

Background: **Triple rule-out (TRO) computed tomography angiography (CTA) is an ECG-gated protocol that enables the simultaneous evaluation of the coronary arteries, thoracic aorta, and pulmonary arteries in a single scan. It is especially useful for patients in the emergency department with low to moderate risk of acute coronary syndrome, particularly when aortic dissection and pulmonary embolism are also considered in the differential diagnosis.**

Objective: **This study aimed to compare two TRO protocols, fully electrocardiogram (ECG)-gated (protocol A) and partially ECG-gated (protocol B), both including coverage of the abdominal aorta, in terms of radiation dose and image quality. Such a comparison of protocols can be useful when iterative reconstruction algorithms are not available and a manual transition between partially ECG-synchronized protocols is required.**

Methods: **Radiation dose was evaluated using dose-length product (DLP), effective dose (ED), and virtual dose. Attenuation values were measured in the coronary and pulmonary arteries, as well as in the descending and abdominal aorta. Image quality and vessel conspicuity were assessed using a 5-point Likert scale.**

Results: **A total of 56 patients were included. Protocol B demonstrated significantly lower radiation exposure compared to protocol A across all metrics: median DLP (1.1 mSv [interquartile range: 0.9 to 1.1] versus 2.2 mSv [interquartile range: 1.6 to 2.8]), ED (17.0 mSv [interquartile range: 14.3 to 18.1] versus 32.6 mSv [interquartile range: 24.4 to 42.7]), and virtual dose (16.2 [interquartile range: 9.3 to 20.4] versus 34.7 [interquartile range: 19.9 to 43.5]); all differences were statistically significant ($p < 0.001$). There were no significant differences in attenuation measurements or qualitative image assessment between the two protocols.**

Conclusion: **Partially ECG-gated TRO CTA provides comparable image quality to the fully ECG-gated technique while significantly reducing radiation exposure, becoming a more radiation dose-efficient alternative when iterative reconstruction algorithms are not available and manual transition is necessary.**

Keywords: **Electrocardiography; Drug Tapering; Radiation Dose-Response Relationship.**

Introduction

Chest pain is one of the most frequent reasons for emergency rooms visits worldwide. Its differential diagnosis is broad, encompassing both cardiac causes (particularly coronary artery disease) and non-cardiac conditions such as aortic dissection and pulmonary embolism. Cardiovascular disorders may be present in up to 20% of patients,[1] with acute coronary syndrome as the most feared condition. A prompt and accurate diagnosis is critical to reducing morbidity and mortality in patients presenting with chest pain. However, distinguishing those who require urgent hospitalization from those with benign conditions who can be safely discharged remains a common challenge in clinical practice.

In this context, computed tomography angiography (CTA) can expedite the evaluation of patients with chest pain by effectively ruling out acute coronary syndrome, offering a high negative predictive value.[2,3] Advances in CT technology and contrast injection protocols have further enabled the implementation of triple rule-out (TRO) CTA.[4] TRO CTA is an electrocardiogram (ECG)-gated protocol that enables the simultaneous evaluation of the coronary arteries, thoracic aorta, and pulmonary arteries in a single scan. It is currently regarded as a cost-effective diagnostic tool for patients in the emergency department with low to moderate risk of acute coronary syndrome,[2] particularly when aortic dissection and pulmonary embolism are also considered in the differential diagnosis.[5,6] However, before

Mailing Address: José Arimateia Batista Araújo-Filho •
Hospital Sírio-Libanês. Adma Jafet. Postal code: 01308-050. São Paulo, SP – Brazil
E-mail: ariaraujocg@gmail.com
Manuscript received April 26, 2025; revised May 5, 2025; accepted May 5, 2025
Editor responsible for the review: Marcelo Tavares

DOI: https://doi.org/10.36660/abcimg.20250025i

Central Illustration: Conventional and Partially ECG-Gated Triple Rule-Out Computed Tomography Angiography with Extension to Abdominal Aorta: Comparative Radiation Dose and Imaging Quality

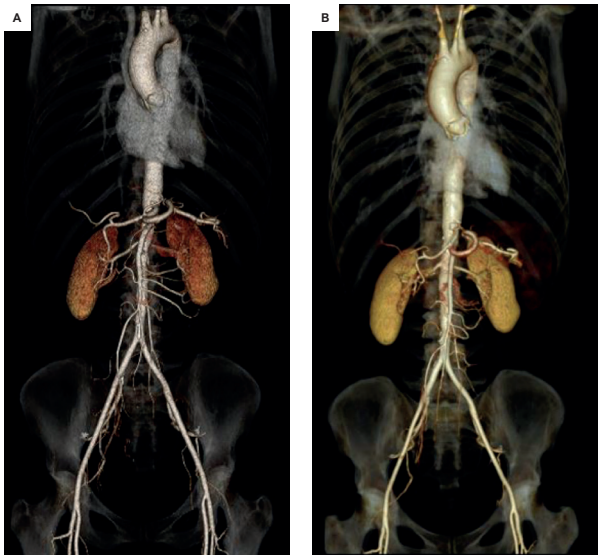

Arq Bras Cardiol: Imagem cardiovasc. 2025;38(2):e20250025

Three-dimensional volume-rendering CTA reconstructions of the same patient showing no significant difference in the overall image quality between fully (A) and partially (B) ECG-gated TRO scans.

implementing TRO CTA, it is essential to consider radiation exposure and technical scanning parameters, as these factors can present challenges depending on the operational capabilities of the available CT system.

Various CT systems can be used to perform the TRO CTA protocol, including 64-slice and 128-slice multidetector scanners, as well as dual-source systems. These typically employ retrospective ECG-gating to enhance coronary arteries visualization. However, the use of expanded anatomic coverage and small pitch values is associated with a significant increase in mean radiation dose.[7,8] Additionally, contrast injection protocols and scan techniques for TRO CTA vary widely across institutions, often leading to inconsistent image quality.[9] Given these challenges, it is essential to maintain high image quality while minimizing radiation exposure.

In recent years, several strategies have been proposed to address this issue.[4,10-14] Ketelsen et al.,[15] for instance, demonstrated a significant reduction in radiation dose using prospective ECG-gated acquisition compared to the traditional retrospective approach. Other studies have explored dose reduction through technical optimizations, such as tube current modulation.[14] To date, existing studies on radiation dose reduction in TRO CTA have not included full coverage of the abdominal aorta, potentially limiting the evaluation of descending aortic dissections. In this context, the aim of our study was to compare radiation dose and diagnostic image quality between two TRO CTA protocols, one using full (protocol A) and the other partial (protocol B) ECG-gating, with both extending to the abdominal aorta.

Materials and methods

Study population

This prospective study was approved by the institutional review board, and informed consent was obtained from all participants. Consecutive patients presenting with chest pain between January and June 2018 and referred for TRO CTA with abdominal aorta extension were enrolled to undergo the partially ECG-gated protocol (protocol B). Inclusion criteria consisted of having previously undergone a fully ECG-gated protocol (protocol A) at our institution within the past 5 years. Patients with contraindications to contrast-enhanced CT, as defined by institutional guidelines, were excluded.

TRO computed tomography

All TRO CTA exams were performed on a single-source 128-slice scanner (SOMATOM Definition AS+, Siemens, Erlangen, Germany) equipped with SAFIRE (sinogram-affirmed iterative reconstruction) technology, using retrospective ECG-gating. Scans were acquired with patients in the supine position (feet first), arms raised, and during breath-hold (apnea) lasting 8 to 20 seconds, depending on body habitus.

Scan parameters included a detector collimation of 128 × 0.6 mm, slice thickness of 0.6 mm, and a gantry rotation time of 0.3 seconds. For both protocols, automatic exposure

control systems (CAREDose 4D for tube current modulation and CAREkV for tube voltage optimization) were activated.

- Protocol A (fully ECG-gated): tube voltage of 120 kV and reference tube current (mAs reference) of 210 mAs.
- Protocol B (partially ECG-gated): two sequential acquisitions:
  - Thoracic aorta phase (ECG-gated): 120 kV, 160 mAs reference, with CAREDose 4D.
  - Abdominal aorta phase (non-ECG-gated): same voltage and mAs settings.
- Table 1 summarizes the main differences between protocols A and B.
- Reconstruction parameters were as follows:
- Chest: 1.0 mm thickness, 0.7 mm increment, D30f medium smooth filter, mediastinal window.
- Aorta (full extent): 1.0 mm thickness, 0.7 mm increment, I26f smooth filter, angiographic window.
- Coronary arteries: 0.6 mm thickness, 0.3 mm increment, D30f filter, angiographic window.

An electromechanical injector pump was used to administer 150 mL of non-ionic iodinated contrast (Omnipaque® 300, Iohexol 300 mg/mL; GE Healthcare, USA) at a flow rate of 4 mL/s. Scan initiation was controlled via bolus tracking software, with a region of interest (ROI) placed in the abdominal aorta.

Radiation dose

Radiation dose was assessed using the dose-length product (DLP) and effective dose (ED), expressed in millisieverts (mSv), calculated according to the European Commission's conversion factors. In addition, organ-specific doses were estimated using VirtualDose™ (Virtual Phantoms Inc., Albany, USA), a tool based on anatomically realistic computational phantoms representing pediatric, pregnant, and adult patients with varying body sizes and morphologies.[16]

Image evaluation

The image sets were anonymized and randomly ordered for review. A board-certified abdominal radiologist with 10 years of experience, blinded to the scan protocol, independently evaluated all examinations for both quantitative and qualitative image analysis.

Attenuation measurements were performed on a post-processing PACS workstation (Carestream Health, Rochester, USA) at four predefined anatomical locations: pulmonary trunk, descending aorta, anterior descending coronary artery, and abdominal aorta. Circular ROIs were manually placed at the center of each vessel with the following dimensions: 0.6 × 0.5 cm (pulmonary trunk), 0.6 × 0.5 cm (descending aorta), 0.1 × 0.1 cm (anterior descending coronary artery), and 0.6 × 0.5 cm (abdominal aorta), as illustrated in Figure 1.

Subjective assessment of image quality was performed using a five-point Likert scale,[17] where 1 = excellent, 2 = good, 3 = sufficient, 4 = suboptimal, and 5 = unsatisfactory.

Table 1 – TRO CTA parameters at our institution

Parameter	Protocol A	Protocol B
Collimation detector (mm)	128 × 0.6	128 × 0.6
Rotation time (s)	0.3	0.3
Tube voltage (kVp)	120	120
mAs reference	210	160

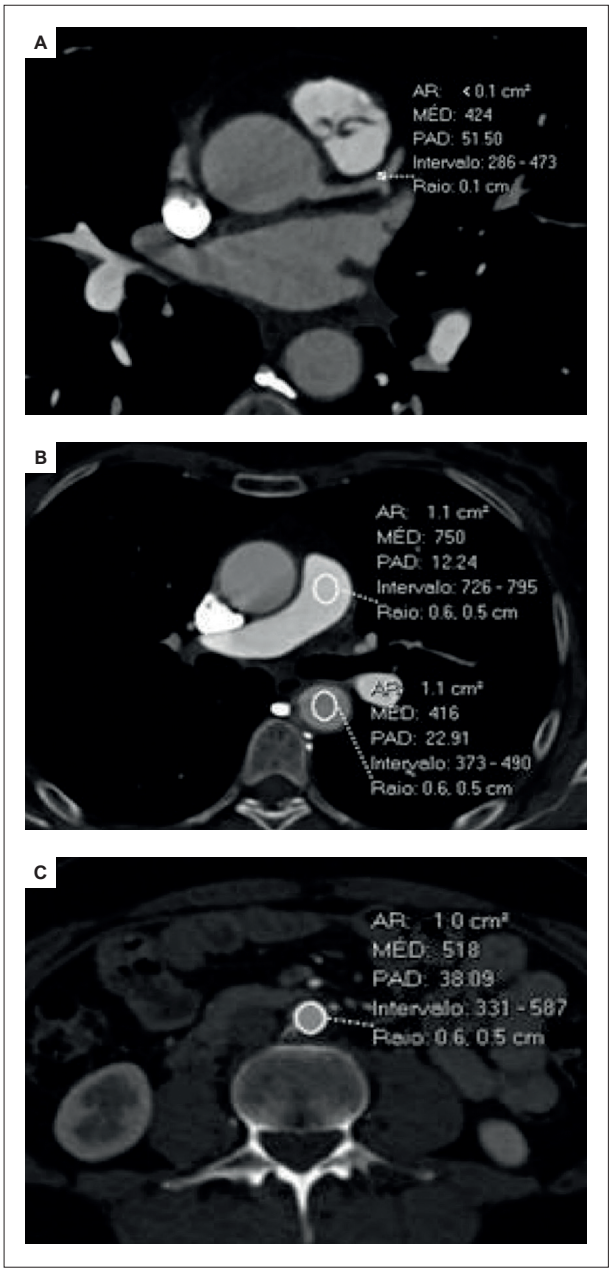

Figure 1 – *CTA in axial plane demonstrating the 4 predefined circle regions of interest to assess the attenuation measurements in the anterior descending coronary artery (A), pulmonary trunk and descending aorta (B), and abdominal aorta (C).*

The radiologist also rated the conspicuity of key thoracic and abdominal vascular structures, including pulmonary trunk, lobar and segmental pulmonary arteries, aortic arch, descending aorta, aortic valve, left coronary trunk, right coronary artery, circumflex artery, celiac trunk, superior and inferior mesenteric arteries, right and left renal arteries, and right and left iliac arteries. Additionally, image quality of relevant findings such as coronary stents and aortic endoprostheses was assessed.

Table 2 – Patient characteristics

Characteristics	Total (N = 56) Median (IQR or %)
Sex (male/female)	38/18 (68%/32%)
Age (years)	66 (59-70)
BMI (kg/m^2)	23.5 (21.0-25.9)
Interval between protocol A and B (months)	24 (14.2-33.3)

BMI: body mass index; IQR: interquartile range.

Table 3 – Radiation doses of protocol A and B

	Protocol A	Protocol B	p
Dose length product, median (IQR)	2.2 (1.6-2.8)	1.1 (0.9-1.1)	< 0.001
ED, median (IQR)	32.6 (24.4-42.7)	17.0 (14.3-18.1)	< 0.001

IQR: interquartile range; ED: effective dose.

Table 4 – Arterial attenuation in Hounsfield unit measurements in protocols A and B

	Protocol A	Protocol B	p
Ascending aorta, median (IQR)	432 (377-390)	439 (387-500)	0.601
Descending aorta, median (IQR)	399 (346-458)	405 (363-451)	0.890
Abdominal aorta, median (IQR)	406 (364-475)	393 (335-456)	0.486
Pulmonary trunk, median (IQR)	460 (387-551)	477 (416-531)	0.835

IQR: interquartile range.

Statistical analysis

Continuous variables were presented as medians with interquartile ranges (IQR), while categorical variables were expressed as counts and proportions. Comparisons between protocols A and B were performed using either Student's t-test or the Wilcoxon rank-sum test, depending on data distribution. A p value < 0.05 was considered statistically significant. All statistical analyses were conducted using SPSS software (version 22.0, IBM Corp.). The statistical methodology was reviewed by an independent statistician.

Results

The final study population included 56 patients, of whom 38 (68%) were men, with a median age of 66 years (IQR: 59 to 70). The median time interval between protocol A and protocol B was 24 months (IQR: 14.2 to 33.3). Patient characteristics are summarized in Table 2.

In terms of radiation dose, the median DLP for Protocol B was 1.1 mSv (IQR: 0.9 to 1.1), while for Protocol A it was 2.2 mSv (IQR: 1.6 to 2.8). The median ED for Protocol B was 17.0 mSv (IQR: 14.3 to 18.1), compared to 32.6 mSv (IQR: 24.4 to 42.7) for Protocol A. Both the DLP and ED values were significantly lower for protocol B compared to protocol A ($p < 0.001$). Additionally, the virtual dose

Table 5 – Comparison of subjective evaluation of overall imaging quality and conspicuity of the main thoracic and abdominal vessels

	p
Overall image quality	0.610
Pulmonary trunk	0.564
Lobular arteries	0.705
Segmental arteries	1.000
Aortic arch	0.317
Descending aorta	0.157
Aortic valve	0.107
Left coronary trunk	1.000
Right coronary artery	0.750
Circumflex artery	0.301
Celiac trunk	0.317
Superior mesenteric artery	1.000
Inferior mesenteric artery	1.000
Right renal artery	1.000
Left renal artery	1.000
Right iliac arteries	0.317
Left iliac arteries	0.317

for protocol B was significantly lower than for protocol A, 16.2 (IQR: 9.3 to 20.4) versus 34.7 (IQR: 19.9 to 43.5), respectively ($p < 0.001$), as shown in Table 3.

Regarding image evaluation, no significant differences were observed in the quantitative attenuation measurements of the ascending aorta, descending aorta, abdominal aorta, and pulmonary trunk between protocols A and B (Table 4). Similarly, no significant differences were found in the qualitative assessment of the conspicuity of the main thoracic and abdominal arteries or in the overall image quality between protocols A and B (Table 5 and Central Illustration).

Discussion

In our study population, the median DLP and ED were significantly lower in protocol B compared to protocol A, with a similarly significant reduction in virtual dose for protocol B. However, there were no significant differences between the two protocols regarding quantitative analysis of ROI measurements in the main thoracic and abdominal arteries or qualitative assessments of vessel conspicuity and overall image quality.

A previous study focusing solely on chest evaluation reported estimated ED values for retrospective ECG-gated TRO CTA ranging from 7.4 to 13.4 mSv for men and 10.1 to 17.5 mSv for women.[15] Another study also including only the chest, using a larger coverage scanner, demonstrated ED of 9.7 to 23.2 mSv, depending on the patient heart rate.[18] In comparison, our results for the partially ECG-gated TRO CTA protocol, which included the abdomen, showed an ED range of 14.3 to 18.1 mSv. This range is consistent with previous studies and has the added advantage of evaluating the abdominal aorta.

In recent years, equipment manufacturers have developed various acquisition protocols to combine thoracic and abdominal images in angiography scans. For example, some manufacturers have implemented automatic switching to non-gated scanning with a faster pitch for imaging the abdominal aorta. However, in certain CT units, automatic iterative reconstruction algorithms are unavailable, requiring manual transitions in partially ECG-gated protocols. This manual switch between gated and non-gated sequences can be time-consuming and may introduce reconstruction artifacts. The CT unit used in our study lacked the automatic iterative reconstruction algorithm, yet no significant loss in image quality was observed. Based on these findings, we strongly advocate for the incorporation of partially ECG-gated protocols when including the abdominal aorta, even in the absence of automatic switching.

Currently, TRO CTA is recognized as an important diagnostic tool for selected patients in the emergency department with acute chest pain.[19,20] However, there are no established guidelines outlining its clinical indications. Very few studies, like ours, have incorporated the abdominal aorta into the protocol to enhance the evaluation of the entire aorta when descending aortic dissections need to be ruled out. The clinical significance of our findings lies in the feasibility of including abdominal aorta scanning in a partially ECG-gated TRO CTA protocol, which provides additional diagnostic information without a substantial increase in effective radiation dose compared to previous thoracic-only studies.[7,8,15,18]

Several limitations of this study should be noted. First, imaging analysis was conducted by a single experienced radiologist, which precluded the assessment of interobserver agreement and may have introduced bias in the evaluation of image quality. Additionally, the impact of heart rate on image quality was not explored in a subgroup comparison. Lastly, we did not compare the procedural times for each protocol or the time required for image reconstruction. These aspects should be addressed in future studies. Furthermore, additional research is needed to assess the cost-benefit ratio of including abdominal scanning in TRO CTA for patients at different risk levels for aortic dissection.

In conclusion, our study demonstrates the feasibility of using a partially ECG-synchronized acquisition protocol as an effective strategy to reduce radiation dose compared to the fully ECG-synchronized technique in CCTA with TRO, when iterative reconstruction algorithms are not available. The proposed protocol maintained image quality, with scan extension to include the abdominal aorta, without loss of image quality when a manual transition between partially ECG-synchronized protocols is necessary.

Author Contributions

Conception and design of the research: Bertolazzi P, Horvat N; acquisition of data: Bertolazzi P, Silva CFG, Oliveira FF, Pereira FP, Viana PCC; analysis and interpretation of the data and critical revision of the manuscript for intellectual content: Horvat N, Araújo-Filho JAB; statistical analysis: Castro I; writing of the manuscript: Bertolazzi P, Silva CFG; Iunes L.

Potential Conflict of Interest

No potential conflict of interest relevant to this article was reported.

Sources of Funding

There were no external funding sources for this study.

Study Association

This study is not associated with any thesis or dissertation work.

Ethics Approval and Consent to Participate

This study was approved by the Ethics Committee of the Instituto de ensino e pesquisa sirio-libanes under the protocol number 2.445.680. All the procedures in this study were in accordance with the 1975 Helsinki Declaration, updated in 2013. Informed consent was obtained from all participants included in the study.

Use of Artificial Intelligence

The authors did not use any artificial intelligence tools in the development of this work.

Availability of Research Data

All datasets supporting the results of this study are available upon request from the corresponding author.

References

1. Hsia RY, Hale Z, Tabas JA. A National Study of the Prevalence of Life-Threatening Diagnoses in Patients with Chest Pain. JAMA Intern Med. 2016;176(7):1029-32. doi: 10.1001/jamainternmed.2016.2498.
2. Takakuwa KM, Halpern EJ. Evaluation of a "Triple Rule-Out" Coronary CT Angiography Protocol: Use of 64-Section CT in Low-to-Moderate Risk Emergency Department Patients Suspected of Having Acute Coronary Syndrome. Radiology. 2008;248(2):438-46. doi: 10.1148/radiol.2482072169.
3. Galperin-Aizenberg M, Cook TS, Hollander JE, Litt HI. Cardiac CT Angiography in the Emergency Department. AJR Am J Roentgenol. 2015;204(3):463-74. doi: 10.2214/AJR.14.12657.
4. Kim HS, Kim SM, Cha MJ, Kim YN, Kim HJ, Choi JH, et al. Triple Rule-Out CT Angiography Protocol with Restricting Field of View for Detection of Pulmonary Thromboembolism and Aortic Dissection in Emergency Department Patients: Simulation of Modified CT Protocol for Reducing Radiation Dose. Acta Radiol. 2017;58(5):521-7. doi: 10.1177/0284185116663044.
5. Burris AC 2nd, Boura JA, Raff GL, Chinnaiyan KM. Triple Rule Out versus Coronary CT Angiography in Patients with Acute Chest Pain: Results from the ACIC Consortium. JACC Cardiovasc Imaging. 2015;8(7):817-25. doi: 10.1016/j.jcmg.2015.02.023.
6. Gaspar T, Halon DA, Peled N. Advantages of Multidetector Computed Tomography Angiography in the Evaluation of Patients with Chest Pain. Coron Artery Dis. 2006;17(2):107-13. doi: 10.1097/00019501-200603000-00003.
7. Madder RD, Raff GL, Hickman L, Foster NJ, McMurray MD, Carlyle LM, et al. Comparative Diagnostic Yield and 3-Month Outcomes of "Triple Rule-Out" and Standard Protocol Coronary CT Angiography in the Evaluation of Acute Chest Pain. J Cardiovasc Comput Tomogr. 2011;5(3):165-71. doi: 10.1016/j.jcct.2011.03.008.
8. Manheimer ED, Peters MR, Wolff SD, Qureshi MA, Atluri P, Pearson GD, et al. Comparison of Radiation Dose and Image Quality of Triple-Rule-Out Computed Tomography Angiography between Conventional Helical Scanning and a Strategy Incorporating Sequential Scanning. Am J Cardiol. 2011;107(7):1093-8. doi: 10.1016/j.amjcard.2010.11.038.
9. Halpern EJ. Triple-Rule-Out CT Angiography for Evaluation of Acute Chest Pain and Possible Acute Coronary Syndrome. Radiology. 2009;252(2):332-45. doi: 10.1148/radiol.2522082335.
10. Chen Y, Wang Q, Li J, Jia Y, Yang Q, He T. Triple-Rule-Out CT Angiography Using Two Axial Scans with 16 cm Wide-Detector for Radiation Dose Reduction. Eur Radiol. 2018;28(11):4654-61. doi: 10.1007/s00330-018-5426-y.
11. Krissak R, Henzler T, Prechel A, Reichert M, Gruettner J, Sueselbeck T, et al. Triple-Rule-Out Dual-Source CT Angiography of Patients with Acute Chest Pain: Dose Reduction Potential of 100 kV Scanning. Eur J Radiol. 2012;81(12):3691-6. doi: 10.1016/j.ejrad.2010.11.021.
12. Takx RAP, Krissak R, Fink C, Bachmann V, Henzler T, Meyer M, et al. Low-Tube-Voltage Selection for Triple-Rule-Out CTA: Relation to Patient Size. Eur Radiol. 2017;27(6):2292-7. doi: 10.1007/s00330-016-4607-9.
13. Kidoh M, Nakaura T, Nakamura S, Namimoto T, Nozaki T, Sakaino N, et al. Contrast Material and Radiation Dose Reduction Strategy for Triple-Rule-Out Cardiac CT Angiography: Feasibility Study of Non-ECG-Gated Low kVp Scan of the Whole Chest Following Coronary CT Angiography. Acta Radiol. 2014;55(10):1186-96. doi: 10.1177/0284185113514886.
14. Takakuwa KM, Halpern EJ, Gingold EL, Levin DC, Shofer FS. Radiation Dose in a "Triple Rule-Out" Coronary CT Angiography Protocol of Emergency Department Patients Using 64-MDCT: The Impact of ECG-Based Tube Current Modulation on Age, Sex, and Body Mass Index. AJR Am J Roentgenol. 2009;192(4):866-72. doi: 10.2214/AJR.08.1758.
15. Ketelsen D, Fenchel M, Thomas C, Buchgeister M, Boehringer N, Tsiflikas I, et al. Estimation of Radiation Exposure of Retrospective Gated and Prospective Triggered 128-Slice Triple-Rule-Out CT Angiography. Acta Radiol. 2011;52(7):762-6. doi: 10.1258/ar.2010.100274.
16. Ding A, Gao Y, Liu H, Caracappa PF, Long DJ, Bolch WE, et al. VirtualDose: A Software for Reporting Organ Doses from CT for Adult and Pediatric Patients. Phys Med Biol. 2015;60(14):5601-25. doi: 10.1088/0031-9155/60/14/5601.
17. Likert R. Rensis Likert on Managing Human Assets. Bull Train. 1978;3(5):1-4.
18. Kang EJ, Lee KN, Kim DW, Kim BS, Choi S, Park BH, et al. Triple Rule-out Acute Chest Pain Evaluation Using a 320-Row-Detector Volume CT: A Comparison of the Wide-Volume and Helical Modes. Int J Cardiovasc Imaging. 2012;28(Suppl 1):7-13. doi: 10.1007/s10554-012-0072-y.
19. Si-Mohamed S, Greffier J, Bobbia X, Larbi A, Delicque J, Khasanova E, et al. Diagnostic Performance of a Low Dose Triple Rule-out CT Angiography Using SAFIRE in Emergency Department. Diagn Interv Imaging. 2017;98(12):881-91. doi: 10.1016/j.diii.2017.09.006.
20. Hiratzka LF, Bakris GL, Beckman JA, Bersin RM, Carr VF, Casey DE Jr, et. 2010 ACCF/AHA/AATS/ACR/ASA/SCA/SCAI/SIR/STS/SVM Guidelines for the Diagnosis and Management of Patients with Thoracic Aortic Disease: A Report of the American College of Cardiology Foundation/American Heart Association Task Force on Practice Guidelines, American Association for Thoracic Surgery, American College of Radiology, American Stroke Association, Society of Cardiovascular Anesthesiologists, Society for Cardiovascular Angiography and Interventions, Society of Interventional Radiology, Society of Thoracic Surgeons, and Society for Vascular Medicine. Circulation. 2010;121(13):e266-369. doi: 10.1161/CIR.0b013e3181d4739e.

"Triple Rule-Out": Including the Abdominal Aorta With a Clear Conscience?

Tiago A. Magalhães[1,2,3]

Complexo Hospital de Clínicas, Universidade Federal do Paraná (CHC-UFPR),[1] *Curitiba, PR – Brazil*
Hcor,[2] *São Paulo, SP – Brazil*
Hospital Sírio Libanês,[3] *São Paulo, SP – Brazil*

Short Editorial related to the article: Conventional and Partially ECG-Gated Triple Rule-Out Computed Tomography Angiography with Extension to Abdominal Aorta: Comparative Radiation Dose and Imaging Quality

The triple rule-out computed tomography angiography (TRO CTA) has been established as a valuable tool in the emergency care of patients with chest pain.[1,2] By allowing simultaneous assessment of the coronary arteries, thoracic aorta, and pulmonary arteries, this approach provides high diagnostic value, particularly in patients at low to intermediate risk of acute coronary syndrome, aortic dissection, and pulmonary thromboembolism. However, the main criticism of TRO CTA remains its significant radiation exposure,[3] especially when retrospective electrocardiographic synchronization techniques are used.

The study by Bertolazzi et al.[4] published in this issue contributes to this debate by comparing two TRO CTA protocols that include an extension to the abdominal aorta – one fully synchronized with the electrocardiogram (ECG) and a second partially (in chest images only) synchronized with the ECG. Although simple, the hypothesis is clinically relevant: would it be possible to maintain diagnostic image quality while significantly reducing radiation exposure with a partially ECG-synchronized protocol?

Less is More – Less Radiation Dose, More Patient Safety

The main strength of the study lies in its methodological approach. The authors selected patients who had previously undergone the TRO CTA protocol including the abdominal aorta with full electrocardiographic synchronization. After obtaining consent, they performed a new examination using the partial electrocardiographic synchronization protocol, enabling a robust comparison through a "matched case-control" model. This approach minimizes bias related to anatomical and technical variability among different individuals.

The results were interesting. The dose reduction was significant: the mean effective dose of the protocol with partial ECG synchronization was 47.9% lower than that of the protocol with full synchronization (17.0 mSv vs. 32.6 mSv, $p<0.001$). It is noteworthy that this reduction in radiation dose was not accompanied by a compromise in image quality. The quantitative assessment of attenuation values in critical vascular regions – such as the ascending aorta, descending aorta, abdominal aorta, and pulmonary trunk – showed no statistically significant differences. Similarly, the subjective qualitative evaluation demonstrated equivalence between the two protocols in terms of image quality of the assessed anatomical structures.

The present study also stands out for including the abdominal aorta in the acquisition, which is not commonly reported in previous publications on TRO CTA. This is particularly relevant as it expands the clinical utility of the exam by allowing a complete evaluation of the aorta when there is suspicion of descending dissections or abdominal involvement – a considerable diagnostic benefit, especially in emergency settings. At this point, however, a comment is warranted: although technically feasible and clinically useful, the TRO CTA protocol with extension to the abdominal aorta should be indicated with caution. The rational use of diagnostic resources should always guide our decisions. An examination evaluating multiple vascular territories, as presented, is only justified when there is clinical uncertainty or a real need to investigate all these segments. In other words, the fact that we can see more, with less radiation, does not mean we should always see everything.

Impact on clinical practice and future perspectives

The implementation of hybrid protocols with partial ECG synchronization represents a realistic and accessible alternative for institutions seeking to optimize their diagnostic workflows with safety and reduced radiation exposure. The study proposes a technical acquisition model that can be replicated by institutions already using TRO CTA and wishing to extend anatomical coverage without proportionally increasing radiation burden. The approach seems accessible and feasible for centers with 'intermediate' CT scanners, available in most major urban centers. Furthermore, the reduced radiation dose protocol should not negatively impact patient flow, exam execution time, or image reconstruction and post-processing times compared to the conventional strategy.

Despite the clear benefit of radiation dose reduction, the future calls for cost-effectiveness and clinical outcome evaluations.[5] While image quality and dose reduction are fundamental, the impact of this protocol in terms of accuracy and cost-effectiveness in real clinical scenarios must be validated in larger cohorts and multicenter studies. As a scientific and clinical community, we must foster discussions and studies that expand this line of investigation, promoting the development of optimized examination protocols that lead to safer and more efficient clinical decisions.

Keywords

X-Ray Computed Tomography; Angiography; Patient Safety

Mailing Address: Tiago Magalhães •
Hospital do Coração. Rua Desembargador Eliseu Guilherme, 147. Postal code: 04004-030. São Paulo, SP – Brazil
E-mail: tiaugusto@gmail.com

DOI: https://doi.org/10.36660/abcimg.20250041i

References

1. Chae MK, Kim EK, Jung KY, Shin TG, Sim MS, Jo IJ, et al. Triple Rule-Out Computed Tomography for Risk Stratification of Patients with Acute Chest Pain. J Cardiovasc Comput Tomogr. 2016;10(4):291-300. doi: 10.1016/j.jcct.2016.06.002.
2. Monica MP, Merkely B, Szilveszter B, Drobni ZD, Maurovich-Horvat P. Computed Tomographic Angiography for Risk Stratification in Patients with Acute Chest Pain - The Triple Rule-out Concept in the Emergency Department. Curr Med Imaging Rev. 2020;16(2):98-110. doi: 10.2174/1573405614666180604095120.
3. Burris AC 2nd, Boura JA, Raff GL, Chinnaiyan KM. Triple Rule Out versus Coronary CT Angiography in Patients with Acute Chest Pain: Results from the ACIC Consortium. JACC Cardiovasc Imaging. 2015;8(7):817-25. doi: 10.1016/j.jcmg.2015.02.023.
4. Bertolazzi P, Silva CFG, Iunes L, Oliveira FF, Pereira FP, Viana PCC et al. Angiotomografia Computadorizada com Descarte Triplo Convencional e Parcialmente Sincronizada ao ECG com Cobertura da Aorta Abdominal: Comparação da Dose de Radiação e da Qualidade da Imagem. Arq Bras Cardiol: Imagem cardiovasc. 2025;38(2):e20250025. doi: https://doi.org/10.36660/abcimg.20250025
5. Ayaram D, Bellolio MF, Murad MH, Laack TA, Sadosty AT, Erwin PJ, et al. Triple Rule-Out Computed Tomographic Angiography for Chest Pain: A Diagnostic Systematic Review and Meta-Analysis. Acad Emerg Med. 2013;20(9):861-71. doi: 10.1111/acem.12210.

Assessment of Left Ventricular Function by MAPSE (Mitral Annular Plane Systolic Excursion): Main Clinical Applications

Andressa Alves de Carvalho,[1] *Wanessa Alves de Carvalho,*[1] *Luis Fabio Barbosa Botelho,*[1] *Marcelo Dantas Tavares de Melo*[1]

Universidade Federal da Paraíba,[1] *João Pessoa, PB – Brazil*

Central Illustration: Assessment of Left Ventricular Function by MAPSE (Mitral Annular Plane Systolic Excursion): Main Clinical Applications

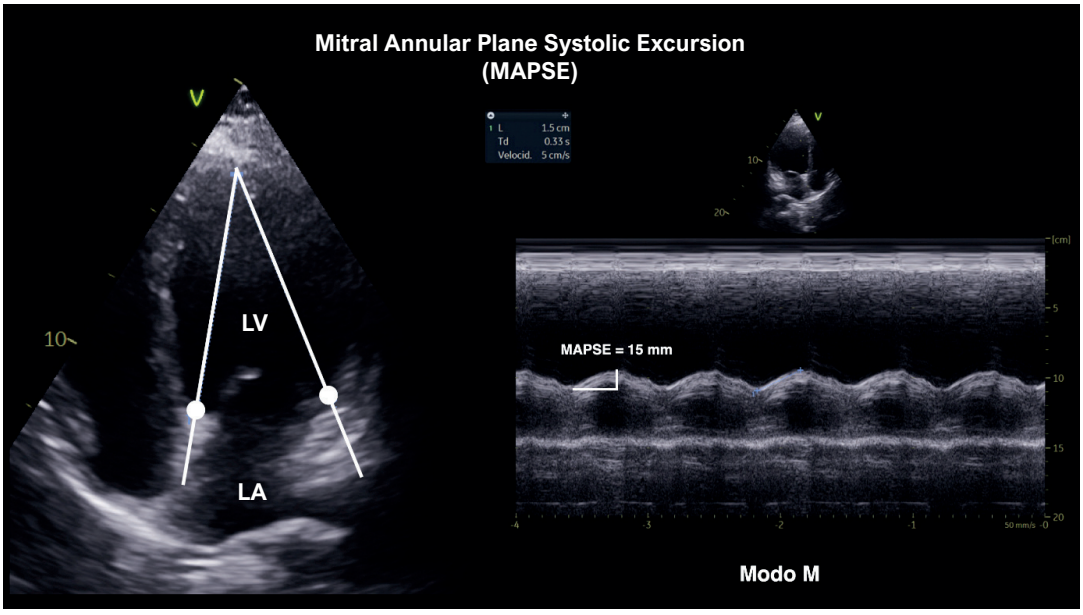

Arq Bras Cardiol: Imagem cardiovasc. 2025;38(2):e20240105

LV: left ventricle; LA: left atrium.

Abstract

Mitral annular plane systolic excursion (MAPSE), a parameter that can be obtained from transthoracic echocardiography or nuclear magnetic resonance (NMR), is capable of reflecting the longitudinal systolic function of the left ventricle (LV) and may change earlier than the LV ejection fraction (LVEF), estimated by usual methods. Furthermore, it also presents a correlation with global longitudinal strain (GLS), assessed by speckle tracking in two-dimensional (2D) echocardiography. The importance of MAPSE extends to the ease with which it can be obtained and reproduced, especially in patients with poor image quality, for whom LVEF and GLS may be inaccurate. This review intends to clarify the evidence available in the literature on MAPSE, which, despite its applicable usefulness in the context of various heart diseases, is an underused index in clinical practice.

Keywords

Função Ventricular; Ecocardiografia; Valva Mitral

Mailing Address: Marcelo Tavares •
Universidade Federal da Paraíba, Departamento de Medicina Interna. Campus I Lot, Cidade Universitária. Postal Code: 58051-900. João Pessoa, PB – Brazil
E-mail: marcelo_dtm@yahoo.com.br
Manuscript received October 23, 2024; revised October 24, 2024; accepted October 24, 2024
Editor responsible for the review: Marcelo Tavares

DOI: https://doi.org/10.36660/abcimg.20240105i

Introduction

Mitral annular plane systolic excursion (MAPSE) is an ultrasound parameter obtained from motion mode (M-mode) over the lateral aspect of the mitral valve annulus. It evaluates its movement during the cardiac cycle (Figure 1). It also presents a good correlation with left ventricular ejection fraction (LVEF), is easy to use, and is readily available. It is also a simple and reproducible index.

The American Society of Echocardiography and European Association of Cardiovascular Imaging Guidelines recommend

its use as a surrogate parameter when LVEF or global longitudinal strain (GLS) cannot be accurately obtained in patients with poor image quality, as both methods require left ventricular (LV) endocardial tracking, which is highly dependent on adequate visualization.[1]

MAPSE can quantitatively reflect LV longitudinal systolic function, as the longitudinal movement of the mitral valve annulus leads LV pumping, unlike the apex, whose position is relatively stationary.[2] Therefore, its measurement only requires the visualization of the mitral annulus, with no need to define the LV endocardial limit, which is essential in performing the other methods mentioned above.

The MAPSE value may be determined from four locations in the atrioventricular plane, equivalent to the septal, lateral, anterior, and posterior walls, viewed in the apical four- and two-chamber windows in M-mode. The cursor must be parallel to the LV walls (Figure 1). The measurement is calculated from the lowest point at the end of the diastole up to the aortic valve closure (Figure 2). In general, MAPSE should be obtained from the septal and lateral mitral annulus, with this value being slightly higher in normal hearts.

A large multicenter study[3] identified normal reference values for MAPSE, established according to age and sex, using M-mode and speckle-tracking 2D echocardiography (Table 1). Women exhibited slightly higher MAPSE values than men, and older individuals had lower values than younger individuals.

There are many studies on the usefulness of MAPSE in assessing LV longitudinal systolic function in heart failure (HF). However, recent publications also present it as a tool with prognostic value in the setting of ischemic heart disease, valvular heart disease, cardiomyopathies, septic shock, and cardio-oncology.[4] It is a sensitive marker of early LV dysfunction, also correlating with some diastolic function indices, such as the E/A ratio, septal e' wave, and lateral e' wave.[5]

In this sense, as this study will show, MAPSE may be altered in certain cardiac conditions even when the LVEF is still normal. Figure 3 illustrates a patient with amyloidosis, with preserved ejection fraction (supranormal), but, disproportionately, with a MAPSE value at the lower limit of normal (10 mm) and with reduced GLS (12.1%).

MAPSE can also be assessed by cardiac nuclear magnetic resonance (NMR) and is considered an important independent predictor of serious adverse cardiac events (death, non-fatal myocardial infarction, hospitalization for HF or unstable angina, and late revascularization). According to the study by Rangarajan et al. (2016),[6] patients with lateral MAPSE <1.11 cm (median value) had a significantly higher incidence of adverse events than did those with MAPSE ≥1.11 cm.

This review article will describe the main clinical applications available in the literature for MAPSE, a parameter that is easy to apply but often forgotten in practice.

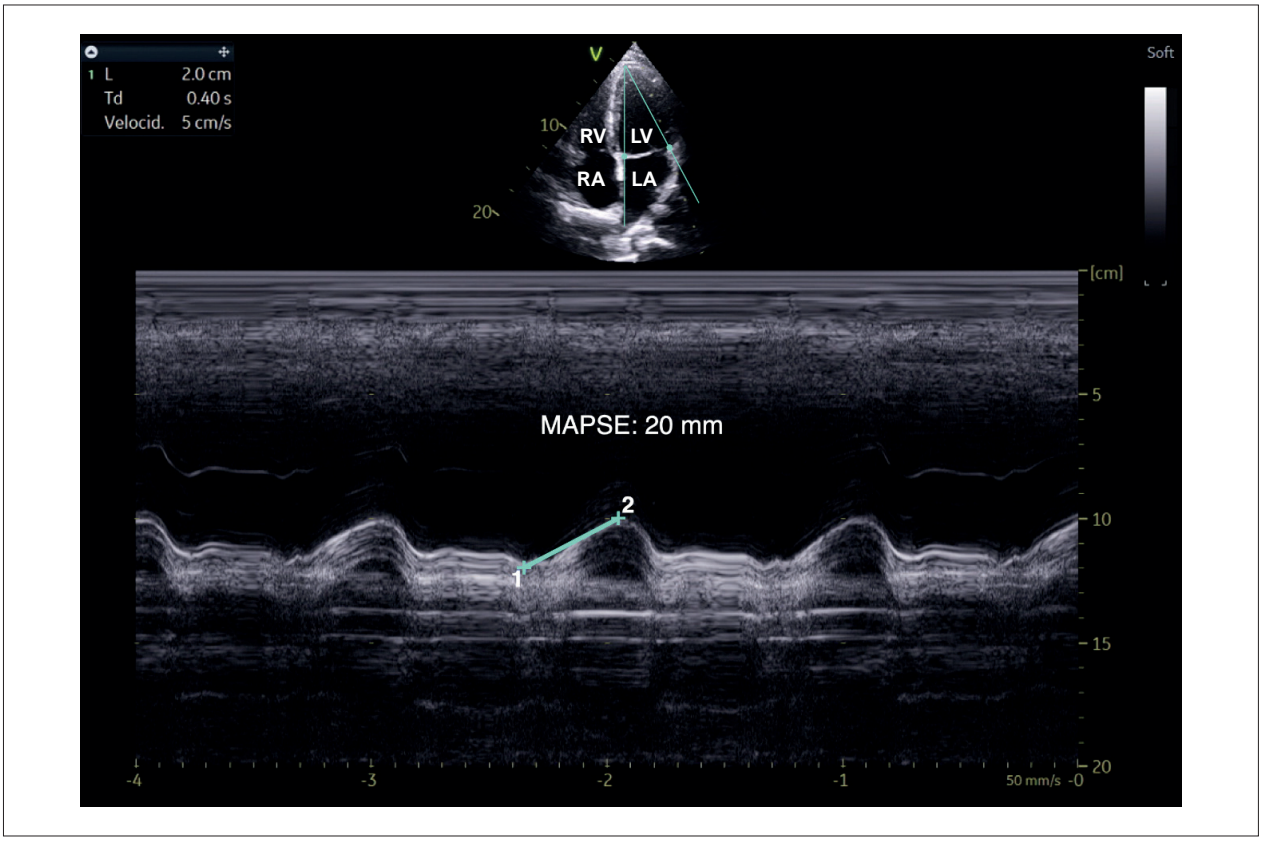

Figure 1 – *MAPSE calculated from M-mode in 2D echocardiography in an athlete patient, obtaining a value of 20 mm, considered normal. Source: created by the authors. RV: right ventricle; LV: left ventricle; RA: right atrium; LA: left atrium; MAPSE: mitral annular plane systolic excursion.*

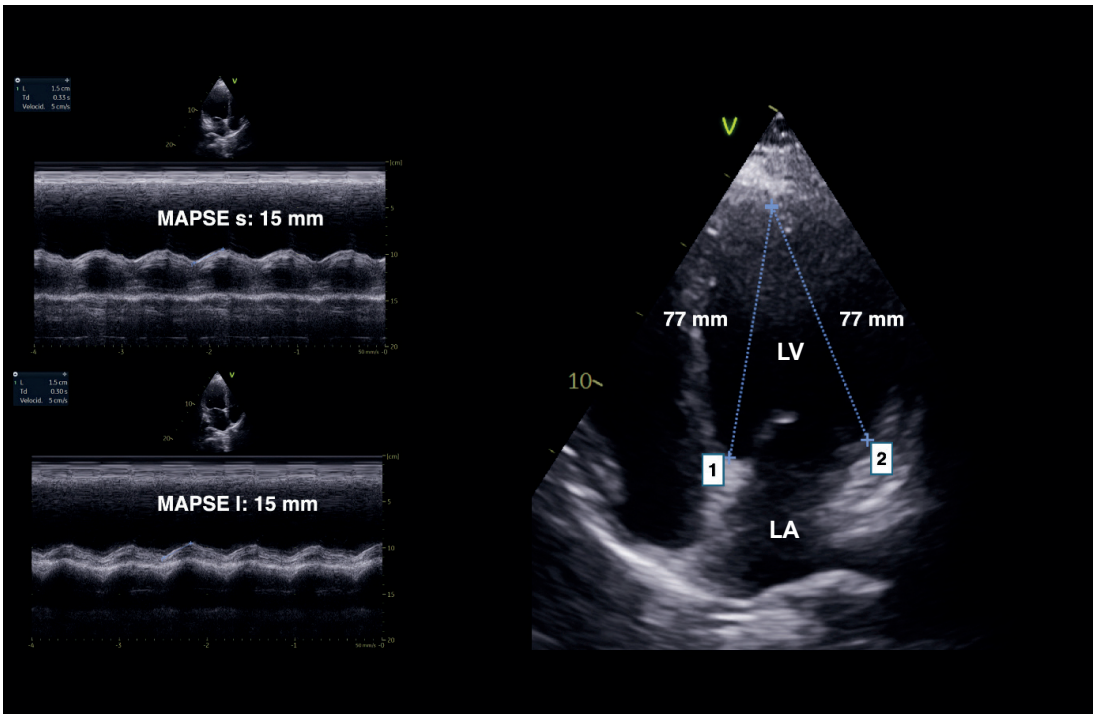

Figure 2 – *Demonstration of the locations where the cursor should be placed on the septal (1) and lateral (2) mitral rings in the apical 4-chamber window. On the left, the echocardiographic measurement in M-mode is observed (above, septal MAPSE; below, lateral MAPSE). MAPSE: mitral annular plane systolic excursion; LV: left ventricle. Source: created by the authors.*

Clinical applications

HF

Reduced MAPSE reflects the presence of impaired longitudinal function, providing complementary information to ejection fraction, which represents the overall result of longitudinal and circumferential contraction.[7] It was shown that patients with chronic HF resulting from dilated cardiomyopathy or myocardial infarction presented a significant reduction in MAPSE, which had a good correlation with ejection fraction.[8]

Patients with preserved LVEF were divided into three groups according to the value of lateral MAPSE: low (<12 mm), relatively preserved (12-15 mm), and high (≥15 mm). The diastolic dysfunction rate and all-cause hospitalization proved to be higher in the low and relatively preserved groups than in the high group, whereas the pro-BNP level and mortality rate were higher in the low group when compared with the relatively preserved and high groups.[9]

There is also evidence that MAPSE, measured at rest and during exercise (on a treadmill using the modified Bruce protocol), correlates well with more sophisticated measurements of ventricular function in patients with HF with preserved ejection fraction (HFpEF), and is, therefore, a useful measure for the early detection of left ventricular dysfunction, which in HFpEF is most evident during exercise testing.[10]

Table 1 – Reference values for a MAPSE by M-mode and 2D-STE.

	Men	Women
Msep (mm)	9-19	9-19
Mlat (mm)	10-20	10-21
STEsep (mm)	7-16	7-16
STElat (mm)	6-18	6-19
STEm (mm)	7-17	8-17
nSTEm (%)	8-19	9-21

M-mode: motion mode; 2D-STE: speckle tracking by 2D echocardiography; Msep and Mlat: Septal and lateral MAPSE by M-mode echocardiography, respectively; STEsep, STElat, and STEmid: septal, lateral, and midpoint MAPSE measured by 2D-STE; nSTEmid: STEmid normalized by LV long axis length in end-diastole. Adapted from WANG et al. (2023).[3]

Systemic arterial hypertension

In the early stages of systemic arterial hypertension (SAH), before the appearance of symptoms related to HF or the reduction in LVEF (<50%), it is already possible to identify abnormalities in the longitudinal components of mechanical contractility and systolic dysfunction. In these patients, parameters were studied to determine the

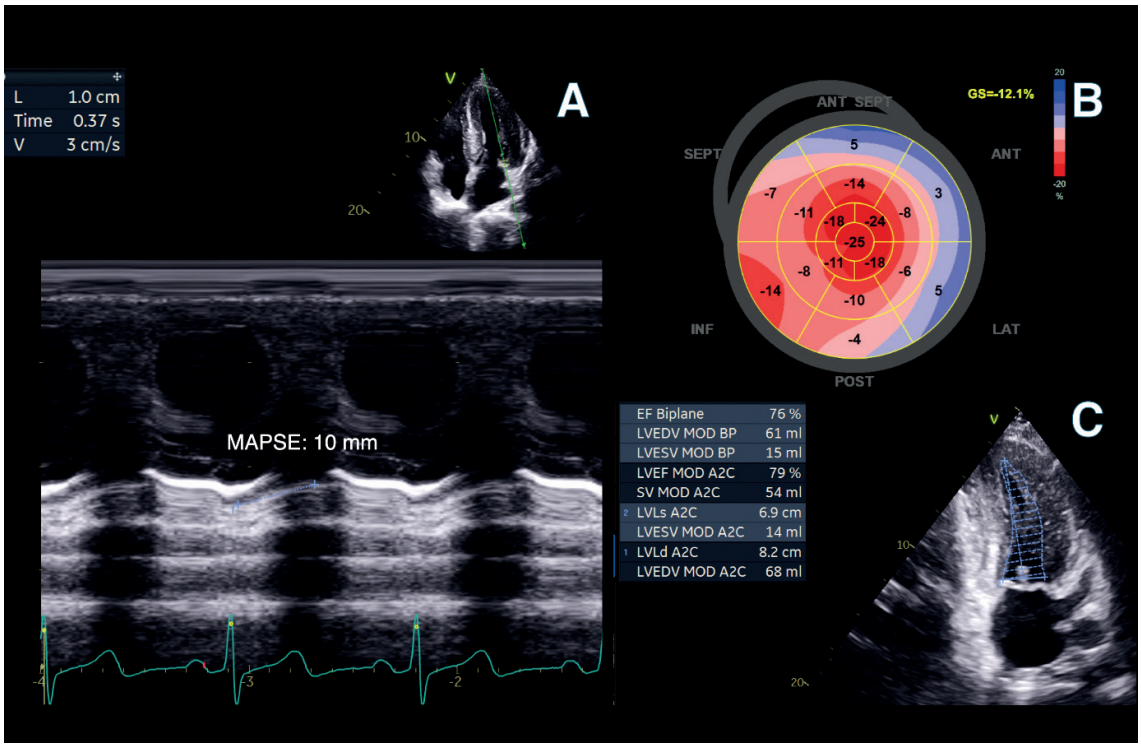

Figure 3 – *Patient with amyloidosis, who exhibits LVEF, MAPSE, and GLS values, respectively, of 76%, 10 mm, and 12.1%. LVEF: left ventricular ejection fraction; MAPSE: mitral annular plane systolic excursion; GLS: global longitudinal strain; EF: ejection fraction; LVEDV: left ventricular end-diastolic volume; MOD: modified; LVEF: left ventricular ejection fraction; BP: biplane; SV: systolic volume; LVL: left ventricular length; LVESV: left ventricular end-systolic volume; LVLd: left ventricular length diastolic. Source: created by the authors.*

transition between structural abnormalities and myocardial dysfunction early.[11]

LVEF was identical in hypertensive and healthy patients, while GLS and MAPSE were lower in the first group. Patients with moderate or severe ventricular hypertrophy (septum ≥13 mm) presented longitudinal systolic dysfunction, with GLS being reduced more than MAPSE even in the presence of small structural changes; conversely, LVEF was insensitive for detecting longitudinal myocardial dysfunction in patients with hypertension.[11] This finding shows that the compensatory increase in circumferential deformation may mask the reduced longitudinal deformation, leading to normal LVEF.

The prognostic value of MAPSE obtained by cardiac NMR was evaluated in a large multicenter population of SAH patients. The risk of death was significantly higher in patients with lateral MAPSE lower than 10 mm, even after adjustment for clinical and imaging risk factors, as well as in the subgroups of patients with preserved LVEF and those without a history of myocardial infarction.[12]

Aortic stenosis

In patients with aortic valve stenosis, MAPSE changes earlier when compared to LVEF or other parameters that assess ventricular function, which may be normal. Furthermore, it has a lower value in symptomatic patients when compared to asymptomatic and severe patients. It is also useful in predicting the onset of symptoms.[13] MAPSE was able to differentiate low-gradient aortic stenosis into moderate or severe in the presence of preserved ejection fraction, using a cutoff value of 9 mm to distinguish them.[14]

Intensive care units and emergency services

Bedside transthoracic echocardiography is essential for the diagnosis and treatment of left ventricular systolic dysfunction in critically ill patients, especially those with septic shock, for whom septic cardiomyopathy may be present in 40% of the cases.[15] Studies show that MAPSE reflects systolic and diastolic function in critically ill patients and is commonly related to ICU mortality when associated with TAPSE, LVEF, and lung ultrasound.[16]

Longitudinal systolic function may be more sensitive in detecting cardiac depression than LVEF. Therefore, when assessing cardiac function in patients with septic shock and normal LVEF, longitudinal function indices, such as MAPSE, should be taken into account.[17] A study with 90 patients, divided evenly between individuals with septic shock and those without sepsis, compared these echocardiographic parameters. No difference was found between groups for LVEF

(64.6% vs. 67.2%, p = 0.161), but a difference was observed for MAPSE, which was significantly worse in those with septic shock (1.2 cm vs. 1.5 cm, p <0.001).[17] Similarly, other authors found that MAPSE, but not LVEF, differed between patients with septic shock with and without myocardial injury, defined as high-sensitivity troponin T ≥45 ng/L upon ICU admission.[18]

A significant advantage, in the emergency or intensive care setting, is that MAPSE assessment does not require good image quality or an experienced operator. The decrease in value correlates with LV systolic dysfunction and may precede changes in LVEF during acute myocardial infarction. It also correlates with elevated levels of brain natriuretic peptides and isolated diastolic dysfunction.[9]

A study with 61 emergency physicians found that MAPSE measurement was easily performed with minimal training and excellent inter-user agreement. An <8 mm value had a moderate predictive value and high specificity for LVEF <50%, and was more specific for identifying a reduced LVEF than the commonly used qualitative assessment.[19]

Acute myocardial infarction

In the context of acute ST-segment elevation myocardial infarction (STEMI), the risk of cardiovascular complications after revascularization, including mortality, is considerable. It is suggested that MAPSE provides significantly greater prognostic validity than LVEF in this patient population.[20] Research shows that MAPSE has a significant incremental predictive value over LVEF; therefore, the combination of both can serve as a good alternative for LV-based risk assessment after STEMI, if GLS is not available.[21,22]

Arrhythmias

In a study of 247 patients undergoing coronary artery bypass grafting surgery, MAPSE was able to predict the development of postoperative atrial fibrillation (AF), with an area under the Receiver Operating Characteristic (ROC) curve (AUC) of 0.831 (95% CI 0.761-0.901, p <0.001), in addition to sensitivity and specificity of 90% and 81%, respectively.[23]

In patients who underwent catheter ablation with pulmonary vein isolation, reduced MAPSE and increased left atrial volume index represented risk factors for AF recurrence.[24] In HFpEF, a reduced MAPSE was associated with right atrial dyssynchrony, a risk predictor for AF.[25]

Oncology

Cardiotoxicity associated with cancer therapies is detected early through GLS and LVEF in echocardiography; however, ultrasound imaging may be affected, especially in postoperative patients with left breast cancer or those with high obesity. The European cardio-oncology guideline[26] recommends using surrogate parameters for evaluation, such as MAPSE.

In breast cancer patients treated with preoperative or postoperative chemotherapy (anthracyclines and trastuzumab), the following cutoff values were identified for septal MAPSE, lateral MAPSE, and mean MAPSE (septal and lateral), respectively: 11.7 mm (AUC = 0.65, p = 0.02; sensitivity 79%; specificity 45%), 13 mm (AUC = 0.82, p = 0.001; sensitivity 94%; specificity 96%) and 11.7 mm (AUC = 0.87, p < 0.001; sensitivity 83%; specificity 80%), respectively.[27]

In another study, MAPSE and peak mitral annular systolic velocity (S') showed good accuracy, sensitivity, and positive predictive value for detecting anthracycline therapy-related cardiac dysfunction (ATRCD), with GLS being used as the gold standard diagnostic test to define it. The authors stated that these conventional echocardiographic parameters may work as screening tools to detect subclinical ATRCD in resource-limited settings.

In patients who underwent neoadjuvant chemoradiotherapy for esophageal or esophagogastric junction cancer, no change was identified in LV GLS after treatment. However, septal MAPSE decreased significantly, showing that chemoradiotherapy appears to induce an acute negative effect on left ventricular systolic function, which was not observed for chemotherapy.[28]

Mapse limitations

MAPSE has some disadvantages inherent to the method. It is not able, for instance, to detect regional dysfunctions in the myocardium, unlike GLS. Furthermore, there are no normalized values for variations in heart size between different patients, especially in children. Its value may also be influenced by moderate to large pericardial effusion, since the cardiac apex, which is relatively stationary under normal conditions, becomes mobile, interfering with the true MAPSE measurement. Similarly, paradoxical septum due to right ventricular dysfunction alters septal MAPSE, and in these conditions, lateral MAPSE should be used. Finally, it is not possible to perform a direct measurement on the mitral annulus when it has significant calcification; in this case, the measurement must be made slightly higher up in the myocardium.[7]

Conclusion

In addition to being readily available and easy to use, MAPSE is a useful parameter in the clinical assessment of LV longitudinal systolic function in different contexts, such as HF, septic cardiomyopathy, and cardio-oncology, and may be altered even when LVEF is normal. Studies on its applicability are still scarce in the literature. Therefore, it is hoped that this review will allow more research to be carried out on MAPSE so that its use can be expanded in medical practice.

Author Contributions

Conception and design of the research: Botelho LFB, Tavares M; acquisition of data: Carvalho AA; analysis and interpretation of the data: Carvalho AA, Carvalho WA, Tavares M; writing of the manuscript and critical revision of the manuscript for intellectual content: Carvalho AA, Carvalho WA, Botelho LFB, Tavares M.

Potential Conflict of Interest

No potential conflict of interest relevant to this article was reported.

Sources of Funding

There were no external funding sources for this study.

Study Association

This study is not associated with any thesis or dissertation work.

Ethics Approval and Consent to Participate

This article does not contain any studies with human participants or animals performed by any of the authors.

References

1. Lang RM, Badano LP, Mor-Avi V, Afilalo J, Armstrong A, Ernande L, et al. Recommendations for Cardiac Chamber Quantification by Echocardiography in Adults: An Update from the American Society of Echocardiography and the European Association of Cardiovascular Imaging. Eur Heart J Cardiovasc Imaging. 2015;16(3):233-70. doi: 10.1093/ehjci/jev014.
2. Carlsson M, Ugander M, Mosén H, Buhre T, Arheden H. Atrioventricular Plane Displacement is the Major Contributor to Left Ventricular Pumping in Healthy Adults, Athletes, and Patients with Dilated Cardiomyopathy. Am J Physiol Heart Circ Physiol. 2007;292(3):H1452-9. doi: 10.1152/ajpheart.01148.2006.
3. Wang YH, Sun L, Li SW, Wang CF, Pan XF, Liu Y, et al. Normal Reference Values for Mitral Annular Plane Systolic Excursion by Motion-mode and Speckle Tracking Echocardiography: A Prospective, Multicentre, Population-based Study. Eur Heart J Cardiovasc Imaging. 2023;24(10):1384-93. doi: 10.1093/ehjci/jead187.
4. Cirin L, Cri□an S, Luca CT, Buza□ R, Lighezan DF, V□c□rescu C, et al. Mitral Annular Plane Systolic Excursion (MAPSE): A Review of a Simple and Forgotten Parameter for Assessing Left Ventricle Function. J Clin Med. 2024;13(17):5265. doi: 10.3390/jcm13175265.
5. Martins AAB, Osaku LY, Camarozano AC, Sá CRF, Carmo DC, Fortunato JA, et al. Excursão Sistólica do Anel Tricúspide e do Anel Mitral: Correlação com Função Diastólica Ventricular Esquerda. Arq Bras Cardiol: Imagem Cardiovasc. 2022;35(1):eabc245. doi: 10.47593/2675-312X/20223501eabc245.
6. Rangarajan V, Chacko SJ, Romano S, Jue J, Jariwala N, Chung J, et al. Left Ventricular Long Axis Function Assessed During Cine-cardiovascular Magnetic Resonance is an Independent Predictor of Adverse Cardiac Events. J Cardiovasc Magn Reson. 2016;18(1):35. doi: 10.1186/s12968-016-0257-y.
7. Hu K, Liu D, Herrmann S, Niemann M, Gaudron PD, Voelker W, et al. Clinical Implication of Mitral Annular Plane Systolic Excursion for Patients with Cardiovascular Disease. Eur Heart J Cardiovasc Imaging. 2013;14(3):205-12. doi: 10.1093/ehjci/jes240.
8. Alam M, Höglund C, Thorstrand C, Philip A. Atrioventricular Plane Displacement in Severe Congestive Heart Failure Following Dilated Cardiomyopathy or Myocardial Infarction. J Intern Med. 1990;228(6):569-75. doi: 10.1111/j.1365-2796.1990.tb00281.x.
9. Ozer PK, Govdeli EA, Demirtakan ZG, Nalbant A, Baykiz D, Orta H, et al. The Relation of Echo-derived Lateral MAPSE to Left Heart Functions and Biochemical Markers in Patients with Preserved Ejection Fraction: Short-term Prognostic Implications. J Clin Ultrasound. 2022;50(5):593-600. doi: 10.1002/jcu.23173.
10. Wenzelburger FW, Tan YT, Choudhary FJ, Lee ES, Leyva F, Sanderson JE. Mitral Annular Plane Systolic Excursion on Exercise: A Simple Diagnostic Tool for Heart Failure with Preserved Ejection Fraction. Eur J Heart Fail. 2011;13(9):953-60. doi: 10.1093/eurjhf/hfr081.
11. Salas-Pacheco JL, Lomelí-Sánchez O, Baltazar-González O, Soto ME. Longitudinal Systolic Dysfunction in Hypertensive Cardiomyopathy with Normal Ejection Fraction. Echocardiography. 2022;39(1):46-53. doi: 10.1111/echo.15267.
12. Romano S, Judd RM, Kim RJ, Kim HW, Heitner JF, Shah DJ, et al. Prognostic Implications of Mitral Annular Plane Systolic Excursion in Patients with Hypertension and a Clinical Indication for Cardiac Magnetic Resonance Imaging: A Multicenter Study. JACC Cardiovasc Imaging. 2019;12(9):1769-79. doi: 10.1016/j.jcmg.2018.10.003.
13. Takeda S, Rimington H, Smeeton N, Chambers J. Long Axis Excursion in Aortic Stenosis. Heart. 2001;86(1):52-6. doi: 10.1136/heart.86.1.52.
14. Herrmann S, Störk S, Niemann M, Lange V, Strotmann JM, Frantz S, et al. Low-gradient Aortic Valve Stenosis Myocardial Fibrosis and its Influence on Function and Outcome. J Am Coll Cardiol. 2011;58(4):402-12. doi: 10.1016/j.jacc.2011.02.059.
15. Lin H, Wang W, Lee M, Meng Q, Ren H. Current Status of Septic Cardiomyopathy: Basic Science and Clinical Progress. Front Pharmacol. 2020;11:210. doi: 10.3389/fphar.2020.00210.
16. Yin W, Li Y, Zeng X, Qin Y, Wang D, Zou T, et al. The Utilization of Critical Care Ultrasound to Assess Hemodynamics and Lung Pathology on ICU Admission and the Potential for Predicting Outcome. PLoS One. 2017;12(8):e0182881. doi: 10.1371/journal.pone.0182881.
17. Zhang HM, Wang XT, Zhang LN, He W, Zhang Q, Liu DW, et al. Left Ventricular Longitudinal Systolic Function in Septic Shock Patients with Normal Ejection Fraction: A Case-control Study. Chin Med J. 2017;130(10):1169-74. doi: 10.4103/0366-6999.205856.
18. Blixt PJ, Nguyen M, Cholley B, Hammarskjöld F, Toiron A, Bouhemad B, et al. Association between Left Ventricular Systolic Function Parameters and Myocardial Injury, Organ Failure and Mortality in Patients with Septic Shock. Ann Intensive Care. 2024;14(1):12. doi: 10.1186/s13613-023-01235-5.
19. Schick AL, Kaine JC, Al-Sadhan NA, Lin T, Baird J, Bahit K, et al. Focused Cardiac Ultrasound with Mitral Annular Plane Systolic Excursion (MAPSE) Detection of Left Ventricular Dysfunction. Am J Emerg Med. 2023;68:52-8. doi: 10.1016/j.ajem.2023.03.018.
20. Mayr A, Pamminger M, Reindl M, Greulich S, Reinstadler SJ, Tiller C, et al. Mitral Annular Plane Systolic Excursion by Cardiac MR is an Easy Tool for Optimized Prognosis Assessment in ST-elevation Myocardial Infarction. Eur Radiol. 2020;30(1):620-9. doi: 10.1007/s00330-019-06393-4.
21. Holzknecht M, Reindl M, Tiller C, Reinstadler SJ, Lechner I, Pamminger M, et al. Global Longitudinal Strain Improves Risk Assessment after ST-segment Elevation Myocardial Infarction: A Comparative Prognostic Evaluation of Left Ventricular Functional Parameters. Clin Res Cardiol. 2021;110(10):1599-611. doi: 10.1007/s00392-021-01855-6.
22. Wang L, Yuan W, Huang X, Zhao X, Zhao X. Cardiac Magnetic Resonance-derived Mitral Annular Plane Systolic Excursion: A Robust Indicator for Risk Stratification after Myocardial Infarction. Int J Cardiovasc Imaging. 2024;40(4):897-906. doi: 10.1007/s10554-024-03058-2..
23. Koseoglu C, Oncel CR, Dagasan G, Coner A, Akkaya O. Mitral Annular Plane Systolic Excursion (MAPSE) as a Predictor of Atrial Fibrillation Development after Coronary Artery Bypass Surgery. Bratisl Lek Listy. 2024;125(8):503-7. doi: 10.4149/BLL_2024_78. PMID: 38989752.

24. Alatic J, Suran D, Vokac D, Naji FH. Mitral Annular Plane Systolic Excursion (MAPSE) as a Predictor of Atrial Fibrillation Recurrence in Patients after Pulmonary Vein Isolation. Cardiol Res Pract. 2022;2022:2746304. doi: 10.1155/2022/2746304.

25. Bytyçi I, Haliti E, Berisha G, Tishukaj A, Shatri F, Bajraktari G. Left Ventricular Longitudinal Systolic Dysfunction is Associated with Right Atrial Dyssynchrony in Heart Failure with Preserved Ejection Fraction. Rev Port Cardiol. 2016;35(4):207-14. doi: 10.1016/j.repc.2015.11.011.

26. Lyon AR, López-Fernández T, Couch LS, Asteggiano R, Aznar MC, Bergler-Klein J, et al. 2022 ESC Guidelines on Cardio-oncology Developed in Collaboration with the European Hematology Association (EHA), the European Society for Therapeutic Radiology and Oncology (ESTRO) and the International Cardio-Oncology Society (IC-OS). Eur Heart J. 2022;43(41):4229-361. doi: 10.1093/eurheartj/ehac244.

27. Ichikawa N, Nishizaki Y, Miyazaki S, Nojima M, Kataoka K, Kasahara R, et al. Efficacy of Mitral Annular Velocity as an Alternative Marker of Left Ventricular Global Longitudinal Strain to Detect the Risk of Cancer Therapy-related Cardiac Disorders. Echocardiography. 2024;41(7):e15877. doi: 10.1111/echo.15877.

28. Lund M, von Döbeln GA, Nilsson M, Winter R, Lundell L, Tsai JA, et al. Effects on Heart Function of Neoadjuvant Chemotherapy and Chemoradiotherapy in Patients with Cancer in the Esophagus or Gastroesophageal Junction - A Prospective Cohort Pilot Study within a Randomized Clinical Trial. Radiat Oncol. 2015;10:16. doi: 10.1186/s13014-014-0310-7.

My Approach to Intracardiac Echocardiography During Atrial Fibrillation Ablation

Simone Nascimento dos Santos,[1] *Benhur Davi Henz,*[1] *Maria Eduarda Leite da Silva,*[2] *Luiz Roberto Leite da Silva*[1]
ECCOS Diagnóstico Cardiovascular,[1] *Brasília, DF – Brazil*
York University,[2] *Toronto, Ontário – Canada*

Central Illustration: My Approach to Intracardiac Echocardiography During Atrial Fibrillation Ablation

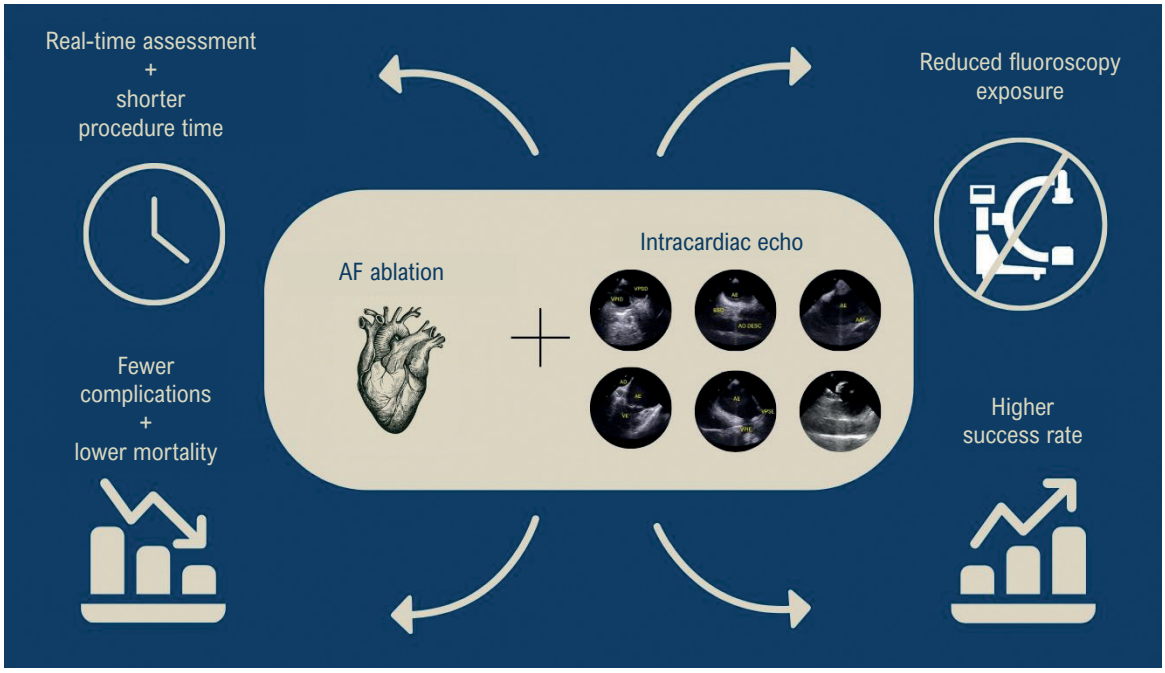

Arq Bras Cardiol: Imagem cardiovasc. 2025;38(2):e20250021

AF: atrial fibrillation.

Abstract

Atrial fibrillation (AF) is the most common arrhythmia encountered in clinical practice and is associated with serious complications such as stroke and heart failure. The prevalence of AF is increasing significantly due to population aging and related comorbidities.[1] In addition, advances in technology — particularly the detection of AF through wearable devices such as smartwatches — have enabled earlier diagnosis. Intracardiac echocardiography (ICE) is a valuable imaging modality in electrophysiology and hemodynamic labs and is well-supported by the literature.[2-5] Since the early studies conducted at the Mayo Clinic,[6,7] ICE has rapidly become an indispensable tool for assessing cardiac anatomy. ICE enables real-time visualization of catheter positioning, tissue contact, its relationship to arrhythmogenic substrates and ablation targets, lesion formation, and procedural complications. Several recent studies have demonstrated the benefits of ICE in complex ablations, including reduced procedure times and complication rates, such as lower risks of cardiac tamponade and mortality, along with higher success rates (Central Illustration).[8-12] ICE-guided procedures are increasingly used in clinical practice across a variety of settings. They are considered feasible, safe, and associated with decreased

Keywords

Intracardiac Echocardiography; Catheter Ablation; Atrial Fibrillation

Mailing Address: Simone Nascimento dos Santos •
ECCOS Diagnóstico Cardiovascular. SMDB Conj 16 Lote 5 Casa A. Postal Code: 71680-160. Brasília, DF – Brazil
E-mail: simone.eccos@gmail.com
Manuscript received April 9, 2025; revised manuscript April 11, 2025; accepted April 14, 2025
Editor responsible for the review: Marcelo Tavares

DOI: https://doi.org/10.36660/abcimg.20250021i

fluoroscopy exposure — or even complete fluoroless procedures, as implemented by several groups in Brazil and worldwide.[8,13-15] This article provides a step-by-step "My Approach to" guide on how to perform ICE during AF ablation.

Step 1 – Getting to know the system

The catheter used employs a phased-array system (8 and 10 Fr) with a high-resolution ultrasound transducer located at the distal tip (5 to 10 MHz). Images are acquired in the longitudinal plane, with the imaging field aligned with the catheter axis. The catheter can be manipulated in four directions using bidirectional steering: anterior-posterior and right-left (Supplementary Video 1).

There are two models currently available in Brazil: i) SoundStar® eco (Biosense Webster), compatible with the GE ultrasound systems Vivid™ i and Vivid™ q; ViewFlex™ Xtra (Abbott), compatible with the Zonare Z.One Ultrasound System (Figure 1A and 1B).

Step 2 – Inserting the catheter

Following ultrasound-guided venous puncture, the catheter is advanced from the left femoral vein through the ipsilateral iliac vein and the inferior vena cava until it reaches the right atrium (RA). During this progression, attention must be paid to possible vessel curvatures and draining veins. At this stage, anterior and/or posterior deflection of the catheter should be used to navigate curves. The catheter should always be advanced within the vessel while visualizing the "echo-free space" on ultrasound, which reduces the risk of vascular perforation and eliminates the need for fluoroscopy (Supplementary Video 2).

Step 3 – Identifying intracardiac anatomy and adjacent structures

With the catheter positioned in the RA, the Eustachian valve and its morphology — whether rigid, prominent, or filamentous — can be identified. A filamentous Eustachian valve with erratic motion within the RA, if not previously recognized, may be mistaken for filamentous thrombi adherent to sheaths or catheters.

From the mid-RA, with the transducer directed toward the tricuspid valve (TV), the image known as the "Home View" is obtained. This view displays the RA, TV, and the inflow tract of the right ventricle (RV). For operators in the early stages of the learning curve, this image serves as a reference point to return to when anatomical structures are not clearly identified. By rotating the catheter clockwise approximately 10-20 degrees from the Home View, the following structures are sequentially visualized: i) aorta and RV outflow tract (RVOT); ii) aorta and left ventricular (LV) outflow tract (LVOT); iii) left atrium (LA) and interatrial septum (IAS); iv) LA, mitral valve (MV), and LV; v) LA and left atrial appendage (LAA); vi) LA and left pulmonary veins (PVs) in longitudinal view; vii) posterior wall (PW) of the LA, esophagus, and descending aorta; and viii) right PVs in transverse view.

There are no mandatory or predefined imaging planes. Cranial advancement or retraction of the catheter, as well as anterior-posterior and right-left flexion, are often required to obtain optimal images. Figure 2 (A-H) illustrates such imaging planes and the corresponding views obtained with the catheter positioned in the RA.

In atrial fibrillation (AF) ablation, it is often necessary to evaluate certain structures with the catheter positioned in the RV, which can be done without the use of fluoroscopy. With the TV in view, the catheter is gently deflected anteriorly and advanced into the RV. Once it crosses the TV, the deflection is released, allowing visualization of the inferior portion of the RV and its anatomical landmarks, such as the moderator band and papillary muscles, as well as the pericardial space. This view is particularly important for detecting any preexisting pericardial effusion (PE) at the start of the procedure. From the RV,

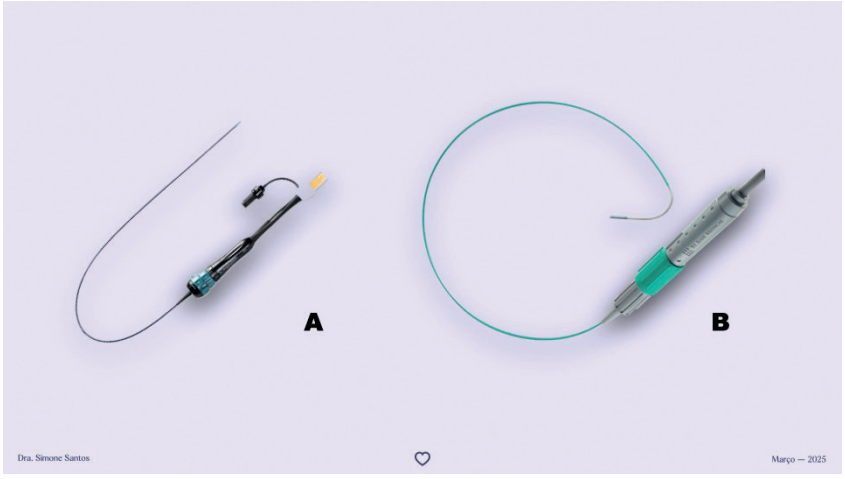

Figure 1 – *Phased-array catheters available in Brazil. A: SoundStar® (Biosense Webster); B: ViewFlex Xtra® (Abbott).*

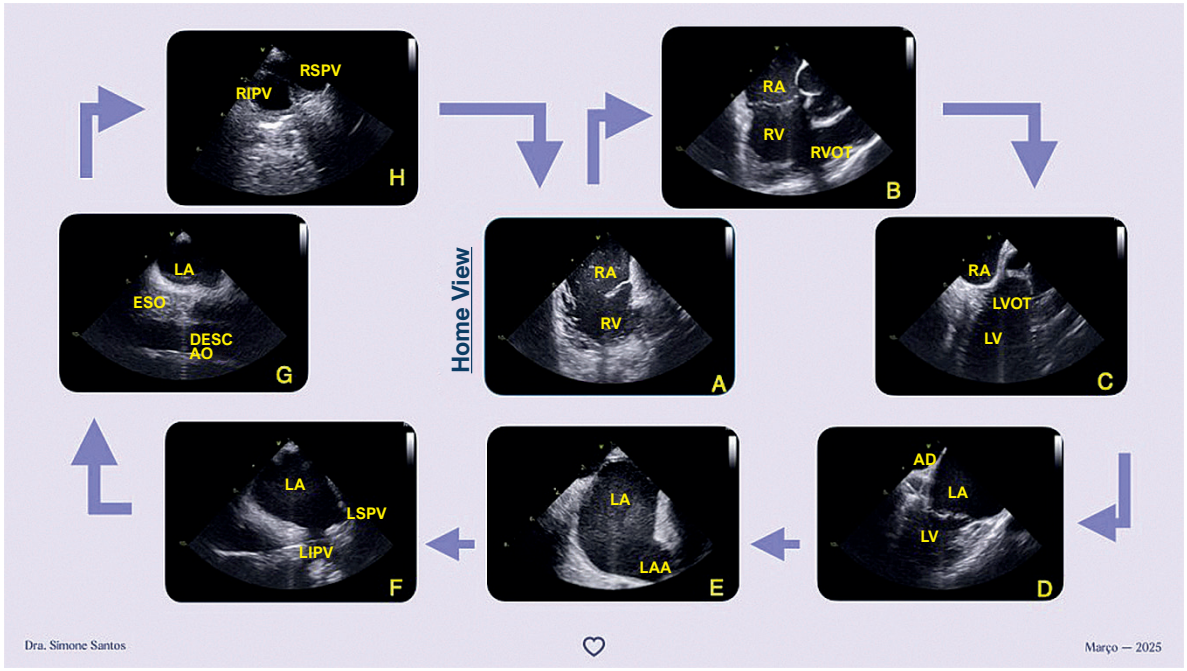

Figure 2 (A-H) – *Image sequence obtained with the catheter in the RA. A: Home View; sequential images from B to H show the progression of views obtained through clockwise catheter rotation starting from the Home View. LA: left atrium; AO: aorta; RV: right ventricle; LV: left ventricle; RA: right atrium; RVOT: right ventricle outflow tract; LVOT: left ventricular outflow tract; LAA: left atrial aappendage; LSPV: left superior pulmonar vein; LIPV: left inferior pulmonary vein; RIPV: right inferior pulmonary vein; RSPV: right superior pulmonary vein.*

clockwise torque enables sequential visualization of the interventricular septum (IVS) and the LV apex, followed by the posteromedial and anterolateral papillary muscles, the MV, the aortic valve in cross-section, the LAA, and the origin of both the left and right coronary arteries. In some cases, it is necessary to advance the catheter through the RVOT and into the pulmonary artery (PA) trunk to improve visualization of the LAA tip and to rule out the presence of thrombi (Figure 3A-F).

Step 4 – Rule out intracavitary thrombi before transeptal puncture

Thrombus detection in the LA or LAA is essential prior to AF ablation in order to prevent thromboembolic events related to the procedure. Although transesophageal echocardiography (TEE) is the gold standard for this purpose, anatomical limitations can lead to false-negative results. In our practice, TEE is performed before the procedure only in high-risk patients — those with persistent AF and MV disease, a history of stroke, or elevated CHA_2DS_2-VASc scores in the setting of poor anticoagulation adherence. We routinely use intracardiac echocardiography (ICE) to rule out thrombi prior to transeptal puncture, visualizing the LAA from the RA, RV (Figures 2 and 3), and PA. ICE catheter positioning in the RVOT, near the pulmonary valve, or within the main PA trunk provides the clearest images for thrombus detection (Supplementary Video 3).[16-18]

Step 5 – Guiding the transeptal puncture

To perform transeptal puncture, the catheter is positioned in the mid-RA, allowing direct visualization of IAS and LA. Since the procedural target is the electrical isolation of PVs — which drain into the PW of the LA — the ideal puncture site on the IAS is at the level of the left PVs or slightly more posterior. This facilitates maneuverability of the ablation catheter and improves safety by avoiding anterior puncture paths that may be directed toward the LAA, aortic root, or ascending aorta (Figure 4). From the Home View, clockwise rotation is performed until the entry of the left PVs into the LA becomes visible. In some cases, posterior deflection is also required, pulling the catheter slightly away from the IAS to optimize the view of the RA, IAS, and LA, thereby facilitating more accurate guidance of the transeptal puncture.

With ICE, we can rapidly identify the anatomy of the IAS and its relatively common anatomical variations that may complicate transeptal puncture, such as lipomatous hypertrophy, aneurysms, double fossa ovalis, and the presence of surgical patches or occluder devices.[19-22]

Whenever possible, we target the thinnest region of the IAS. In cases of redundant or aneurysmal septa, we select the lowest possible puncture site — while carefully avoiding the risk of perforating a pericardial recess. This strategy provides better anchoring of the needle and facilitates transeptal access in these more challenging scenarios.

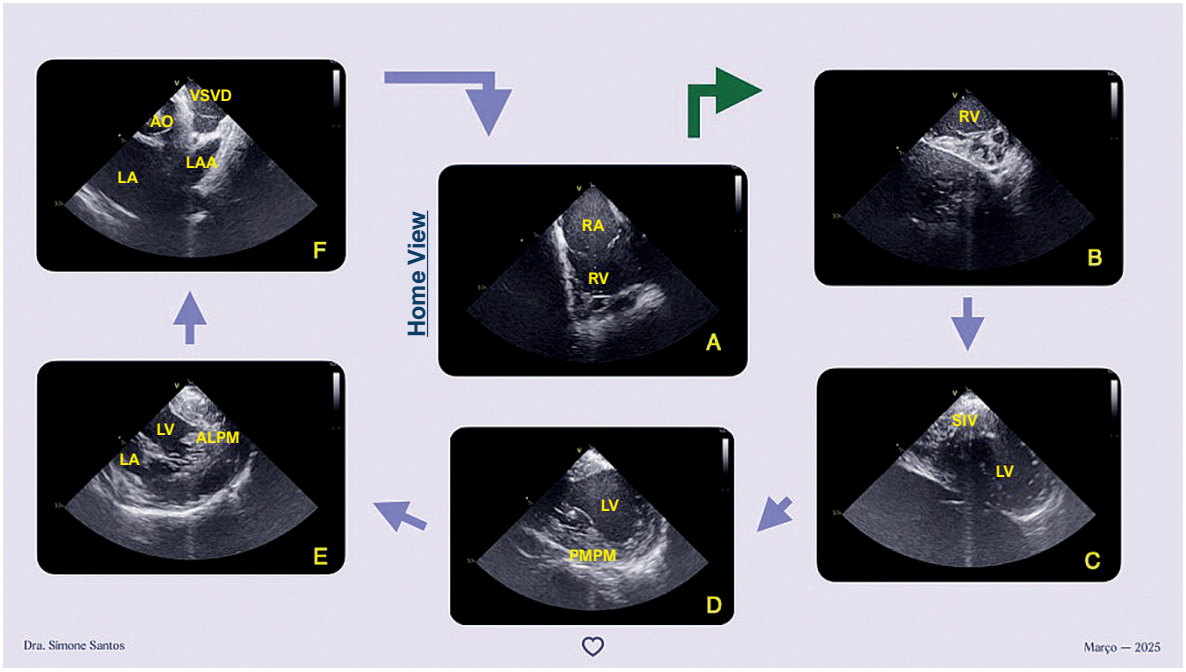

Figure 3 (A-F) – *Image sequence obtained from the RV. A: Home View; B: Green arrow shows anterior deflection with catheter positioned in the RV; C-F: Sequential views acquired via clockwise rotation of the catheter in the RV (blue arrows). PMPM: posteromedial papillary muscle; ALPM: anterolateral papillary muscle; AO: aorta; LA: left atrium; AO: aorta; RV: right ventricle; LV: left ventricle; RA: right atrium; LAA: left atrial appendage.*

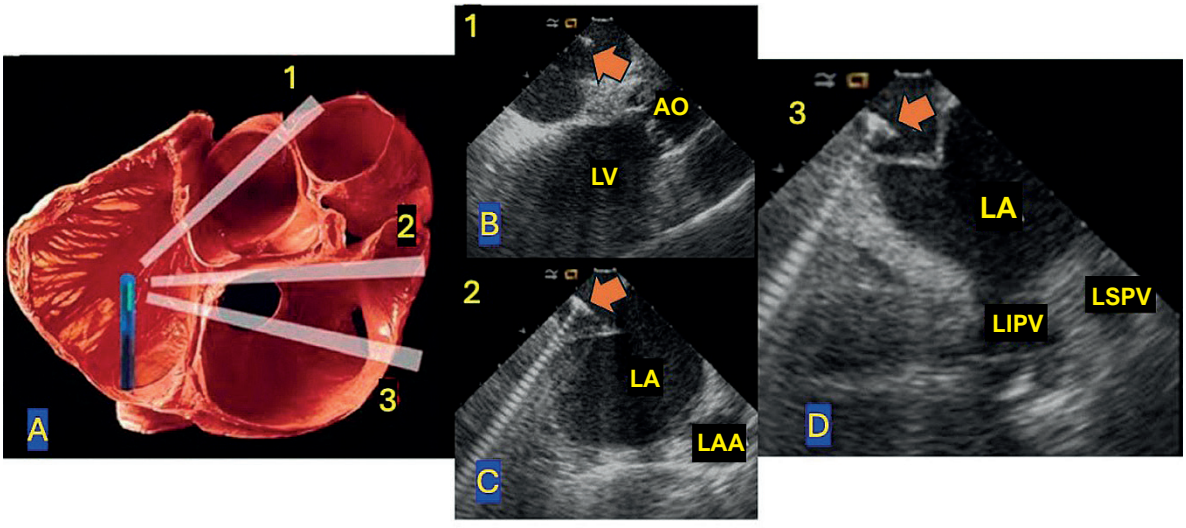

Figure 4 (A-D) – *Imaging planes for transeptal puncture. A: Schematic view of the heart and corresponding ICE imaging planes (1-3); B: Plane 1 – more anterior, with risk of aortic perforation; C: Plane 2 – anterior view of the LAA, which may hinder catheter manipulation; D: Plane 3 – ideal for transeptal puncture in AF ablation procedures, visualizing the entry of the left PVs. The orange arrow indicates the transeptal needle. Figure adapted from Enriquez, A. et al.19 LA: left atrium; LV: left ventricle; LAA: left atrial appendage; LSPV: left superior pulmonar vein; LIPV: left inferior pulmonary vein.*

Step 6 – Guiding circular catheter contact during electroanatomic mapping

We perform two ICE-guided transeptal punctures and insert two long sheaths: one for the electroanatomic mapping catheter and another for the ablation catheter. Once the anatomy of the LA and PVs is defined — whether there is a common trunk, separate ostia, or their relationship with the LAA — ICE is used to guide the mapping catheter's contact with atrial tissue, avoid proximity to the MV, and identify the ridge separating the left PVs from the LAA. This facilitates the rapid construction of the electroanatomic map of the LA and PVs. In some centers, the CARTOSOUND™ system (Biosense Webster) is used to generate chamber geometry based on multiple ICE imaging slices.

Step 7 – Monitoring ablation catheter contact and lesion formation

Once electroanatomic mapping is complete, the next step is real-time, accurate monitoring of the ablation catheter's contact with atrial tissue. This improves the efficacy of energy delivery while reducing the risk of complications. Inadequate tissue contact may result in ineffective lesion formation, leading to incomplete electrical isolation and increased blood heating, which raises the risk of thrombus formation. Energy delivery can also be titrated based on the gradual increase in tissue echogenicity observed on ICE. A sudden or excessive increase in echogenicity may precede a steam pop, which is associated with tissue perforation and an increased risk of cardiac tamponade (Supplementary Video 4). Such events are often accompanied by the formation of microbubbles, reflecting tissue heating and cellular leakage, and may pose a risk of cerebral microembolization.[5] Although current technologies provide contact force monitoring and recommend specific energy parameters for radiofrequency delivery, individual variations must be considered. Fragile patients, atrial scarring, or calcifications may result in either excessive or ineffective lesions.[23]

Step 8 – Monitoring esophageal proximity to ablation sites

Ablation of the PW — either for PV isolation or direct PW targeting — carries a potential risk of esophageal injury due to the close anatomical relationship between the esophagus and the LA. This may result in an atrioesophageal fistula.[24,25] To prevent esophageal injury, energy delivery near the esophagus is typically reduced in both force and duration, and esophageal temperature monitoring is routinely employed. However, despite these precautions, cases of esophageal injury detected by upper endoscopy after ablation have been reported.[26,27] In our esophageal temperature monitoring protocol, we first use ICE to visualize the position of the esophagus and its relationship to the PVs. We then insert a deflectable catheter orally for temperature monitoring, with excellent outcomes[28] (Figure 5).

Detecting complications

ICE imaging is used throughout the entire AF ablation procedure. Therefore, the early detection of potential complications should not be considered a single step in the process. From the initial femoral venous puncture, ICE can assist in identifying thrombi, occlusions, dissections, and extrinsic venous compressions along the pathway to the RA. Below, we highlight the most common complications that may occur during the procedure.

Pericardial effusion

One of the potential complications of radiofrequency ablation (RFA) for AF is cardiac tamponade. ICE allows for the rapid detection of PE, often before hemodynamic instability or tamponade develops.[29] This enables early intervention, reversal of anticoagulation, and, if necessary, pericardiocentesis. Initially, PE is typically visualized in the inferior region of the RV and the posterior aspect of the RA, and may progressively extend to the apical and anterior regions of the RV, eventually surrounding the entire heart.

Upon reaching the RA, the catheter is advanced into the RV, and clockwise rotation allows visualization of the pericardial space adjacent to both the RV and the LV (Figure 3). This approach enables early identification of any preexisting PE before catheter manipulation begins. With this baseline reference, if there is any suspicion of perforation or an episode of arterial hypotension, the pericardial space is promptly reassessed and compared to the initial images. As part of our standard protocol, we perform repeated ICE evaluations of the pericardial space from the RV at specific stages of the procedure: after isolation of the left PVs, after isolation of the right PVs, following any additional RF applications, and again after catheter withdrawal at the end of the procedure.

Intracavitary thrombi

Thrombus formation on sheaths and catheters can be readily detected in real time using ICE, allowing for immediate intervention and the prevention of potentially imminent embolic events.[30,31] Although less common due to the use of irrigated-tip catheters and direct oral anticoagulants, thrombi may still be observed adherent to sheaths or catheters while they are positioned in the RA, enabling early management before transeptal puncture. If thrombi are identified on catheters within the LA during the procedure, management strategies may include intensifying systemic heparinization, aspirating the thrombus into the sheath, or, in extreme cases, deploying bilateral carotid artery filters to prevent cerebral embolization.

Conclusion

ICE is the only tool that provides direct, real-time visualization throughout all phases of AF ablation. Mastery and systematic use of ICE enhance both the effectiveness and safety of the procedure.

Author Contributions

Conception and design of the research and writing of the manuscript: Santos SN; critical revision of the manuscript for intellectual content: Santos SN, Henz BD, Silva LRL, Silva MEL.

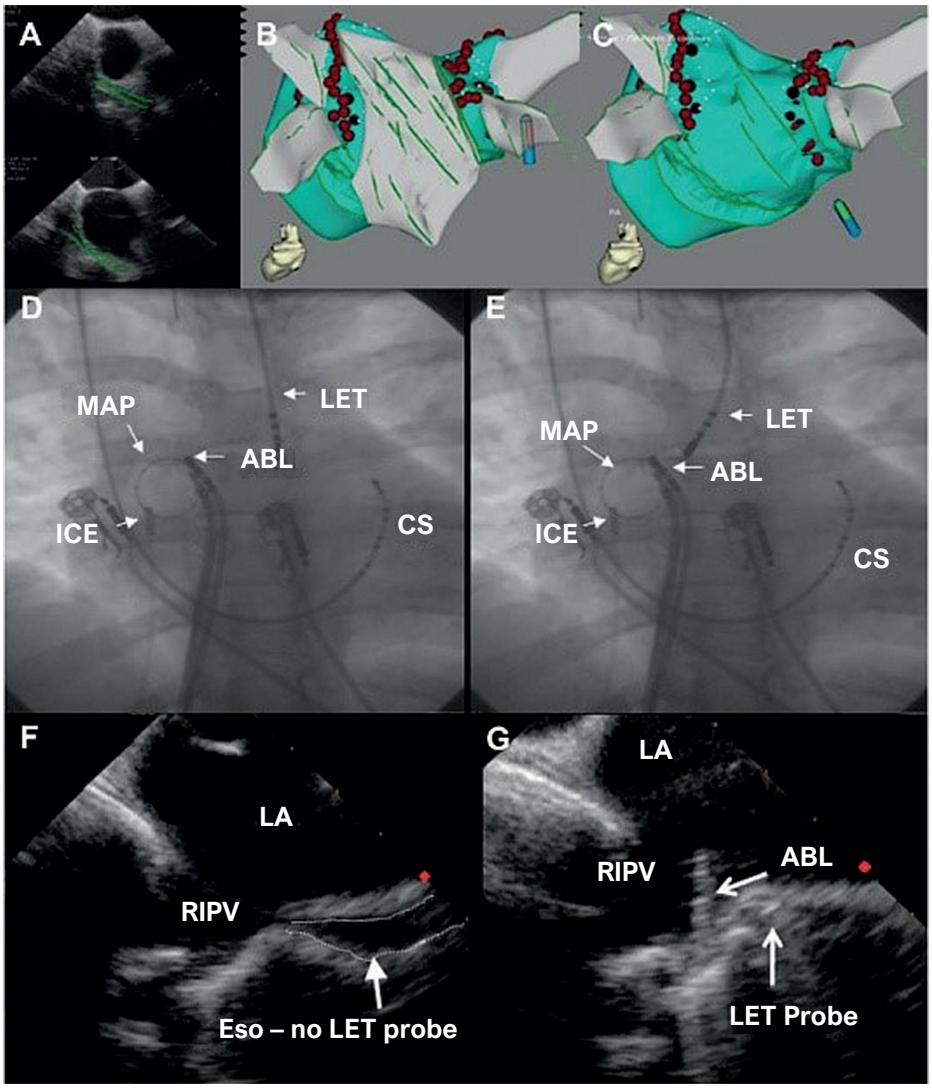

Figure 5 – *ICE-guided deflection of the esophageal temperature monitoring catheter. A: ICE showing the esophagus in relation to the left and right PVs (green contours); B: Esophagus (in gray) visualized in the electroanatomic map, broad and in contact with both left and right PVs; C: Electroanatomic map with black markers indicating esophageal temperature rise >2 °C; D: Fluoroscopy showing the luminal esophageal temperature (LET) probe in a neutral position, apparently distant from the right PVs; E: Fluoroscopy showing LET deflected to the right, approaching the ablation catheter; F: ICE image of the right PVs and esophagus without LET positioning, corresponding to fluoroscopic image D; G: ICE image with LET probe in place and in close proximity to the ablation catheter, corresponding to fluoroscopic image E. Eso: esophagus; MAP: circular mapping catheter; CS: coronary sinus catheter; LET: luminal esophageal temperature; ICE: Intracardiac echocardiography; LA: left atrium; RIPV: right inferior pulmonary vein; ABL: ablation catheter. Figure reproduced with permission from Leite L.R. et al.*[28]

Potential Conflict of Interest

No potential conflict of interest relevant to this article was reported.

Sources of Funding

There were no external funding sources for this study.

Study Association

This study is not associated with any thesis or dissertation work.

Ethics Approval and Consent to Participate

This article does not contain any studies with human participants or animals performed by any of the authors.

Use of Artificial Intelligence

The authors did not use any artificial intelligence tools in the development of this work.

Availability of Research Data

The underlying content of the research text is contained within the manuscript.

References

1. van Gelder IC, Rienstra M, Bunting KV, Casado-Arroyo R, Caso V, Crijns HJGM, et. 2024 ESC Guidelines for the Management of Atrial Fibrillation Developed in Collaboration with the European Association for Cardio-Thoracic Surgery (EACTS). Eur Heart J. 2024;45(36):3314-414. doi: 10.1093/eurheartj/ehae176.
2. Earing MG, Cabalka AK, Seward JB, Bruce CJ, Reeder GS, Hagler DJ. Intracardiac Echocardiographic Guidance during Transcatheter Device Closure of Atrial Septal Defect and Patent Foramen Ovale. Mayo Clin Proc. 2004;79(1):24-34. doi: 10.4065/79.1.24.
3. Medford BA, Taggart NW, Cabalka AK, Cetta F, Reeder GS, Hagler DJ, et al. Intracardiac Echocardiography during Atrial Septal Defect and Patent Foramen Ovale Device Closure in Pediatric and Adolescent Patients. J Am Soc Echocardiogr. 2014;27(9):984-90. doi: 10.1016/j.echo.2014.05.017.
4. Jongbloed MR, Bax JJ, van der Burg AE, van der Wall EE, Schalij MJ. Radiofrequency Catheter Ablation of Ventricular Tachycardia Guided by Intracardiac Echocardiography. Eur J Echocardiogr. 2004;5(1):34-40. doi: 10.1016/s1525-2167(03)00051-9.
5. Marrouche NF, Martin DO, Wazni O, Gillinov AM, Klein A, Bhargava M, et al. Phased-Array Intracardiac Echocardiography Monitoring during Pulmonary Vein Isolation in Patients with Atrial Fibrillation: Impact on Outcome and Complications. Circulation. 2003;107(21):2710-6. doi: 10.1161/01.CIR.0000070541.83326.15.
6. Bruce CJ, Packer DL, Seward JB. Transvascular Imaging: Feasibility Study Using a Vector Phased Array Ultrasound Catheter. Echocardiography. 1999;16(5):425-30. doi: 10.1111/j.1540-8175.1999.tb00086.x.
7. Bruce CJ, Packer DL, Seward JB. Intracardiac Doppler Hemodynamics and Flow: New Vector, Phased-Array Ultrasound-Tipped Catheter. Am J Cardiol. 1999;83(10):1509-12, A9. doi: 10.1016/s0002-9149(99)00136-8.
8. Goya M, Frame D, Gache L, Ichishima Y, Tayar DO, Goldstein L, et al. The Use of Intracardiac Echocardiography Catheters in Endocardial Ablation of Cardiac Arrhythmia: Meta-Analysis of Efficiency, Effectiveness, and Safety Outcomes. J Cardiovasc Electrophysiol. 2020;31(3):664-73. doi: 10.1111/jce.14367.
9. Friedman DJ, Pokorney SD, Ghanem A, Marcello S, Kalsekar I, Yadalam S, et al. Predictors of Cardiac Perforation with Catheter Ablation of Atrial Fibrillation. JACC Clin Electrophysiol. 2020;6(6):636-45. doi: 10.1016/j.jacep.2020.01.011.
10. Field ME, Gold MR, Reynolds MR, Goldstein L, Lee SHY, Kalsekar I, et al. Real-World Outcomes of Ventricular Tachycardia Catheter Ablation with versus without Intracardiac Echocardiography. J Cardiovasc Electrophysiol. 2020;31(2):417-22. doi: 10.1111/jce.14324.
11. Isath A, Padmanabhan D, Haider SW, Siroky G, Perimbeti S, Correa A, et al. Does the use of Intracardiac Echocardiography during Atrial Fibrillation Catheter Ablation Improve Outcomes and Cost? A Nationwide 14-Year Analysis from 2001 to 2014. J Interv Card Electrophysiol. 2021;61(3):461-8. doi: 10.1007/s10840-020-00844-5.
12. Pimentel RC, Rahai N, Maccioni S, Khanna R. Differences in Outcomes Among Patients with Atrial Fibrillation Undergoing Catheter Ablation with versus without Intracardiac Echocardiography. J Cardiovasc Electrophysiol. 2022 Sep;33(9):2015-47. doi: 10.1111/jce.15599.
13. Saad EB, Slater C, Inácio LAO Jr, Santos GVD, Dias LC, Camanho LEM. Catheter Ablation for Treatment of Atrial Fibrillation and Supraventricular Arrhythmias without Fluoroscopy Use: Acute Efficacy and Safety. Arq Bras Cardiol. 2020;114(6):1015-26. doi: 10.36660/abc.20200096.
14. Bulava A, Hanis J, Eisenberger M. Catheter Ablation of Atrial Fibrillation Using Zero-Fluoroscopy Technique: A Randomized Trial. Pacing Clin Electrophysiol. 2015;38(7):797-806. doi: 10.1111/pace.12634.
15. Razminia M, Willoughby MC, Demo H, Keshmiri H, Wang T, D'Silva OJ, et al. Fluoroless Catheter Ablation of Cardiac Arrhythmias: A 5-Year Experience. Pacing Clin Electrophysiol. 2017;40(4):425-33. doi: 10.1111/pace.13038.
16. Ikegami Y, Tanimoto K, Inagawa K, Shiraishi Y, Fuse J, Sakamoto M, et al. Identification of Left Atrial Appendage Thrombi in Patients with Persistent and Long-Standing Persistent Atrial Fibrillation Using Intra-Cardiac Echocardiography and Cardiac Computed Tomography. Circ J. 2017;82(1):46-52. doi: 10.1253/circj.CJ-17-0077.
17. Minga I, Lee K, Golemi L, Varley A, Thorne C, Osorio J, et al. Comparative Analysis of Transesophageal Echocardiography (TEE) and Intracardiac Echocardiography (ICE) in Atrial Fibrillation Ablation: Insights from the Real-World Experience Registry. J Interv Card Electrophysiol. 2025. doi: 10.1007/s10840-025-02013-y.
18. Sriram CS, Banchs JE, Moukabary T, Moradkhan R, Gonzalez MD. Detection of Left Atrial Thrombus by Intracardiac Echocardiography in Patients Undergoing Ablation of Atrial Fibrillation. J Interv Card Electrophysiol. 2015;43(3):227-36. doi: 10.1007/s10840-015-0008-2.
19. Lakkireddy D, Rangisetty U, Prasad S, Verma A, Biria M, Berenbom L, et al. Intracardiac Echo-Guided Radiofrequency Catheter Ablation of Atrial Fibrillation in Patients with Atrial Septal Defect or Patent Foramen Ovale Repair: A Feasibility, Safety, and Efficacy Study. J Cardiovasc Electrophysiol. 2008;19(11):1137-42. doi: 10.1111/j.1540-8167.2008.01249.x.
20. Santangeli P, Di Biase L, Burkhardt JD, Horton R, Sanchez J, Bailey S, et al. Transseptal Access and Atrial Fibrillation Ablation Guided by Intracardiac Echocardiography in Patients with Atrial Septal Closure Devices. Heart Rhythm. 2011;8(11):1669-75. doi: 10.1016/j.hrthm.2011.06.023.
21. Hsu JC, Badhwar N, Gerstenfeld EP, Lee RJ, Mandyam MC, Dewland TA, et al. Randomized Trial of Conventional Transseptal Needle versus Radiofrequency Energy Needle Puncture for Left Atrial Access (the TRAVERSE-LA Study). J Am Heart Assoc. 2013;2(5):e000428. doi: 10.1161/JAHA.113.000428.
22. JFM. R. Monitoring and Early Diagnosis of Procedural Complications. In: Ren J-F, Marchlinski FE, Callans DJ, Schwartzman D, editors. Practical Intracardiac Echocardiography in Electrophysiology. Oxford: Blackwell Science; 2006. p. 180-207.
23. Santos SN, Silva LRL, Medeiros F, Zanatta AR, Botelho FMN, Henz BD. Left Atrial Intramural Hematoma during Radiofrequency Catheter Ablation for Atrial Fibrillation: The Important Role of Intracardiac Echocardiography. Heart Rhythm Case Reports. 2025;11(4):311-7. doi: 10.1016/j.hrcr.2024.12.017.
24. Sánchez-Quintana D, Cabrera JA, Climent V, Farré J, Mendonça MC, Ho SY. Anatomic Relations between the Esophagus and Left Atrium and Relevance for Ablation of Atrial Fibrillation. Circulation. 2005;112(10):1400-5. doi: 10.1161/CIRCULATIONAHA.105.551291.
25. Di Biase L, Saenz LC, Burkhardt DJ, Vacca M, Elayi CS, Barrett CD, et al. Esophageal Capsule Endoscopy after Radiofrequency Catheter Ablation for Atrial Fibrillation: Documented Higher Risk of Luminal Esophageal Damage with General Anesthesia as Compared with Conscious Sedation. Circ Arrhythm Electrophysiol. 2009;2(2):108-12. doi: 10.1161/CIRCEP.108.815266.

26. Singh SM, d'Avila A, Doshi SK, Brugge WR, Bedford RA, Mela T, et al. Esophageal Injury and Temperature Monitoring during Atrial Fibrillation Ablation. Circ Arrhythm Electrophysiol. 2008;1(3):162-8. doi: 10.1161/CIRCEP.107.789552.

27. Rillig A, Meyerfeldt U, Birkemeyer R, Wiest S, Sauer BM, Staritz M, et al. Oesophageal Temperature Monitoring and Incidence of Oesophageal Lesions after Pulmonary Vein Isolation Using a Remote Robotic Navigation System. Europace. 2010;12(5):655-61. doi: 10.1093/europace/euq061.

28. Leite LR, Santos SN, Maia H, Henz BD, Giuseppin F, Oliverira A, et al. Luminal Esophageal Temperature Monitoring with a Deflectable Esophageal Temperature Probe and Intracardiac Echocardiography May Reduce Esophageal Injury during Atrial Fibrillation Ablation Procedures: Results of a Pilot Study. Circ Arrhythm Electrophysiol. 2011;4(2):149-56. doi: 10.1161/CIRCEP.110.960328.

29. Doldi F, Geßler N, Anwar O, Kahle AK, Scherschel K, Rath B, et al. In-Hospital Mortality and Major Complications Related to Radiofrequency Catheter Ablations of Over 10 000 Supraventricular Arrhythmias from 2005 to 2020: Individualized Case Analysis of Multicentric Administrative Data. Europace. 2023;25(1):130-6. doi: 10.1093/europace/euac146.

30. Ren JF, Marchlinski FE, Callans DJ. Left Atrial Thrombus Associated with Ablation for Atrial Fibrillation: Identification with Intracardiac Echocardiography. J Am Coll Cardiol. 2004;43(10):1861-7. doi: 10.1016/j.jacc.2004.01.031.

31. Macedo PG, Oliveira EM, Henz BD, Santos S, Barreto JR, Zanatta A, et al. Thrombus Detection by Intracardiac Ecocardiography During Atrial Fibrillation Ablation: Implications in Stroke and Peripheral Embolism Prevention. . Heart Rhythm 2016;13:5:166-232. doi: 10.1016/j.hrthm.2016.03.028.

32. Enriquez A, Saenz LC, Rosso R, Silvestry FE, Callans D, Marchlinski FE, et al. Use of Intracardiac Echocardiography in Interventional Cardiology: Working with the Anatomy Rather Than Fighting It. Circulation. 2018;137(21):2278-94. doi: 10.1161/CIRCULATIONAHA.117.031343.

*Supplemental Materials

See the Supplemental Video 1, please click here.

See the Supplemental Video 2, please click here.

See the Supplemental Video 3, please click here.

See the Supplemental Video 4, please click here.

My Approach To Echocardiographic Evaluation in Pediatric Patients with Sickle Cell Disease

Viviane Thome Gonçalves Dias,[1] *Mirela Frederico de Almeida*[2,3]
Hospital Santa Izabel,[1] *Salvador, BA – Brazil*
Universidade Federal da Bahia,[2] *Salvador, BA – Brazil*
Hospital Alianca,[3] *Salvador, BA – Brazil*

Central Illustration: My Approach To Echocardiographic Evaluation in Pediatric Patients with Sickle Cell Disease

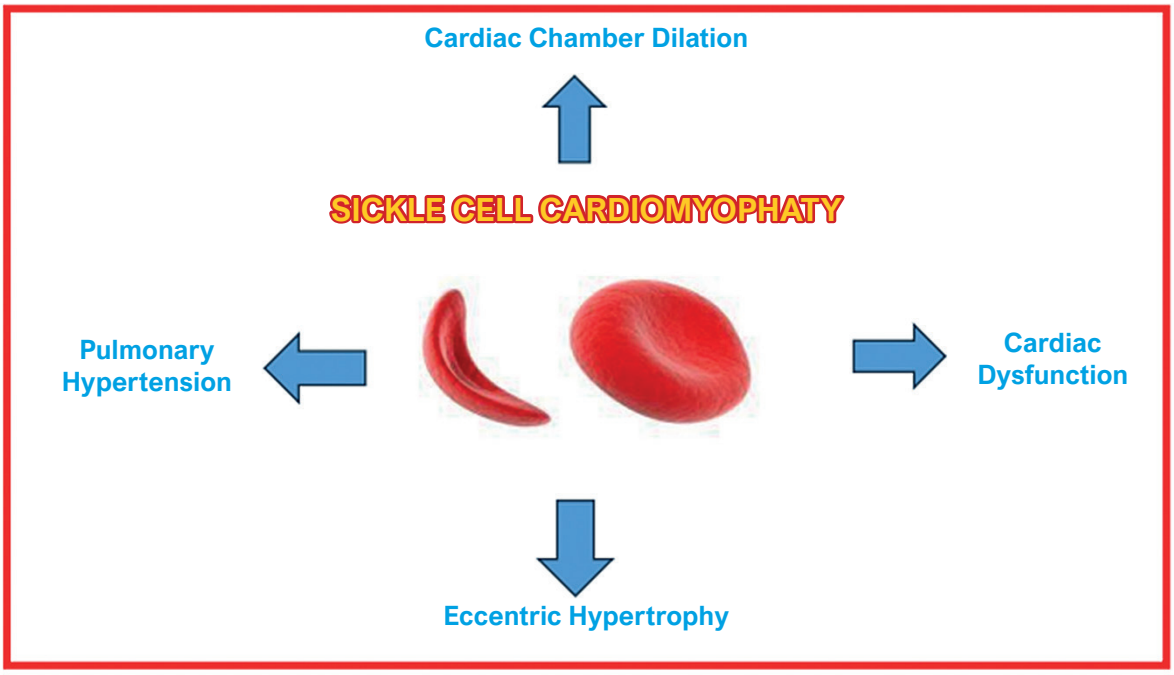

Arq Bras Cardiol: Imagem cardiovasc. 2025;38(2):e20240128

Echocardiographic evaluation in patients with sickle cell disease.

Keywords

Echocardiography; Sickle Cell Anemia; Child

Mailing Address: Viviane Thome G. Dias •
Rede D'or Aliança. Avenida Juracy Magalhaes, 2096. Postal code: 41920-900. Salvador, BA – Brazil.
E-mail: diasvivi82@gmail.com
Manuscript received November 30, 2024; revised March 27, 2025; accepted April 18, 2025
Editor responsible for the review: Marcelo Tavares

DOI: https://doi.org/10.36660/abcimg.20240128i

Abstract

Sickle cell disease (SCD) is the most prevalent hereditary genetic disorder worldwide, and cardiovascular alterations are the main cause of death among patients with this disease.

Therefore, the early identification of markers of sickle cell cardiomyopathy using echocardiographic parameters (Central Illustration) is essential for the appropriate management of the cardiovascular condition in these patients.

This review provides a comprehensive overview of the use of echocardiography in pediatric patients with SCD, highlighting the main characteristics of the condition and the importance of regular follow-up.

Introduction

Sickle cell disease (SCD) is considered the most prevalent hereditary genetic disorder worldwide.

In Brazil, this condition affects between 60,000 and 100,000 individuals and has a higher incidence among the Afro-descendant population (8%). The distribution across the Brazilian territory is heterogeneous, with a higher incidence in the states of Bahia, Distrito Federal, and Piauí. The national incidence is approximately 1:1,200 live births, while it reaches 1:650 live births in Bahia.[1]

SCD is characterized by a recessive autosomal hereditary mutation, in which the glutamic acid is replaced by valine at the sixth position of the hemoglobin (Hb) beta chain. As a result, the organism produces Hb S , an abnormal type of Hb responsible for the physiopathology of SCD. Hb S has a shorter half-life (approximately one-sixth of the normal Hb A) due to its increased susceptibility to hemolysis and increased adhesiveness, contributing to vaso-occlusive events.

The disease may manifest as a homozygous form (Hb SS), known as sickle cell anemia, which is the most severe and prevalent form (approximately 60% to 75% of cases), with symptoms typically beginning within the first year of life. The heterozygous form occurs in approximately 25% to 40% of cases, tends to be milder, and results from the association of Hb S with other abnormal Hb, such as Hb SC and Hb SE. On the other hand, the sickle cell trait occurs when there is an association between Hb S and Hb A.[2] Individuals with sickle cell trait are usually asymptomatic.

Under stress conditions (e.g., extreme temperatures, infection, or dehydration), the deoxygenated Hb S undergoes polymerization, causing red blood cells to assume a sickle shape. This condition makes Hb more prone to hemolysis, leading to chronic anemia. Moreover, the increased Hb rigidity impairs its passage through the microvasculature, triggering repeated painful vasoconstriction, endothelial dysfunction, inflammation, and ischemia-reperfusion injury.

The cardiac involvement in SCD arises from multiple mechanisms:

- Chronic hemolytic anemia leads to reflex peripheral vasodilation to improve tissue oxygen delivery. This condition activates the renin-angiotensin-aldosterone system to retain sodium and water and, consequently, increase preload and chronic cardiac chamber **dilation**, particularly in the left chambers. Over time, this results in compensatory **eccentric hypertrophy**.
- Chronic vaso-occlusive crises may cause microvascular myocardial dysfunction, renal failure, and systemic arterial hypertension. These conditions promote myocardial fibrosis and consequent **systolic** (less common) and **diastolic dysfunction** (more frequent).
- **Pulmonary hypertension** in patients with SCD is multifactorial (Group 5): it may present with pre-capillary (arterial) characteristics secondary to intravascular hemolysis and Hb release into the plasma, which consumes nitric oxide and causes vasoconstriction, and post-capillary (venous) characteristics, in which diastolic dysfunction increases ventricular filling pressure, impairing blood flow through pulmonary veins and increasing pulmonary venous pressure. Additionally, chronic hypoxia and pulmonary thromboembolism may further contribute to elevated pulmonary pressure in patients with SCD.

Given these alterations, qualified and regular echocardiographic assessments are essential in patients with SCD.

Echocardiographic evaluation in patients with SCD

Dilation of cardiac chambers

The dilation of cardiac chambers, particularly the left chamber, occurs in approximately 30% to 65% of patients with SCD and is more prevalent in adults and those with the most severe form.

Atrium dilation is the earliest cardiac alteration resulting from volume overload secondary to compensatory vasodilation in response to anemia as a mechanism to improve oxygen delivery to tissues.

Sabatini et al. demonstrated an inverse association between serum Hb levels (degree of anemia) and left atrial dilation, and a direct association between reticulocyte levels (a marker for hemolytic anemia) and left atrial dilation[3] (Figure 1).

Eccentric hypertrophy

Eccentric hypertrophy (more common in the left chambers) occurs in 25% to 45% of patients with SCD and is more prevalent among older adults and individuals with more severe hemolytic anemia.

Koyunku et al. conducted a retrospective study on 146 patients with SCD aged over 18 years and found that 45 (30.8%) patients presented eccentric hypertrophy. After a 5-year follow-up, 31 (21.2%) patients had died. Survival analysis showed that patients presenting eccentric hypertrophy had a worse prognosis (the greater the eccentric hypertrophy, the higher the risk of death).[4]

Cardiac dysfunction

Chronic hemolytic anemia and recurrent vaso-occlusive episodes are physiopathological mechanisms for microvascular dysfunction and myocardial fibrosis. Moreover, disease-related systemic alterations, such as renal dysfunction, systemic arterial hypertension, and iron overload (which may occur in patients receiving periodical blood transfusions), contribute to the development or worsening of cardiac dysfunction, or both.

Diastolic dysfunction is common in adults with SCD (approximately 15% to 20% of cases) and is associated with an increased risk of premature death.[5] Evaluating diastolic

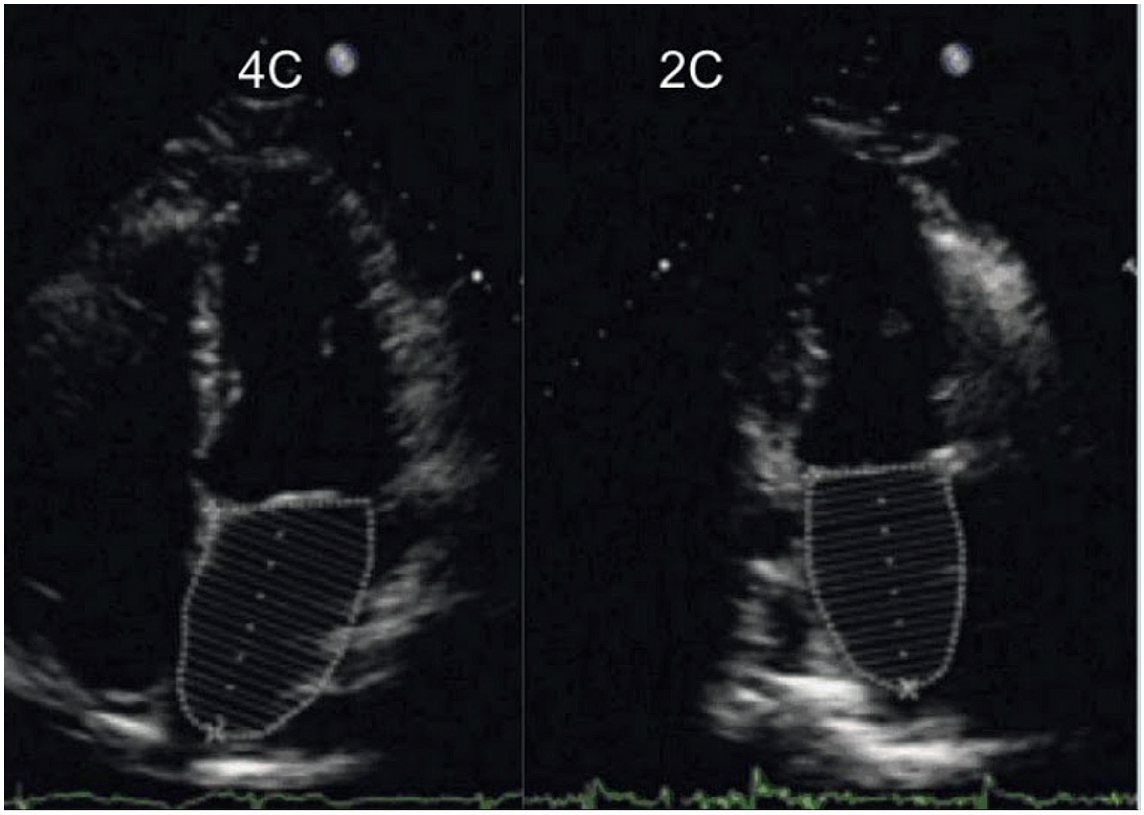

Figure 1 – *Apical 2- and 4-chamber views for left atrial volume calculation.*

function in patients with SCD is needed but also challenging for echocardiographers.

In children, the assessment of diastolic function is limited because the Doppler parameters vary significantly according to age, body surface area, and heart rate. Unlike systolic function, which can be evaluated using one parameter (e.g., ejection fraction), there is no single gold-standard marker for diastolic function.

Even invasive measurements obtained by cardiac catheterization have limitations and provide only partial information on ventricular diastolic characteristics. Also, the parameters used to define diastolic dysfunction may be affected by the underlying disease physiopathology without truly reflecting diastolic function alterations, such as atrial dilation.[6,7]

In the general population, atrial dilation is associated with increased ventricular filling pressures. However, this dilation in patients with SCD occurs early in the development of the disease due to volume overload from the compensatory physiopathology of the condition and may not reflect elevated filling pressures. Hammoudi et al. evaluated 127 patients with SCD and found that most presented with left atrial dilation, but this finding was not associated with diastolic dysfunction. Instead, it correlated with disease severity and duration.[5]

Tricuspid regurgitation velocity peak is another parameter used to assess diastolic function. However, an increase in this parameter in patients with SCD may not necessarily indicate elevated pulmonary arterial pressure but rather increased cardiac preload or pre-capillary pulmonary hypertension. Hence, tricuspid regurgitation velocity data must be interpreted with caution in this population.[5]

The ratio between early diastolic transmitral flow velocity and tissue Doppler velocity (E/e′) is also used to estimate the left ventricular filling pressure in SCD. Sachdev et al. assessed 436 patients with SCD (homozygous for Hb S) and found that the E/e′ ratio independently correlated with reduced exercise capacity measured using the six-minute walk test.[8]

Another parameter used to evaluate diastolic function is the ratio between early and late diastolic flow velocity (E/A ratio). In a study of 141 patients with SCD, Sachdev et al. found that a low E/A ratio (i.e., indicative of diastolic dysfunction) was associated with increased mortality risk (hazard ratio of 3.5).[9]

Systolic dysfunction (assessed by conventional echocardiography) is rare in children with SCD.[4] Poludasu et al. performed a meta-analysis of 19 case-control studies and found no significant difference in systolic function between 841 patients with SCD (homozygous Hb S) and

554 controls when evaluated using echocardiographic parameters[10] (Figure 2).

Strain analysis in SCD: what is new?

The development of 2D strain imaging enabled the early detection of cardiac damage in many chronic diseases and has become an increasingly important tool in prognostic stratification. The aim is to highlight the contribution of 2D strain in detecting subclinical ventricular myocardial damage in patients with SCD.

Cardiac dilation and eccentric ventricular hypertrophy in patients with SCD occur in response to increased preload and may progressively alter the cardiac function. These alterations contribute to morbidity and mortality in patients with SCD.

The global longitudinal strain of the left ventricle is a more specific predictor of myocardial remodeling than the left ventricle ejection fraction (LVEF), making it a sensitive tool for detecting early systolic dysfunction even when LVEF is preserved.

Studies have shown that patients with SCD presenting lower Hb levels (Hb < 9 g/dl) and increased preload are more likely to develop long-term subclinical systolic dysfunction in the left ventricle due to the limited adaptability of the heart to chronic preload increases. Resende et al. followed 219 patients with SCD for 30 months and observed that those with abnormal strain had worse clinical outcomes (pain crises, acute chest syndrome, and SCD-related death), independent of age, tricuspid regurgitation velocity peak, and ejection fraction assessed using conventional echocardiography. Thus, patients with SCD who present abnormal strain are at greater risk for adverse outcomes[11] (Figure 3).

Pulmonary hypertension

Pulmonary hypertension is characterized by reduced blood flow through the pulmonary arterial circulation due to increased pulmonary vascular resistance and elevated arterial pressures.

The prevalence of pulmonary hypertension is higher in patients with Hb SS disease than in those with SC, Sβ+, or Sβ° thalassemia.

Studies using echocardiography to measure tricuspid regurgitation velocity peak as an index of systolic pulmonary artery pressure demonstrated a high prevalence (30%) of pulmonary hypertension in patients with SCD.[5]

The physiopathology of pulmonary hypertension varies. First, since pulmonary pressure is a product of flow and pulmonary vascular resistance, the high cardiac output in SCD leads to increased pulmonary pressure regardless of altered pulmonary vascular resistance. Second, chronic volume overload may lead to left ventricular failure and subsequent pulmonary venous hypertension. Third, intravascular hemolysis may induce pulmonary arterial vasculopathy, mainly driven by nitric oxide depletion due to free plasma Hb.

Last, several other mechanisms may contribute, including hypoxemia, post-embolic pulmonary hypertension, lung injury related to SCD, and chronic liver disease. Importantly, several of these factors often occur simultaneously in the same patient with SCD and pulmonary hypertension. This represents a major challenge in the clinical management of the disease. Therefore, these patients are currently classified into Group 5 of the WHO classification system for pulmonary hypertension.[5]

Mehari et al. studied 531 patients and found associations between pulmonary pressure and reduced exercise tolerance and increased mortality rate in patients with SCD.[12]

Given the impact of pulmonary hypertension on the morbidity and mortality of patients with SCD, the American Thoracic Association published a management guideline in 2014 recommending diagnostic cardiac catheterization when tricuspid regurgitation velocity was ≥ 3 m/s or between 2.5 and 2.9 m/s in symptomatic patients (e.g., reduced performance in the six-minute walk test or elevated serum NT-pro-BNP) [13] (Figure 4).

Echocardiographic assessment during SCD treatment

Symptomatic patients with SCD or those with pulmonary hypertension are candidates for disease-modifying treatments.

Hydroxyurea is one of the drugs used to treat SCD. One of its mechanisms of action is to increase fetal Hb levels; thus, reducing pathological Hb S levels and its physiopathological consequences.

Dhar et al. analyzed 100 patients with SCD, including 60 who received hydroxyurea, and observed that left ventricular dilation and hypertrophy significantly improved with hydroxyurea therapy. Additionally, left ventricular volume and mass were inversely correlated with treatment duration, demonstrating that pharmacological therapy may lead to cardiac remodeling.[14]

Another recommended therapy in symptomatic patients with SCD is chronic blood transfusion, aimed at reducing levels of pathological Hb S.

Turpin et al. evaluated 13 patients with SCD (homozygous Hb S) before and after chronic blood transfusion therapy and observed improved functional class and reduced tricuspid regurgitation jet velocity following transfusion.[15]

Therefore, patients with SCD undergoing disease-modifying treatment should also be regularly evaluated by echocardiography for a better definition of the cardiovascular status.

Echocardiographic assessment during SCD crises

Patients with SCD may present numerous acute events throughout life, such as pain crises, acute chest syndrome, splenic sequestration, and stroke.

Onalo et al. followed 176 patients for two years (92 without crisis and 84 with at least one crisis) and found a higher prevalence of pulmonary hypertension and cardiac dysfunction in those who experienced a crisis during this period.[16]

Therefore, patients with SCD who present with a sickle cell crisis must have their cardiovascular status re-evaluated to ensure appropriate cardiac management during these episodes.

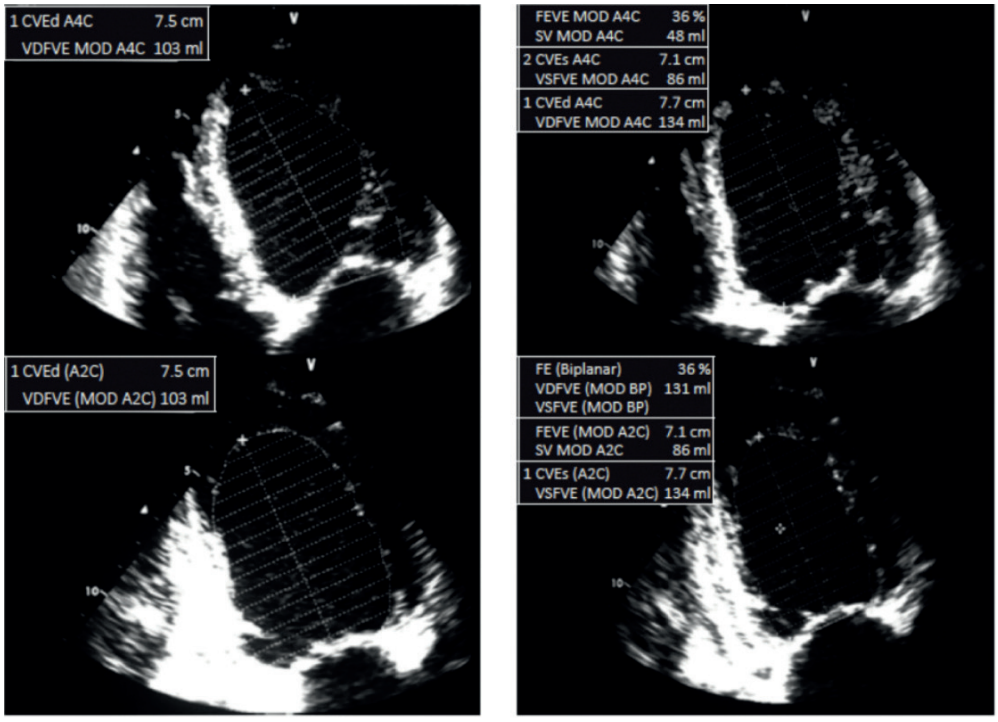

Figure 2 – *Apical 2- and 4-chamber views for the analysis of ventricular function during systole and diastole. Ejection fraction was calculated using Simpson's method. CVEd/VDFVE: Left Ventricular End-Diastolic Volume; MOD: Simpson's Method; FEVE/FE: Left Ventricular Ejection Fraction; CVE/VSFVE: Left Ventricular End-Systolic Volume; SV: Stroke Volume.*

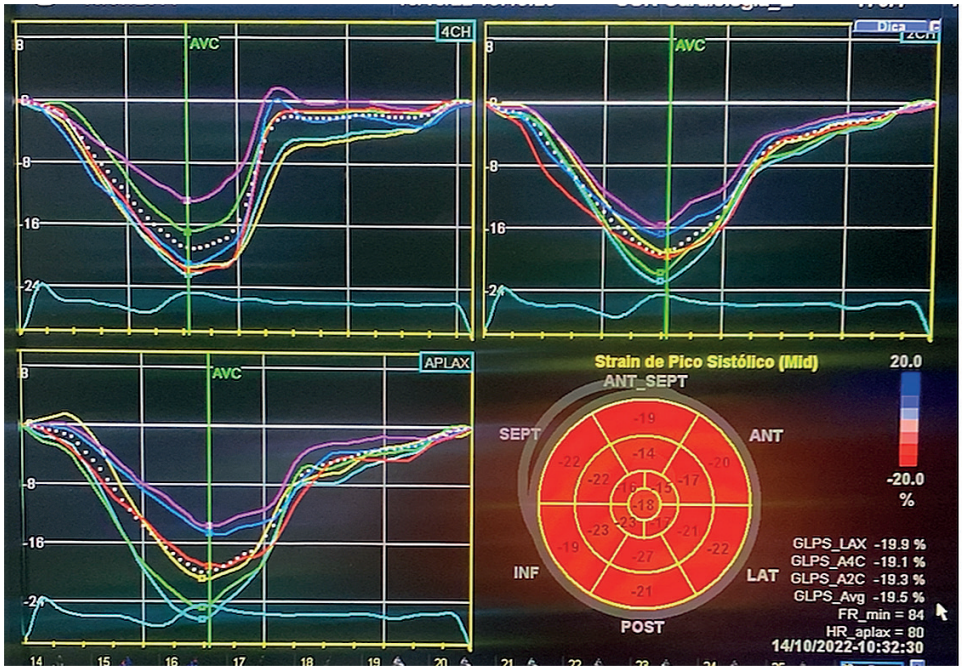

Figure 3 – *Left ventricle global longitudinal strain of -19.5% in a child with SCD. Sept: Septal wall; Ant: Anterior wall; Inf: Inferior wall; Lat: Lateral wall; Post: Posterior wall; GLPS: Global Longitudinal Peak Strain; FR: Frame Rate*

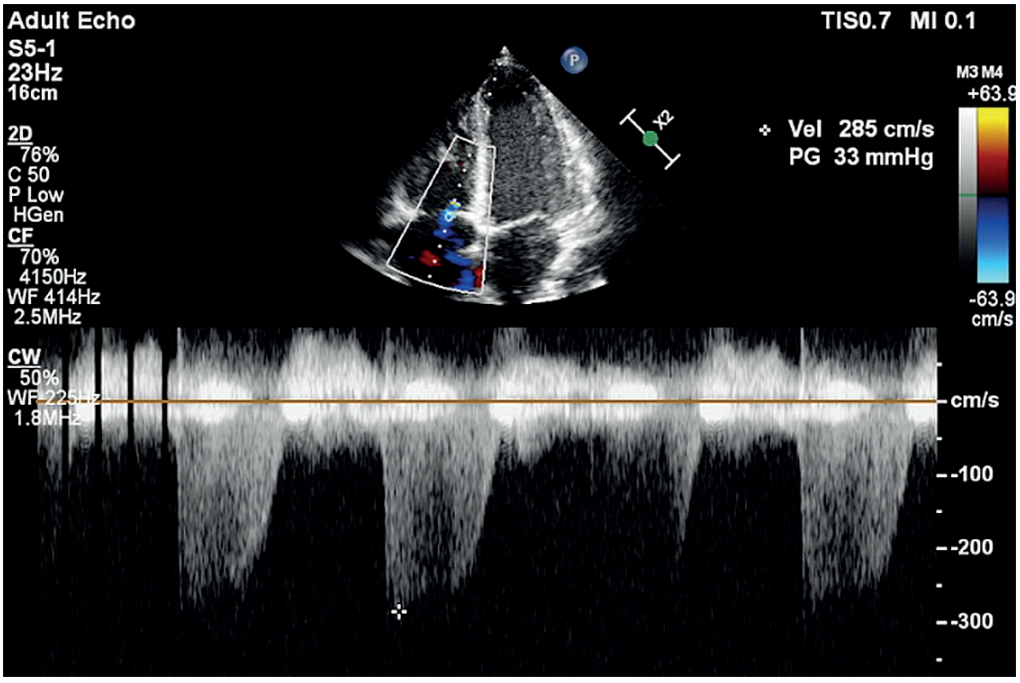

Figure 4 – *Apical 4-chamber view for the analysis of tricuspid regurgitation using continuous Doppler in a patient with SCD. PG: Pressure Gradient; CW: Continuous Wave Doppler; WF: Waveform; CF: Color Flow Doppler*

Conclusion

Routine echocardiogram for asymptomatic pediatric patients with SCD is not yet a reality in clinical practice. However, the significant impact of cardiac alterations can be already observed from childhood.

Serial echocardiography exams must be considered to allow an early diagnosis of cardiac complications, improve clinical care for patients with SCD, and reduce cardiovascular morbidity and mortality in this population.

Author Contributions

Conception and design of the research, acquisition of data, analysis and interpretation of the data, writing of the manuscript and critical revision of the manuscript for intellectual content: Dias VTG, Andrade MFA.

Potential Conflict of Interest

No potential conflict of interest relevant to this article was reported.

Sources of Funding

There were no external funding sources for this study.

Study Association

This study is not associated with any thesis or dissertation work.

Ethics Approval and Consent to Participate

This article does not contain any studies with human participants or animals performed by any of the authors.

Use of Artificial Intelligence

The authors did not use any artificial intelligence tools in the development of this work.

Availability of Research Data

The underlying content of the research text is contained within the manuscript.

References

1. Agência Nacional de Vigilância Sanitária. Manual de Diagnóstico e Tratamento de Doenças Falciformes. Brasília: ANVISA; 2001.
2. Brasil. Ministério da Saúde. Doença Falciforme [Internet]. Brasília: Ministério da Saúde; 2025 [cited 2025 May 19]. Available from: https://www.gov.br/saude/pt-br/assuntos/saude-de-a-a-z/d/doenca-falciforme.
3. Sabatini L, Chinali M, Franceschini A, Di Mauro M, Marchesani S, Fini F, et al. Echocardiographic Evaluation in Paediatric Sickle Cell Disease Patients: A Pilot Study. J Clin Med. 2022;12(1):7. doi: 10.3390/jcm12010007.
4. Koyuncu MB, Tombak A, Orscelik O, Koseci T, Turker A, Basir H, et al. Cardiac Chamber Quantification by Echocardiography in Adults with

Sickle Cell Disease: Need Attention to Eccentric Hypertrophy. Cureus. 2021;13(6):e15592. doi: 10.7759/cureus.15592.

5. Hammoudi N, Lionnet F, Redheuil A, Montalescot G. Cardiovascular Manifestations of Sickle Cell Disease. Eur Heart J. 2020;41(13):1365-73. doi: 10.1093/eurheartj/ehz217.

6. Rosa LM, Morhy SS. My Approach to Managing Left Ventricular Diastolic Function of Children and in Congenital Heart Disease. Arq Bras Cardiol: Imagem Cardiovasc. 2022;35(3):ecom29. doi: 10.47593/2675-312X/20223503ecom29.

7. Hammoudi N, Charbonnier M, Levy P, Djebbar M, Stojanovic KS, Ederhy S, et al. Left Atrial Volume is Not an Index of Left Ventricular Diastolic Dysfunction in Patients with Sickle Cell Anaemia. Arch Cardiovasc Dis. 2015;108(3):156-62. doi: 10.1016/j.acvd.2014.09.010.

8. Sachdev V, Kato GJ, Gibbs JS, Barst RJ, Machado RF, Nouraie M, et al. Echocardiographic Markers of Elevated Pulmonary Pressure and Left Ventricular Diastolic Dysfunction are Associated with Exercise Intolerance in Adults and Adolescents with Homozygous Sickle Cell Anemia in the United States and United Kingdom. Circulation. 2011;124(13):1452-60. doi: 10.1161/CIRCULATIONAHA.111.032920.

9. Sachdev V, Machado RF, Shizukuda Y, Rao YN, Sidenko S, Ernst I, et al. Diastolic Dysfunction is an Independent Risk Factor for Death in Patients with Sickle Cell Disease. J Am Coll Cardiol. 2007;49(4):472-9. doi: 10.1016/j.jacc.2006.09.038.

10. Poludasu S, Ramkissoon K, Salciccioli L, Kamran H, Lazar JM. Left Ventricular Systolic Function in Sickle Cell Anemia: A Meta-Analysis. J Card Fail. 2013;19(5):333-41. doi: 10.1016/j.cardfail.2013.03.009.

11. Resende MBS, Ferrari TCA, Araujo CG, Vasconcelos MCM, Tupinambás JT, Dias RCTM, et al. Prognostic Value of Left Ventricular Longitudinal Strain by Speckle-Tracking Echocardiography in Patients with Sickle Cell Disease. Int J Cardiovasc Imaging. 2020;36(11):2145-53. doi: 10.1007/s10554-020-01924-3.

12. Mehari A, Gladwin MT, Tian X, Machado RF, Kato GJ. Mortality in Adults with Sickle Cell Disease and Pulmonary Hypertension. JAMA. 2012;307(12):1254-6. doi: 10.1001/jama.2012.358.

13. Klings ES, Machado RF, Barst RJ, Morris CR, Mubarak KK, Gordeuk VR, et al. An Official American Thoracic Society Clinical Practice Guideline: Diagnosis, Risk Stratification, and Management of Pulmonary Hypertension of Sickle Cell Disease. Am J Respir Crit Care Med. 2014;189(6):727-40. doi: 10.1164/rccm.201401-0065ST.

14. Dhar A, Leung TM, Appiah-Kubi A, Gruber D, Aygun B, Serigano O, et al. Longitudinal Analysis of Cardiac Abnormalities in Pediatric Patients with Sickle Cell Anemia and Effect of Hydroxyurea Therapy. Blood Adv. 2021;5(21):4406-12. doi: 10.1182/bloodadvances.2021005076.

15. Turpin M, Chantalat-Auger C, Parent F, Driss F, Lionnet F, Habibi A, et al. Chronic Blood Exchange Transfusions in the Management of Pre-Capillary Pulmonary Hypertension Complicating Sickle Cell Disease. Eur Respir J. 2018;52(4):1800272. doi: 10.1183/13993003.00272-2018.

16. Onalo R, Cooper P, Cilliers A, Nnebe-Agumadu U. Cardiovascular Changes in Children with Sickle Cell Crisis. Cardiol Young. 2020;30(2):162-70. doi: 10.1017/S1047951120000037.

My Approach to Point-of-Care Ultrasound for Dyspnea Assessment

Adriana Brentegani,[1,2] Fernando Arturo Effio Solis,[3] Milena de Paulis,[3] Marcelo Luiz Campos Vieira[1,3]

Instituto do Coração do Hospital das Clínicas da Faculdade de Medicina da Universidade de São Paulo,[1] São Paulo, SP – Brazil

Hospital Sírio-Libanês,[2] São Paulo, SP – Brazil

Hospital Israelita Albert Einstein,[3] São Paulo, SP – Brazil

Central Illustration: My Approach to Point-of-Care Ultrasound for Dyspnea Assessment

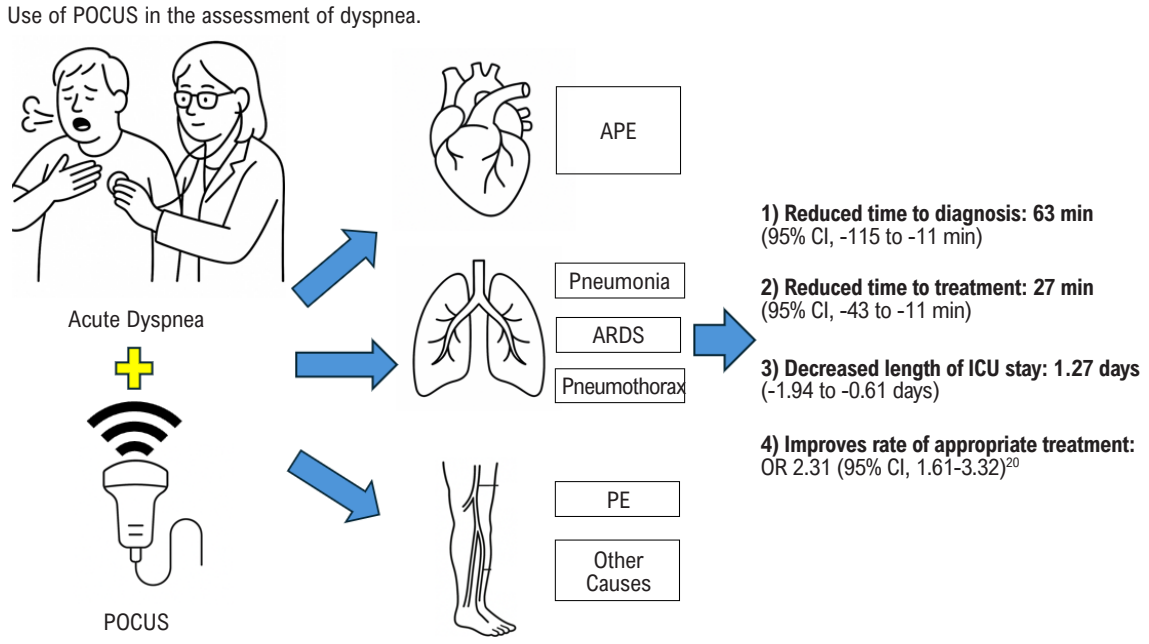

Arq Bras Cardiol: Imagem cardiovasc. 2025;38(2):e20250023

POCUS: Point-of-care ultrasound; ARDS: acute respiratory distress syndrome; PE: pulmonary embolism; APE: Acute Pulmonary Edema.

Abstract

Dyspnea is a common and potentially serious symptom whose traditional diagnostic approach, based on physical examination and complementary tests, may present significant limitations. Point-of-care ultrasound (POCUS) has emerged as an effective tool for the rapid and accurate assessment of this symptom, both in outpatient settings and in emergency and critical care environments.

This article provides a practical, illustrated guide to the integrated application of POCUS in the evaluation of dyspnea, with an emphasis on distinguishing cardiac from pulmonary causes. It describes techniques for acquiring cardiac, pulmonary, and venous ultrasound images, highlights key sonographic findings, and outlines a step-by-step approach to clinical application. Lung POCUS has demonstrated high sensitivity in detecting differential diagnoses of dyspnea. Its integration with echocardiography and lower limb ultrasound further refines diagnosis by identifying specific clinical patterns such as acute pulmonary edema (APE), pulmonary embolism (PE), and acute respiratory distress syndrome (ARDS).

The structured use of POCUS represents a significant advancement in the modern physical exam, enabling faster and more accurate bedside clinical decision-making. Its adoption should be encouraged among cardiologists,

Keywords

Ultrasonography; Echocardiography; Dyspnea

Mailing Address: Adriana Brentegani •
Hospital Sírio-Libanês. Rua Adma Jafet, 115. Postal code: 01308-050. São Paulo, SP – Brazil
E-mail: dribrentegani@gmail.com
Manuscript received April 24, 2025; revised May 5, 2025; accepted May 5, 2025
Editor responsible for the review: Marcelo Tavares

DOI: https://doi.org/10.36660/abcimg.20250023i

intensivists, and healthcare professionals working in critical care settings.

Introduction

Dyspnea is a common and potentially serious complaint encountered in emergency departments, intensive care units, and outpatient settings. Traditionally, clinical reasoning around this symptom relies on correlating patient history, physical examination, and complementary tests such as chest X-ray (CXR), computed tomography, or biomarkers like D-dimer and BNP. However, these methods have significant limitations, including the low sensitivity of physical examination and delays in obtaining complementary test results.

In this context, point-of-care ultrasound (POCUS) has become an essential tool for enhancing diagnostic sensitivity in the evaluation of dyspnea (Central Illustration).[1,2] Several studies have shown that lung POCUS is more sensitive than auscultation and CXR for detecting pulmonary congestion,[1,3] and can even identify abnormalities before the onset of clinical symptoms (Figure 1).[4] Moreover, ultrasound findings such as the presence of multiple B-lines correlate with invasive hemodynamic measurements, including elevated left ventricular (LV) filling pressures and pulmonary capillary wedge pressure, especially in patients with heart failure. Nonetheless, interpretation must always consider the clinical context, particularly differential diagnoses such as interstitial lung diseases or acute inflammatory injuries.[1,3,4]

This article presents a step-by-step approach to evaluating patients with dyspnea of unclear etiology using an integrated POCUS strategy, including assessment of the lungs, heart, and deep venous system of the lower limbs. The aim is to demonstrate how this approach can efficiently support clinical reasoning.

For cardiologists seeking to go beyond traditional physical examination, mastering POCUS means embracing what Braunwald, Narula, and colleagues have termed the "fifth pillar of the modern physical exam": insonation, alongside inspection, palpation, percussion, and auscultation.[5] This tool is transforming clinical practice by enabling real-time, portable, bedside visualization of conditions that previously depended on slower or unavailable complementary tests. In emergency settings, especially in the evaluation of dyspnea, POCUS has become a frontline modality for differentiating causes such as pulmonary edema, pneumonia, and pneumothorax.[1]

Just as the stethoscope revolutionized auscultation two centuries ago, the ultrasound probe is now beginning to play a comparable role in the physical exam of the modern cardiologist.

Technique and Probe Positioning

The POCUS assessment of a dyspneic patient involves different probes and scanning windows, tailored to the anatomical target.[6]

- **Heart:** phased array transducer, with parasternal long- and short-axis, apical and subcostal windows being the most commonly used (Figure 2).[7]
- **Lungs**: For pulmonary ultrasound, using a high-frequency linear transducer (7–13 MHz) is preferable to obtain detailed views of the pleural line and its dynamic features, such as lung sliding.[8] The convex transducer, with its greater penetration and wider field of view, is better suited for evaluating pulmonary artifacts such as A-lines and B-lines (Figure 3).

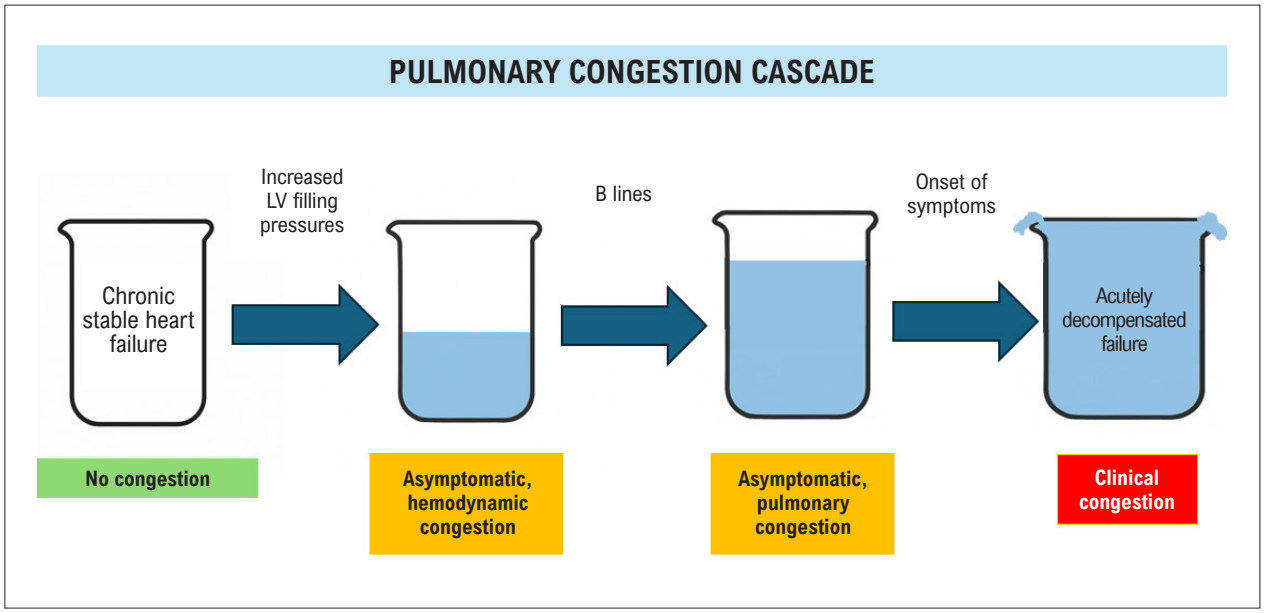

Figure 1 – *Hemodynamic congestion is the first step in the sequence leading to pulmonary congestion. Initially, exertion-induced B-lines emerge, marking a subclinical stage. Resting B-lines appear subsequently, preceding overt clinical signs that may take hours or days to develop. Therapeutic interventions are likely more effective when initiated during the early, asymptomatic stages of the preclinical and pre-radiological cascade. Adapted from Picano E, Scali MC, Ciampi Q, et al. LV: left ventricular*

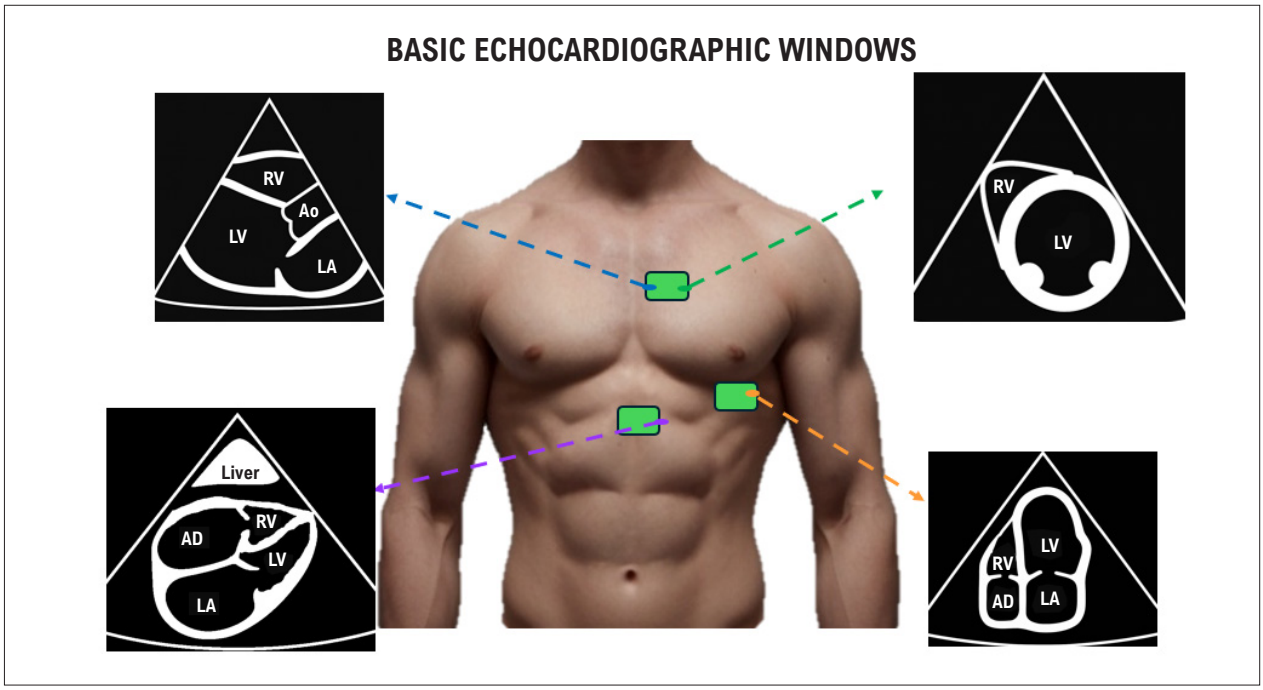

Figure 2 – *Basic echocardiographic windows. Ao: aorta. LA: left atrium. RA: right atrium. LV: left ventricle. RV: right ventricle.*

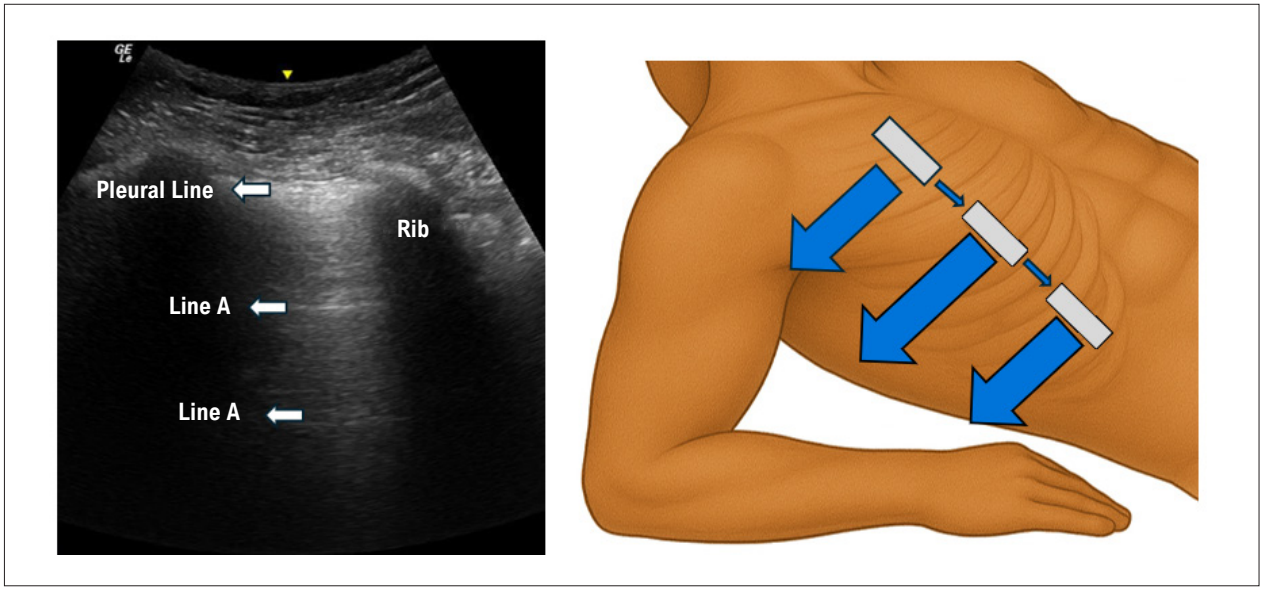

Figure 3 – *Lung ultrasound assessment in the lateral decubitus position: A-pattern. Left: B-mode image showing the A-pattern, with a hyperechoic pleural line and multiple horizontal A-lines (reverberation artifacts), indicating well-aerated lung. Also visible is the acoustic shadow of the rib (marked with an asterisk). Right: schematic representation of the ultrasound scan of the right hemithorax, with the probe positioned perpendicular to the rib cage. Blue arrows indicate the sequential scan direction along the intercostal spaces.*

The scan begins in the longitudinal orientation with the probe marker facing cephalad, allowing identification of the rib spaces and pleural line.[8] Next, a transverse sweep is performed by sliding the probe from anterior to lateral regions, either covering the entire thoracic surface or focusing on the zone of interest—a reasoning process analogous to auscultation during the traditional physical exam.

The anterosuperior thoracic quadrant is best for pneumothorax assessment, while the inferolateral quadrant along the posterior axillary line is preferred for evaluating

pleural effusion and consolidations. The exam can be performed with the patient in the supine or semi-upright position, depending on clinical condition and diagnostic goal (Figure 4).

• **Lower limb deep veins:** high-frequency linear transducer for compression ultrasound from the common femoral vein[9] down to the popliteal vein (Figure 5).

Why use POCUS? Advantages over physical exam and CXR

Standalone physical examination has low sensitivity for detecting pulmonary congestion, ranging from 17% to 33%, whereas POCUS can exceed 90% sensitivity for the same purpose.[10,11] Studies have also shown that the presence of 15 or more B-lines strongly correlates with biomarkers such as NT-proBNP, the E/e' ratio, and functional class in patients with decompensated heart failure, reinforcing its prognostic value[4,12,13] (Figure 6). Furthermore, a reduction in B-lines during treatment is associated with clinical improvement and hemodynamic compensation, validating POCUS as both a diagnostic and therapeutic monitoring tool.[3] In contrast, CXR may show delayed or inconclusive findings in early stages. Pulmonary ultrasound can detect congestion before symptom onset and demonstrate early resolution after therapy, sometimes within a few hours.[3,14-17]

It is essential to remember that POCUS should not replace the traditional physical exam or formal tests such as echocardiography, computered tomography, lower limb Doppler, or biomarkers, but rather serve as a complementary tool to support more informed clinical decision-making.

Bedside protocols: which one to choose?

Several POCUS protocols have been developed for evaluating dyspnea, including the Bedside Lung Ultrasound in Emergency (BLUE) protocol,[1] used in emergency contexts, the FALLS protocol,[19] for hemodynamic assessment in shock, and the Rapid Ultrasound for Shock and Hypotension (RUSH) protocol,[20] for undifferentiated shock. Each offers a specific and structured approach tailored to different clinical scenarios.

The BLUE protocol is the most widely validated and utilized for ultrasonographic assessment of acute respiratory failure. A study involving over 300 patients demonstrated a sensitivity of 90.5% and specificity of 98.2% for identifying the main causes of respiratory failure, with an average scan time of under three minutes. Developed by Daniel Lichtenstein in 2008, its primary goal is to enable a rapid, structured, and accurate approach to diagnosing the most common causes of dyspnea in adults.

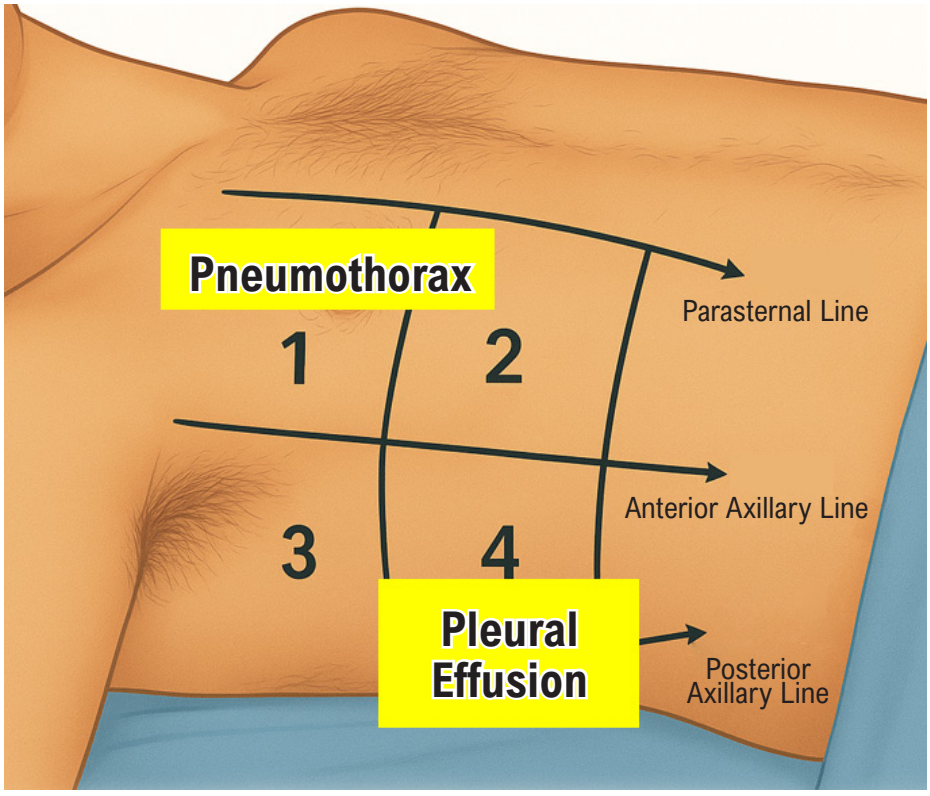

Figure 4 – *Division of the hemithorax into quadrants for lung assessment, with the patient in supine position. 1: anterosuperior region; 2: anteroinferior region; 3: upper lateral region; 4: lower lateral region.*

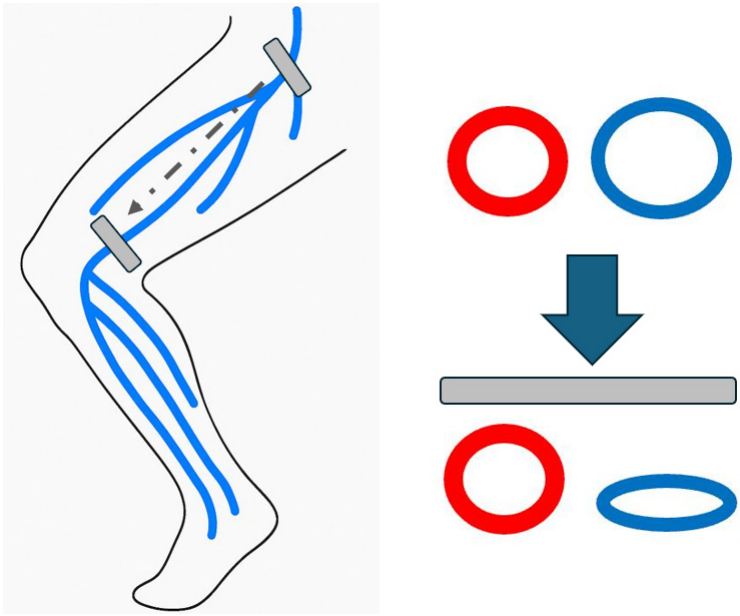

Figure 5 – *Venous compression protocol for deep vein thrombosis (DVT) evaluation—normal exam with vein collapse upon probe compression. This choice allows clear visualization of anatomical structures while respecting the regional anatomy. The gray arrow indicates the scan direction.*

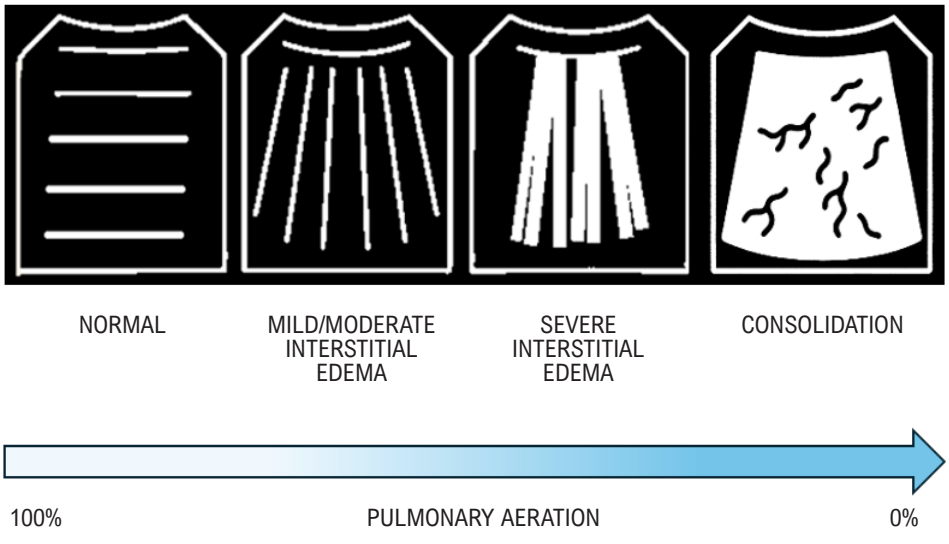

Figura 6 – *Schematic representation of interstitial pulmonary edema progression as evaluated by lung ultrasound, reflecting the gradual loss of aeration. Based on Gargani.*[18]

The BLUE protocol is based on syndromic reasoning, as it begins with assessing the presence or absence of lung sliding, followed by the analysis of pulmonary artifacts (A-lines and B-lines), subpleural and pulmonary consolidations (C-lines), and pleural effusions. Based on these findings, specific ultrasonographic profiles are generated that correlate with clinical syndromes such as Chronic obstructive pulmonary disease (COPD), asthma, heart failure, pneumonia, pulmonary embolism (PE), and pneumothorax.

It is important to remember that the goal of any protocol is to guide clinical reasoning, not to restrict it. Understanding

the available tools, knowing when to apply them, and how to interpret the results is more valuable than rigidly following any given model.

Step-by-step guide to the BLUE protocol

The exam begins by placing the transducer on the anterosuperior chest wall, followed by the anteroinferior and finally the inferolateral regions of both hemithoraces, with the patient lying supine or semi-upright. The transducer is oriented longitudinally to clearly identify the pleural line[5] between the intercostal spaces (also known as the "bat sign"). The following are assessed:

1. Lung sliding;
2. Horizontal artifacts (A lines);
3. Vertical artifacts (B lines);
4. Subpleural and pulmonary consolidations;
5. Evaluation of pleural effusion.

Lung sliding refers to the dynamic, horizontal movement of the pleural line seen on lung ultrasound, occurring in sync with respiration. It represents the visceral pleura gliding against the parietal pleura during breathing, indicating normal contact and well-aerated lungs. In B-mode, this movement appears as a horizontal shimmering of the pleural line; in M-mode, it creates the classic "**sea-shore sign**", with a static upper section (chest wall) and a granular lower section (moving lung) (Figure 7).

The presence or absence of lung sliding, combined with the analysis of pulmonary artifacts (A-lines and B-lines) or direct visualization of lung parenchyma in cases of consolidation, will define the BLUE protocol diagnostic profiles listed below.

These profiles should be complemented by evaluating DVT in the lower limbs, especially in patients with an A-profile and suspected PE. Compression of the common femoral and popliteal veins using a linear transducer allows for quick confirmation or exclusion of DVT.

Diagnostic profiles in the BLUE protocol

By assessing the structures described above, the following classic ultrasonographic profiles are identified, as defined by Lichtenstein et al.,[1,19] with the patient in the supine or semi-upright position (Figure 8):

- **A-profile:** presence of repetitive horizontal A-lines originating from the pleural line, with bilateral lung sliding preserved. Suggests normally aerated lungs or patterns typical of COPD or asthma. When combined with evidence of DVT, it increases the likelihood of PE.
- **A'-profile:** same as the A-profile, but with absent lung sliding and presence of the pathognomonic lung point—the transition zone between areas with and without lung sliding—indicative of pneumothorax with 100% specificity.
- **B-profile:** bilateral, predominant B-lines (long, vertical, hyperechoic, well-defined, dynamic comet-tail artifacts that erase A-lines), with lung sliding preserved. It indicates pulmonary congestion.

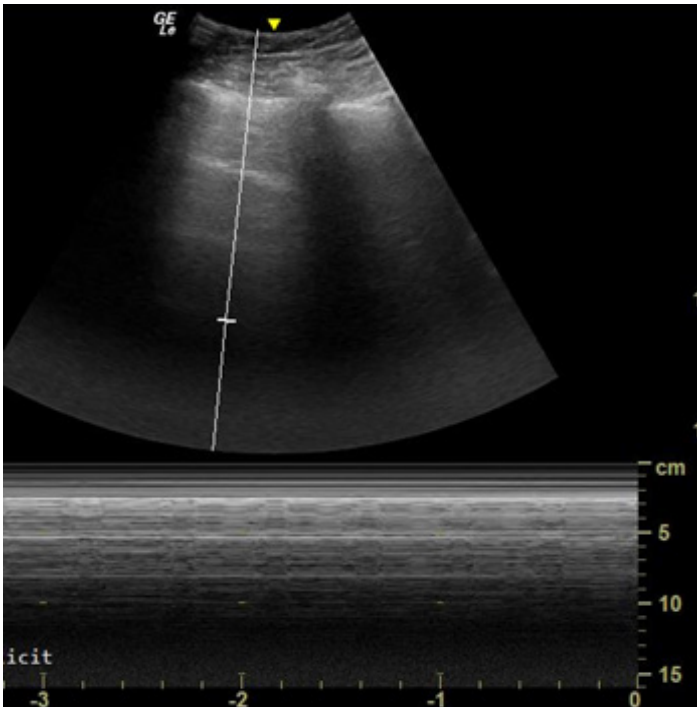

Figure 7 – *Sea-shore sign: the M-mode representation of normal lung sliding.*

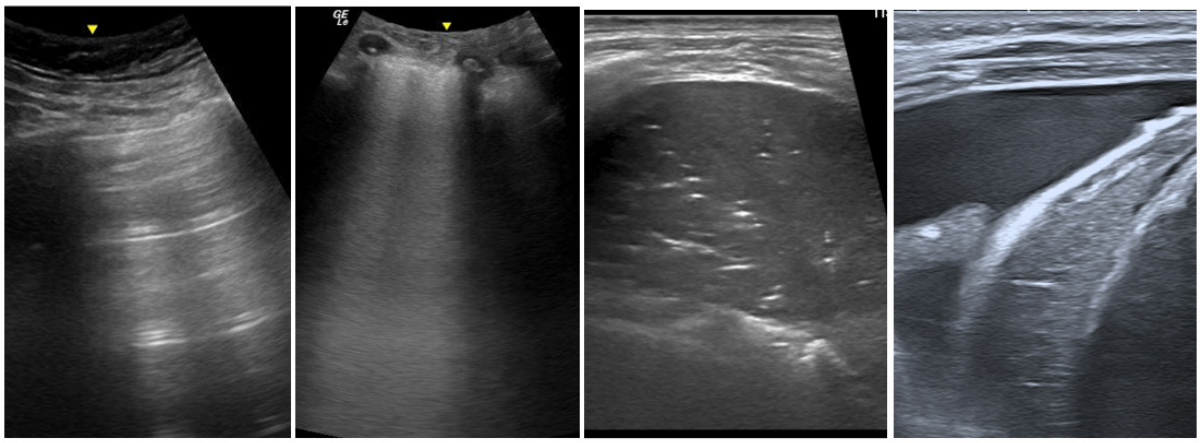

Figure 8 – *Lung ultrasound profiles described in the BLUE protocol.*

• **B'-profile:** same as B-profile, but with absent lung sliding. It may indicate interstitial pneumonia or ARDS.

• **A/B-profile:** asymmetric pattern with B-lines on one hemithorax and A-lines on the other. It suggests mixed pathologies or early stages of congestion.

• **C-profile:** presence of anterior alveolar consolidations, with or without air bronchograms, typically representing pneumonia.

• **PLAPS -profile:** presence of posterior and/or lateral alveolar consolidations or pleural effusions.

• **Pleural Effusion Profile:** an anechoic space between the lung and diaphragm and/or pleura, associated with conditions such as heart failure, pneumonia, or malignancy.

Image-Guided Clinical Reasoning

Once the main ultrasound findings have been identified and the pulmonary profiles classified according to the BLUE protocol,[1] clinical reasoning can be organized into a systematic flowchart (Flowchart 1). This approach streamlines the bedside differential diagnosis of dyspnea and speeds up decision-making by integrating pulmonary, cardiac, and venous data, as described below:

Multisystem Integration: Lungs, Heart, and Vessels

Although the BLUE protocol prioritizes lung assessment, incorporating echocardiography and venous ultrasound enhances interpretation and expands the diagnostic capabilities of POCUS in patients with dyspnea. Two key questions can guide cardiac evaluation:

1. Is there LV dysfunction? Findings such as reduced anterior mitral valve leaflet systolic excursion toward the interventricular septum (EPSS, E-point septal separation), decreased mitral annular plane systolic excursion (MAPSE), ventricular dilation, and diffuse hypokinesia suggest LV systolic dysfunction.[17]

Additionally, the mitral E/e' ratio[12] plays a central role in indirectly estimating LV filling pressures. To obtain this ratio:

• Use the apical four-chamber view with pulsed Doppler to measure the E wave of mitral inflow;

• Then, using tissue Doppler imaging (TDI), place the cursor at the septal and lateral mitral annulus to measure the e' wave;

• An E/e' ratio ≥ 15 strongly suggests elevated left-sided filling pressures, while values < 8 indicate normal pressures. Intermediate values require clinical correlation.

This parameter is especially useful in patients with diffuse B-lines on lung ultrasound, as it helps distinguish between cardiogenic pulmonary congestion and non-cardiogenic causes such as ARDS. When combined with pulmonary findings and clinical data, diagnostic accuracy improves, enabling more targeted and timely management.

2. Is there right ventricular (RV) overload or dysfunction? Key findings include:[11]

• RV dilation (RV/LV ratio > 1);

• Paradoxical septal motion ("D-shape");

• McConnell's sign (hypokinesia of the mid and basal free RV wall with preserved apical contractility);

• Tricuspid regurgitation with elevated estimated pulmonary artery systolic pressure.

These findings are strongly suggestive of acute *cor pulmonale*, particularly in the context of PE or decompensated pulmonary hypertension.

How to integrate lung ultrasound with echocardiography to identify the congestion pattern?

Echocardiography can be integrated with lung ultrasound, allowing different types of congestion to be distinguished: absent, purely hemodynamic, combined hemodynamic and pulmonary, or purely pulmonary with possible non-cardiac etiology.[16]

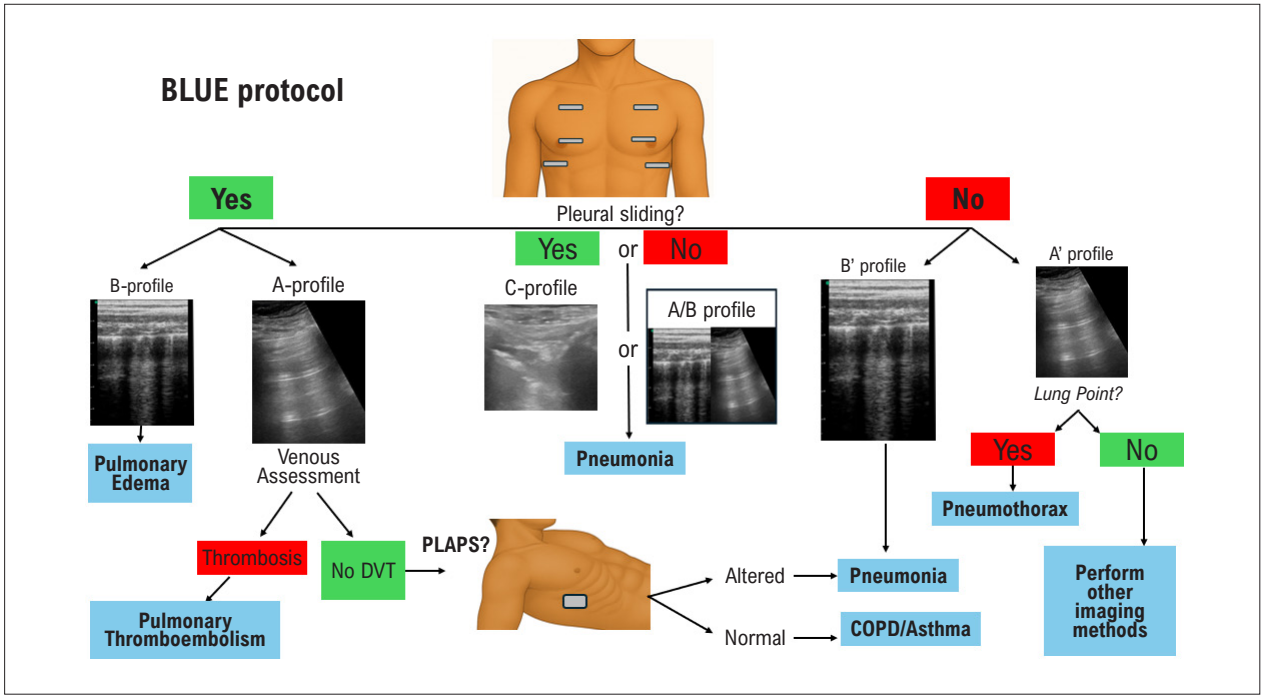

Flowchart 1 – *BLUE Protocol flowchart for the assessment of acute dyspnea by bedside lung ultrasound (adapted from Lichtenstein et al.).[1] BLUE: Bedside Lung Ultrasound in Emergency; DVT: deep vein thrombosis; PLAPS: Posterolateral Alveolar and/or Pleural Syndrome; COPD: Chronic obstructive pulmonary disease*

These four congestion profiles, resulting from the integration of echocardiography (presence or absence of increased filling pressures based on the E/e' ratio) and lung ultrasound (presence or absence of pulmonary congestion based on the identification of diffuse B lines), are explained as follows:

1. No Congestion: When echocardiography shows no evidence of elevated LV filling pressure (normal E/e') and lung ultrasound reveals no B-lines, the patient is classified as not congested (Figure 9).

2. Hemodynamic Congestion: If echocardiography indicates elevated LV filling pressure (high E/e') but lung ultrasound does not detect B-lines, the patient presents with hemodynamic congestion. This reflects increased pressure on the left side of the heart without a detectable fluid overload in the lungs, possibly an early stage of cardiac congestion (Figure 10).

3. Hemodynamic and Pulmonary Congestion: When echocardiography reveals elevated LV filling pressure and lung ultrasound shows multiple, bilateral diffuse B-lines, the patient has both hemodynamic and pulmonary congestion. This reflects increased pressure on the left side of the heart that has resulted in fluid leakage into the pulmonary interstitium, as manifested by B-lines (clinical congestion) (Figure 11).

4. Pulmonary Congestion without Hemodynamic Congestion: If echocardiography shows no signs of elevated LV filling pressure, but lung ultrasound reveals multiple, bilateral diffuse B-lines, the patient has pulmonary congestion without hemodynamic overload. This suggests a non-cardiac cause for the B-lines, such as acute lung injury (ALI) or acute respiratory distress syndrome (ARDS) (Figure 12 and Table 2).

Conclusion

The integration of POCUS in the evaluation of dyspnea marks a major advance in contemporary clinical practice. Its high diagnostic accuracy, combined with the ability to provide dynamic monitoring, makes it an indispensable tool in emergency medicine, critical care, and even outpatient settings.

Despite these advantages, POCUS remains underused by cardiologists,[6] even though it has proven reproducibility and a positive impact on diagnostic accuracy. Evidence suggests that the main barriers to adoption are related to medical training and access to proper education.

Mastery of ultrasound techniques and familiarity with sonographic profiles, such as those outlined in the BLUE protocol, will enable an objective and effective syndromic approach.

Acknowledgments

To Dr. Marcelo Dutra and Dr. Natalia Tavares, for kindly providing the ultrasound images in Figure 8.

Author Contributions

Conception and design of the research, acquisition of data, analysis and interpretation of the data, writing of the manuscript and critical revision of the manuscript for intellectual content: Brentegani A, Solis FAE, Paulis M, Vieira MLC.

Table 1 – Ultrasound profiles and differential diagnosis

Diagnosis	Pulmonary profile (BLUE)	US of lower limbs (DVT)	Cardiac POCUS
Pulmonary edema	B-profile	Negative	LV dysfunction, E/e´≥ 15
COPD / Asthma	A-profile	Negative	Normal
Pneumothorax	A'-profile	Not applicable	Normal
PE	A-profile	Positive (non-compressible vein)	RV overload (D-shape, McConnell, RV > LV)
Pneumonia	B', C or PLAPS profile	Negative	Normal or hyperdynamic LV
ARDS / Interstitial pneumonitis	B'-profile	Negative	Normal, E/e´<15, or RV dysfunction in severe cases
Pleural Effusion	Pleural effusion or PLAPS	Variable	LV dysfunction or signs of associated systemic disease

**Adapted from Lichtenstein et al.[1] PE: pulmonary embolism; BLUE: Bedside Lung Ultrasound in Emergency; DVT: deep vein thrombosis; POCUS: Point-Of-Care Ultrasound; ARDS: acute respiratory distress syndrome; LV: left ventricule; RV: right ventricle; COPD: Chronic obstructive pulmonary disease.*

Table 2 – Differentiation between Cardiogenic Acute Pulmonary Edema (APE) and ARDS

Ultrasound finding	Cardiogenic APE	ARDS
Anterior pleural line	Regular, thin	Irregular, thickened
Pleural motion	Normal glide	Reduced glide
Multiple B-line distribution	Diffuse anterior	Random
Right and left lung	Symmetrical	May have spared areas
Pleural effusion	Frequent and bilateral	May be present
Dependent consolidation	Usually present	Usually present
Anterior (non-dependent) consolidation	Never visible	Sometimes present
Cardiac POCUS (LV function)	Abnormal	Often normal

**Adapted from Picano et al.[4] LV: left ventricular*

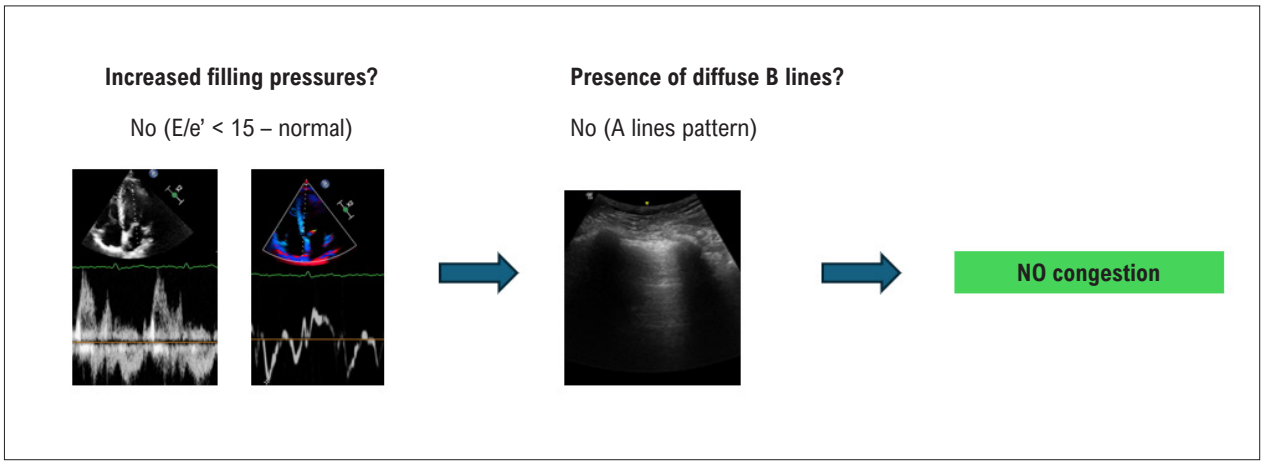

Figure 9 – *Integration of echocardiography with lung ultrasound: Normal E/e' and A-profile on lung ultrasound indicate absence of congestion.*

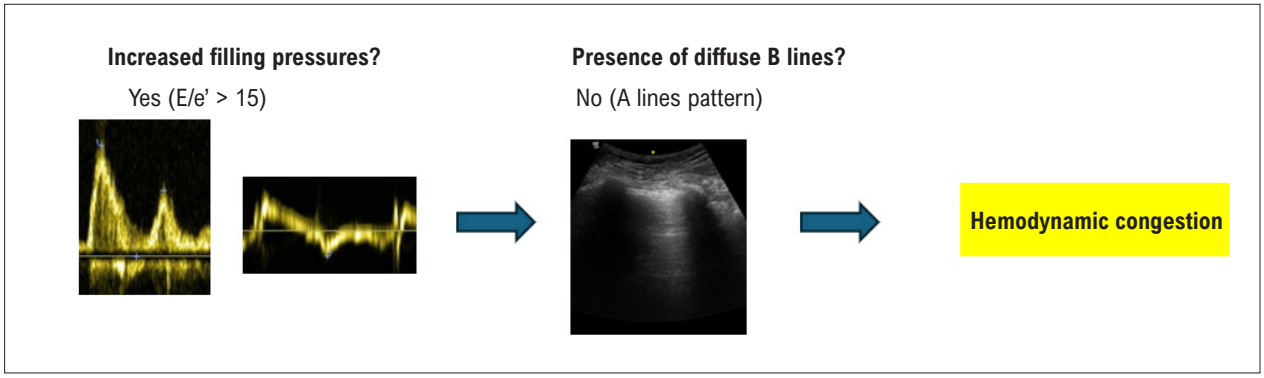

Figure 10 – *Integration of echocardiography with lung ultrasound: Elevated E/e' and A-profile on lung ultrasound indicate hemodynamic congestion.*

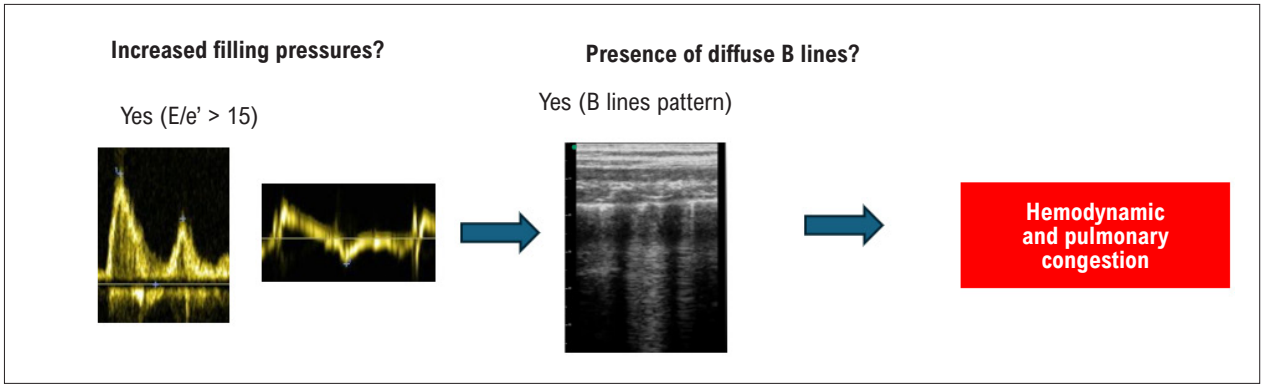

Figure 11 – *Integration of echocardiography with lung ultrasound: Elevated E/e' and B-profile on lung ultrasound indicate both hemodynamic and pulmonary congestion.*

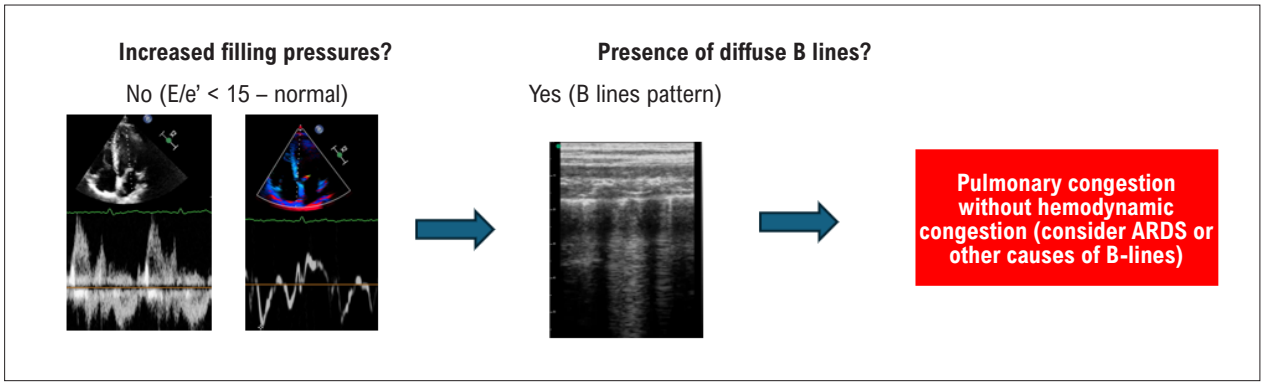

Figure 12 – *Integration of echocardiography with lung ultrasound: Normal E/e' ratio and B-profile on lung ultrasound indicate pulmonary involvement without hemodynamic congestion. ARDS: acute respiratory distress syndrome.*

Potential Conflict of Interest

There is a declaration of potential conflict of interest from the authors Adriana Brentegani, Fernando Arturo Solis, and Milena de Paulis, who serve as instructors and coordinators of point-of-care ultrasound (POCUS) courses for physicians, without any affiliation with companies or institutional sponsorship.

Sources of Funding

There were no external funding sources for this study.

Study Association

This study is not associated with any thesis or dissertation work.

Ethics Approval and Consent to Participate

This article does not contain any studies with human participants or animals performed by any of the authors.

Use of Artificial Intelligence

During the preparation of this work, the authors used ChatGPT for suggestions on restructuring and improving textual flow, as well as for generating and transforming illustrative medical images. Following the use of this tool, the authors reviewed and edited the content as necessary and take full responsibility for the content of the published article.

Availability of Research Data

The underlying content of the research text is contained within the manuscript.

References

1. Lichtenstein DA, Mezière GA. Relevance of Lung Ultrasound in the Diagnosis of Acute Respiratory Failure: The BLUE Protocol. Chest. 2008;134(1):117-25. doi: 10.1378/chest.07-2800.
2. Francisco MJ Neto, Lira EB Filho, Queiroz MRG. Point-of-Care in Clinical Practice: Consolidated Reality. Arq Bras Cardiol. 2024;121(1):e20230688. doi: 10.36660/abc.20230688.
3. Coiro S, Rastogi T, Girerd N. How and When to Use Lung Ultrasound in Patients with Heart Failure? Rev Cardiovasc Med. 2022;23(6):198. doi: 10.31083/j.rcm2306198.
4. Picano E, Scali MC, Ciampi Q, Lichtenstein D. Lung Ultrasound for the Cardiologist. JACC Cardiovasc Imaging. 2018;11(11):1692-705. doi: 10.1016/j.jcmg.2018.06.023.
5. Narula J, Chandrashekhar Y, Braunwald E. Time to Add a Fifth Pillar to Bedside Physical Examination: Inspection, Palpation, Percussion, Auscultation, and Insonation. JAMA Cardiol. 2018;3(4):346-50. doi: 10.1001/jamacardio.2018.0001.
6. Mayo PH, Copetti R, Feller-Kopman D, Mathis G, Maury E, Mongodi S, et al. Thoracic Ultrasonography: A Narrative Review. Intensive Care Med. 2019;45(9):1200-11. doi: 10.1007/s00134-019-05725-8.
7. Accorsi TAD, Amorim EF. Princípios Básicos de Ultrassonografia para o Clínico. Rev Soc Cardiol Estado São Paulo. 2024;34(2):101-7. doi:10.29381/0103-8559/20243402101-7.
8. Volpicelli G, Elbarbary M, Blaivas M, Lichtenstein DA, Mathis G, Kirkpatrick AW, et al. International Evidence-Based Recommendations for Point-of-Care Lung Ultrasound. Intensive Care Med. 2012;38(4):577-91. doi: 10.1007/s00134-012-2513-4.
9. Martinez EC, Diarte E, Martinez DO, Reyes LR, Cano DAA, Navarro CC, et al. Point-of-Care Ultrasound for the Diagnosis of Frequent Cardiovascular Diseases: A Review. Cureus. 2023;15(12):e51032. doi: 10.7759/cureus.51032.
10. Pivetta E, Goffi A, Lupia E, Tizzani M, Porrino G, Ferreri E, et al. Lung Ultrasound-Implemented Diagnosis of Acute Decompensated Heart Failure in the ED: A SIMEU Multicenter Study. Chest. 2015;148(1):202-10. doi: 10.1378/chest.14-2608.
11. Price S, Platz E, Cullen L, Tavazzi G, Christ M, Cowie MR, et al. Expert Consensus Document: Echocardiography and Lung Ultrasonography for the Assessment and Management of Acute Heart Failure. Nat Rev Cardiol. 2017;14(7):427-40. doi: 10.1038/nrcardio.2017.56.
12. Nagueh SF, Appleton CP, Gillebert TC, Marino PN, Oh JK, Smiseth OA, et al. Recommendations for the Evaluation of Left Ventricular Diastolic Function by Echocardiography. Eur J Echocardiogr. 2009;10(2):165-93. doi: 10.1093/ejechocard/jep007.
13. Miglioranza MH, Gargani L, Sant'Anna RT, Rover MM, Martins VM, Mantovani A, et al. Lung Ultrasound for the Evaluation of Pulmonary Congestion in Outpatients: A Comparison with Clinical Assessment, Natriuretic Peptides, and Echocardiography. JACC Cardiovasc Imaging. 2013;6(11):1141-51. doi: 10.1016/j.jcmg.2013.08.004.
14. Platz E, Merz AA, Jhund PS, Vazir A, Campbell R, McMurray JJ. Dynamic Changes and Prognostic Value of Pulmonary Congestion by Lung Ultrasound in Acute and Chronic Heart Failure: A Systematic Review. Eur J Heart Fail. 2017;19(9):1154-63. doi: 10.1002/ejhf.839.
15. Gargani L, Volpicelli G. How I do it: Lung Ultrasound. Cardiovasc Ultrasound. 2014;12:25. doi: 10.1186/1476-7120-12-25.
16. Gargani L, Girerd N, Platz E, Pellicori P, Stankovic I, Palazzuoli A, et al. Lung Ultrasound in Acute and Chronic Heart Failure: A Clinical Consensus Statement of the European Association of Cardiovascular Imaging (EACVI). Eur Heart J Cardiovasc Imaging. 2023;24(12):1569-82. doi: 10.1093/ehjci/jead169.
17. Noritomi DT, Vieira ML, Mohovic T, Bastos JF, Cordioli RL, Akamine N, et al. Echocardiography for Hemodynamic Evaluation in the Intensive Care Unit. Shock. 2010;34 (Suppl 1):59-62. doi: 10.1097/SHK.0b013e3181e7e8ed.
18. Gargani L. Lung Ultrasound: A New Tool for the Cardiologist. Cardiovasc Ultrasound. 2011;9:6. doi: 10.1186/1476-7120-9-6.
19. Lichtenstein D. FALLS-Protocol: Lung Ultrasound in Hemodynamic Assessment of Shock. Heart Lung Vessel. 2013;5(3):142-7.
20. Perera P, Mailhot T, Riley D, Mandavia D. The RUSH Exam: Rapid Ultrasound in SHock in the Evaluation of the Critically lll. Emerg Med Clin North Am. 2010;28(1):29-56. doi: 10.1016/j.emc.2009.09.010.
21. Szabó GV, Szigetváry C, Szabó L, Dembrovszky F, Rottler M, Ocskay K, et al. Point-of-Care Ultrasound Improves Clinical Outcomes in Patients with Acute Onset Dyspnea: A Systematic Review and Meta-Analysis. Intern Emerg Med. 2023;18(2):639-53. doi: 10.1007/s11739-022-03126-2.

My Approach to Estimate Pulmonary Pressures: Practical Aspects

Halsted Alarcão Gomes Pereira da Silva,[1] *Helder Moura Gomes*[2]
Instituto Dante Pazzanese de Cardiologia,[1] *São Paulo, SP – Brasil*
Hospital Metropolitano Dom José Maria Pires,[2] *João Pessoa, PB – Brasil*

Central Illustration: My Approach to Estimate Pulmonary Pressures: Practical Aspects

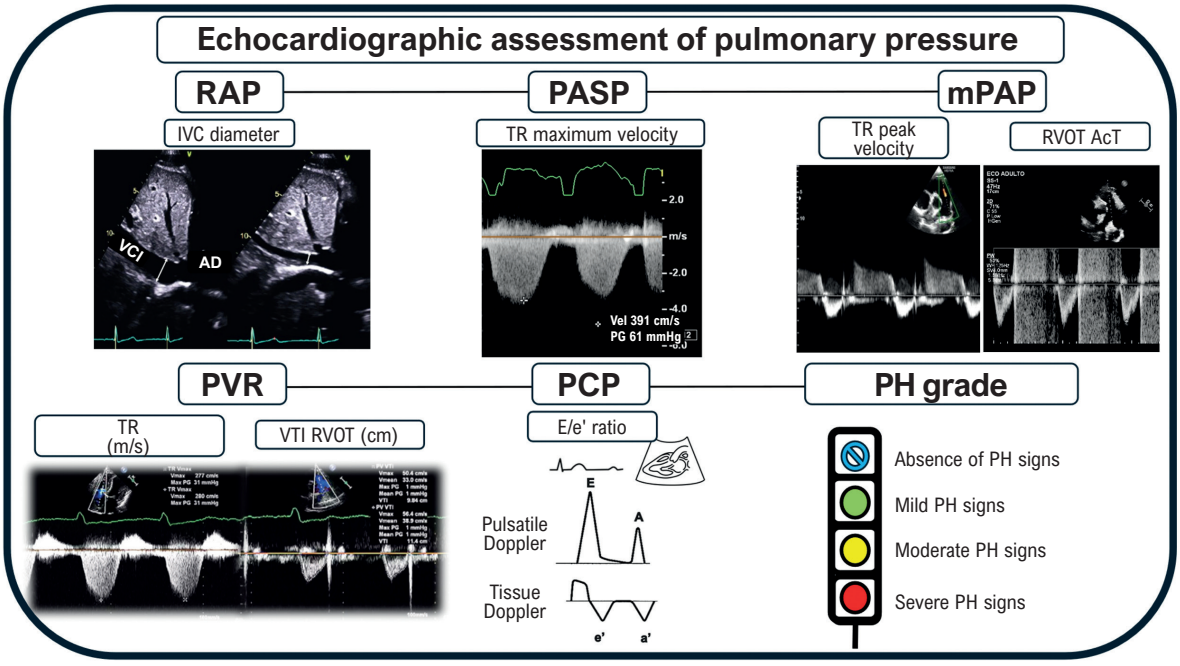

Arq Bras Cardiol: Imagem cardiovasc. 2025;38(2):e20250028

IVC: inferior vena cava; VTI RVOT: velocity-time integral right ventricular outflow tract; TR: Tricuspid regurgitation; PASP: Pulmonary artery systolic pressure.

Abstract

Pulmonary hypertension (PH) is a global disease and is increasingly present in echocardiography laboratories, given the progressive rise in its prevalence with population aging. Previously diagnosed only through invasive methods, echocardiographic assessment of pulmonary pressures has become fundamental in screening and monitoring patients with PH. This topic was revisited by the American Society of Echocardiography in a new guideline published in March 2025, reinforcing the importance of echocardiography in clinical stratification, considering recent updates in the definition of PH. Among the main assessment parameters, systolic pulmonary artery pressure, mean pulmonary artery pressure (mPAP), pulmonary vascular resistance (PVR), and pulmonary capillary pressure (PCP) are described, along with a series of precautions for the correct estimation and interpretation of these values. The classification of PH levels has also been revised in a new framework. As an accessible and reproducible method, the assessment of pulmonary pressures through echocardiography stands out as an essential tool in the evaluation and follow-up of PH.

Keywords

Pulmonary Hypertension; Echocardiography; Doppler Ultrasonography; Pulmonary Wedge Pressure.

Mailing Address: Halsted Alarcão Gomes Pereira da Silva •
Instituto Dante Pazzanese de Cardiologia. Rua Dr. Dante Pazzanese, 500. Postal code: 04012-909. São Paulo, SP – Brazil
E-mail: halstedufg@hotmail.com
Manuscript received April 28, 2025; revised May 6, 2025; accepted May 8, 2025
Editor responsible for the review: Marcelo Tavares

DOI: https://doi.org/10.36660/abcimg.20250028i

Introduction

Pulmonary hypertension (PH) has an estimated prevalence of about 1% of the global population, with a gradual increase

with aging due to its direct relationship with cardiac and pulmonary diseases. It has prognostic implications due to its severe hemodynamic consequences and serves as a fundamental parameter for clinical decision-making and therapeutic guidance.[1]

The assessment of pulmonary pressures has been a constant pursuit for a better hemodynamic understanding of diseases affecting both acquired and congenital heart conditions. Initially, this type of evaluation was performed exclusively through invasive hemodynamic methods, predominantly using pulmonary artery catheters such as the Swan-Ganz and right heart catheterization.[2]

The incorporation of the color Doppler method and the ability to correlate intracavitary flow velocities with hemodynamic gradients, with reasonable agreement with invasive parameters, has enabled the rapid evolution of echocardiography in this field. As a non-invasive, reproducible, and replicable method, performed at the bedside and with relatively low cost, echocardiography presents a significant advantage as an initial assessment tool.[3]

Definition of PH

The currently accepted definition of PH was proposed during the 6th World Symposium on PH in 2018, where 124 experts gathered and reviewed it.[4]

Previous definition of PH

- Mean pulmonary artery pressure (mPAP): ≥ 25 mmHg
- Pulmonary vascular resistance (PVR): ≥ 3 Wood Units (WU) – Precapillary hypertension
- Pulmonary capillary pressure (PCP): ≤ 15 mmHg – Precapillary hypertension

Proposed (current) definition:

- mPAP: > 20 mmHg
- PVR: > 2 Wood Units (WU) – Precapillary hypertension
- PCP: ≤ 15 mmHg – Precapillary hypertension

This change was based on data from healthy individuals, in which resting mPAP was identified as approximately 14.0±3.3 mmHg. Considering a variation of two standard deviations as still within normal limits, a mPAP value >20 mmHg would be the threshold for abnormal pulmonary artery pressure (above the 97.5th percentile).[4]

Based on these values, the echocardiographic parameters described below were studied in relation to invasive assessment, not with the aim of replacing this examination, but rather as an initial screening proposal, since performing right heart catheterization at a population level is impractical and not cost-effective.

The concept of communicating vessels

The echocardiographic assessment of pulmonary pressures is based on the concept of communicating vessels. This concept establishes that a fluid with the same specific mass and at the same height would have the same pressure at any point in the system. Based on this, echocardiography can identify the pulmonary artery systolic pressure (PASP) by calculating the right ventricular systolic pressure (RVSP).

To calculate RVSP, the systolic gradient between the right ventricle (RV) and the right atrium (RA) must first be evaluated using the maximum velocity of tricuspid regurgitation (TR), applying the modified Bernoulli equation, which derives the gradient based on velocity. By adding the estimated right atrial pressure (RAP) to this pressure estimate, RVSP is obtained, which, in a system without flow obstruction, will be similar to PASP.

Mean RAP

For this estimation, we first examine how to assess the mean RAP. Throughout its evolution, transthoracic echocardiography has identified various metrics to estimate RAP with reasonable accuracy. Despite several limitations in its analysis, the most commonly used parameter for this inference is the measurement of the inferior vena cava (IVC) diameter during an expiratory pause and its respiratory variability, as shown in Figure 1.

Depending on the initial measurement of the IVC and its variation with respiratory phasicity, RAP can be estimated as follows:

- RAP < 3 mmHg
- RAP: 3 mmHg (0 - 5 mmHg)
- RAP: 8 mmHg (5 - 10 mmHg)
- RAP: 15 mmHg (10 - 20 mmHg)
- RAP: 20 mmHg

The IVC can be measured in most patients using the subcostal window, making it easily reproducible during hospitalization or outpatient follow-up. As we will see below, this index is not always representative of RAP in certain scenarios, which should be interpreted with caution.

Precautions in the acquisition and interpretation of the IVC:

- Acquire the IVC image longitudinally with a central axis cut throughout the respiratory cycle (the measurement of the transverse axis can help avoid errors).
- Be cautious when evaluating patients with chronic hypervolemia (heart failure and advanced chronic kidney disease)
- Be cautious when evaluating athletes (IVC distended due to excellent preload).

In cases of diagnostic uncertainty or indeterminate cases, secondary indices for estimating RAP can be considered, such as a tricuspid E/e' ratio > 6, predominance of diastolic flow in the hepatic veins*, and identification of a restrictive diastolic filling pattern in the right chambers.[5]

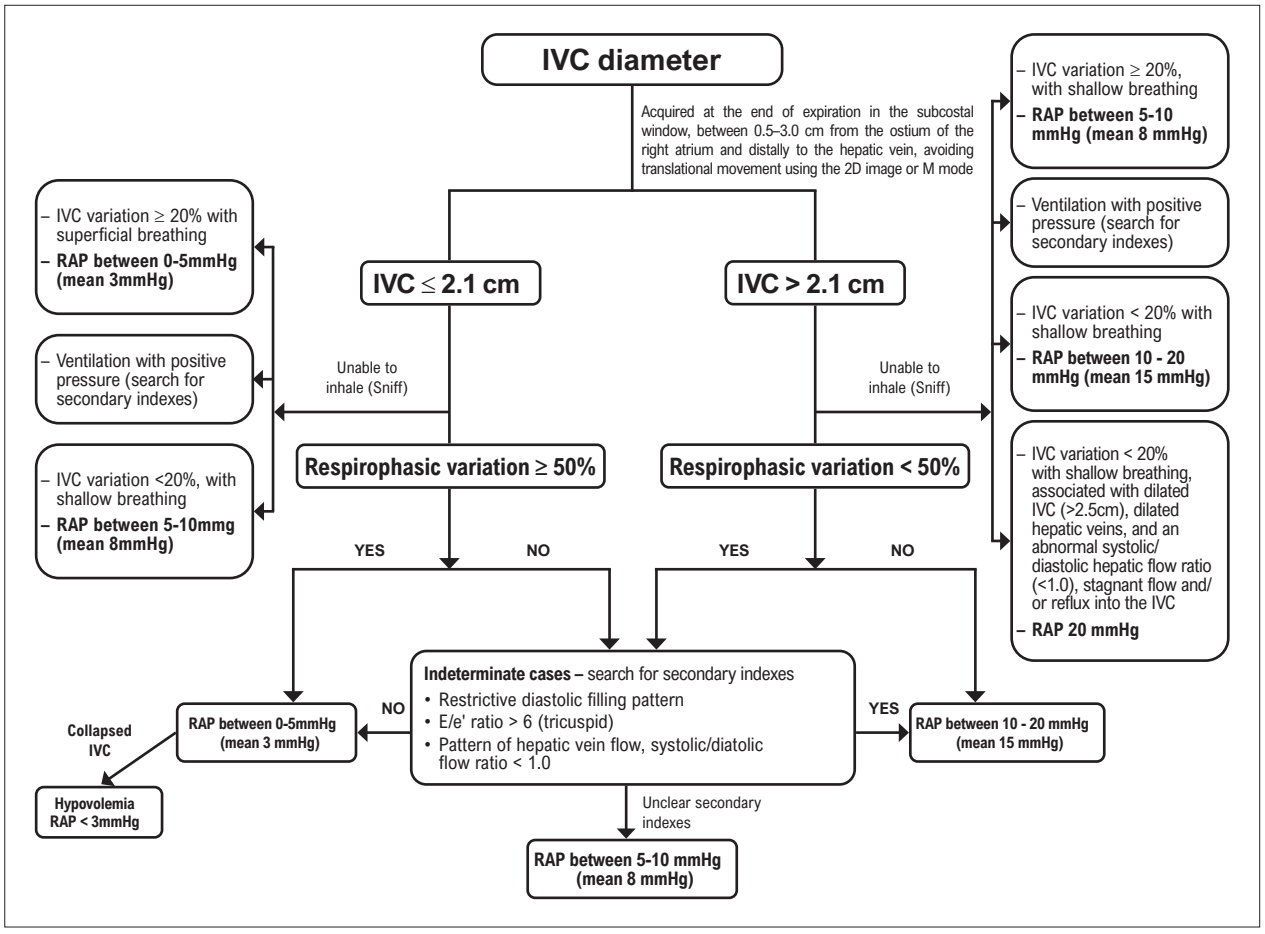

Figure 1 – *Flowchart for the assessment of mean RAP proposed by the American Society of Echocardiography in its latest guideline (ASE 2025);[5] IVC: inferior vena cava; RAP: right atrial pressure; RV: right ventricle.*

$$*SFF = \frac{VTI\ of\ the\ S\ wave}{VTI\ of\ the\ S\ wave + VTI\ of\ the\ D\ wave} \times 100$$

(Values < 55 % are sensitive and specific for increases in RAP)

The systolic filling fraction (SFF) equation VTI: velocity-time integral; S: systolic; D: diastolic

PASP

Still regarding the concept of communicating vessels without flow obstruction, it can be inferred that RVSP will be equivalent to PASP, which is the hemodynamic parameter that is actually being investigated.

Figure 2 illustrates a case of a significant increase in pulmonary pressures and how the final PASP value is calculated.

Precautions in the acquisition and interpretation of PASP:

– When measuring the maximum velocity of TR (RV–RA gradient), proper Doppler angle alignment (< 20°) should be maintained to avoid possible underestimation due to measurement error.

– Excessive gain should be avoided when acquiring the spectral Doppler image to prevent overestimation of the actual transvalvular gradient, as shown in Figure 3.

– To ensure accuracy and account for respiratory variation, RVSP should ideally be calculated from the average of three consecutive beats in echocardiographic windows with the highest velocities and best spectral Doppler envelopes.

Other parameters for estimating PASP have been described using the acceleration time (AcT) of systolic flow in the right ventricular outflow tract (RVOT). As a region of low pressure and high compliance, the pulmonary bed generates a flow pattern with low velocities and a long AcT during the systolic period.

A progressive increase in pulmonary pressures, particularly in its precapillary component, will result in a progressively shorter AcT, associated with an earlier-than-usual systolic peak (Figure 4).

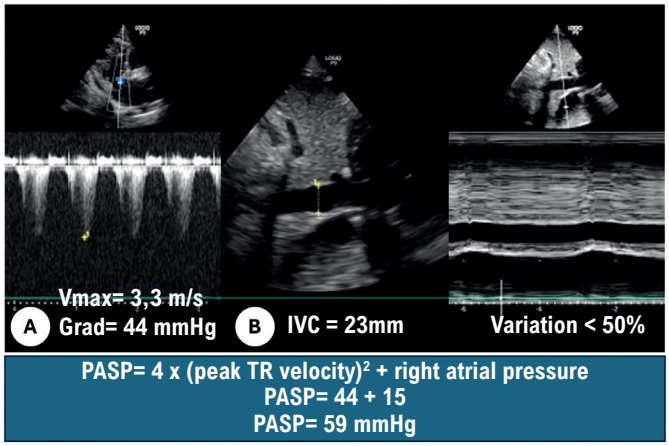

Figure 2 – *Estimation of PASP, measured at 59 mmHg in this patient. A) TR assessed with continuous-wave Doppler. B) Estimation of RAP by evaluating the diameter of the IVC and collapsibility with the respiratory cycle in M-mode. IVC: inferior vena cava; PASP: Pulmonary arterial systolic pressure; RAP: right atrial pressure.*

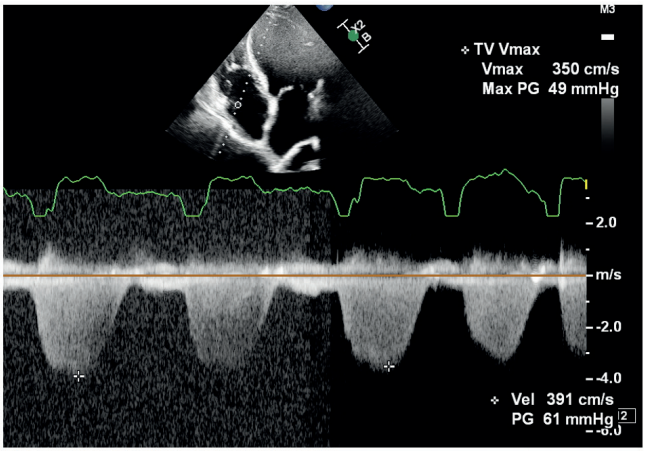

Figure 3 – *TR on continuous-wave Doppler with excessive gain (left, with a maximum velocity of 3.9 m/s) and with appropriate gain (right, with a maximum velocity of 3.5 m/s).*

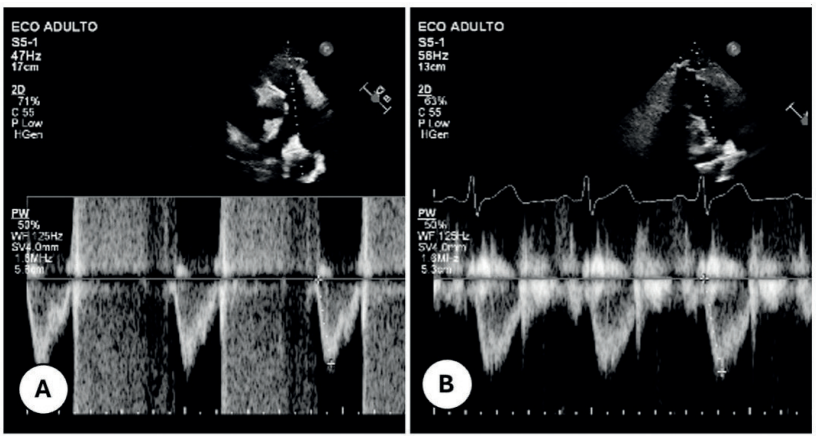

Figure 4 – *Assessment of AcT considering the sample volume at the level of the pulmonary valve; A) Shortened AcT (81ms) associated with mid-systolic notch in the tracing, confirming the finding of PH; B) Normal AcT (113ms).*

Based on this important hemodynamic concept, correlation studies between these two variables were conducted, allowing for the identification and validation of the formulas presented in Table 1.

Precautions in the acquisition and interpretation of AcT

- Window: Parasternal short-axis at the level of the great vessels, directed toward the pulmonary valve.
- Sample volume position: Acquired using pulsed Doppler in the RVOT, with the sample volume positioned just below the pulmonary valve at the end of expiration.
- Measurement: From the beginning of pulmonary flow to the peak velocity.
- The greatest validation of pulmonary ATc has been conducted in cases of precapillary PH.
- ATc in the RVOT may be less reliable in patients with low or high heart rates (<60 and >100 beats/min).

mPAP

Considered the reference measure for defining PH and severity stratification, the determination of mPAP is very important for clinical cardiologists. Over the past decades, several studies have validated this non-invasive estimate, culminating in the recommendation of the American guideline for the echocardiographic evaluation of the right heart in adults in 2010. This document provided a detailed description of the formulas for calculating both mPAP and pulmonary artery diastolic pressure (PADP), which were replicated in the 2025 guideline.

Based on current knowledge, mPAP values greater than 20 mmHg are considered pathological and should be reported in the echocardiographic report.

The step-by-step process for calculating mPAP after acquiring PASP and PADP is illustrated in Figure 5 and Table 2.

Precautions in acquisition and interpretation

- The calculation of mPAP involves other variables, so its estimation should be performed using the best possible technique.

Table 1 – Main Clinically Validated Formulas for Estimating Pulmonary Artery Systolic Pressure (PASP)

Parameter	Formula	Condition
PASP	4 x maximum velocity of TR + RAP [6,7]	
PASP	134 – (0,9 X AcT) [5]	
PASP		RVOT AcT > 105 ms (without PH*)[6] * Considered normal, based on epidemiological studies involving healthy populations.
PASP		RVOT AcT < 80 ms (probable HP)[5]

PASP: pulmonary artery systolic pressure; TR: tricuspid regurgitation; RAP: right atrial pressure; AcT: acceleration time; PH: pulmonary hypertension; RVOT: right ventricular outflow tract.[5]

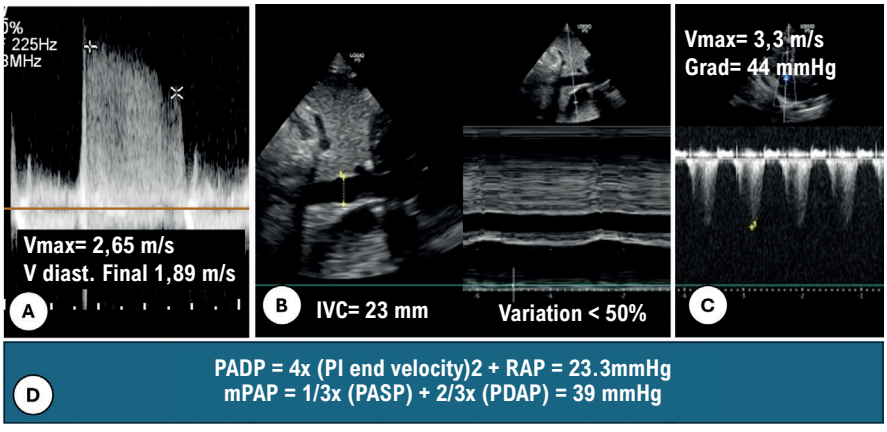

Figure 5 – *Estimation of mPAP and pulmonary artery diastolic pressure (PADP) using the initial and final velocities of pulmonary insufficiency (PI): A) PI on continuous-wave Doppler; mPAP is obtained by summing RAP with the peak gradient of PI calculated using the Bernoulli equation. PADP is obtained by calculating the gradient considering the end-diastolic velocity of PI added to RAP; B) Estimation of RAP by evaluating the IVC and its respiratory collapsibility; C) TR; D) Application of formulas for calculating mPAP and PADP; PASP: pulmonary artery systolic pressure; IVC: inferior vena cava.*

– mPAP uses Pulmonary Insufficiency (PI) as an analysis parameter for its calculation. The initial velocity of the PI jet, added to RAP, allows for the determination of mPAP.
– PADP uses the final velocity of the PI jet, added to RAP, to determine the PADP value.

PVR

Concept describing the measurement of resistance that the pulmonary vascular system offers to blood flow from the RV. This parameter provides an important discriminatory factor, allowing stratification between the precapillary and postcapillary components of PH.

The identification of this measurement in a non-invasive manner originates from the classic work of Abbas et al.[12] The study was published in the Journal of the American College of Cardiology (JACC) in 2003, and their formula was later validated in a new publication in 2013 in the Journal of the American Society of Echocardiography (JASE).[12]

For the calculation of PVR, two basic evaluation parameters are required (Figure 6).

The formulas used for PVR calculation are described in Table 3.

PCP

The combined assessment of pulmonary pressures, PVR, and PCP allows for the classification of PH into one of the five categories described below, according to the latest PH classification (ESC 2022):

1. Pulmonary Arterial Hypertension (PAH)
2. PH associated with left ventricular disease
3. PH associated with lung disease
4. PH associated with obstructive lung disease
5. PH with unclear or multifactorial mechanisms (etiology)

Table 2 – Main clinically validated formulas used for mPAP estimation

Parameter	Formula	Condition
mPAP	$\frac{1}{3}(PSAP) + \frac{2}{3} PADP$	
mPAP	79 – 0.45x(*AcT*)[8]	AcT ≥ 120ms (HR 60 – 100bpm)
mPAP	90 – 0.62x(*AcT*)[9]	AcT < 120ms (HR 60 – 100bpm)
mPAP	0.61x(*PASP*) + 2[10]	
mPAP	VTI da IT + RAP11	

mPAP: mean pulmonary artery pressure; AcT: acceleration time of the right ventricular outflow tract; HR: heart rate; TR: tricuspid regurgitation; VTI: velocity-time integral; RAP: right atrial pressure.[5]

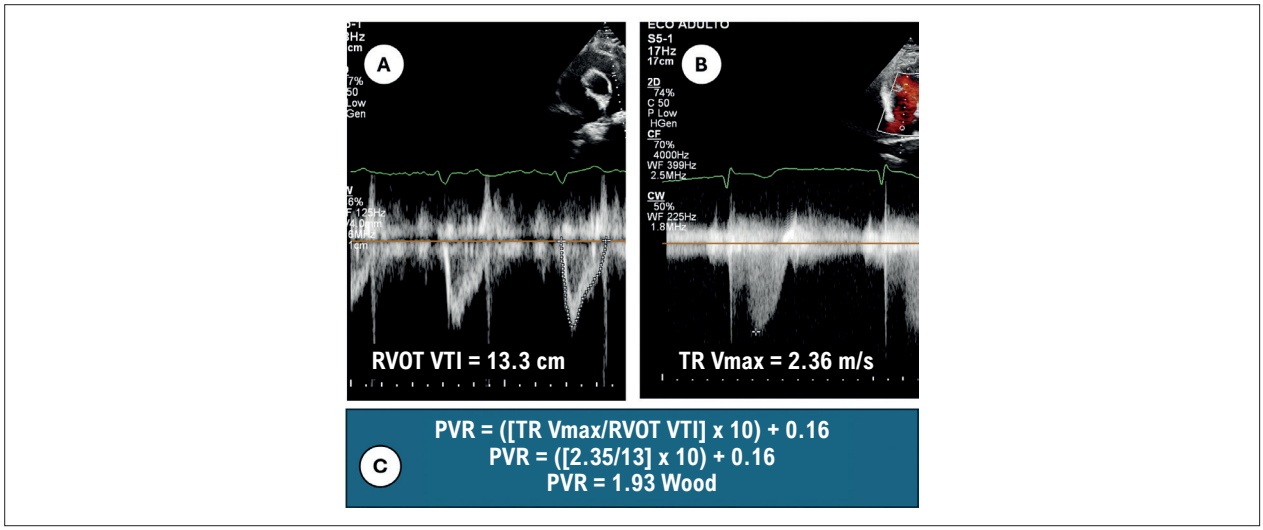

Figure 6 – *Calculation of PVR using velocity-time integral (VTI) of the RVOT' (A); maximum velocity of TR (B); application of the formula (C).*

Thus, the evaluation of PCP will determine whether capillary pressures – and consequently, left atrial pressure – are elevated or not, enabling an initial stratification between groups with and without left heart involvement (postcapillary and precapillary hypertension).

The main formulas for this calculation are described below (Table 4), with Nagueh's formula being the most widely used. In their original study, the findings of Nagueh et al.[13] were strongly correlated with left ventricular filling pressures and, therefore, with PCP.

Precautions in acquisition and interpretation:

– The evaluation of E/e' variables is routinely performed in the assessment of diastolic function and therefore does not add extra time to the examination.

Table 3 – Main clinically validated formulas used for PVR estimation

Parameter	Formula	Condition
PVR	$\frac{TR\ maximum\ velocity\ (m/s)}{RVOT\ VTI\ (cm)}$ X 10 + 0.16[12]	RVP > 2.0 Woods is considered abnormal
PVR	$\frac{RVSP - PCP}{CO}$	RVSP, RVDP and CO values may be obtained from echocardiographic data

PVR: Pulmonary Vascular Resistance; TR: Tricuspid Regurgitation; VTI: Velocity-Time Integral; RVOT: Right Ventricular Outflow Tract; RVSP: Right Ventricular Systolic Pressure; PCP: Pulmonary Capillary Pressure; CO: Cardiac Output.[5]

Table 4 – Main clinically validated formulas used for PCP estimation

Parameter	Formula	Condition
PCP	1,24 X E/e' ratio + 1,9 [13]	– Normality values: < 12 – 15 mmHg E/e' > 15 was correlated with PCP > 15 mmHg Original study: Sensitivity: 89% - Specificity: 91% - Accuracy: 0.92
PCP	PCP = 5,7 X E/VP + 4,6 [14]	Study with 45 patients (LVEF: 40% ± 15%)

PCP: pulmonary capillary pressure; LVEF: left ventricle ejection fraction; CO: cardiac output; PVR: Pulmonary vascular resistance.

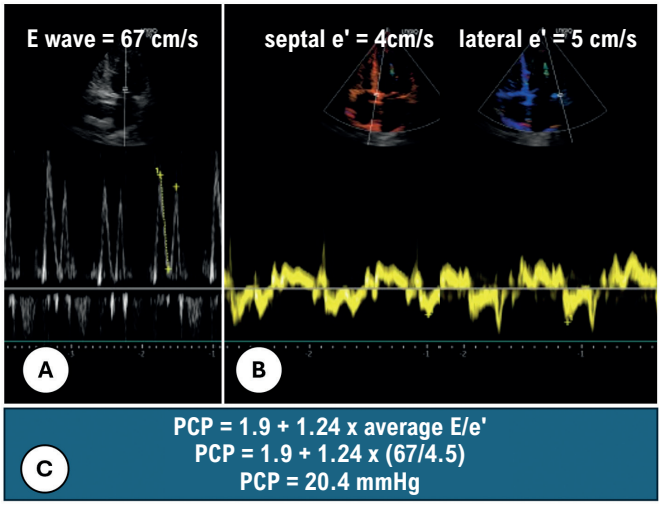

Figure 7 – *Calculation of PCP using Nagueh's formula; A) E and A waves of mitral inflow on pulsed Doppler; B) e' wave of the mitral annulus on tissue Doppler; C) Nagueh's formula with the estimation of a significant increase in PCP.*

Table 5 – Classification of pulmonary pressure levels according to the 2025 American Society of Echocardiography guidelines

Variable	Normality	Abnormality grade		
		Discrete	Moderate	Important
TR velocity	< 2.8m/s	2.8 -3.1m/s	3.2 - 3.5m/s	≥3.6m/s
PASP	≤34mmHg	35 – 49 mmHg	50 -69 mmHg	≥70mmHg
RAP	0 - 4 (Mean 3 mmHg)	5 a 9 (Médio 8 mmHg)	10 a 14 mmHg	≥15mmHg
AcT	>105ms	80 – 105ms	61 -79ms	≤ 60ms

PVR: pulmonary vascular resistance; TR: tricuspid regurgitation; PASP: pulmonary artery systolic pressure; RAP: right atrial pressure; AcT: acceleration time[3]

- Since they use the Doppler method, these variables are influenced by the insonation angle.
- In patients with significant mitral valve disease, the A wave may be increased due to the valvulopathy, limiting the analysis of PCP.
- PCP assessment is impaired in the presence of arrhythmias.

Summary of main warnings and pitfalls

1. Measure the densest primary edge of the continuous-wave Doppler signal ("chin") and not the faint spectra ("beard"), optimizing gain and brightness across multiple imaging planes.
2. Ultrasound contrast agents, saline blood contrast, and agitated saline solution can be used to enhance the Doppler signal, improving diagnostic accuracy.
3. Position the ultrasound beam parallel to the direction of blood flow, ideally at an angle $<20°$ to minimize any errors in velocity measurement.
4. If there is significant TR, the shape of the continuous-wave Doppler signal can help guide the accuracy of right ventricular systolic pressure (RVSP) estimates. A triangular continuous-wave Doppler contour will underestimate RVSP, while accuracy improves with a parabolic Doppler contour.
5. Do not consider velocity after a pause or premature contraction (extrasystole).
6. Consider the average velocity over five to seven beats in patients with arrhythmia.
7. Measure the IVC while visualizing its walls throughout the entire respiratory cycle, avoiding possible false collapsibility due to sampling error.
8. Physiological aging and an increase in body surface area can elevate pulmonary artery systolic pressure (PASP) without necessarily indicating pathology.

Clinical interpretation

Although there are several echocardiographic methods to calculate PMAP, the standard reporting of RVSP is generally preferred for several reasons. First, RVSP is measured directly from the peak velocity of the TR jet, making it a more direct and reliable estimate. In contrast, methods such as AcT of RVOT and the estimation of mPAP and PADP rely on indirect calculations and assumptions, which can introduce measurement errors.

The correct quantification and stratification of pulmonary pressures will allow their classification as mild, moderate, and severe. This classification was revisited in the guideline for echocardiographic assessment of the right heart in adults and special considerations in PH by the American Society of Echocardiography (ASE), grading the abnormality of the values presented in Table 5.

Due to the significant limitation in correctly identifying pulmonary vascular resistance (PVR), PH can be assessed by considering only the maximum velocity of TR to avoid inference errors, a parameter that had already been corroborated by the European Society of Cardiology (ESC) in its 2022 PH guidelines.

The definitive assessment of mPAP for diagnosis, classification, and initiation of pharmacological therapy for PH requires direct hemodynamic measurement via invasive right heart catheterization.

Conclusion

The evaluation of pulmonary pressures has been a cornerstone in identifying adult patients and patients with congenital diseases who have a worse clinical prognosis. The identification of pulmonary pressure levels is still based on invasive quantification through hemodynamic assessment, which remains the gold standard method. Doppler echocardiography emerges as an excellent alternative for the initial stratification of these patients, adding other parameters such as ventricular function and valve assessment.

Author Contributions

Conception and design of the research, writing of the manuscript and critical revision of the manuscript for intellectual content: Silva HAGP, Gomes HM.

Potential Conflict of Interest

No potential conflict of interest relevant to this article was reported.

Sources of Funding

There were no external funding sources for this study.

Study Association

This study is not associated with any thesis or dissertation work.

Ethics Approval and Consent to Participate

This article does not contain any studies with human participants or animals performed by any of the authors.

Use of Artificial Intelligence

The authors did not use any artificial intelligence tools in the development of this work.

Availability of Research Data

The underlying content of the research text is contained within the manuscript.

References

1. Humbert M, Kovacs G, Hoeper MM, Badagliacca R, Berger RMF, Brida M, et al. 2022 ESC/ERS Guidelines for the Diagnosis and Treatment of Pulmonary Hypertension. Eur Respir J. 2023;61(1):2200879. doi: 10.1183/13993003.00879-2022.
2. Holen J, Simonsen S. Determination of Pressure Gradient in Mitral Stenosis with Doppler Echocardiography. Br Heart J. 1979;41(5):529-35. doi: 10.1136/hrt.41.5.529.
3. Hatle L, Angelsen BA, Tromsdal A. Non-Invasive Assessment of Aortic Stenosis by Doppler Ultrasound. Br Heart J. 1980;43(3):284-92. doi: 10.1136/hrt.43.3.284.
4. Galiè N, McLaughlin VV, Rubin LJ, Simonneau G. An Overview of the 6th World Symposium on Pulmonary Hypertension. Eur Respir J. 2019;53(1):1802148. doi: 10.1183/13993003.02148-2018.
5. Mukherjee M, Rudski LG, Addetia K, Afilalo J, D'Alto M, Freed BH, et al. Guidelines for the Echocardiographic Assessment of the Right Heart in Adults and Special Considerations in Pulmonary Hypertension: Recommendations from the American Society of Echocardiography. J Am Soc Echocardiogr. 2025;38(3):141-86. doi: 10.1016/j.echo.2025.01.006.
6. D'Alto M, Di Maio M, Romeo E, Argiento P, Blasi E, Di Vilio A, et al. Echocardiographic Probability of Pulmonary Hypertension: A Validation Study. Eur Respir J. 2022;60(2):2102548. doi: 10.1183/13993003.02548-2021.
7. Badesch DB, Champion HC, Sanchez MAG, Hoeper MM, Loyd JE, Manes A, et al. Diagnosis and Assessment of Pulmonary Arterial Hypertension. J Am Coll Cardiol. 2009;54(1 Suppl):S55-S66. doi: 10.1016/j.jacc.2009.04.011.
8. Mahan G, Dabestani A, Gardin J, Allfie A, Burn C, HenryW. Estimation of Pulmonary Artery Pressure by Pulsed Doppler Echocardiography. Circulation. 1983;68(3):367.
9. Dabestani A, Mahan G, Gardin JM, Takenaka K, Burn C, Allfie A, et al. Evaluation of Pulmonary Artery Pressure and Resistance by Pulsed Doppler Echocardiography. Am J Cardiol. 1987;59(6):662-8. doi: 10.1016/0002-9149(87)91189-1.
10. Chemla D, Castelain V, Humbert M, Hébert JL, Simonneau G, Lecarpentier Y, et al. New Formula for Predicting Mean Pulmonary Artery Pressure Using Systolic Pulmonary Artery Pressure. Chest. 2004;126(4):1313-7. doi: 10.1378/chest.126.4.1313.
11. Aduen JF, Castello R, Lozano MM, Hepler GN, Keller CA, Alvarez F, et al. An Alternative Echocardiographic Method to Estimate Mean Pulmonary Artery Pressure: Diagnostic and Clinical Implications. J Am Soc Echocardiogr. 2009;22(7):814-9. doi: 10.1016/j.echo.2009.04.007.
12. Abbas AE, Franey LM, Marwick T, Maeder MT, Kaye DM, Vlahos AP, et al. Noninvasive Assessment of Pulmonary Vascular Resistance by Doppler Echocardiography. J Am Soc Echocardiogr. 2013;26(10):1170-7. doi: 10.1016/j.echo.2013.06.003.
13. Nagueh SF, Middleton KJ, Kopelen HA, Zoghbi WA, Quiñones MA. Doppler Tissue Imaging: A Noninvasive Technique for Evaluation of Left Ventricular Relaxation and Estimation of Filling Pressures. J Am Coll Cardiol. 1997;30(6):1527-33. doi: 10.1016/s0735-1097(97)00344-6.
14. Garcia MJ, Ares MA, Asher C, Rodriguez L, Vandervoort P, Thomas JD. An Index of Early Left Ventricular Filling that Combined with Pulsed Doppler Peak E Velocity May Estimate Capillary Wedge Pressure. J Am Coll Cardiol. 1997;29(2):448-54. doi: 10.1016/s0735-1097(96)00496-2.

My Approach to Diagnose Fabry Disease

Sandra Marques e Silva[1]
Hospital de Base do Distrito Federal,[1] *Brasília, DF – Brazil*

Central Illustration: My Approach to Diagnose Fabry Disease

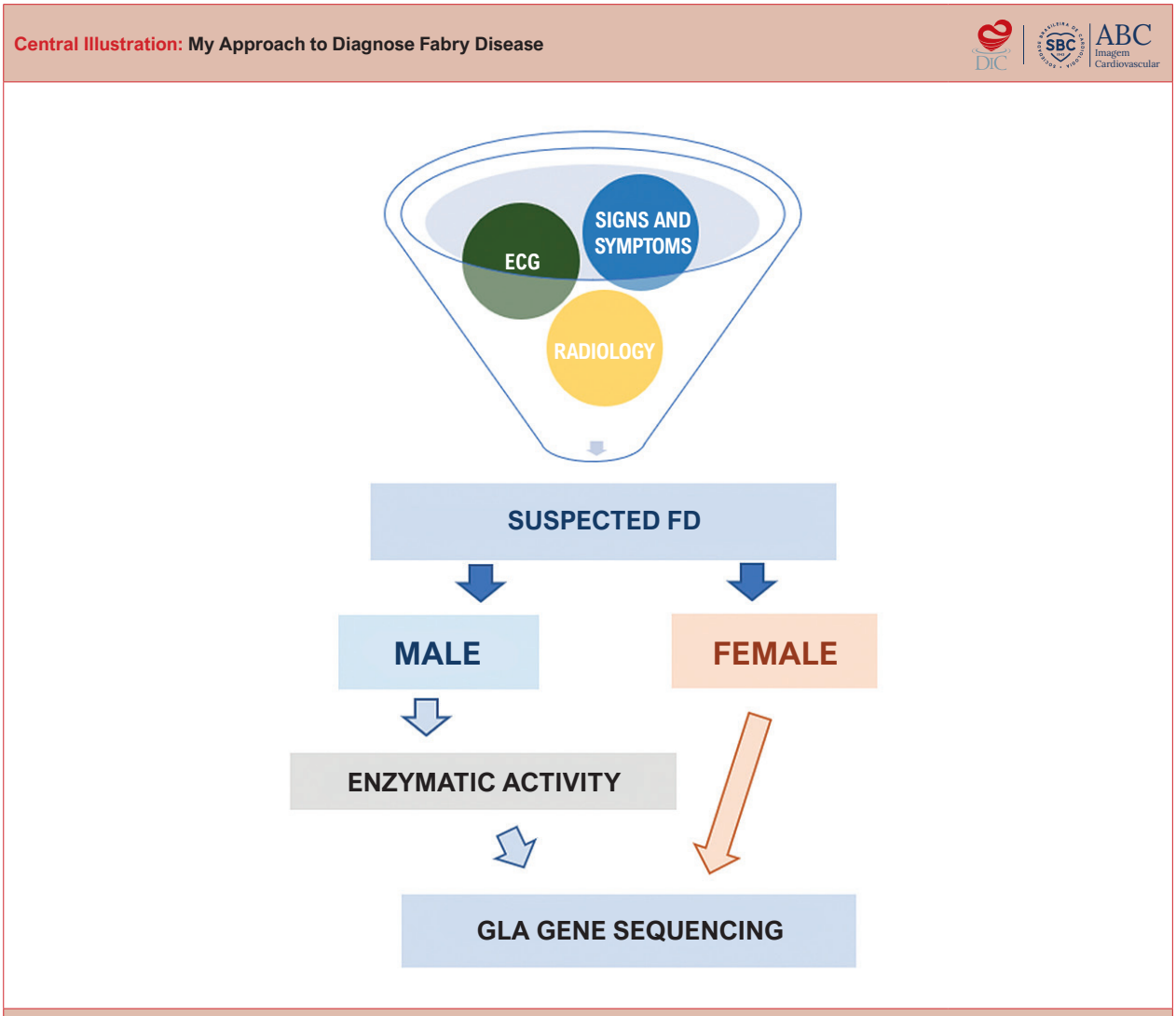

Arq Bras Cardiol: Imagem cardiovasc. 2025;38(2):e20240091

Diagnostic sequence of FD: ancillary tests. ECG: electrocardiogram; GLA: gene associated with FD (X chromosome); FD: Fabry

Keywords

Fabry Disease; Glycosphingolipids; Hypertrophic Cardiomyopathy

Mailing Address: Sandra Marques e Silva •
Área especial. Quadra 101 / 301. Postal code: 70719-040. Brasília, DF – Brazil
E-mail: smarquesmd@gmail.com
Manuscript received April 27, 2025; revised May 5, 2025; accepted May 5, 2025
Editor responsible for the review: Marcelo Tavares

DOI: https://doi.org/10.36660/abcimg.20240091i

Abstract

Fabry disease (FD) is an inherited lysosomal storage disorder caused by a deficiency of the enzyme alpha-galactosidase A (α-Gal A). This enzymatic defect leads to the cytoplasmic lysosomal accumulation of globotriaosylceramides (GB3 and LysoGB3), resulting in multisystemic clinical manifestations. Cardiovascular involvement, often mimicking hypertrophic cardiomyopathy, is the main determinant of morbidity and mortality, due to the development of arrhythmia,

myocardial ischemia, and heart failure. Although FD is a rare condition in the general population, the availability of specific enzyme replacement therapy, which can alter the natural course of the disease, underscores the importance of including FD as a key differential diagnosis among storage cardiomyopathies. Diagnostic evaluation should encompass a thorough clinical assessment, with particular attention to patient history and physical examination, complemented by laboratory testing and imaging studies, such as electrocardiography and echocardiography. Cardiac magnetic resonance imaging, including late gadolinium enhancement and T1 and T2 parametric mapping, provides additional diagnostic and prognostic information and should ideally be performed at the time of initial diagnosis. Definitive diagnosis is established by genetic sequencing of the GLA gene, located on the long arm of the X chromosome, enabling the selection of the most appropriate therapeutic strategy for each patient.

Introduction

Fabry disease (FD; OMIM 301500) is a rare, X-linked lysosomal storage disorder. Pathogenic variants in the GLA gene, located on the long arm of the X chromosome, lead to a deficiency of the enzyme alpha-galactosidase A (α-Gal A), which is responsible for the catabolism of glycosphingolipids, such as globotriaosylceramide (GB3) and its deacetylated form, Lyso-GB3, within lysosomes. The accumulation of these substrates begins in the intrauterine period and triggers an intense tissue inflammatory response, coupled with local oxidative stress. This cascade promotes cellular injury, apoptosis, and, progressively, organ dysfunction and failure.[1]

Cardiovascular involvement, which can mimic hypertrophic cardiomyopathy (phenocopy), is the leading cause of morbidity and mortality among Brazilian patients, primarily due to the development of arrhythmias, myocardial ischemia, and heart failure.[2] Despite its low prevalence in the general population, the availability of disease-specific enzyme replacement therapy, capable of modifying the disease course, highlights FD as a key differential diagnosis among storage cardiomyopathies.

The diagnostic approach to FD-associated cardiomyopathy should include a comprehensive clinical evaluation, encompassing a detailed medical history and physical examination, as well as accessible laboratory and imaging studies, such as electrocardiography and echocardiography. Cardiac magnetic resonance imaging provides additional diagnostic and prognostic insights and should preferably be performed during the initial diagnostic workup. Definitive diagnosis is established through genetic sequencing of the GLA gene, which also guides the selection of the most appropriate therapeutic strategy for each patient.[3]

My approach to

Diagnosing a rare cardiomyopathy poses a significant challenge for cardiologists, particularly when dealing with phenocopies. The estimated prevalence of FD in the general population is approximately 1 in 117,000 cases.[4] However, this figure may reach as high as 1 in 3,100 when considering neonatal screening, a strategy that has been progressively incorporated into the Brazilian public health care system, as already implemented in certain regions, such as the Distrito Federal.[5]

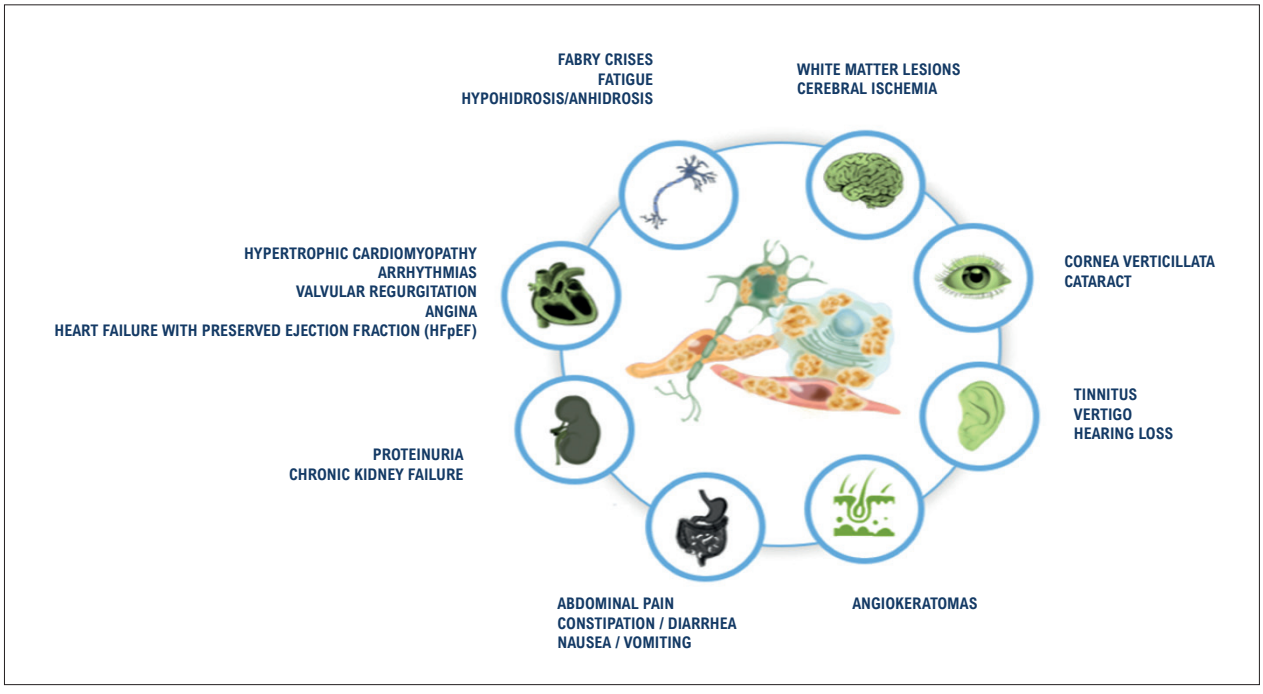

Figure 1 – *Multisystemic manifestations of FD.*

The low prevalence of FD in the general population highlights two key considerations. First, it emphasizes the importance of including FD in the differential diagnosis of cardiomyopathies, given the availability of specific treatment through enzyme replacement therapy, which has been recently incorporated into Brazil's Unified Health System (*Sistema Único de Saúde*, SUS). This therapy has the potential to positively alter the natural history of the disease and improve patients' symptom-free survival. Second, it reinforces the need to thoroughly identify and manage more prevalent conditions — such as systemic hypertension, valvular heart disease, and, in the Brazilian context, rheumatic heart disease — before considering FD as the underlying cause of the presenting symptoms.

The diagnostic workup for FD should begin with a thorough clinical history. Figure 1 outlines the key elements that may raise clinical suspicion of FD. Patient age and sex should also be considered, as the clinical expression of the disease varies depending on the type of pathogenic variant identified in the GLA gene.

In the classic form of FD, cardiovascular manifestations — such as palpitations and exercise intolerance — may appear as early as childhood. These symptoms are often accompanied by other early manifestations, including characteristic neuropathic pain (Fabry crises) triggered by exposure to extreme temperatures, hypohidrosis or anhidrosis with impaired thermoregulation, gastrointestinal disturbances with alternating constipation and diarrhea, tinnitus or hearing loss, as well as cornea verticillata and angiokeratomas typically located in the pelvic region and/or mucosal surfaces.[6]

In contrast, in the nonclassic form of FD, also referred to as late-onset FD, these early systemic manifestations are often absent, with clinical presentation predominantly characterized by cardiac or renal involvement. These may occasionally be associated with central nervous system ischemic events, such as strokes occurring at relatively young ages.[7]

A careful assessment of the patient's personal history of symptoms and prior disorders is also essential, as is gathering information on first-degree relatives. Commonly reported symptoms include exertional chest pain, palpitations, exercise intolerance, orthostatic hypotension, and/or syncope, which may be associated with renal dysfunction, ischemic neurological events, or polyneuropathy. Family history should include targeted questions regarding known cases of FD, cardiomyopathies, strokes, sudden cardiac death, and/or renal failure requiring dialysis.[8] Based on these data, it is advisable to construct a family pedigree, ideally encompassing at least three generations, in order to identify the familial inheritance pattern, which in the case of FD is X-linked.[9]

Once the clinical data have been collected, electrocardiography is the first ancillary tool available in the evaluation of FD-associated cardiomyopathy. The most frequent electrocardiographic findings are summarized in Table 1. Although PR interval shortening combined with signs of left ventricular overload is not specific to FD, its presence may suggest glycosphingolipid deposition in cardiac tissues. These findings can aid in differential diagnosis with other cardiomyopathies presenting

Table 1 – Findings of FD-associated cardiomyopathy on ancillary tests

Method	Findings
Clinical evaluation	Clinical complaints from the index case and family members
	Detailed physical examination
Electrocardiogram	Short PR interval
	Arrhythmias of undefined origin (tachyarrhythmia/bradyarrhythmia)
	Left ventricular overload pattern
	Repolarization abnormalities suggestive of myocardial ischemia
	Corrected QT interval <440 ms
Echocardiogram	Increased left ventricular wall thickness >12 mm
	Papillary muscle hypertrophy
	Diastolic dysfunction (early) and left ventricular systolic dysfunction (late)
	Regional wall motion abnormalities (basal inferolateral wall)
	Reduced longitudinal and radial strain (basal inferolateral wall)
Cardiac magnetic resonance imaging	Mid-myocardial late gadolinium enhancement in the basal inferolateral wall
	Low native T1 mapping values
	Valores elevados no mapa T2

with a hypertrophic phenotype, such as sarcomeric cardiomyopathy or cardiac amyloidosis.

Early conduction abnormalities may be detected as early as childhood; however, they typically become clinically apparent during adolescence, manifesting as palpitations or exercise intolerance. Additional findings include corrected QT interval abnormalities, electrocardiographic signs suggestive of myocardial ischemia secondary to microvascular dysfunction (MINOCA), as well as ventricular or supraventricular arrhythmias, the latter carrying a potential risk of adverse outcomes, such as embolic events or sudden cardiac death at a young age.[10,11]

More advanced diagnostic tools are required for phenotypic characterization of the disease, contributing to the definition of the therapeutic strategy and the planning of long-term follow-up. In this context, echocardiography stands out as a widely accessible, low-cost, easy-to-perform imaging modality. The most common echocardiographic findings are presented in Table 1.

The earliest sign of cardiac involvement is diastolic dysfunction, which cannot be attributed to pressure or volume overload, nor to conditions such as systemic hypertension, valvular heart disease, or diabetes mellitus. Another characteristic finding is increased left ventricular wall thickness, with lower cutoff values than those established for sarcomeric hypertrophic cardiomyopathy: ≥11 mm in women and ≥12 mm in men. This distinction is justified by the fact that, in storage diseases, wall thickness equal to or greater than 15 mm is often associated with myocardial fibrosis, which serves as an arrhythmogenic substrate and a marker of poor prognosis.

Concentric hypertrophy is the most common presentation; however, eccentric or isolated apical patterns have also been described. Glycosphingolipid deposits also affect the chordae tendineae and papillary muscles, leading to significant thickening, as well as the endocardium, resulting in the so-called "binary sign." Biventricular ejection fraction tends to remain preserved throughout the natural course of the disease, except in the presence of myocardial fibrosis, which increases the risk of progressive systolic dysfunction.

Emerging techniques, such as global longitudinal strain (GLS) analysis, provide additional valuable information for the differential diagnosis with other causes of hypertrophy and with the athlete's heart. GLS reduction, particularly due to impaired strain in the basal segment of the inferolateral wall, is strongly correlated with the presence of myocardial fibrosis detected by cardiac magnetic resonance imaging. Moreover, mild valvular regurgitation — especially of the mitral and aortic valves — as well as proximal thoracic aortic ectasia, are additional echocardiographic findings commonly observed in FD with cardiac involvement.[12,13]

Cardiac magnetic resonance imaging is considered the gold standard for the diagnosis of FD-associated cardiomyopathy, given the comprehensive diagnostic and prognostic information it provides. Late gadolinium enhancement, typically located in the mid-myocardial layer of the basal inferolateral wall, has significant prognostic value due to its association with an increased risk of heart failure and arrhythmia, as well as serving as a marker of chronic cardiac involvement.[14]

Native T1 parametric mapping typically shows characteristically reduced values in FD, which may be altered even before the development of ventricular hypertrophy. The only other condition that shares this pattern of reduced T1 values is cardiac-involved hemochromatosis, which can be differentiated through serum iron metabolism markers and liver ultrasound. Conversely, T2 mapping in FD reveals characteristically elevated values, contributing — together with T1 mapping — to the early diagnosis of cardiomyopathy as well as aiding in the differential diagnosis with other etiologies of cardiomyopathy.[15,16]

Cardiac biomarkers, such as high-sensitivity troponin and NT-proBNP, are elevated in the presence of FD-associated cardiomyopathy. Lyso-GB3 is considered the most specific biomarker for the disease, with markedly elevated plasma levels, particularly in the classic form. Following the initiation of enzyme replacement therapy, a reduction in Lyso-GB3 levels is observed, making it a useful marker for monitoring therapeutic effectiveness. In contrast, GB3 levels in plasma and urine are not routinely assessed in clinical practice, especially in women, as they may present altered levels even in individuals without the disease, thus limiting their diagnostic utility.[17,18]

Definitive diagnosis of FD is established by identifying a pathogenic variant in the GLA gene through genetic testing. As illustrated in Central Illustration, in male individuals, genetic testing may be preceded by measurement of enzymatic activity, which typically shows markedly low levels in this population. In females, however, due to the presence of two X chromosomes, enzymatic activity may be normal or only slightly reduced, limiting its diagnostic utility. Moreover, to confirm the diagnosis, at least one of the following criteria must be present: signs or symptoms suggestive of FD (e.g., neuropathic pain, cornea verticillata, or angiokeratomas); elevated plasma Lyso-GB3 levels; or a family history of FD confirmed by the same pathogenic variant.[19,20]

This diagnostic pathway is crucial for the appropriate therapeutic management of patients with FD-associated cardiomyopathy, especially considering the recent approval by the Brazilian National Committee for the Incorporation of Technologies into the Unified Health System of specific therapies capable of modifying the prognosis and natural course of the disease. Enzyme replacement therapies are currently available through the SUS high-cost pharmacy network nationwide. Therefore, it is the cardiologist's responsibility to actively ensure early access to the most appropriate and available treatment for these patients.

Author Contributions

Conception and design of the research, acquisition of data, analysis and interpretation of the data, writing of the manuscript and critical revision of the manuscript for intellectual content: Silva SM.

Potential Conflict of Interest

No potential conflict of interest relevant to this article was reported.

Sources of Funding

There were no external funding sources for this study.

Study Association

This study is not associated with any thesis or dissertation work.

Ethics Approval and Consent to Participate

This article does not contain any studies with human participants or animals performed by any of the authors.

Use of Artificial Intelligence

The authors did not use any artificial intelligence tools in the development of this work.

Availability of Research Data

The underlying content of the research text is contained within the manuscript.

References

1. Pastores GM, Lien YH. Biochemical and Molecular Genetic Basis of Fabry Disease. J Am Soc Nephrol. 2002;13(Suppl 2):S130-3.
2. Martins AM, Kyosen SO, Garrote J, Marques FM, Guilhem JG, Macedo E, et al. Demographic Characterization of Brazilian Patients Enrolled in the Fabry Registry. Genet Mol Res. 2013;12(1):136-42. doi: 10.4238/2013.January.24.5.
3. Ortiz A, Germain DP, Desnick RJ, Politei J, Mauer M, Burlina A, et al. Fabry Disease Revisited: Management and Treatment Recommendations for Adult Patients. Mol Genet Metab. 2018;123(4):416-27. doi: 10.1016/j.ymgme.2018.02.014.
4. Desnick RJ. Fabry Disease: α-Galactosidase A Deficiency. Academic Press. 2025;1:695-708. doi: 10.1016/B978-0-443-19041-4.00079-0.
5. Spada M, Pagliardini S, Yasuda M, Tukel T, Thiagarajan G, Sakuraba H, et al. High Incidence of Later-Onset Fabry Disease Revealed by Newborn Screening. Am J Hum Genet. 2006;79(1):31-40. doi: 10.1086/504601.
6. Hopkin RJ, Jefferies JL, Laney DA, Lawson VH, Mauer M, Taylor MR, et al. The Management and Treatment of Children with Fabry Disease: A United States-Based Perspective. Mol Genet Metab. 2016;117(2):104-13. doi: 10.1016/j.ymgme.2015.10.007.
7. Desnick RJ, Brady R, Barranger J, Collins AJ, Germain DP, Goldman M, et al. Fabry Disease, an Under-Recognized Multisystemic Disorder: Expert Recommendations for Diagnosis, Management, and Enzyme Replacement Therapy. Ann Intern Med. 2003;138(4):338-46. doi: 10.7326/0003-4819-138-4-200302180-00014.
8. Yogasundaram H, Kim D, Oudit O, Thompson RB, Weidemann F, Oudit GY. Clinical Features, Diagnosis, and Management of Patients with Anderson-Fabry Cardiomyopathy. Can J Cardiol. 2017;33(7):883-97. doi: 10.1016/j.cjca.2017.04.015.
9. Bennett RL, Hart KA, O'Rourke E, Barranger JA, Johnson J, MacDermot KD, et al. Fabry Disease in Genetic Counseling Practice: Recommendations of the National Society of Genetic Counselors. J Genet Couns. 2002;11(2):121-46. doi: 10.1023/a:1014545521753.
10. Zada M, Lo Q, Trivedi SJ, Harapoz M, Boyd AC, Devine K, et al. Electrocardiographic Characteristics and Their Correlation with Echocardiographic Alterations in Fabry Disease. J Cardiovasc Dev Dis. 2022;9(1):11. doi: 10.3390/jcdd9010011.
11. Namdar M, Steffel J, Vidovic M, Brunckhorst CB, Holzmeister J, Lüscher TF, et al. Electrocardiographic Changes in Early Recognition of Fabry Disease. Heart. 2011;97(6):485-90. doi: 10.1136/hrt.2010.211789.
12. Yeung DF, Sirrs S, Tsang MYC, Gin K, Luong C, Jue J, et al. Echocardiographic Assessment of Patients with Fabry Disease. J Am Soc Echocardiogr. 2018;31(6):639-49.e2. doi: 10.1016/j.echo.2018.01.016.
13. Pieroni M, Moon JC, Arbustini E, Barriales-Villa R, Camporeale A, Vujkovac AC, et al. Cardiac Involvement in Fabry Disease: JACC Review Topic of the Week. J Am Coll Cardiol. 2021;77(7):922-36. doi: 10.1016/j.jacc.2020.12.024.
14. Nordin S, Kozor R, Bulluck H, Castelletti S, Rosmini S, Abdel-Gadir A, et al. Cardiac Fabry Disease with Late Gadolinium Enhancement is a Chronic Inflammatory Cardiomyopathy. J Am Coll Cardiol. 2016;68(15):1707-8. doi: 10.1016/j.jacc.2016.07.741.
15. Augusto JB, Johner N, Shah D, Nordin S, Knott KD, Rosmini S, et al. The Myocardial Phenotype of Fabry Disease Pre-Hypertrophy and Pre-Detectable Storage. Eur Heart J Cardiovasc Imaging. 2021;22(7):790-9. doi: 10.1093/ehjci/jeaa101.
16. Perry R, Shah R, Saiedi M, Patil S, Ganesan A, Linhart A, et al. The Role of Cardiac Imaging in the Diagnosis and Management of Anderson-Fabry Disease. JACC Cardiovasc Imaging. 2019;12(7 Pt 1):1230-42. doi: 10.1016/j.jcmg.2018.11.039.
17. Yogasundaram H, Nikhanj A, Putko BN, Boutin M, Jain-Ghai S, Khan A, et al. Elevated Inflammatory Plasma Biomarkers in Patients with Fabry Disease: A Critical Link to Heart Failure with Preserved Ejection Fraction. J Am Heart Assoc. 2018;7(21):e009098. doi: 10.1161/JAHA.118.009098.
18. Carnicer-Cáceres C, Arranz-Amo JA, Cea-Arestin C, Camprodon-Gomez M, Moreno-Martinez D, Lucas-Del-Pozo S, et al. Biomarkers in Fabry Disease. Implications for Clinical Diagnosis and Follow-up. J Clin Med. 2021;10(8):1664. doi: 10.3390/jcm10081664.
19. Sirrs S, Bichet DG, Iwanochko RM, Khan A, Moore D, Oudit G, et al. 2017 Canadian Fabry Disease Guidelines Canadian Fabry Disease Treatment Guidelines 2017 [Internet]. Toronto: The Canadian Fabry Association; 2017 [cited 2025 Mar 3]. Available from: https://www.fabrycanada.com/content/uploads/Final-Can-FD-Treatment-Guidelines-2017Oct18.pdf.
20. Arbelo E, Protonotarios A, Gimeno JR, Arbustini E, Barriales-Villa R, Basso C, et al. 2023 ESC Guidelines for the Management of Cardiomyopathies. Eur Heart J. 2023;44(37):3503-626. doi: 10.1093/eurheartj/ehad194.

Large Heterogeneous Mass in the Right Chambers: A Case Report in Cardio-Oncology

João Pedro Perfeito Frigo,[1] *Themissa Helena Voss*[2]
Universidade Federal de Uberlândia,[1] *Uberlândia, MG – Brazil*
Hospital de Clínicas de Uberlândia,[2] *Uberlândia, MG – Brazil*

Abstract

Renal cell carcinoma (RCC) is one of the most lethal cancers. It is frequently associated with the formation of tumor thrombi (TT), an intravascular extension of the tumor. Approximately 4% to 10% of patients with RCC have TT, which can reach the renal vein (10% to 18%), the inferior vena cava (4% to 23%), and, rarely, the right atrium (1%). These thrombi generally accompany advanced tumors, with distant metastases, and they reflect an aggressive biology. Treatment is challenging, especially in metastatic cases, and surgical resection is indicated in the absence of metastases. Anticoagulation remains controversial due to the neoplastic composition of TT. We report the case of a 51-year-old male patient with clear cell RCC and lung and liver metastases treated with pazopanib. The patient presented right heart failure and was diagnosed with extensive TT up to the right atrium, identified by transthoracic echocardiography. In an advanced stage, with clinical deterioration, palliative care was chosen, and the patient died within a few weeks. The diagnosis of TT is crucial to define prognosis and therapeutic strategies. Echocardiography, combined with advanced imaging techniques, plays a fundamental role in differentiating between TT and thromboembolism. This case highlights the importance of a multidisciplinary approach and technological advances for managing complex conditions such as TT, with the goals of early diagnosis and reduced complications.

Introduction

Renal cell carcinoma (RCC) is one of the most lethal cancers, associated with the formation of tumor thrombi (TT), characterized by intravascular tumor extension. RCC represents approximately 3% of all cancers, and it is estimated that 4% to 10% of patients with RCC have some degree of TT. The reported prevalence of venous TT in RCC is 10% to 18% with invasion of the renal vein, 4% to 23% with involvement of the inferior vena cava, and 1% with extension to the right atrium.[1,2]

TT is strongly associated with pulmonary embolism, and it is challenging to distinguish it from thromboembolism by radiographic findings. However, biopsy can assist in definitive diagnosis, although it is rarely performed.[1] Other common outcomes of TT include thrombotic or hemorrhagic complications and death.

With respect to treatment, in the absence of distant metastases, surgical resection is indicated for local control. In metastatic disease, therapy aims to control symptoms, with a primary focus on palliative treatment.[3]

Regarding anticoagulation, it is still debatable, since TT behaves differently from a conventional thrombus, exhibiting organized tumor cells instead of only a fibrin clot.[1,2] Because it is a rare condition and, in the majority of cases, it is diagnosed late, treatment still poses a challenge, especially when the disease is in the metastatic phase.

Keywords

Cardio-Oncology; Renal Cell Carcinoma; Thrombosis; Relatos de Casos

Mailing Address: João Pedro Perfeito Frigo •
Universidade Federal de Uberlândia. Rua Ceara. Postal code: 38400-694. Uberlândia, MG – Brazil
E-mail: joaopedroperfeito1@gmail.com
Manuscript received January 15, 2025; revised January 16, 2025; accepted January 26, 2025
Editor responsible for the review: Marcelo Tavares

DOI: https://doi.org/10.36660/abcimg.20250002i

Case report

We report the case of a 51-year-old male patient, with smoking and alcoholism, who was diagnosed with a clear cell renal tumor, clinical stage IV, with lung and liver metastases. He began treatment with the vascular endothelial growth factor inhibitor pazopanib. He developed significant peripheral edema and ascites and was hospitalized for further assessment.

The patient underwent a transthoracic echocardiogram, which revealed the presence of a large heterogeneous mass with well-defined borders, measuring 8.3 × 4.0 cm in the right chambers, obstructing anterograde flow in the tricuspid valve (mean gradient of 5 mmHg). Subcostal imaging revealed the continuity of the mass in the right chambers with the inferior vena cava, suggesting the presence of an extensive TT. These findings explain the etiology of the clinical signs and symptoms of right heart failure, initially attributed to a possible pulmonary thromboembolism.

During hospitalization, due to difficulties in improving symptoms and signs of clinical deterioration, in addition to the advanced stage of the disease, exclusive palliative care was chosen. The patient died within a few weeks.

Discussion

Intravascular tumor extension is known as TT, which occurs in diverse tumor types, RCC being the most common in adults. Of these, 10% to 18% reach the renal vein only; 4% to 23% reach the inferior vena cava, and only 1% extend into the right atrium. They are generally associated with

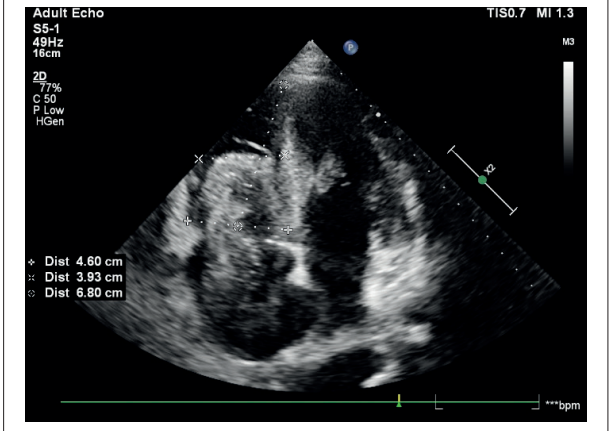

Figure 1 – *Enlargement of the right heart chambers observed in the apical four-chamber view.*

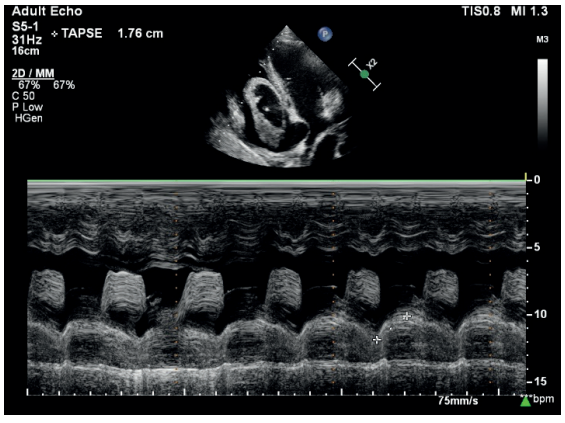

Figure 2 – *Preserved right ventricular systolic function based on TAPSE.*

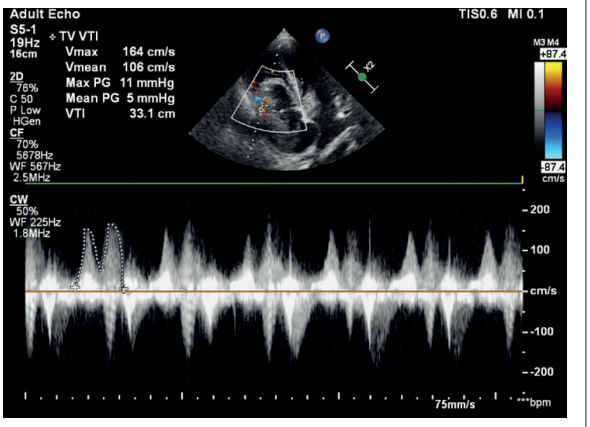

Figure 3 – *Turbulent flow and a mean gradient of 5 mmHg across the tricuspid valve (relative obstruction due to mass protrusion).*

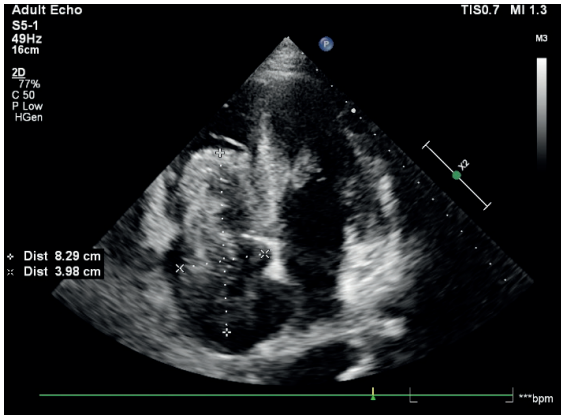

Figure 4 – *Dimensions of the mass within the right heart chambers.*

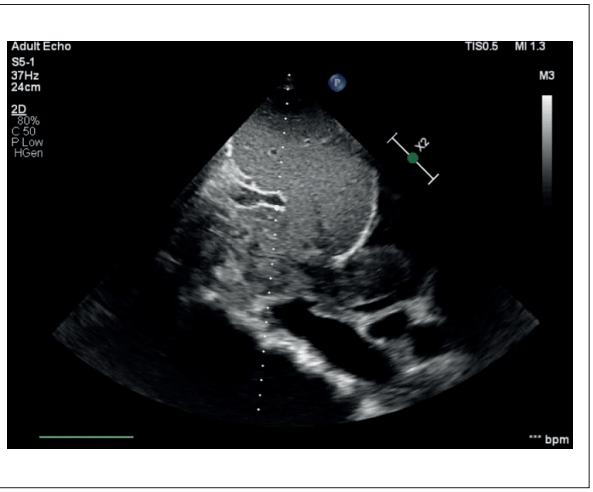

Figure 5 – *Mass in the inferior vena cava.*

larger tumors and advanced stages, often accompanied by distant metastases, which reflect a more aggressive biology and may explain the worse prognosis.[4]

Patients without associated metastases may undergo tumor resection, including the TT, by means of various techniques. Anticoagulation is debatable, given that the behavior of TT differs from simple thrombi due to the presence of organized neoplastic cells. In 1.5% to 3.4% of patients with TT, embolization to the pulmonary arteries may occur, mainly during the intraoperative period, and this complication is associated with a high mortality rate (up to 75%). It is noteworthy that TT, in spite of their extension, are not considered metastases. Moreover, there is a possibility of recurrence of the TT after the initial resection. Diagnosis of TT implies a 65% greater chance of mortality.[5]

Transthoracic echocardiography is the initial imaging modality, whereas cardiac magnetic resonance imaging

plays an important role in the differential diagnosis between thrombus and cardiac tumor. The associated use of ultrasound enhancement agents in transthoracic echocardiography increases diagnostic accuracy. This finding is decisive in a patient's journey, indicating an unfavorable prognosis and demanding a differentiated surgical approach.

The complexity of TT management reinforces the importance of a multidisciplinary approach. Teams composed of specialists in oncology, cardiology, vascular surgery, and radiology are essential to ensure early diagnosis, personalized treatment planning, and reduced complications. Furthermore, advances in imaging techniques have the potential to enhance detection and differentiation between tumor and non-TT, contributing to more precise treatment and better survival prospects for patients.[6]

In conclusion, this case highlights the relevance of echocardiography as an essential tool for the diagnosis of pathologies in which the signs and symptoms suggest a cardiac component, in addition to guiding therapeutic management.

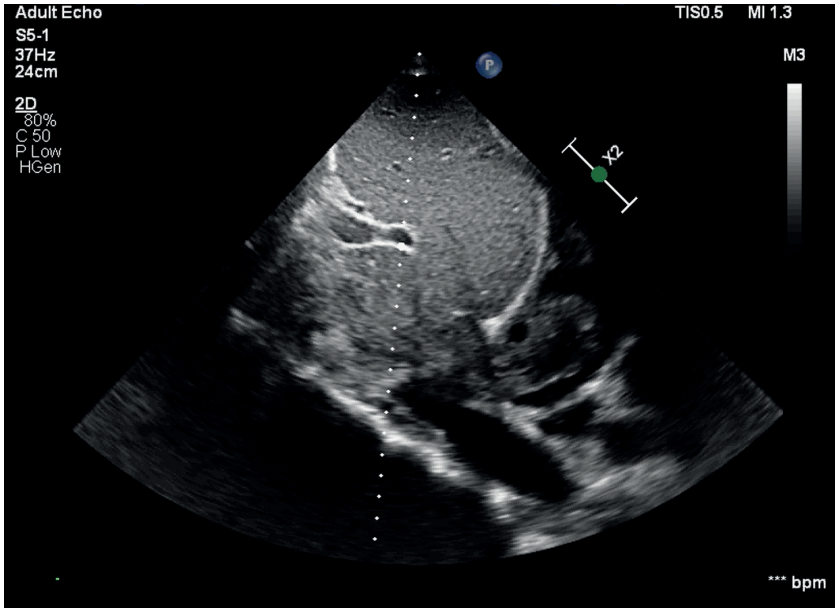

Video 1 – *Access: http://abcimaging.org/supplementary-material/2025/3801/2025-0002_RC_Video1.mp4*

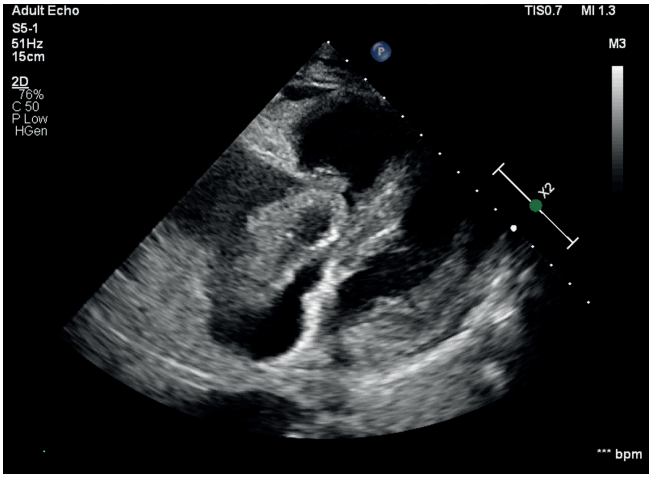

Video 2 – *Access: http://abcimaging.org/supplementary-material/2025/3801/2025-0002_RC_Video2.mp4*

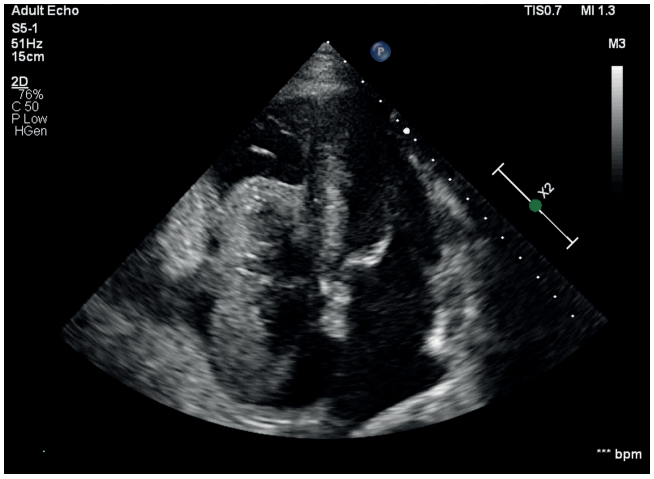

Video 3 – *Access: http://abcimaging.org/supplementary-material/2025/3801/2025-0002_RC_Video3.mp4*

Author Contributions

Conception and design of the research, acquisition of data, analysis and interpretation of the data, writing of the manuscript and critical revision of the manuscript for intellectual content: Frigo JPP, Voss TH.

Potential Conflict of Interest

No potential conflict of interest relevant to this article was reported.

Sources of Funding

There were no external funding sources for this study.

Study Association

This study is not associated with any thesis or dissertation work.

Ethics Approval and Consent to Participate

This study was approved by the Ethics Committee of the Universidade Federal de Uberlândia under the protocol number 7.534.313. All the procedures in this study were in accordance with the 1975 Helsinki Declaration, updated in 2013. Informed consent was obtained from all participants included in the study.

References

1. Kaptein FHJ, van der Hulle T, Braken SJE, van Gennep EJ, Buijs JT, Burgmans MC, et al. Prevalence, Treatment, and Prognosis of Tumor Thrombi in Renal Cell Carcinoma. JACC CardioOncol. 2022;4(4):522-31. doi: 10.1016/j.jaccao.2022.07.011.
2. Almatari AL, Sathe A, Wideman L, Dewan CA, Vaughan JP, Bennie IC, et al. Renal Cell Carcinoma with Tumor Thrombus: A Review of Relevant Anatomy and Surgical Techniques for the General Urologist. Urol Oncol. 2023;41(4):153-65. doi: 10.1016/j.urolonc.2022.11.021.
3. Pouliot F, Shuch B, Larochelle JC, Pantuck A, Belldegrun AS. Contemporary Management of Renal Tumors with Venous Tumor Thrombus. J Urol. 2010;184(3):833-41. doi: 10.1016/j.juro.2010.04.071.
4. Palaskas N, Thompson K, Gladish G, Agha AM, Hassan S, Iliescu C, et al. Evaluation and Management of Cardiac Tumors. Curr Treat Options Cardiovasc Med. 2018;20(4):29. doi: 10.1007/s11936-018-0625-z. PMID: 29556752..
5. Psutka SP, Leibovich BC. Management of Inferior Vena Cava Tumor Thrombus in Locally Advanced Renal Cell Carcinoma. Ther Adv Urol. 2015;7(4):216-29. doi: 10.1177/1756287215576443.
6. Chen Z, Yang F, Ge L, Qiu M, Liu Z, Liu C, et al. Outcomes of Renal Cell Carcinoma with Associated Venous Tumor Thrombus: Experience from a Large Cohort and Short Time Span in a Single Center. BMC Cancer. 2021;21(1):766. doi: 10.1186/s12885-021-08508-x.

Important Mitral Regurgitation and Ventricular Dysfunction in Hypereosinophilic Syndrome: A Case Report

Marcel Pina Ciuffo,[1] *Lucas Mori,*[2] *Tais Araújo,*[1] *Ingrid Kowatsch,*[1] *Ana Clara Tude Rodrigues*[1]

Hospital das Clinicas da Faculdade de Medicina da Universidade de São Paulo,[1] *São Paulo, SP – Brazil*

Universidawde de São Paulo, Instituto do Coração,[2] *São Paulo, SP – Brazil*

Introduction

Hypereosinophilic syndrome (HES) represents a group of rare hematologic diseases characterized by an increased number of eosinophils in the peripheral blood. Once activated, these eosinophils can cause damage to host tissues and organs. Patients with HES generally present with dermatological, respiratory, and gastrointestinal signs and symptoms. Involvement of the cardiovascular system is uncommon and can lead to serious consequences such as heart failure, arrhythmias, and thromboembolic phenomena.

This article describes a case of eosinophilic endomyocardial disease, also known as Loeffler syndrome, a manifestation of HES characterized by eosinophil-mediated cardiac damage. Despite adequate treatment and control of the hematologic disease, the patient developed biventricular systolic dysfunction and important mitral regurgitation (MR).

Case report

A 29-year-old male patient, with no comorbidities, history of fever, night sweats, and 17-kg weight loss in the last 4 months, sought medical care with fatigue upon mild exertion, pain in the left hypochondrium, and increased abdominal volume. Physical examination revealed pale skin, tachycardia, hepatosplenomegaly, and edema of the lower limbs.

Laboratory tests showed hemoglobin 7.0 g/dL, hematocrit 21.2%, leukocytes 161,000/mm^3, neutrophils 120,000/mm^3, eosinophils 35,000/mm^3, and platelets 87,000/mm^3. Given the hypothesis of HES, a bone marrow biopsy was performed, which showed absolute granulocytic predominance and eosinophilia in all maturation stages, suggesting chronic myeloproliferative disease.

Keywords

Mitral Valve Insufficiency; Heart Failure; Hypereosinophilic Syndrome

Mailing Address: Marcel Pina Ciuffo •
Hospital das Clínicas da Faculdade de Medicina da Universidade de São Paulo. Avenida Doutor Enéas Carvalho de Aguiar, S/N. Postal code: 05403-010. São Paulo, SP – Brazil
E-mail: marcelpina.cardio@gmail.com
Manuscript received April 29, 2025; revised May 5, 2025; accepted May 5, 2025
Editor responsible for the review: Marcelo Tavares

DOI: https://doi.org/10.36660/abcimg.20250029i

An echocardiogram was performed, showing diffuse endocardial thickening in the left ventricle (LV), which was more pronounced in the apical region, extending to the base of the posterior leaflet of the mitral valve, preserved systolic function, ejection fraction of 68%, and reduced global longitudinal strain (GLS) of −11.6 (Figure 1). There was an echogenic intracavitary image covering the apex and the anterolateral wall, and an ultrasound contrast agent (Sonovue) was infused, suggesting an intracavitary thrombus (Figure 2). The right ventricle did not show any abnormalities, and analysis of diastolic function was impaired by tachycardia. The mitral valve had restricted movement of the posterior leaflet and moderate eccentric MR.

Intravenous furosemide and full anticoagulation with enoxaparin were initiated, due to the clinical condition and the intracardiac thrombus. The patient showed improved congestion symptoms, followed treatment with hematology, and was discharged from hospital 30 days later.

The patient was asymptomatic from a cardiovascular perspective when he returned for follow-up echocardiography 1 year after the onset of the disease. The examination showed mild systolic dysfunction of the LV, ejection fraction of 50%, inferior hypokinesia, and rectified septum. The right ventricle showed mild to moderate systolic dysfunction (tricuspid annular plane systolic excursion 13 mm and fractional area change 30%). Assessment of diastolic function was impaired by significant mitral reflux, and the mitral valve showed reduced mobility and important MR filling the entire left atrium (Figure 3).

Discussion

HES represents a group of rare diseases defined by peripheral blood eosinophil counts greater than 1.5 × 10^9/L. It can be classified as primary (myeloid or lymphocytic neoplasm), secondary (infectious, autoimmune, drug-related, allergic, and metabolic causes), and idiopathic.

HES generally affects individuals between 20 and 50 years of age, and it is more common in men, especially HES of myeloproliferative origin. It can affect different tissues and organs, causing signs and symptoms such as skin lesions, diarrhea, abdominal pain, fever, and weight loss. When it affects the cardiovascular system, it represents a severe form of the disease with high morbidity and mortality.[2]

Loeffler syndrome is the manifestation of HES characterized by eosinophil-mediated cardiac damage. In its early stages, it is asymptomatic, but it causes inflammation and necrosis of the endocardium with formation of intracardiac thrombi and fibrosis. It can

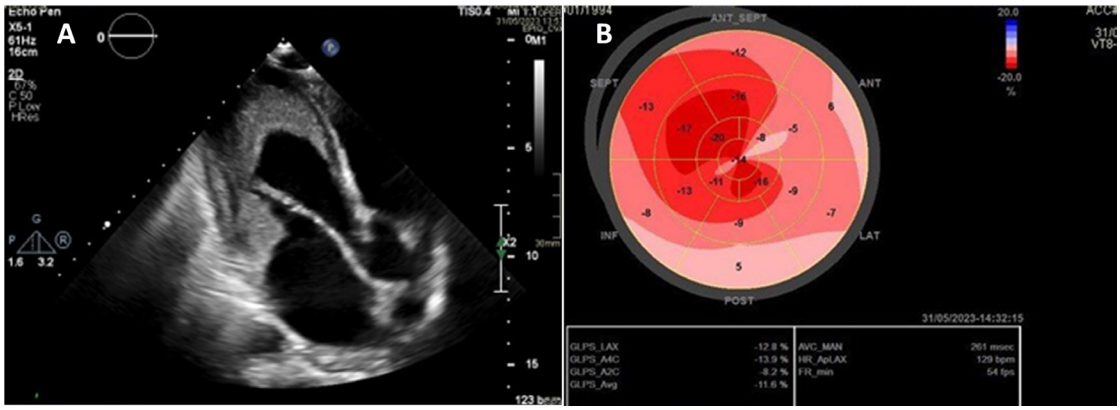

Figure 1 – *(A) Diffuse endocardial thickening, more pronounced in the apical region and the papillary muscle. (B) Bull's-eye plot showing reduced GLS.*

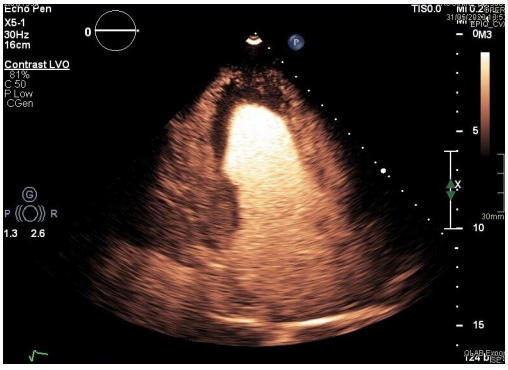

Figure 2 – *Ultrasound contrast agent showing an echogenic image compatible with a thrombus in the apical region of the LV.*

cause heart failure (systolic and diastolic dysfunction), thromboembolic phenomena, arrhythmias, and valvular diseases, mainly regurgitation of the atrioventricular valves, resulting from valvular involvement due to fibrosis.

It is worth highlighting that MR can decrease after treatment of the underlying disease with corticosteroids.[7] Nonetheless, in this case, MR worsened, even after treatment. Furthermore, the patient developed biventricular systolic dysfunction, and he had already presented reduced GLS since diagnosis of the disease, reinforcing the ability of GLS to detect ventricular systolic dysfunction early.

Echocardiography is essential in the evaluation of patients with Loeffler syndrome. In the initial (inflammatory) phase, increased echogenicity of the subendocardium is observed. Subsequently, intracardiac thrombi may appear, which are typically located in the apex of the LV and the subvalvular regions of atrioventricular valves. The use of an ultrasound contrast agents increases the sensitivity of thrombus detection, in addition to allowing differential diagnosis of other conditions, such as apical hypertrophic cardiomyopathy and noncompaction of the myocardium.

Following identification of ventricular dysfunction on echocardiography, cardiac magnetic resonance imaging was performed for further evaluation, as this is the most accurate exam for tissue characterization, helping to define inflammation, edema, and fibrosis in all disease stages (Figure 4).

Endomyocardial biopsy is the gold standard for diagnosis, providing evidence of eosinophilic infiltrate in the cardiac tissue.[4] However, due to the potential for complications, it is only performed in select cases.

Treatment depends on the stage of the disease and the degree of fibrosis. The main goals are to reduce hypereosinophilia and to prevent the progression of tissue damage and thrombus formation. Corticosteroids are the most commonly used medication, but many patients do not respond well. Other options include interferon-alpha, hydroxyurea, imatinib, mepolizumab, and immunomodulatory drugs.[1-3]

The prognosis of HES has improved in recent years due to a better understanding of the disease and the emergence of new therapeutic modalities. However, cardiac dysfunction remains the leading cause of mortality.[8]

Conclusion

We have reported a case of Loeffler syndrome secondary to chronic myeloproliferative disease. Despite adequate diagnosis and treatment, the patient developed biventricular systolic dysfunction and important MR. We emphasize the importance of early diagnosis, treatment, and long-term follow-up as means of reducing the morbidity and mortality of this disease.

Author Contributions

Conception and design of the research and critical revision of the manuscript for intellectual content: Rodrigues ACT; acquisition of data: Ciuffo MP, Araújo T,

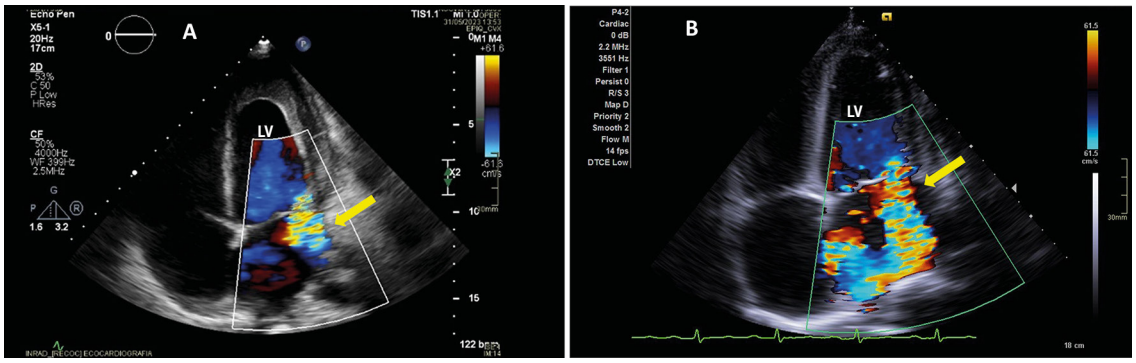

Figure 3 – *(A) Moderate MR jet (yellow arrow) before antineoplastic treatment. (B) Important MR jet, even after treatment. LV: left ventricle.*

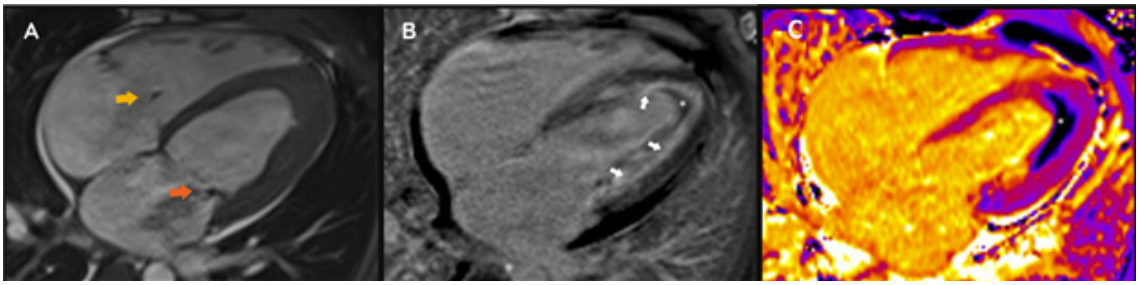

Figure 4 – *(A) Cine magnetic resonance imaging showing attachment of the papillary muscles to the lateral wall of the LV with loss of trabeculation and mitral (orange arrow) and tricuspid (yellow arrow) regurgitation jets. (B) Delayed enhancement showing diffuse circumferential subendocardial fibrosis, without corresponding to a coronary territory (white arrows) and associated with thrombus covering the left ventricular subendocardium (asterisks). (C) Native T1 mapping showing diffusely increased T1, mainly in the septal wall, indicating edema and fibrosis, associated with the thrombus (asterisk).*

Kowatsch I, Mori L; analysis and interpretation of the data: Ciuffo MP, Araújo T, Kowatsch I, Mori L, Rodrigues ACT; writing of the manuscript: Ciuffo MP.

Potential Conflict of Interest

No potential conflict of interest relevant to this article was reported.

Sources of Funding

There were no external funding sources for this study.

Study Association

This study is not associated with any thesis or dissertation work.

Ethics Approval and Consent to Participate

This study was approved by the Ethics Committee of the Hospital das Clínicas da Faculdade de Medina da USP under the protocol number 7.469.009. All the procedures in this study were in accordance with the 1975 Helsinki Declaration, updated in 2013. Informed consent was obtained from all participants included in the study.

Use of Artificial Intelligence

The authors did not use any artificial intelligence tools in the development of this work.

Availability of Research Data

The underlying content of the research text is contained within the manuscript.

References

1. Shomali W, Gotlib J. World Health Organization and International Consensus Classification of Eosinophilic Disorders: 2024 Update on Diagnosis, Risk Stratification, and Management. Am J Hematol. 2024;99(5):946-68. doi: 10.1002/ajh.27287.
2. Requena G, van den Bosch J, Akuthota P, Kovalszki A, Steinfeld J, Kwon N, et al. Clinical Profile and Treatment in Hypereosinophilic Syndrome Variants: A Pragmatic Review. J Allergy Clin Immunol Pract. 2022;10(8):2125-34. doi: 10.1016/j.jaip.2022.03.034.
3. Takla A, Shah P, Sbenghe M, Baibhav B, Feitell S. Incessant Ventricular Tachycardia: An Atypical Presentation of Chronic Eosinophilic Leukemia. JACC Case Rep. 2024;29(16):102461. doi: 10.1016/j.jaccas.2024.102461.
4. Bondue A, Carpentier C, Roufosse F. Hypereosinophilic Syndrome: Considerations for the Cardiologist. Heart. 2022;108(3):164-71. doi: 10.1136/heartjnl-2020-317202.
5. Inoue T, Watanabe C, Ayukawa H, Nadahama T, Hosokawa A, Beppu K, et al. Biopsy-Proven Loeffler Endocarditis Successfully Treated with Steroids. Circulation. 2015;131(8):e353-4. doi: 10.1161/CIRCULATIONAHA.114.012976.
6. van Dongen IM, van Kraaij DJW, Schalla S, La Rocca HPB, Driessen RGH. Severe Mitral Regurgitation Caused by Eosinophilic Endocarditis. J Cardiol Cases. 2014;10(3):108-10. doi: 10.1016/j.jccase.2014.05.012.
7. Jin X, Ma C, Wang Y, Yang J. A Case of Loeffler Endocarditis That Showed Endomyocardial Systolic Dysfunction Detected by Layer Specific Strain Analysis. Int Heart J. 2017;58(6):1001-3. doi: 10.1536/ihj.16-422.
8. Polito MV, Hagendorff A, Citro R, Prota C, Silverio A, De Angelis E, et al. Loeffler's Endocarditis: An Integrated Multimodality Approach. J Am Soc Echocardiogr. 2020;33(12):1427-41. doi: 10.1016/j.echo.2020.09.002.
9. Bonanad C, Monmeneu JV, López-Lereu MP. Loeffler Endocarditis of the Left Ventricle: Cardiac Magnetic Resonance Findings. Heart Lung Circ. 2013;22(12):1056-7. doi: 10.1016/j.hlc.2013.03.087.

Case Report

Assessment of Coronary Flow Reserve by Myocardial Perfusion Scintigraphy using CZT Equipment

Wilter dos Santos Ker,[1,3] Davi Shunji Yahiro,[2] Gabriel de Moraes Mangas,[2] Isabelle Mendes Rodrigues Salomão,[1,2] José Augusto Antonio Alves Flor,[2] Hugo Matheus Silvestre Vianna,[2] Cláudio Tinoco Mesquita[1,2,3]

Hospital Pró-Cardíaco,[1] Rio de Janeiro, RJ – Brazil

Universidade Federal Fluminense,[2] Niterói, RJ – Brazil

Hospital Vitória e Hospital Samaritano Barra,[3] Rio de Janeiro, RJ – Brazil

Abstract

This case report presents a myocardial perfusion analysis in a 67-year-old asymptomatic male patient with known coronary artery disease (CAD) and multiple risk factors. While myocardial perfusion Imaging (MPI) with single-photon emission computed tomography (SPECT) revealed a 5% area of ischemia, the myocardial blood flow quantification assessment in a camera equipped with cadmium-zinc-telluride (CZT) detectors demonstrated a reduced global myocardial flow reserve (MFR) of 1.57. Coronary angiography confirmed extensive multivessel disease, including an 80% stenosis in the left anterior descending artery (LAD) and an occlusion of the circumflex artery (LCx), findings not fully identified by the semi-quantitative SPECT MPI. This case underscores the importance of MFR assessment, particularly using CZT technology, in detecting significant CAD that may be underestimated by traditional SPECT methods. It highlights the potential of dynamic CZT SPECT to provide more comprehensive functional information, enhancing risk stratification and potentially influencing patient management in complex cases of suspected or known CAD.

Introduction

Myocardial perfusion imaging (MPI) using single-photon emission computed tomography (SPECT) plays a crucial role in the diagnosis, risk stratification, and prognostic evaluation of coronary artery disease (CAD), with its clinical value being well established.[1,2] Although SPECT provides valuable information, it also has certain limitations.[2,3] Recent advancements in novel cameras using cadmium-zinc-telluride (CZT) detectors offer improved spatial and temporal resolution, enabling dynamic imaging and assessment of myocardial flow reserve (MFR).[2-4] MFR serves as an indicator of microvascular function and has been shown to provide incremental information beyond perfusion analysis alone.[2] Studies have demonstrated good correlation between CZT SPECT and positron emission tomography (PET) for myocardial blood flow (MBF) quantification.[3,5]

This case report highlights the limitations of SPECT without myocardial blood flow quantification in a patient with suspected CAD and underscores the importance of MFR assessment using CZT SPECT. It demonstrates how quantitative flow data can reveal critical information that is not readily apparent through traditional qualitative or semi-quantitative SPECT analysis, with potential implications for clinical decision-making and patient management.

Case report

A 67-year-old asymptomatic male patient with a medical history of systemic arterial hypertension, dyslipidemia, type 2 diabetes mellitus, sedentary lifestyle, and former smoking. He reported undergoing coronary angioplasty 10 years ago in the right coronary artery (RCA). The patient was on beta-blockers, statins, calcium channel blockers, spironolactone, antiplatelet agents, and proton pump inhibitors. He underwent myocardial perfusion scintigraphy at rest and after pharmacologic stress with dipyridamole, using 12 mCi and 36 mCi, respectively, of the radiopharmaceutical 99mTc-sestamibi on a D-SPECT CARDIO system (Spectrum Dynamics Medical) for the evaluation of myocardial ischemia and coronary flow reserve (CFR). Pharmacologic stress was performed using dipyridamole (0.568 mg/kg) over 4 minutes, with 99mTc-sestamibi administered at the 7th minute for acquisition of both dynamic and perfusion images.

Perfusion analysis revealed an estimated ischemic defect involving 5% of the left ventricle, affecting the mid anterior, mid anterolateral, and mid inferior segments. The global MFR was reduced, with an estimated value of 1.57 (normal > 2.0). Segmental MFR values (stress/rest) were estimated at 1.60 in the RCA, 1.02 in the circumflex artery (LCx), and 1.83 in the left anterior descending artery (LAD) (Figure 1). The patient subsequently underwent coronary angiography, which showed a patent previous stent, a calcified 80% stenosis in the LAD, 50% in the RCA, 90% in the posterior descending artery (PDA), and total occlusion of the LCx (Figure 1).

Discussion

This case report highlights how myocardial perfusion scintigraphy can underestimate the extent of myocardial

Keywords

Coronary Artery Disease; Single-Photon Emission-Computed Tomography; Myocardial Ischemia

Mailing Address: Gabriel de Moraes Mangas •
Universidade Federal Fluminense. R. Des. Athayde Parreiras, 100. Postal Code: 24220-900. Niterói, RJ – Brazil
E-mail: gabrielmangas@gmail.com
Manuscript received March 30, 2025, revised manuscript April 4, 2025, accepted April 9, 2025
Editor responsible for the review: Marcelo Tavares

DOI: https://doi.org/10.36660/abcimg.20250020i

ischemia. It underscores the importance of evaluating coronary flow reserve (CFR). CFR provides a more comprehensive assessment of myocardial perfusion through the absolute quantification of blood flow.[6] Although the patient was asymptomatic, with known coronary artery disease (CAD) and a low ischemic burden, the reduced CFR indicates a high risk of extensive CAD and future cardiac events.[1] The coronary microvasculature plays a crucial role in myocardial perfusion, and its assessment improves risk stratification.[7,8]

CZT cameras offer higher resolution, 3D dynamic acquisition capability, and accurate myocardial flow reserve (MFR) assessments, which enhance the detection of ischemic regions—particularly in patients with obstructive coronary artery disease (CAD).[9,10] In this case, a D-SPECT system (CZT camera) was used, revealing a discrepancy between the findings of semi-quantitative SPECT and the blood flow quantification data obtained through dynamic CZT SPECT imaging. The detection of a globally impaired flow reserve is associated with more extensive anatomic coronary disease, and the territory of the circumflex artery—where a coronary occlusion was identified—showed the most pronounced reduction in regional MFR, demonstrating the superior diagnostic accuracy of CZT technology.

Conclusion

The reported case highlights the importance of considering myocardial flow reserve (MFR) and the potential use of CZT gamma cameras in the evaluation of patients with suspected or known coronary artery disease (CAD), especially when myocardial perfusion findings are inconclusive or inconsistent with the clinical presentation.

Author Contributions

Conception and design of the research and acquisition of data: Ker WS, Yahiro DS, Mangas GM, Mesquita CT; analysis and interpretation of the data: Salomão IMR; Writing of the manuscript: Yahiro DS, Mangas GM, Salomão IMR, Flor JAAA, Vianna HMS; critical revision of the manuscript for intellectual content: Ker WS, Mesquita CT.

Potential Conflict of Interest

No potential conflict of interest relevant to this article was reported.

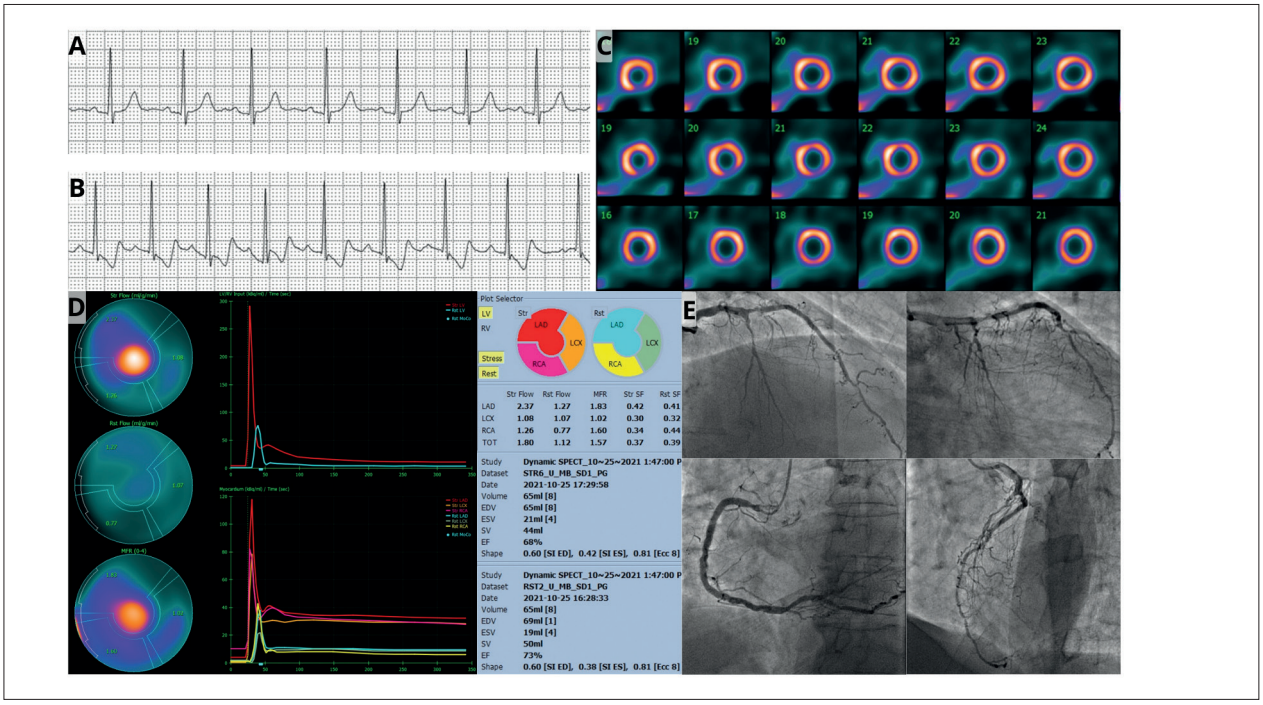

Figure 1 – *A) Electrocardiogram (resting): sinus rhythm, nonspecific ventricular repolarization abnormalities. B) Electrocardiogram: Peak pharmacological stress showing ST-segment depression. C) Perfusion analysis relative to stress-induced myocardial ischemia in the anterior (middle), anterolateral (middle), and inferior (middle) segments. Estimated ischemic defect area in 5% of the left ventricle. Fixed defect in the inferior segment (apical). D) Coronary flow reserve: There was no adequate increase in blood flow in the myocardium under stress. Global MBF reserve = 1.57. Reserve (stress/rest) in the LAD = 1.83; LCX = 1.02; RCA = 1.60. Post-stress ejection fraction was estimated at 68%. E) Coronary angiography: Obstructive three-vessel atherosclerotic CAD. Left coronary artery: left coronary artery trunk with diffuse non-obstructive irregularities and calcifications. LAD with 70% lesions in the middle third and 80% in the distal third. LCX occluded in the proximal third. RCA with 50% lesion in the proximal third, 30% in the distal third. Posterior descending artery with 90% lesion in the middle third. Posterior ventricular branch with 40% lesion in the proximal third intrastent. LAD: left anterior descending artery; LCX: left circumflex artery; RCA: right coronary artery.*

Sources of Funding

There were no external funding sources for this study.

Study Association

This study is not associated with any thesis or dissertation work.

Ethics Approval and Consent to Participate

This study was approved by the Ethics Committee of the Hospital Pró-Cardíaco under the protocol number 80960324.0.0000.5533. All the procedures in this study were in accordance with the 1975 Helsinki Declaration, updated in 2013. Informed consent was obtained from all participants included in the study.

Use of Artificial Intelligence

The authors did not use any artificial intelligence tools in the development of this work.

Availability of Research Data and Other Materials

The underlying content of the research text is contained within the manuscript.

References

1. Zavadovsky KV, Mochula AV, Maltseva AN, Boshchenko AA, Baev AE, Andreev SL, et al. The Diagnostic Value of SPECT CZT Quantitative Myocardial Blood Flow in High-Risk Patients. J Nucl Cardiol. 2022;29(3):1051-63. doi: 10.1007/s12350-020-02395-8.
2. Wang J, Li S, Chen W, Chen Y, Pang Z, Li J. Diagnostic Efficiency of Quantification of Myocardial Blood Flow and Coronary Flow Reserve with CZT Dynamic SPECT Imaging for Patients with Suspected Coronary Artery Disease: A Comparative Study with Traditional Semi-Quantitative Evaluation. Cardiovasc Diagn Ther. 2021;11(1):56-67. doi: 10.21037/cdt-20-728.
3. Bailly M, Thibault F, Courtehoux M, Metrard G, Angoulvant D, Ribeiro MJ. Myocardial Flow Reserve Measurement During CZT-SPECT Perfusion Imaging for Coronary Artery Disease Screening: Correlation with Clinical Findings and Invasive Coronary Angiography-The CFR-OR Study. Front Med. 2021;8:691893. doi: 10.3389/fmed.2021.691893.
4. Souza ACDAH, Gonçalves BKD, Tedeschi A, Lima RSL. Quantification of Coronary Flow Reserve with CZT Gamma Camera in the Evaluation of Multivessel Coronary Disease. Arq Bras Cardiol. 2018;111(4):635-37. doi: 10.5935/abc.20180196.
5. Mesquita C, Palazzo I, Pacheco J, Ker W, Sabra MMM, Chambi A, et al. Assessing Myocardial Flow Reserve Using CZT SPECT Perfusion Imaging: A Step Towards Clinical Application. Eur Heart J Cardiovasc Imaging. 2024;25(Suppl_1):jeae142.073. doi: 10.1093/ehjci/jeae142.073.
6. Acampa W, Zampella E, Assante R, Genova A, Simini G, Mannarino T, et al. Quantification of Myocardial Perfusion Reserve by CZT-SPECT: A Head to Head Comparison with 82Rubidium PET Imaging. J Nucl Cardiol. 2021;28(6):2827-39. doi: 10.1007/s12350-020-02129-w.
7. Sakuma H, Ishida M. Advances in Myocardial Perfusion MR Imaging: Physiological Implications, the Importance of Quantitative Analysis, and Impact on Patient Care in Coronary Artery Disease. Magn Reson Med Sci. 2022;21(1):195-211. doi: 10.2463/mrms.rev.2021-0033.
8. Assante R, Zampella E, Cantoni V, Green R, D'Antonio A, Mannarino T, et al. Prognostic Value of Myocardial Perfusion Imaging by Cadmium Zinc Telluride Single-Photon Emission Computed Tomography in Patients with Suspected or Known Coronary Artery Disease: A Systematic Review and Meta-Analysis. Eur J Nucl Med Mol Imaging. 2023;50(12):3647-58. doi: 10.1007/s00259-023-06344-8.
9. Kelshiker MA, Seligman H, Howard JP, Rahman H, Foley M, Nowbar AN, et al. Coronary Flow Reserve and Cardiovascular Outcomes: A Systematic Review and Meta-Analysis. Eur Heart J. 2022;43(16):1582-93. doi: 10.1093/eurheartj/ehab775.
10. Lima R, Bezerra ALF, Daibes M, Domenico C, Lorenzo A. Clinical Impact of Assessment of Myocardial Flow Reserve in Identifying the Cause of Chest Discomfort. Arq Bras Cardiol. 2024;121(6):e20230700. doi: 10.36660/abc.20230700.

Coronary Artery Dissection Following Pharmacologic Stress Echocardiography and the Follow-Up of Clinical Management: A Case Report

Thiago Artioli,[1] *Bruno Querido Marcondes Santos,*[1] *Denis Cárdenas Monteiro,*[1] *Layane Bonfante Batista,*[1] *Matheus Zavaris Lorenzoni,*[1] *Hsu Gwo Jen,*[1] *Kelvyn Melo Vital,*[1] *Kelvin Henrique Vilalva*[1]

Instituto Dante Pazzanese de Cardiologia,[1] *São Paulo, SP – Brazil*

Introduction

Spontaneous coronary artery dissection (SCAD) remains a diagnostic and therapeutic challenge in the evaluation of chest pain. Misinterpretation of symptom characteristics and failure to consider the patient's epidemiological profile may lead to inappropriate diagnostic workups and treatment strategies. The case described herein represents only the second report with similar characteristics published in major medical databases.[1] This case underscores the importance of considering uncommon causes of chest pain and acute coronary syndrome (ACS), while also providing a brief review of relevant literature. The report was prepared in accordance with the CAse REport (CARE) guidelines.[2]

Case report

The patient is a 42-year-old white female from São Paulo, Brazil. She is divorced, has completed high school, works as an administrative secretary, and identifies as Catholic. Her weight was 72 kg and height 1.75 m at presentation.

Primary symptoms

The patient reported the onset of chest pain, initially suggestive of noncardiac origin, in January 2024. The pain was described as mild, located in the thoracic region, and not associated with physical exertion. The symptoms persisted until March 2024, prompting her to seek evaluation by a private cardiologist. During the initial consultation, the clinical impression was that the patient likely had stable angina. The following medications were prescribed: acetylsalicylic acid at 100 mg/day, simvastatin at 20 mg/day, metoprolol at 50 mg/day, and enalapril at 20 mg/day. Previously, the patient was only taking desogestrel at 75 mg/day as an oral contraceptive. A dobutamine stress echocardiography was requested for further functional assessment.

Keywords

Blood Vessel Dissection; Coronary Disease; Stress Echocardiography; Case Reports

Mailing Address: Thiago Artioli •
Instituto Dante Pazzanese de Cardiologia. Av. Dr. Dante Pazzanese, 500. Postal code: 04012-909. Vila Mariana, São Paulo, SP – Brasil
E-mail: thiago.artioli48@gmail.com
Manuscript received May 5, 2025; revised manuscript May 5, 2025; accepted May 5, 2025
Editor responsible for the review: Marcelo Tavares

DOI: https://doi.org/10.36660/abcimg.20250034i

Medical, family, and psychosocial history

The patient had a known history of sporadic migraine and iron-deficiency anemia. She denied smoking, alcohol consumption, and maintained a sedentary lifestyle. Her surgical history included cesarean section, saphenectomy for venous insufficiency, and partial thyroidectomy for a benign thyroid nodule. She reported four pregnancies, including three cesarean deliveries and one spontaneous abortion of unknown etiology. There was no significant family history of cardiovascular or rheumatologic diseases.

Relevant past interventions

On March 20, 2024, the patient underwent a dobutamine stress echocardiography at a private hospital. During the examination, she experienced a sudden onset of severe precordial pain, distinct from her previous symptoms, described as a crushing sensation rated 10/10 in intensity, radiating to the head, and accompanied by nausea and vomiting. The procedure was immediately interrupted.

She was referred to a public emergency department, where she was admitted with a working diagnosis of non-ST-segment elevation ACS (NSTE-ACS). Electrocardiogram findings were nonischemic; however, serial troponin measurements showed a positive curve. Diagnostic coronary angiography revealed a tortuous and elongated left anterior descending artery, which also supplied the inferior wall, with an image consistent with a type 1 coronary dissection (Figure 1) in the mid to distal segment. Transthoracic echocardiography showed a preserved left ventricular ejection fraction (47%), with hypokinesia of the basal segment of the inferior wall and the apical region. She was discharged on her initial medications, with the addition of clopidogrel at 75 mg/day and sublingual isosorbide dinitrate at 5 mg as needed for chest pain. She was referred to our tertiary public cardiology center for outpatient follow-up.

Physical examination and clinical findings at the tertiary cardiology center

The patient was first evaluated at our tertiary cardiology center on May 10, 2024. She reported persistent angina classified as Canadian Cardiovascular Society (CCS) class II, with characteristics distinct from the initial atypical pain in January 2024, but similar to the pain experienced during the ACS event. Physical examination was unremarkable, and both electrocardiogram and chest X-ray performed at our center were within normal limits.

Following clinical assessment, myocardial perfusion scintigraphy at rest and under pharmacologic stress using

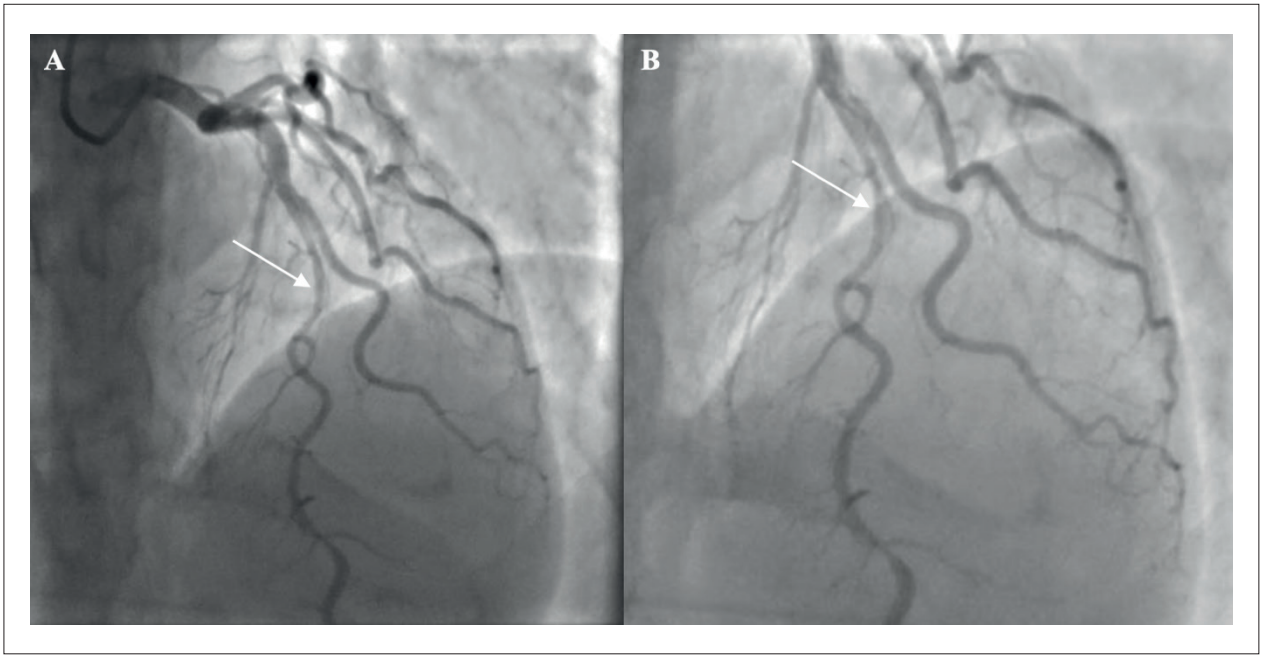

Figure 1 – *Dissection of the left anterior descending artery visualized in the right anterior oblique cranial view during cardiac catheterization (A). Magnified view of the dissection (B).*

sestamibi and dipyridamole was requested, along with coronary computed tomography (CT) angiography to monitor coronary anatomy and assess the dissection plane. It was decided to maintain clinical management with no indication for percutaneous intervention at that time. Anti-anginal therapy was optimized by increasing the metoprolol dose to 100 mg/day.

Follow-up and outcomes

The patient returned for follow-up on July 15, 2024. Clinically, she continued to experience episodes of nonspecific chest discomfort, associated with atypical chest pain described as a burning sensation lasting for hours, radiating to the left upper limb, and worsening when lying on the left side.

Laboratory tests revealed normal blood count, renal and liver function, no electrolyte abnormalities, urinalysis without crystals, and negative serologies for HIV, syphilis, and hepatitis B and C. Her LDL cholesterol level was 62 mg/dL, and NT-proBNP was 53 pg/mL. Myocardial perfusion scintigraphy showed no evidence of myocardial ischemia. Coronary CT angiography demonstrated a zero calcium score (Agatston method), no luminal coronary stenosis, and no residual signs of dissection (Figure 2).

Etiology and future follow-up

Following the July 2024 appointment, the patient continued regular follow-up at our center. She did not experience any further episodes of chest pain with characteristics suggestive of angina. Further investigation into the etiology of the coronary dissection was conducted, including assessments for Marfan syndrome, vasculitis, and collagen vascular diseases. All clinical and laboratory evaluations were negative.

Discussion

SCAD accounts for 0.1% to 4% of ACS and is more frequently observed in women, particularly young females.[3] The pathophysiology of nonatherosclerotic SCAD is not yet fully understood; proposed mechanisms include intimal tears, bleeding of the vasa vasorum, arterial inflammation, and vessel tortuosity. Approximately 20% of cases are classified as idiopathic. Other reported etiologies include pregnancy, use of oral contraceptives, genetic predisposition, and associations with certain conditions such as migraines, connective tissue disorders, and others.[4,5]

SCAD should be considered in any young patient presenting with ACS or cardiac arrest, particularly in females without traditional coronary artery disease risk factors.[6] Emotional stress, physical exertion, and hormonal influences have been identified as potential triggers for SCAD. The diagnostic workup should include electrocardiography, cardiac biomarkers, and coronary angiography. Echocardiography is valuable for assessing ventricular function, prognosis, and for differentiating from other conditions, such as Takotsubo syndrome. SCAD is classified into three angiographic types: type 1, characterized by contrast dye staining of the arterial wall with multiple radiolucent lumens; type 2, presenting as diffuse stenosis of varying severity, from mild narrowing to complete occlusion; and type 3, which mimics atherosclerosis, presenting as focal or tubular stenosis. Intracoronary imaging, coronary CT angiography, or cardiac magnetic resonance imaging may aid in diagnosis, particularly in ambiguous cases.[7,8]

Revascularization in patients with SCAD remains challenging and is associated with higher rates of procedural failure and complications. Therefore, conservative management is

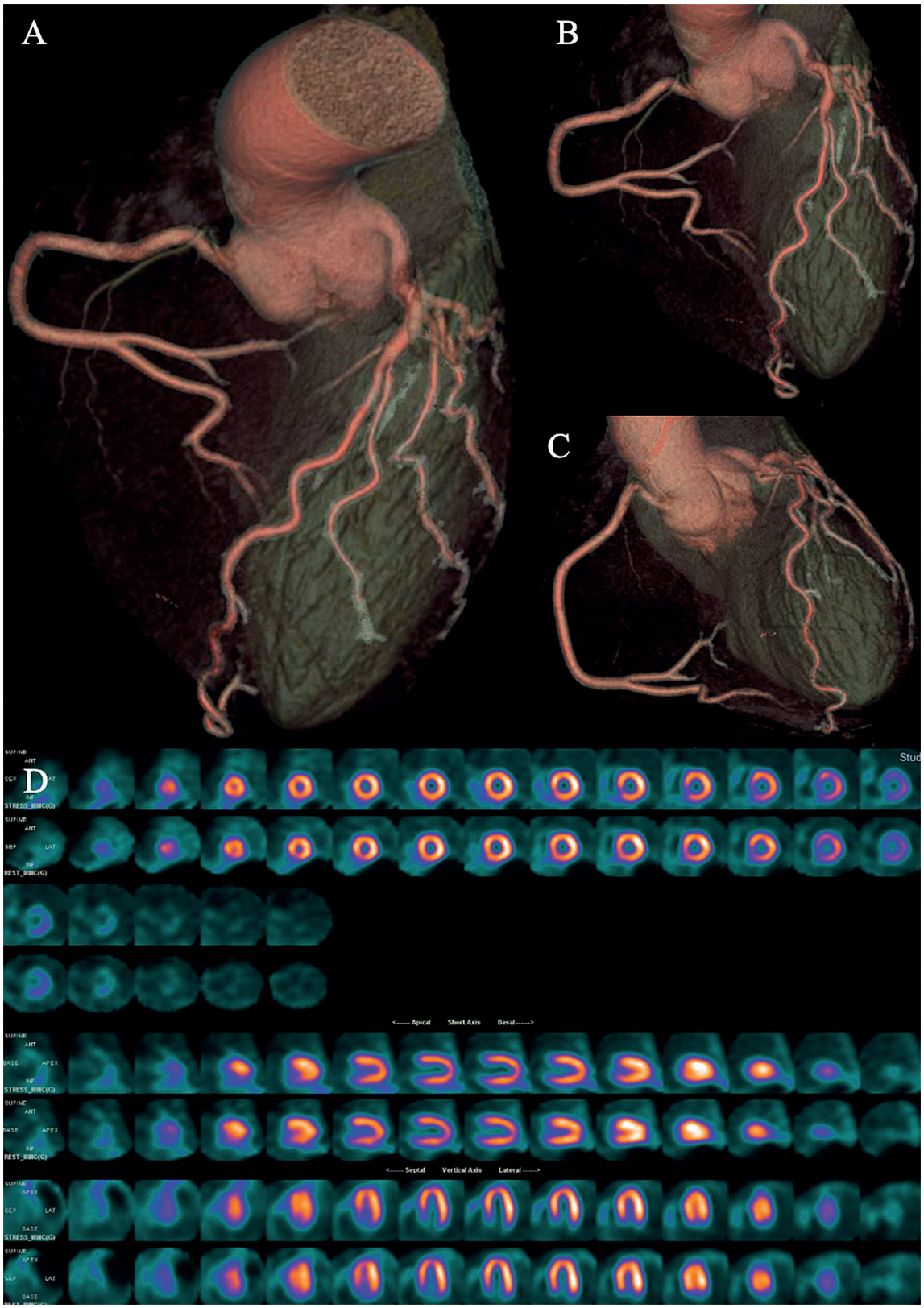

Figure 2 – *Coronary computed tomography angiography and myocardial perfusion scintigraphy during follow-up.*

generally recommended as the first-line treatment, unless the patient presents with ongoing ischemia, hemodynamic instability, or left main coronary artery involvement.[9] Angiographic "healing" of SCAD lesions has been frequently observed following conservative management. Regarding long-term management, there are currently no studies directly comparing different therapeutic strategies. As such, treatment is often extrapolated from ACS guidelines, typically including aspirin, beta-blockers, statins, and antianginal agents. It is considered reasonable to discontinue dual antiplatelet therapy once dissection healing is confirmed, which is generally expected to occur within 4 to 6 weeks following the event.[7,8]

To date, only one case report describing coronary artery dissection following stress echocardiography has been identified in major medical databases. In that case, a middle-aged male patient presented with significant ST-segment elevation followed by an accelerated idioventricular rhythm. Similar to our case, the patient was managed conservatively, with complete restoration of vessel patency.[1] A limitation of our report is the inability to definitively determine whether the dissection occurred during the dobutamine stress echocardiography or whether the exam exacerbated a pre-existing SCAD, as we do not have prior imaging of the patient's coronary anatomy. Nevertheless, the notable difference in the patient's symptoms before, during, and after the examination supports the possibility that the test acted as a potential trigger for the dissection.

Author Contributions

Conception and design of the research and writing of the manuscript: Artioli T, Santos BQM, Monteiro DC, Batista LB, Lorenzoni MZ, Jen HG, Vital KM, Vilalva KH; acquisition of data: Artioli T, Santos BQM, Monteiro DC, Batista LB, Lorenzoni MZ; analysis and interpretation of the data: Artioli T, Santos BQM, Monteiro DC, Batista LB; critical revision of the manuscript for intellectual content: Artioli T, Lorenzoni MZ, Jen HG, Vital KM, Vilalva KH.

Potential Conflict of Interest

No potential conflict of interest relevant to this article was reported.

Sources of Funding

There were no external funding sources for this study.

Study Association

This study is not associated with any thesis or dissertation work.

Ethics Approval and Consent to Participate

This study was approved by the Ethics Committee of the Instituto Dante Pazzanese de Cardiologia under the protocol number 89472225.7.0000.5462. All the procedures in this study were in accordance with the 1975 Helsinki Declaration, updated in 2013. Informed consent was obtained from all participants included in the study.

Use of Artificial Intelligence

The authors did not use any artificial intelligence tools in the development of this work.

Availability of Research Data

The underlying content of the research text is contained within the manuscript.

References

1. Karabinos I, Papadopoulos A, Koulouris S, Kranidis A, Korovesis S, Katritsis D. Spontaneous Coronary Artery Dissection during a Dobutamine Stress Echocardiography. Echocardiography. 2006;23(3):232-4. doi: 10.1111/j.1540-8175.2006.00141.x.
2. Riley DS, Barber MS, Kienle GS, Aronson JK, von Schoen-Angerer T, Tugwell P, et al. CARE Guidelines for Case Reports: Explanation and Elaboration Document. J Clin Epidemiol. 2017;89:218-35. doi: 10.1016/j.jclinepi.2017.04.026.
3. Saw J, Starovoytov A, Aymong E, Inohara T, Alfadhel M, McAlister C, et al. Canadian Spontaneous Coronary Artery Dissection Cohort Study: 3-Year Outcomes. J Am Coll Cardiol. 2022;80(17):1585-97. doi: 10.1016/j.jacc.2022.08.759.
4. Djokovic A, Krljanac G, Matic P, Zivic R, Djulejic V, Haljilji MM, et al. Pathophysiology of Spontaneous Coronary Artery Dissection: Hematoma, Not Thrombus. Front Cardiovasc Med. 2023;10:1260478. doi: 10.3389/fcvm.2023.1260478.
5. Stanojevic D, Apostolovic S, Kostic T, Mitov V, Kutlesic-Kurtovic D, Kovacevic M, et al. A Review of the Risk and Precipitating Factors for Spontaneous Coronary Artery Dissection. Front Cardiovasc Med. 2023;10:1273301. doi: 10.3389/fcvm.2023.1273301.
6. Offen S, Yang C, Saw J. Spontaneous Coronary Artery Dissection (SCAD): A Contemporary Review. Clin Cardiol. 2024;47(6):e24236. doi: 10.1002/clc.24236.
7. Hayes SN, Kim ESH, Saw J, Adlam D, Arslanian-Engoren C, Economy KE, et al. Spontaneous Coronary Artery Dissection: Current State of the Science: A Scientific Statement from the American Heart Association. Circulation. 2018;137(19):523-57. doi: 10.1161/CIR.0000000000000564.
8. Hayes SN, Tweet MS, Adlam D, Kim ESH, Gulati R, Price JE, et al. Spontaneous Coronary Artery Dissection: JACC State-of-the-Art Review. J Am Coll Cardiol. 2020;76(8):961-84. doi: 10.1016/j.jacc.2020.05.084.
9. Tweet MS, Eleid MF, Best PJ, Lennon RJ, Lerman A, Rihal CS, et al. Spontaneous Coronary Artery Dissection: Revascularization versus Conservative Therapy. Circ Cardiovasc Interv. 2014;7(6):777-86. doi: 10.1161/CIRCINTERVENTIONS.114.001659.

Idiopathic Multiple Coronary Artery Aneurysms

Alberto Vera,[1] *Virginia Álvarez*[1]
Navarre Hospital Complex,[1] *Pamplona, Navarra – Spain*

Case presentation

A 54-year-old patient with no previous medical history was evaluated in the cardiology clinic for chest pain with atypical characteristics. Due to a pretest probability of ischemic heart disease of 20%, a coronary computed tomography scan was performed, which showed a coronary aneurysm (10 × 11 mm) from the origin of the right coronary artery (RCA) to the mid-segment (Figure 1A, white arrow; Figure 2C). In the RCA mid-segment, there was partial circumferential thrombosis with 50% lumen stenosis (Figure 1B and C; Figure 2C, white asterisks). The rest of the RCA showed no coronary artery obstruction. A 9 × 9 mm aneurysm was also observed in the left main coronary artery extending to the bifurcation and proximal portion of the left anterior descending coronary artery, without significant lesions (Figure 1A and D, white arrows; Figure 2A). A 5 × 6 mm aneurysm was also observed in the proximal left circumflex artery, without significant coronary lesions (Figure 1A, white arrow; Figure 2B). The study was completed with a regadenoson stress cardiac magnetic resonance that was negative for inducible ischemia. Serologies and autoantibodies were also requested, and they were negative. The decision was made to initiate medical treatment with acetylsalicylic acid and atorvastatin. During the 6-month follow-up, the patient did not present coronary outcomes and remained asymptomatic.

A coronary artery aneurysm (CAA) is typically defined as a focal dilation of a coronary artery that exceeds 1.5 times the diameter of an adjacent normal segment, whereas coronary ectasia refers to a diffuse dilation involving at least 50% of the artery's length. Giant coronary aneurysms, although rare, are classified as those measuring more than 20 mm in diameter. This distinction is clinically significant, as ectasia represents a more extensive and generalized involvement of the artery, whereas aneurysms are focal and may carry a different prognosis and management approach.

Considering the definitions provided above, we classified our case as multiple CAAs because the dilations observed were focal rather than diffuse, which differentiates them from coronary ectasia. We have explicitly compared our case with the coronary ectasia classification proposed by Kawsara et al.[1] In particular, type I coronary ectasia, which affects multiple arteries and may present focal superimposed dilations, could have a similar radiological phenotype. However, in our case, the imaging findings demonstrated well-demarcated aneurysms rather than extensive arterial involvement. This distinction supports our classification of the lesions as aneurysms rather than ectasia. CAAs are uncommon, yet clinically significant findings, often associated with atherosclerosis, Kawasaki disease, or other inflammatory conditions. Their management is complex and depends on factors such as aneurysm size, location, and the presence of complications like thrombosis or rupture.[1] The treatment of CAAs can range from conservative medical management to invasive interventions. Medical therapy typically includes antiplatelet agents, anticoagulation, and statins to reduce thrombotic risk and control underlying atherosclerosis. For patients with large or symptomatic aneurysms or those with a high risk of rupture, surgical or percutaneous interventions may be necessary. These approaches include aneurysm resection, coronary artery bypass grafting, or stenting.[1]

Multiple CAAs have been reported in the literature, including cases affecting more than one coronary artery.[2] However, our case presents some particular features that make it unique. The aneurysms were discovered incidentally during the evaluation of atypical chest pain, rather than being diagnosed due to acute complications or symptomatic presentation. Additionally, there was involvement of all three major coronary arteries, which remains a rare finding. Another distinctive aspect of our case is that the patient was successfully managed with a conservative medical approach, without requiring interventional or surgical treatment. These aspects highlight the importance of considering conservative management in stable patients with multiple CAAs, emphasizing the need for individualized decision-making in such rare presentations.

In conclusion, the novelty of our case lies in being the first reported case of idiopathic CAAs present in the three main coronary arteries and the presence of 50% partial asymptomatic circumferential thrombosis of the RCA aneurysm, which was successfully managed with medical therapy.

Author Contributions

Conception and design of the research, writing of the manuscript and critical revision of the manuscript for intellectual content: Vera A, Álvarez V.

Keywords

Coronary Aneurysm; Case Reports

Mailing Address: Alberto Vera •
Navarre Hospital Complex. Irunlarea, 3. Postal code: 31008. Pamplona – Spain
E-mail: verasainz1604@gmail.com
Manuscript received October 24, 2024; revised March 27, 2025; accepted April 24, 2025
Editor responsible for the review: Marcelo Dantas

DOI: https://doi.org/10.36660/abcimg.20240106i

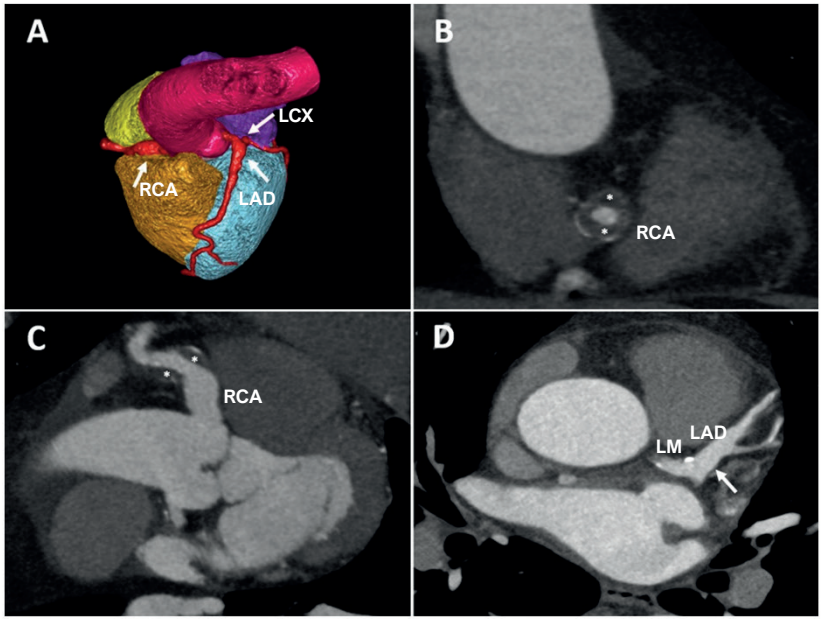

Figure 1 – *(A) Three-dimensional volume rendering. (B) RCA mid-segment. Partial circumferential thrombosis with 50% lumen stenosis. (C) RCA mid-segment. Partial thrombosis with 50% lumen stenosis. (D) LAD aneurysm. LAD: left anterior descending artery; LCX: left circumflex artery; LM: left main coronary artery; RCA: right coronary artery.*

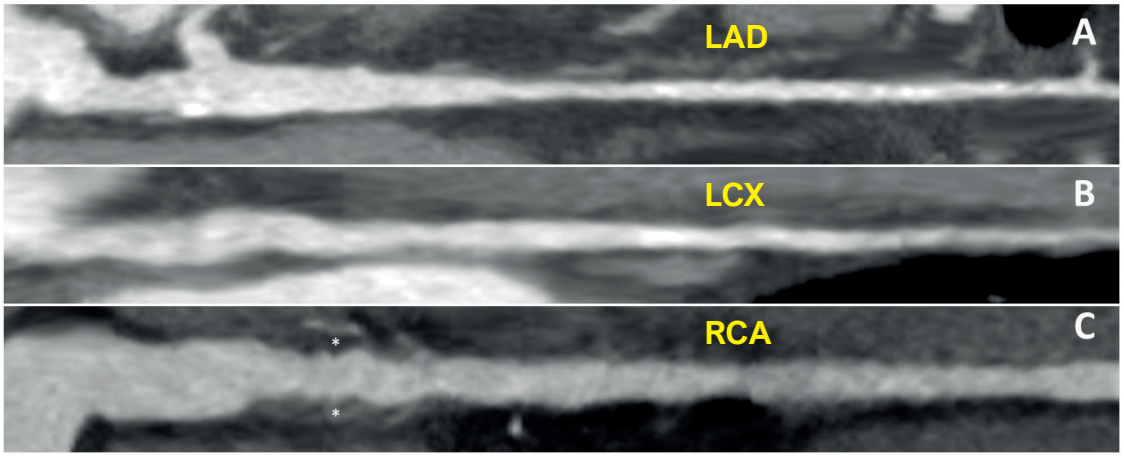

Figure 2 – *Multiplanar reconstruction. (A) LAD. (B) CX. (C) RCA. CX: left circumflex artery; LAD: left anterior descending artery; RCA: right coronary artery.*

Potential Conflict of Interest

No potential conflict of interest relevant to this article was reported.

Sources of Funding

There were no external funding sources for this study.

Study Association

This study is not associated with any thesis or dissertation work.

Ethics Apprand Consent to Participate

This article does not contain any studies with human participants or animals performed by any of the authors.

Use of Artificial Intelligence

The authors did not use any artificial intelligence tools in the development of this work.

Availability of Research Data

All datasets supporting the results of this study are available upon request from the corresponding author, Alberto Vera.

References

1. Kawsara A, Núñez Gil IJ, Alqahtani F, Moreland J, Rihal CS, Alkhouli M. Management of Coronary Artery Aneurysms. JACC Cardiovasc Interv. 2018;11(13):1211-23. doi: 10.1016/j.jcin.2018.02.041.
2. Khouzam MS, Khouzam N. Giant Coronary Artery Aneurysms Involving More than One Coronary Artery: Case Report. J Cardiothorac Surg. 2021;16(1):177. doi: 10.1186/s13019-021-01560-5.